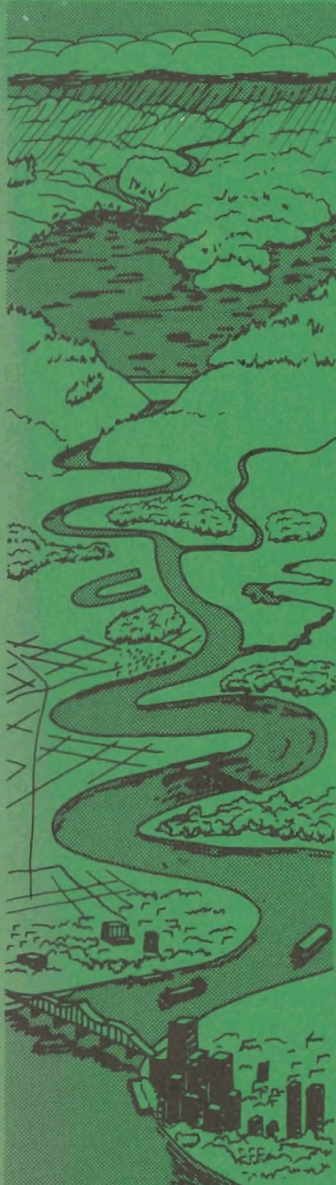




US Army Corps  
of Engineers



HERRMANN  
ENVIRONMENTAL AND WATER QUALITY  
OPERATIONAL STUDIES

CHIEF, HYD LAB COPY

MISCELLANEOUS PAPER E-84-4

# CONVECTION SCHEMES FOR USE WITH CURVILINEAR COORDINATE SYSTEMS - A SURVEY

by

Joe F. Thompson

Department of Aerospace Engineering  
Mississippi State University  
Mississippi State, Mississippi 39762



June 1984

Final Report

Approved For Public Release; Distribution Unlimited

Prepared for **DEPARTMENT OF THE ARMY**  
**US Army Corps of Engineers**  
Washington, DC 20314

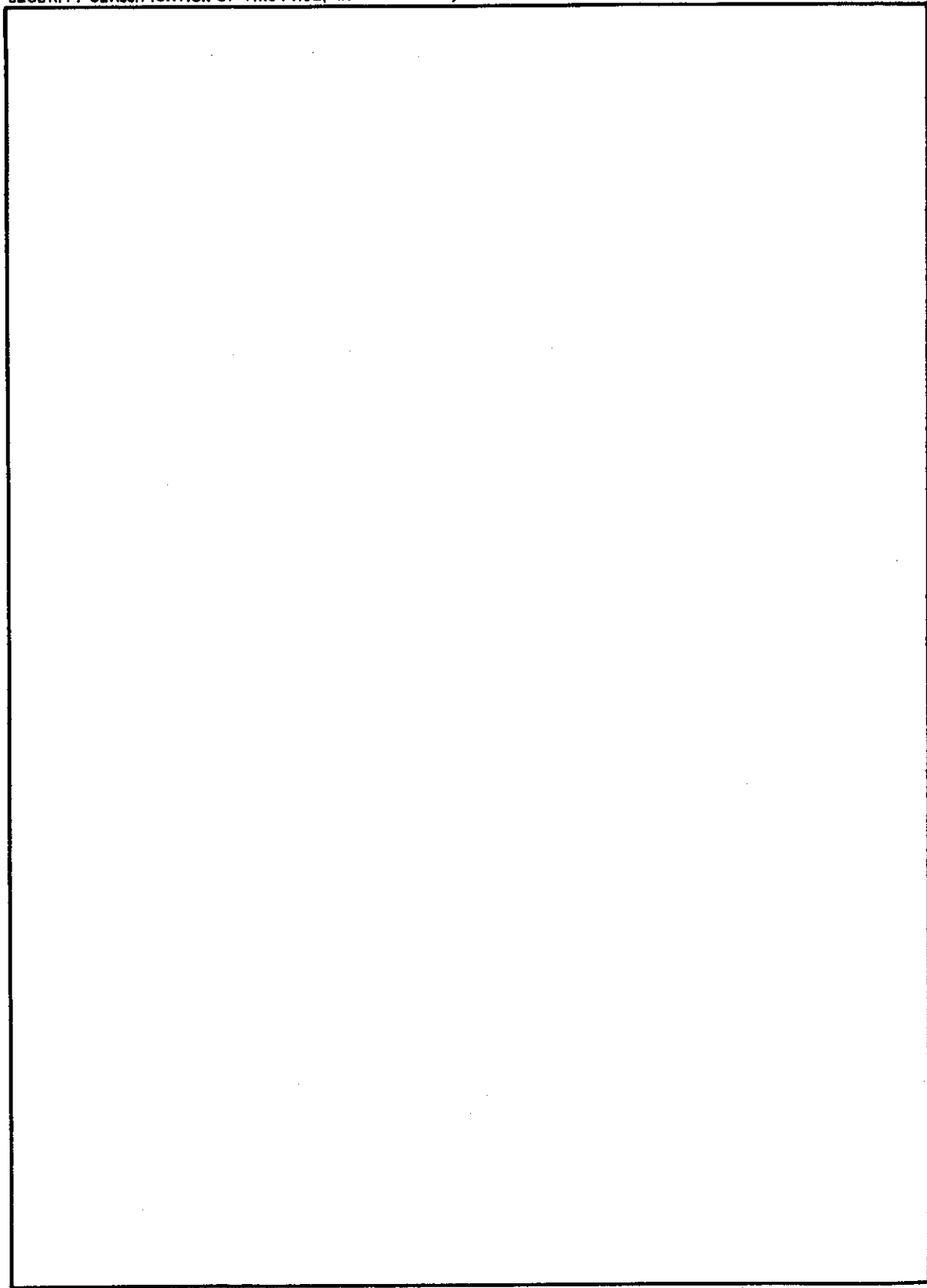
Under **Contract No. DACW39-81-C-0069**  
**(EWQOS Work Unit IC.2)**

Monitored by **Hydraulics Laboratory**  
**US Army Engineer Waterways Experiment Station**  
PO Box 631, Vicksburg, Mississippi 39180





**SECURITY CLASSIFICATION OF THIS PAGE(When Data Entered)**



**SECURITY CLASSIFICATION OF THIS PAGE(When Data Entered)**

## PREFACE

The work described in this report was performed under Contract No. DACW39-81-C-0069, entitled "Assessment of Multi-Dimensional Transport Schemes Applied on Boundary Fitted Coordinate Systems," dated 21 August 1981, between the U. S. Army Engineer Waterways Experiment Station (WES), Vicksburg, Mississippi, and Mississippi State University, Starkville, Mississippi. The study was sponsored by the Office, Chief of Engineers (OCE), U. S. Army, as part of the Civil Works General Investigations, Environmental and Water Quality Operational Studies (EWQOS) Work Unit IC.2 entitled Develop and Evaluate Multidimensional Reservoir Water Quality and Ecological Predictive Techniques. The OCE Technical Monitors were Mr. Earl Eiker, Mr. John Bushman, and Mr. James L. Gottesman.

The study was conducted and the report prepared by Dr. J. F. Thompson, Department of Aerospace Engineering, Mississippi State University, during the period August 1981 to February 1983. Dr. B. H. Johnson of the Hydraulic Analysis Division, Hydraulics Laboratory, monitored the effort. Messrs. M. B. Boyd, Chief of the Hydraulic Analysis Division, and H. B. Simmons, Chief of the Hydraulics Laboratory, provided general supervision. Program Manager of EWQOS was Dr. J. L. Mahloch, Environmental Laboratory.

Commanders and Directors of WES during this study and the preparation and publication of this report were COL Nelson P. Conover, CE, and COL Tilford C. Creel, CE. Technical Director was Mr. F. R. Brown.

This report should be cited as follows:

Thompson, J. F. 1984. "Convection Schemes for Use with Curvilinear Coordinate Systems - A Survey," Miscellaneous Paper E-84-4, prepared by Mississippi State University, for the US Army Engineer Waterways Experiment Station, Vicksburg, Mississippi.

### ACKNOWLEDGMENT

The stimulating interest of Dr. Billy H. Johnson of WES throughout this project is gratefully acknowledged. The conscientious secretarial and editorial efforts of Rita Curry of MSU were an essential part of the preparation of this report.

TABLE OF CONTENTS

	<u>Page</u>
PREFACE . . . . .	i
ACKNOWLEDGMENT . . . . .	iii
CHAPTER	
I. INTRODUCTION . . . . .	1
II. FOUNDATIONS . . . . .	2
Conventions . . . . .	2
Curvilinear Coordinates. . . . .	2
Higher Dimensions. . . . .	4
Differences. . . . .	4
Nonlinear Equations. . . . .	4
Numerical Techniques . . . . .	5
Interpolation Functions. . . . .	5
Differential Approach - Taylor Series. . . . .	6
Differential Approach - Characteristics. . . . .	8
Integral Approach - Time . . . . .	10
Integral Approach - Space. . . . .	11
Integral Approach - Time and Space . . . . .	11
Multi-Level Methods. . . . .	12
Multi-Stage Methods. . . . .	12
Explicit and Implicit Forms. . . . .	13
Difference - Differential Methods. . . . .	13
Finite Element Methods . . . . .	14
Truncation Error . . . . .	14
Difference Expressions . . . . .	15
Dissipation and Dispersion . . . . .	20

CHAPTER	<u>Page</u>
III. LOW-ORDER METHODS . . . . .	24
First-Order Upwind Methods . . . . .	24
Purely Upwind Methods . . . . .	24
Hybrid Methods. . . . .	25
Riemann Solver Methods. . . . .	27
Second-Order Methods . . . . .	28
Symmetric Methods . . . . .	28
Spatial Oscillations . . . . .	34
Upwind-Biased Methods . . . . .	35
Comparisons . . . . .	39
IV. HIGHER-ORDER METHODS. . . . .	59
Symmetric Methods. . . . .	59
Upwind-Biased Methods. . . . .	62
Multi-Stage Methods . . . . .	85
Compact Methods. . . . .	94
Hermite Methods . . . . .	94
Pade Difference Methods . . . . .	114
Spline Methods. . . . .	116
Operator Compact Methods. . . . .	119
Local Solution Methods . . . . .	121
Spectral and Pseudospectral Methods. . . . .	125
Moment Methods . . . . .	129
Finite Element Methods . . . . .	139
Ordinary Differential Equation Methods. . . . .	147
Comparisons . . . . .	147

CHAPTER	<u>Page</u>
V. FILTERS . . . . .	178
Switched Shuman Filter . . . . .	178
Flux-Corrected Transport . . . . .	179
Hybrid Methods . . . . .	186
Waveform Filters . . . . .	204
Implicit Filters . . . . .	208
Artificial Viscosity . . . . .	209
VI. TIME-SPLITTING. . . . .	212
Multiple Dimensions. . . . .	212
Multiple Processes . . . . .	214
Numerical Considerations . . . . .	214
VII. VARIOUS CONSIDERATIONS. . . . .	217
Stability. . . . .	217
Curvilinear Coordinate Systems . . . . .	220
Derivative Representations . . . . .	222
Nonuniform Grid - Exact Metric . . . . .	223
Nonuniform Grid - Difference Metric . . . . .	230
Nonorthogonality. . . . .	231
Conservative Forms. . . . .	232
VIII. CONCLUSION. . . . .	236
REFERENCES. . . . .	245

CONVECTION SCHEMES FOR USE WITH  
CURVILINEAR COORDINATE SYSTEMS -  
A SURVEY

I. INTRODUCTION

The convection of a concentration is a problem that needs no introduction. The present survey concerns this problem in regard to the use of general boundary-conforming coordinate systems in the form of numerically generated grids. The intent here has been to cover all schemes with promise in application in this context, with a representative discussion of all types of schemes, rather than to cite all works in the area.

Figure titles are duplicated from the original references and, therefore, may contain reference to equations or other items in the references. Citations of other figures, however, have been changed to correspond to the numbers in this report. Various symbols are used for the Courant number on the figures, but this item should be easily recognized in each case.

## II. FOUNDATIONS

The basic convection equation in 2D is

$$\phi_t + u(x,y,t)\phi_x + v(x,y,t)\phi_y = 0 \quad (1)$$

where, in general, the velocity is nonuniform and time dependent.

### Conventions

#### Curvilinear Coordinates

Transforming the first derivatives we have

$$\begin{aligned} \phi_x &= \frac{1}{J}(y_\eta \phi_\xi - y_\xi \phi_\eta) \\ \phi_y &= \frac{1}{J}(x_\xi \phi_\eta - x_\eta \phi_\xi) \end{aligned} \quad (2)$$

where the Jacobian of the transformation is given by

$$J = x_\xi y_\eta - x_\eta y_\xi \quad (3)$$

Then the partial differential equation becomes, in the transformed region,

$$J\phi_t + (uy_\eta - vx_\eta)\phi_\xi + (vx_\xi - uy_\xi)\phi_\eta = 0$$

or

$$J\phi_t + \bar{u}\phi_\xi + \bar{v}\phi_\eta = 0 \quad (4)$$

where

$$\begin{aligned} \bar{u} &\equiv uy_\eta - vx_\eta \\ \bar{v} &\equiv vx_\xi - uy_\xi \end{aligned} \quad (5)$$

Therefore, in the transformed region the problem has essentially the same form as the cartesian equations, but with the velocity components,  $u$  and  $v$ , replaced by the contra-variant velocity components,  $\bar{u}$  and  $\bar{v}$ . Note, however, that even with a uniform physical velocity field, these contra-variant velocity components will vary in space for a nonuniform coordinate system. (The Jacobian could be included in the definition of  $\bar{u}$  and  $\bar{v}$  if desired, of course.) It is thus possible to apply any scheme valid for Eq. (1) with nonuniform velocity to Eq. (4) directly in the transformed region. The only real complication introduced by the curvilinear coordinate system is the imposition of an effective nonuniform velocity.

Therefore, cartesian coordinate notation will be used in this review, in conformance with the notation in the articles cited, with the understanding that the schemes are to be applied in the transformed region using the effective nonuniform velocity components appearing in Eq. (4), and with the Jacobian either appearing as a multiplicative factor on the time derivative or included in the effective velocities. In this application, the symbols  $x$  and  $y$  carry over directly to the symbols for the curvilinear coordinates  $\xi$  and  $\eta$ . Schemes for which the order is degraded when the velocity is nonuniform will likewise be of lower order when applied in the transformed region. With application understood to be in the transformed region, it is only necessary to consider a uniform square grid with unit spacing. However, certain considerations are necessary to preserve the order of a scheme when the coordinate line spacing in the physical region is not uniform, as is discussed in a later section.

### Higher Dimensions

Most schemes will be presented in one dimension for economy of presentation. Application in higher dimensions is discussed in a later section, where it is noted that any one-dimensional scheme can be applied with multiple dimensions through time-splitting (sometimes called factoring). Even when a scheme has a natural generalization to higher dimensions, the time-split approach is often preferable.

### Differences

In the discussion to follow, differences are understood to be central and symmetric unless otherwise indicated. Schemes are assumed to be applicable to nonuniform velocity fields without loss of order, and grid spacing is taken to be uniform, unless stated otherwise. Precise difference expressions are not given in this review; rather the points involved are indicated by diagrams referred to as "stencils." In these diagrams for 1D schemes, the space direction is shown across the page, while the time direction is up the page. Solid lines intersect at grid points at integral time levels. For 2D schemes both directions are spatial, with values at intermediate time levels to be understood in multi-stage methods. Intermediate points and time levels are indicated by dotted lines. Circles identify the points involved, with the point at which a new value is obtained being indicated by a filled circle.

### Nonlinear Equations

Schemes are generally analyzed in the quasi-linear form with uniform velocity, so conclusions regarding stability, dissipation, and phase error must be considered to be local for the nonlinear case or with nonuniform velocity. Thus for the general nonlinear equation

$$\phi_t + [f(\phi)]_x + [g(\phi)]_y = 0 \quad (6)$$

the equation actually analyzed is

$$\phi_t + A\phi_x + B\phi_y + 0 \quad (7)$$

where A and B are the Jacobian matrices of f and g, respectively, with respect to  $\phi$ , i.e., with

$$\phi = \begin{bmatrix} \phi_1 \\ \phi_2 \\ \cdot \\ \cdot \\ \cdot \\ \phi_n \end{bmatrix} \quad f = \begin{bmatrix} f_1 \\ f_2 \\ \cdot \\ \cdot \\ \cdot \\ f_n \end{bmatrix} \quad (8)$$

where each element of  $\phi$  represents a different dependent variable, the elements of the Jacobian matrix of f are given by

$$A_{ij} = \frac{\partial f_i}{\partial \phi_j} \quad i, j = 1, 2, \dots, n \quad (9)$$

It is actually the linear single-component problem defined simply by Eq. (1) which is of direct concern in the present review.

#### Numerical Techniques

Numerical solution of Eq. (1) can be approached in several ways, of course. One basic demarcation is foundation on the differential form given by Eq. (1), or an integral form obtained by integrating Eq. (1) with respect to space and/or time.

#### Interpolation Functions

In either approach, the basic technique involved in the construction of a numerical method is the approximation of the solution by an interpolation function fitted to the solution values, and perhaps to some of its derivatives, at certain discrete points. Derivatives, or integrals,

are then approximated by differentiating, or integrating, the interpolation function. The most common form of interpolation function is a polynomial, the Lagrange interpolation polynomials being fitted to solution values only, and the Hermite interpolation polynomials being fitted to derivatives as well. Splines are a form of interpolation polynomial fitted to solution values and some derivatives on the ends of each successive interval between grid points. The imposition of continuity of certain higher derivatives at the grid points yields difference relations among the solution values and the derivatives that are fitted. The spline representation is thus a piecewise continuous approximation over the entire field. In contrast, the Lagrange and Hermite polynomials are usually applied locally over small overlapping sets of points neighboring the point of evaluation. Any polynomial representation will be exact, of course, if the solution function is a polynomial of degree equal to, or less than, that of the interpolation polynomial.

Other interpolation functions are also used, such as exponentials or functions obtained as local solutions of the differential equation. The spectral methods use eigenfunction expansions of the solution. Still another form is the expansion of the solution in a finite Fourier series, as in the pseudospectral methods. The derivatives (integrals) obtained by differentiation (integration) of the series in the spectral and pseudospectral methods are essentially of infinite order.

#### Differential Approach - Taylor Series

By differentiation of the one-dimensional form of the partial differential equation (1), we have

$$\phi_{tt} = -u\phi_{xt} - u_t\phi_x \quad (10)$$

But,

$$\phi_{xt} = (\phi_t)_x = - (u\phi_{xx} + u_x\phi_x) \quad (11)$$

so that

$$\phi_{tt} = u^2\phi_{xx} + (uu_x - u_t)\phi_x \quad (12)$$

Higher derivatives may be obtained in a similar fashion, and thus all time derivatives can be expressed in terms of space derivatives. A Taylor series expansion in time then gives

$$\begin{aligned} \phi^{n+1} &= \phi^n + \phi_t \Delta t + \phi_{tt} \frac{\Delta t^2}{2} + O(\Delta t^3) \\ &= \phi^n - u\phi_x \Delta t + [u^2\phi_{xx} + (uu_x - u_t)\phi_x] \frac{\Delta t^2}{2} \\ &\quad + O(\Delta t^3) \end{aligned} \quad (13)$$

Thus a second-order scheme results if  $\phi_x$  in the  $\Delta t$  term is approximated to second order, and  $\phi_{xx}$ ,  $u_x\phi_x$ , and  $u_t\phi_x$  in the  $\Delta t^2$  term are approximated to first order. This second-order scheme is the single equation version of the Lax-Wendroff scheme. Higher-order expressions can be obtained by retaining more terms in the Taylor series expansion, using successive differentiations of the differential equation to express the additional time derivatives in terms of space derivatives of  $\phi$ , and expressing all the derivatives to the necessary order in each term of the resulting expression. Difference representations of the various derivatives are obtained by approximating the solution by an interpolation function, differentiating this function, and evaluating the result at the point in question. This topic is discussed further later in this section.

All schemes in this review that are not indicated to be dependent on interpolation functions other than polynomials are assumed to be

based on polynomials and are, therefore, derivable from Taylor series expansions of the function at the grid points that appear in the final difference expressions, with all time derivatives in the series being expressed in terms of space derivatives through repeated differentiation of the differential equation as illustrated above.

#### Differential Approach-Characteristics

Taking another approach, we have  $\phi = \text{constant}$  on the trajectories given by  $x_t = u$ , i.e., on

$$x = \int_0^t u dt + x_0 \quad (14)$$

These trajectories define the characteristic curves of the partial differential equation. Therefore we can write

$$\phi(x, t + \Delta t) = \phi\left(x - \int_t^{t+\Delta t} u dt', t\right) \quad (15)$$

i.e., the solution at  $x$  at the new time level,  $t + \Delta t$ , is equal to the solution at  $x - \int_t^{t+\Delta t} u dt'$  at the previous time level. This type of method is constructed by approximating the solution by an interpolation function and evaluating the function at the location given by the first argument in the right side of Eq. (15).

Now with

$$\Delta \zeta \equiv \int_t^{t+\Delta t} u dt' \quad (16)$$

we have by a Taylor series expansion,

$$\phi(x - \Delta \zeta, t) = \phi(x, t) - \phi_x \Delta \zeta + \phi_{xx} \frac{\Delta \zeta^2}{2} + O(\Delta \zeta^3) \quad (17)$$

Now redefine the variable of integration  $t'$  such that

$$\Delta \zeta = \int_0^{\Delta t} u[x(t + t'), t + t'] dt' \quad (18)$$

and expand  $u$  in a Taylor series so that

$$\Delta \zeta = \int_0^{\Delta t} \{u(x, t) + u_x [x(t + t') - x(t)] + u_t t' + O(\Delta t^2)\} dt' \quad (19)$$

But

$$\begin{aligned} x(t + t') &= x(t) - \int_t^{t+t'} u dt'' \\ &= x(t) - \int_0^{t'} u dt'' \quad (\text{with } t'' \text{ redefined}) \\ &= x - ut' + O(\Delta t^2) \end{aligned} \quad (20)$$

Then

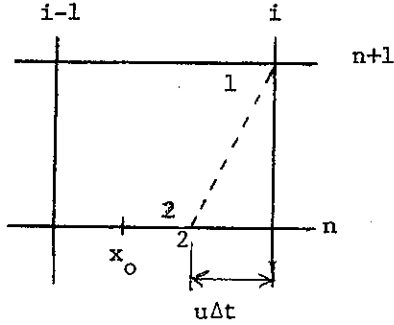
$$\begin{aligned} \Delta \zeta &= \int_0^{\Delta t} (u - u_x ut' + u_t t') dt' + O(\Delta t^3) \\ &= u \Delta t - (u u_x - u_t) \frac{\Delta t^2}{2} + O(\Delta t^3) \end{aligned} \quad (21)$$

Then

$$\begin{aligned} \phi(x - \int_t^{t+\Delta t} u dt', t) &= \phi(x, t) - u \phi_x \Delta t + (u u_x - u_t) \frac{\Delta t^2}{2} \phi_x \\ &\quad + \frac{1}{2} u^2 \phi_{xx} \Delta t^2 + O(\Delta t^3) \end{aligned} \quad (22)$$

which agrees exactly with Eq. (13).

Thus in constructing a convective scheme, the same results follow from expanding the function at grid points on adjacent time levels and from expanding the function at the intersection on the present time level of characteristics from grid points on the adjacent time levels. This is true, of course, to arbitrary order in the series expansion. Thus in the diagram below, the same scheme will result whether point 1 or 2 is used in the construction. In either case it is the grid point 1 that will appear in the final difference expression.



This development also illustrates that expansion of the solution at the new time level about the previous level, with all time derivatives in the series expressed in terms of spatial derivatives through repeated differentiation of the differential equation, followed by substitution of spatial difference expressions, is equivalent to expressing the advanced time solution in terms of the solution at the previous time level at a position  $\Delta\zeta$  upstream, this value being determined by interpolation among the grid points at the previous time level.

#### Integral Approach - Time

Integrating the one-dimensional form of Eq. (1) over a time interval  $\Delta t$  we have

$$\phi^{n+1} - \phi^n = - \int_t^{t+\Delta t} u \phi_x dt \quad (23)$$

With the integrand approximated by a linear function, the second-order Crank-Nicholson form results:

$$\phi^{n+1} - \phi^n = - \frac{1}{2} [(u\phi_x)^n + (u\phi_x)^{n+1}] \Delta t \quad (24)$$

which involves a temporal average of the convective flux. Higher-order representations are, of course, possible using higher-degree approximations of the integrand (one degree lower than the order) involving more time levels or perhaps some intermediate time levels.

### Integral Approach - Space

With the integration taken over space instead of time we have, using integration by parts in the last step,

$$\begin{aligned} \int_{x_{i-\frac{1}{2}}}^{x_{i+\frac{1}{2}}} \phi_t dx &= - \int_{x_{i-\frac{1}{2}}}^{x_{i+\frac{1}{2}}} u \phi_x dx \\ &= - (u\phi)_{i+\frac{1}{2}} + (u\phi)_{i-\frac{1}{2}} + \int_{x_{i-\frac{1}{2}}}^{x_{i+\frac{1}{2}}} \phi u_x dx \end{aligned} \quad (25)$$

The first two terms on the right are the fluxes through the sides of a cell. The last integral vanishes for uniform velocity.

Methods of various orders are produced using different degrees of approximation functions for the integrands, which again must be represented by functions of no more than one degree less than the intended order of the method. Note that this approach involves a spatial average of the time derivative.

### Integral Approach - Time and Space

Integration over both space and time produces

$$\begin{aligned} \int_{x_{i-\frac{1}{2}}}^{x_{i+\frac{1}{2}}} (\phi^{n+1} - \phi^n) dx &= - \int_t^{t+\Delta t} [(u\phi)_{i+\frac{1}{2}} - (u\phi)_{i-\frac{1}{2}}] dt \\ &\quad + \int_t^{t+\Delta t} \int_{x_{i-\frac{1}{2}}}^{x_{i+\frac{1}{2}}} \phi u_x dx \end{aligned} \quad (26)$$

Again the last integral vanishes for uniform velocity or the conservative form. The first integral on the right is now the time-average of the fluxes through the cell sides.

In Eq. (26) the integrals can be approximated using Eq. (15) with

$\phi$  expanded in a Taylor series as in Eq. (17). Thus with  $d\zeta \equiv udt$  and  $\Delta\zeta =$

$\int_t^{t+\Delta t} udt'$ , we have

$$\begin{aligned} \int_t^{t+\Delta t} u\phi dt' &= \int_0^{\Delta\zeta} \phi(x - \zeta, t) d\zeta \\ &= \int_0^{\Delta\zeta} [\phi(x, t) - \phi_x \zeta + \phi_{xx} \frac{\zeta^2}{2} + O(\zeta^3)] d\zeta \\ &= \phi \Delta\zeta - \phi_x \frac{\Delta\zeta^2}{2} + \phi_{xx} \frac{\Delta\zeta^3}{6} + O(\Delta\zeta^4) \end{aligned} \quad (27)$$

Using the approximation for  $\Delta\zeta$  given by Eq. (21) this becomes, to third order,

$$\int_t^{t+\Delta t} u\phi dt = \phi [u\Delta t - (uu_x - u_t) \frac{\Delta t^2}{2}] - \phi_x \frac{u^2 \Delta t^2}{2} + O(\Delta t^3) \quad (28)$$

Higher-order forms can be developed in a similar manner. An alternative approach here is to represent the flux,  $u\phi$ , directly by an approximating function of degree one less than the desired order of the method.

#### Multi-Level Methods

Another way to achieve higher order in time is to represent the time derivative directly by higher-order difference representations involving more than one previous time level. Chief among such methods is the three-level "leapfrog" scheme, which is constructed using a second-order central time difference.

#### Multi-Stage Methods

In many methods several stages may be involved in progressing to the next time level. These stages often involve intermediate time levels and points between grid points. The schemes forming the intermediate

stages are usually of lower order than the overall scheme. It is possible, of course to algebraically combine these stages into a single step. However, the actual computation is done in the separate stages, and the presentation is certainly not elucidated by the combination. Truncation error, phase error, and stability analyses do require the single-step form. Stencils are shown for each stage of such methods. It is clear from the stencils that the single-step form would involve an expanded stencil.

#### Explicit and Implicit Forms

Explicit methods produce values at new time levels directly at each point in succession, since the new values at each point depend only on old values at neighboring points. Implicit methods require the solution of a system of algebraic equations at each new time level, since the new values at each point depend on the new values at adjacent points as well as on the old values. Implicit methods allow larger time steps but it is generally not possible to take advantage of this increased stability in convection problems without sacrificing accuracy because of dispersion in the solution. Implicit methods are more important with stiff systems of equations, which have widely different time scales for the various components.

#### Difference - Differential Methods

In some schemes difference approximations are made only in space or only in time, and the resulting set of simultaneous ordinary differential equations is solved by one of many established, highly accurate procedures for such equations. When the ordinary differential equations are in time, the scheme is referred to as the "method of lines." In this case the size of the system of ordinary differential equations

to be solved is equal to the product of the number of dependent variables and the number of points in the field. With spatial ordinary differential equations, however, the system is much smaller, consisting of simply one equation for each dependent variable.

### Finite Element Methods

Finite element methods involve representing the solution as a finite series of basis functions, with the coefficients in the series being the values of the solution, and perhaps some of its derivatives, at certain points on the elements which fit together to cover the field in space and perhaps time also. This representation is substituted in the differential equation, and the residual is required to be orthogonal to the basis functions over the element. The result is a system of algebraic equations which must be solved over the field. Such methods are inherently implicit.

### Truncation Error

The truncation error of a difference scheme is obtained by expanding all variables in the difference equations in Taylor series about some certain point, and invoking the partial differential equation and its derivatives to cancel terms wherever possible. Certain difference expressions are common to many schemes, so the truncation error analysis can be facilitated by first evaluating the error of these component expressions. Thus

$$\delta f_i \equiv f_{i+\frac{1}{2}} - f_{i-\frac{1}{2}} = f_x \Delta x + f_{xxx} \frac{\Delta x^3}{24} + O(\Delta x^5) \quad (29.a)$$

$$\mu f_i \equiv \frac{1}{2}(f_{i+\frac{1}{2}} + f_{i-\frac{1}{2}}) = f + f_{xx} \frac{\Delta x^2}{8} + O(\Delta x^4) \quad (29.b)$$

$$\mu \delta f_i \equiv \frac{1}{2}(f_{i+1} - f_{i-1}) = f_x \Delta x + f_{xxx} \frac{\Delta x^3}{6} + O(\Delta x^5) \quad (29.c)$$

$$\Delta f_i \equiv f_{i+1} - f_i = f_x \Delta x + f_{xx} \frac{\Delta x^2}{2} + O(\Delta x^3) \quad (29.d)$$

$$\nabla f_i \equiv f_i - f_{i-1} = f_x \Delta x - f_{xx} \frac{\Delta x^2}{2} + O(\Delta x^3) \quad (29.e)$$

$$\delta^2 f_i = f_{i+1} - 2f_i + f_{i-1} = f_{xx} \Delta x^2 + f_{xxx} \frac{\Delta x^3}{6} + O(\Delta x^4) \quad (29.f)$$

with similar relations for time derivatives. With these relations, the truncation error of the scheme

$$\begin{aligned} \phi_i^{n+1} &= \phi_i^n - \frac{u \Delta t}{2 \Delta x} (\phi_{i+1}^n - \phi_{i-1}^n) + \frac{u^2 \Delta t^2}{2 \Delta x^2} (\phi_{i+1}^n - 2\phi_i^n + \phi_{i-1}^n) \\ &= [1 - \frac{u \Delta t}{\Delta x} u \delta + \frac{1}{2} (\frac{u \Delta t}{\Delta x})^2 \delta^2] \phi_i^n \end{aligned} \quad (30)$$

for uniform velocity is given by

$$\begin{aligned} T &= [\phi_t \Delta t + \phi_{tt} \frac{\Delta t^2}{2} + \phi_{ttt} \frac{\Delta t^3}{6} + O(\Delta t^4)] + \frac{u \Delta t}{\Delta x} [\phi_x \Delta x \\ &\quad + \phi_{xxx} \frac{\Delta x^3}{6} + O(\Delta x^5)] - \frac{1}{2} (\frac{u \Delta t}{\Delta x})^2 [\phi_{xx} \Delta x^2 \\ &\quad + \phi_{xxxx} \frac{\Delta x^4}{12} + O(\Delta x^6)] \\ &= (\phi_t + u \phi_x) \Delta t + (\phi_{tt} - u^2 \phi_{xx}) \frac{\Delta t^2}{2} + \phi_{ttt} \frac{\Delta t^3}{6} \\ &\quad + u \phi_{xxx} \frac{\Delta t \Delta x^2}{6} + O(\Delta t^4, \Delta t^2 \Delta x^2) \end{aligned} \quad (31)$$

But by Eq. (1) and (12) the first two terms vanish. Also  $\phi_{ttt} = -u^3 \phi_{xxx}$  so that the final truncation error expression is

$$T = [1 - (\frac{u \Delta t}{\Delta x})^2] u \phi_{xxx} \frac{\Delta t \Delta x^2}{6} \quad (32)$$

and the scheme is thus second order.

### Difference Expressions

Difference expressions for derivatives obtained by differentiating interpolation polynomials may be generalized to arbitrary order as follows. With the displacement operator defined as

$$E f_i \equiv f_{i+1} \quad (33)$$

we have from the definitions of the difference operators in Eq. (29)

the following operator equivalences:

$$\delta = E^{\frac{1}{2}} - E^{-\frac{1}{2}} \quad (34.a)$$

$$\mu = \frac{1}{2}(E^{\frac{1}{2}} + E^{-\frac{1}{2}}) \quad (34.b)$$

$$\Delta = E - 1 \quad (34.c)$$

$$\nabla = 1 - E \quad (34.d)$$

Now by Taylor series expansion on a uniform grid,

$$f_{i+1} = \sum_{k=0}^{\infty} f_i^{(k)} \frac{(\Delta x)^k}{k!} \quad (35)$$

where the superscript (k) indicates the k-th derivative. With the derivative operator defined as  $Df = f_x$ , Eq. (35) can be written

$$Ef = \sum_{k=0}^{\infty} \frac{(\Delta x)^k}{k!} D^k f = \left( \sum_{k=0}^{\infty} \frac{(\Delta x)^k}{k!} D^k \right) f$$

which yields the operator equivalence

$$E = \sum_{k=0}^{\infty} \frac{(\Delta x D)^k}{k!} = e^{\Delta x D} \quad (36)$$

and then

$$\Delta x D = \ln E \quad (37)$$

Using the equivalences of Eq. (34) we have

$$\Delta x D = 2 \sinh^{-1} \left( \frac{\delta}{2} \right) \quad (38.a)$$

$$= \ln (1 + \Delta) \quad (38.b)$$

$$= -\ln (1 + \nabla) \quad (38.c)$$

Difference expressions for approximation of derivatives to any order may then be obtained from truncated expansions of the expressions in Eq. (38). From Eq. (29), the leading terms of the expansions of  $\delta f$ ,  $\Delta f$ , and  $\nabla f$  are all  $f_x \Delta x$ . Therefore, the truncation error of the difference expressions obtained from Eq. (38) is obtained by replacing the operator with  $\Delta x D$  in the first term following the truncation.

For example

$$\begin{aligned} f_x &= \frac{1}{\Delta x} \Delta x Df \\ &= \frac{1}{\Delta x} \ln(1 + \Delta) f \\ &= \frac{1}{\Delta x} (\Delta - \frac{1}{2} \Delta^2 + 1/3 \Delta^3 \dots) f \end{aligned}$$

If this expression is truncated after the first power of  $\Delta$ , we have

$$f_x \cong \frac{1}{\Delta x} \Delta f = \frac{1}{\Delta x} (f_{i+1} - f_i)$$

with truncation error  $-\frac{\Delta x}{2} f_{xx}$ . If the second power of  $\Delta$  is retained then

$$f_x \cong \frac{1}{\Delta x} (\Delta - \frac{1}{2} \Delta^2) f = \frac{1}{\Delta x} (\Delta f - \frac{1}{2} \Delta^2 f)$$

Now  $\Delta f = f_{i+1} - f_i$  so that

$$\begin{aligned} \Delta^2 f &= \Delta(\Delta f) = \Delta f_{i+1} - \Delta f_i = (f_{i+2} - f_{i+1}) - (f_{i+1} - f_i) \\ &= f_{i+2} - 2f_{i+1} + f_i \end{aligned}$$

Then

$$\begin{aligned} f_x &\cong \frac{1}{\Delta x} [(f_{i+1} - f_i) - \frac{1}{2}(f_{i+2} - 2f_{i+1} + f_i)] \\ &= \frac{1}{\Delta x} (-\frac{1}{2}f_{i+2} + 2f_{i+1} - \frac{3}{2}f_i) \end{aligned}$$

with truncation error  $\frac{\Delta x^2}{3} f_{xxx}$ . Higher approximations are developed in like manner.

Also

$$\begin{aligned} f_x &= \frac{1}{\Delta x} [2 \sinh^{-1}(\frac{\delta}{2})] f \\ &= \frac{2}{\Delta x} (\frac{\delta}{2} - \frac{\delta^3}{48} + \frac{\delta^5}{460} \dots) f \end{aligned}$$

But note that this would require  $f_{i+\frac{1}{2}}$ ,  $f_{i+\frac{3}{2}}$ , etc., instead of  $f_{i+1}$ ,

$f_{i+2}$ , etc. This can be avoided by using the identity:  $\mu^2 = 1 + \frac{1}{4}\delta^2$ .

Then we may write

$$\begin{aligned} f_x &= \frac{1}{\Delta x} \left[ \mu \left(1 + \frac{1}{4}\delta^2\right)^{-\frac{1}{2}} 2 \sinh^{-1} \left(\frac{\delta}{2}\right) \right] f \\ &= \frac{1}{\Delta x} \left( \mu\delta - \frac{\mu\delta^3}{6} + \frac{\mu\delta^5}{30} \dots \right) f \end{aligned}$$

Here truncation after the first power of  $\delta$  yields

$$\begin{aligned} f_x &\approx \frac{1}{\Delta x} \mu\delta f = \frac{1}{\Delta x} \mu \left( f_{i+\frac{1}{2}} - f_{i-\frac{1}{2}} \right) \\ &= \frac{1}{2\Delta x} \left[ (f_{i+1} + f_i) - (f_i + f_{i-1}) \right] \\ &= \frac{1}{2\Delta x} (f_{i+1} - f_{i-1}) \end{aligned}$$

which is the familiar central difference approximation, with truncation error  $-\frac{\Delta x^2}{6} f_{xxx}$ .

Higher derivatives are obtained in an analogous manner:

$$\begin{aligned} f_{xx} &= \frac{1}{\Delta x^2} (\Delta x D)^2 f \\ &= \frac{1}{\Delta x^2} [\ln(1 + \Delta)]^2 f \\ &= \frac{1}{\Delta x^2} \left( \Delta - \frac{1}{2} \Delta^2 + \frac{1}{3} \Delta^3 \dots \right)^2 f \\ &= \frac{1}{\Delta x^2} \left( \Delta^2 - \Delta^3 + \frac{11}{12} \Delta^4 - \frac{5}{6} \Delta^5 + \dots \right) f \end{aligned}$$

Also,

$$\begin{aligned} f_{xx} &= \frac{1}{\Delta x^2} \left[ 2 \sinh^{-1} \left(\frac{\delta}{2}\right) \right]^2 f \\ &= \frac{1}{\Delta x^2} \left( \delta^2 - \frac{1}{12} \delta^4 + \frac{1}{90} \delta^6 \dots \right) f \end{aligned}$$

Truncation after the first term in this last expression yields the familiar three-point central difference approximation for the second derivative:

$$f_{xx} = \frac{1}{\Delta x^2} \delta^2 f = \frac{1}{\Delta x^2} (f_{i+1} - 2f_i + f_{i-1})$$

with truncation error  $-\frac{x^2}{12} f_{xxxx}$ .

Another variation of the above is as follows: Using the displacement operator E, we may write

$$\begin{aligned} f_x &= \frac{1}{\Delta x} \Delta x D f = \frac{1}{\Delta x} \Delta x D (E f_{i-1}) = \frac{1}{\Delta x} (\ln E) E f_{i-1} \\ &= \frac{1}{\Delta x} [\ln(1 + \Delta)] (1 + \Delta) f_{i-1} \\ &= \frac{1}{\Delta x} [-\ln(1 - \nabla)] (1 - \nabla)^{-1} f_{i-1} \\ &= \frac{1}{\Delta x} [2 \sinh^{-1}(\frac{\delta}{2})] \exp[2 \sinh^{-1}(\frac{\delta}{2})] f_{i-1} \\ &= \frac{1}{\Delta x} \mu(1 + \frac{1}{4} \delta^2)^{-\frac{1}{2}} [2 \sinh^{-1}(\frac{\delta}{2})] \exp[2 \sinh^{-1}(\frac{\delta}{2})] f_{i-1} \end{aligned}$$

Expressions of this type yield the derivatives at  $x_i$  without using the value of  $f$  at  $x_i$ . Obviously the displacement operator may be used to generate similar expressions not involving  $f_{i+1}$ ,  $f_{i-1}$ , or any others desired. The extension to higher derivatives is obvious also:

$$f_{xx} = \frac{1}{\Delta x^2} (\Delta x D)^2 f = \frac{1}{\Delta x^2} (\Delta x D)^2 E f_{i-1}$$

Note also that

$$f_x = \frac{1}{\Delta x} \Delta x D f = \frac{1}{\Delta x} \Delta x D E^{-1} f_{i+1}, \text{ etc.}$$

Note also that expressions involving differences of the derivatives can be obtained. Thus, using Eq. (38),

$$f_x = Df$$

But then

$$D^{-1}f_x = f \quad (39)$$

With  $D$  represented by an expression such as is given in Eq. (38), this becomes a representation involving differences of  $f_x$  instead of  $f$ . Similarly, we may write

$$f_{xx} = D^2f$$

and then either

$$D^{-1}f_{xx} = Df = f_x \quad (40)$$

or

$$D^{-2}f_{xx} = f \quad (41)$$

The first of these, with the expressions of Eq. (38), represents  $f_x$  in terms of differences of  $f_{xx}$ , while the second is a relation between  $f$  and differences of  $f_{xx}$ . Clearly a wide variety of expressions can be obtained by algebraic manipulation of these operators. Use of the identity  $\mu^2 = 1 + \frac{\delta^2}{4}$ , or other identities, increases the variety even further.

#### Dissipation and Dispersion

Stability and phase error (dispersion) are analyzed by substituting the basic wave form,  $w = e^{i(kx - \omega t)}$ , with  $k$  real and  $\omega$  complex, into the difference equation. Since this is one element of a Fourier series, any error can be represented as a superposition of such elementary wave forms. Noting that

$$w = e^{i(kx - \omega t)} = e^{I(\omega)t} e^{i[kx - R(\omega)t]} \quad (42)$$

where  $R(\omega)$  and  $I(\omega)$  represent the real and imaginary parts, respectively, we have that  $e^{I(\omega)t}$  is the amplitude of the wave and  $R(\omega)t$  is the phase shift. If the wave form is written as  $\zeta^t e^{ikx}$ , where  $\zeta = e^{-i\omega}$  then with  $t = n\Delta t$  we have  $\zeta^t = \zeta^{n\Delta t} = (\zeta^{\Delta t})^n = G^n$  with  $G \equiv \zeta^{\Delta t}$ . The wave form then is  $w = G^n e^{ikx}$ . Now note that  $G = \zeta^{\Delta t} = e^{-i\omega\Delta t} = e^{I(\omega)\Delta t} e^{-iR(\omega)\Delta t}$ . Thus

$$R(G) + iI(G) = e^{I(\omega)\Delta t} [\cos R(\omega)\Delta t - i \sin R(\omega)\Delta t]$$

so that

$$R(G) = e^{I(\omega)\Delta t} \cos R(\omega)\Delta t \quad (43.a)$$

$$I(G) = -e^{I(\omega)\Delta t} \sin R(\omega)\Delta t \quad (43.b)$$

Then

$$\frac{I(G)}{R(G)} = -\tan R(\omega)\Delta t$$

so that

$$R(\omega)\Delta t = -\tan^{-1} \left[ \frac{I(G)}{R(G)} \right] \quad (44)$$

which is the phaseshift that occurs at a fixed location during time  $\Delta t$ .

Now the phase shift that occurs during  $\Delta t$  due to the convection of the wave is

$$k(u\Delta t) = k\sigma\Delta x, \text{ where } \sigma \leq \frac{u\Delta t}{\Delta x}, \text{ the Courant number.}$$

Therefore the dispersion of the wave during time  $\Delta t$  is the difference between these two phase shifts:

$$\epsilon = k\sigma\Delta x + \tan^{-1} \left[ \frac{I(G)}{R(G)} \right] \quad (45)$$

The dissipation is given by

$$\tau = 1 - |G| \quad (46)$$

Stability requires that  $|G| \leq 1$ .

Again it is convenient to have available the results of substitution

of the basic wave form into the expansion of the difference operators given in Eq. (29). Thus, with  $\beta \equiv k\Delta x$ ,

$$\delta w = i\left(\beta - \frac{\beta^3}{24}\right)w + O(\beta^5) \quad (47.a)$$

$$\mu w = \left(1 - \frac{\beta^2}{8}\right)w + O(\beta^4) \quad (47.b)$$

$$\mu\delta w = i\left(\beta - \frac{\beta^3}{6}\right)w + O(\beta^4) \quad (47.c)$$

$$\Delta w = \left(i\beta - \frac{1}{2}\beta^2\right)w + O(\beta^3) \quad (47.d)$$

$$\nabla w = \left(i\beta + \frac{1}{2}\beta^2\right)w + O(\beta^3) \quad (47.e)$$

$$\delta^2 w = -\left(\beta^2 - \frac{\beta^4}{12}\right)w + O(\beta^6) \quad (47.f)$$

Alternatively, the full expression can be derived by substitution of the wave form directly into the difference expressions. Thus, for example,

$$\begin{aligned} \delta w &= w_{i+\frac{1}{2}} - w_{i-\frac{1}{2}} = G^n \left[ e^{ik\left(x + \frac{\Delta x}{2}\right)} - e^{ik\left(x - \frac{\Delta x}{2}\right)} \right] \\ &= \left( e^{i\frac{\beta}{2}} - e^{-i\frac{\beta}{2}} \right) w \\ &= 2i \sin\left(\frac{\beta}{2}\right) w \end{aligned} \quad (48.a)$$

Similarly,

$$\mu w = \cos\left(\frac{\beta}{2}\right) w \quad (48.b)$$

$$\mu\delta w = i \sin \beta \cdot w \quad (48.c)$$

$$\Delta w = \left( e^{i\beta} - 1 \right) w \quad (48.d)$$

$$\nabla w = \left( 1 - e^{-i\beta} \right) w \quad (48.e)$$

$$\delta^2 w = 2(\cos \beta - 1)w \quad (48.f)$$

The expressions in Eq. (47) are simply the truncated expansions of those in Eq. (48). Considering again the scheme given by Eq. (30) with uniform velocity as an example, we have

$$G^{n+1} e^{ikx} = [1 - i\sigma(\beta - \frac{\beta^3}{6}) - \frac{\sigma^2}{2} \beta^2] w + O(\beta^4) \quad (49)$$

Thus

$$G = 1 - i\sigma(\beta - \frac{\beta^3}{6}) - \frac{\sigma^2}{2} \beta^2 + O(\beta^4) \quad (50)$$

The phase error then is

$$\begin{aligned} G &= \sigma\beta + \tan^{-1} \left[ \frac{-\sigma(\beta - \frac{\beta^3}{6})}{1 - \frac{\sigma^2}{2} \beta^2} \right] \\ &= \frac{\sigma\beta^3}{6} (1 - \sigma^2) + O(\beta^4) \end{aligned} \quad (51)$$

and the dissipation is  $O(\beta^4)$ .

It is the phase error that causes oscillations in the solution of the difference equation in the vicinity of sharp gradients. The dissipation causes the solution to be smoothed out.

### III. LOW-ORDER METHODS

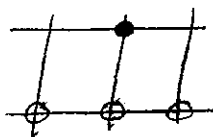
#### First-Order Upwind Methods

##### Purely Upwind Methods

The use of first-order upwind difference expressions for the convective terms, which with flow to the right has the stencil



yields a very stable scheme because large numerical dissipation is introduced. However, this dissipation is excessive and will obliterate solution gradients in long-range solutions. Second-order central difference expressions with the stencil



have much less dissipation but are unstable without some physical diffusion unless some numerical dissipation is added to the equation. With physical diffusion present, central differences lead to spatial oscillations, often called "wiggles," near sharp gradients when the cell Reynolds number exceeds 2. Hybrid methods have been constructed which represent the convective terms as a weighted average of upwind and central differences, switching more toward the former as the cell Reynolds number increases. It should be recognized, however, that the large dissipation introduced by first-order upwind differences makes the solution in essence a low Reynolds number solution.

First-order upwind differences were used by Narayanan and Shankar

(Ref. 151) to model flow in a shallow estuary. The results show considerable dissipation as expected. In Ref. 59, de Vahl Davis and Mallinson found that the first-order upwind scheme severely misrepresented the solution for a cavity flow problem.

#### Hybrid Methods

The hybrid method used by Spalding (Ref. 192) for convective-diffusion equations employs first-order upwind differencing when the cell Reynolds number is greater than 2, and second-order central differencing otherwise. Raithby and Torrance, Ref. 168, also used the hybrid approach in the form of a weighted average of second-order central and first-order upwind differences. In one version the weights were determined by the local cell Reynolds number, upwind differences being used for Reynolds number greater than 2, with a continuous transition to central differences as the Reynolds number approaches zero. In another version the weights were determined to satisfy a local exact solution, in a manner similar to that used by Chien (Ref. 43).

Runchal (Ref. 182) found the averaged central-upwind scheme useful for a fluid in solid-body rotation. However, Leschziner and Rodi (Ref. 131) found the use of weighted average of second-order central differences and first-order upwind differences to be highly deficient because of the strong dissipation. Heydweiller (Ref. 100) used a weighted average of second-order central differences and first-order upwind in a method-of-lines form. Comparisons are given for convection of a triangular wave on the following page:

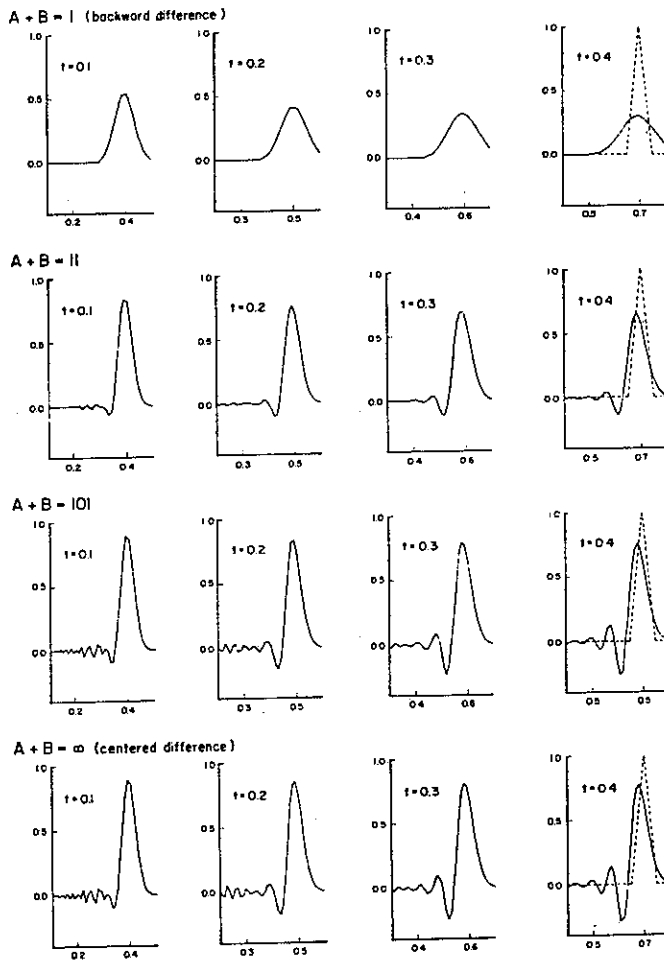


Fig. 1. Effect of  $A + B$  on solution of Eq. (19) (---exact solution). (Ref. 100)

No combination is satisfactory because of the low order of the scheme.

A variant of the first-order upwind scheme in a hybrid context is given by Blottner in Ref. 27 for a steady-state problem. Here the difference equation is applied at mid-points, so that the two-point convective difference expression between grid points can be interpreted as a central difference at the mid-point, and hence as second-order accurate. The three-point diffusion difference representation on grid

points then must be interpreted as first order, since it is unsymmetric in regard to this mid-point. Actually this scheme was only used outside a boundary layer, where diffusion was small, with the conventional second-order central differencing used inside. With spatial averaging of the time derivative, this procedure would be related to the Keller box scheme for time-dependent equations.

Khosla and Rubin, Ref.113, represent the convective derivative as the sum of the first-order upwind difference evaluated at the advanced time level and the second-order central difference for the second derivative at the previous level. This is inconsistent in time-dependent problems, but reduces to second-order central differencing for the convective terms in the steady state. The difference equations have diagonal dominance at all Reynolds numbers.

#### Riemann Solver Methods

Another form of low-order upwind scheme is based on random sampling of the results of Riemann solvers, i.e., characteristic solutions which track discontinuities. Random choice methods based on Riemann solvers have been used by Glimm (Ref. 81), Concus and Proskurowski (Ref. 53), Chorin (Ref. 46 and 47), Colella (Ref. 51), Flores and Holt (Ref. 70) DiPerna (Ref. 61), and others. Some of these applications have been to petroleum reservoir problems, while others have treated shocks.

The scheme of Osher and Solomon, also based on Riemann solvers, (Ref. 157) is designed to handle discontinuities such as shocks and reduces to conventional first-order upwind differencing with smooth solutions. This approach has also been used by Roe (Ref. 175), and Chakravarthy and Osher (Ref.38), and related earlier work is given in Majda and Osher (Ref. 140).

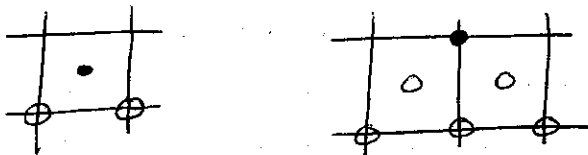
### Second-Order Methods

Srinivas, Gururaja and Prasad (Ref. 194) note that first-order schemes yield smooth profiles of discontinuities and resist nonlinear instability, but are too dissipative. Second-order schemes give sharper profiles, but exhibit oscillations near the discontinuities. Higher-order schemes do not attain their order near discontinuities.

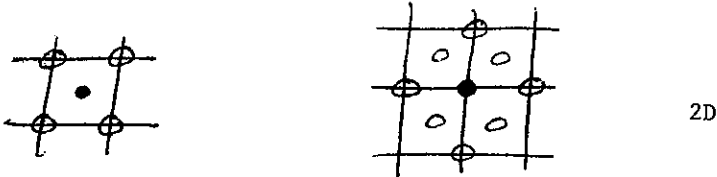
#### Symmetric Methods

The classic second-order method is the Lax-Wendroff scheme mentioned on p. 7, which can be obtained by expanding the solution in a Taylor series about the previous time level and replacing all time derivatives with space derivatives obtained by repeated differentiation of the differential equation. (As noted on p. 9 such schemes can also be obtained via the characteristics approach). Higher-order schemes of this type follow analogously. Abarbanel and Goldberg (Ref. 1) generalized the Lax-Wendroff scheme to include a source term.

The Lax-Wendroff method is often implemented as a two-stage scheme involving mid-points between grid points and a half-integer intermediate time level as given by Richtmyer (Ref. 171). Some such schemes are mentioned later in the following section on Comparisons. McGuire and Morris (Ref. 145) generalize this two-stage rendering of the Lax-Wendroff method to include a free parameter. The stencil is

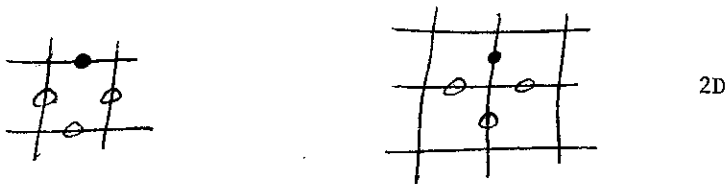


The original Richtmyer scheme (Ref. 171) and the method of Rubin and Burstein (Ref. 177) are contained in this formulation. The Burstein two-stage, second-order scheme (Ref. 36) in 2D uses the stencils



This scheme is of the same order as the Lax-Wendroff scheme, but has more dissipation.

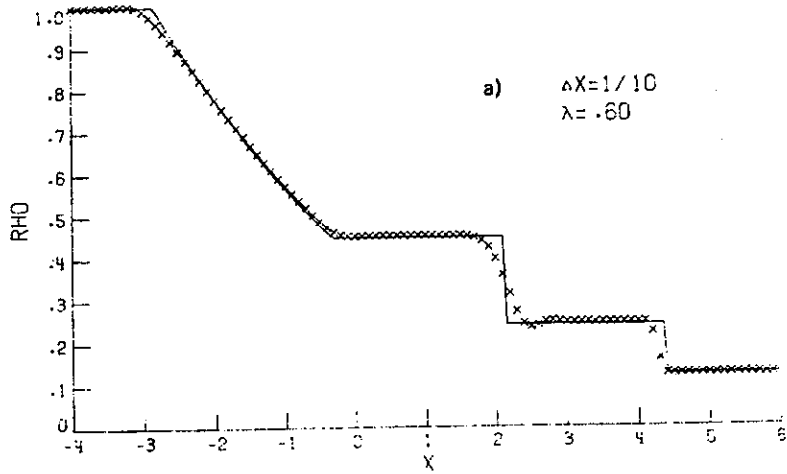
Philips and Rose (Ref. 163) give a two-stage scheme which is second order in time and space. This scheme is a leapfrog second stage written between half-integer time steps, which is set up by an averaging first stage. The stencils are



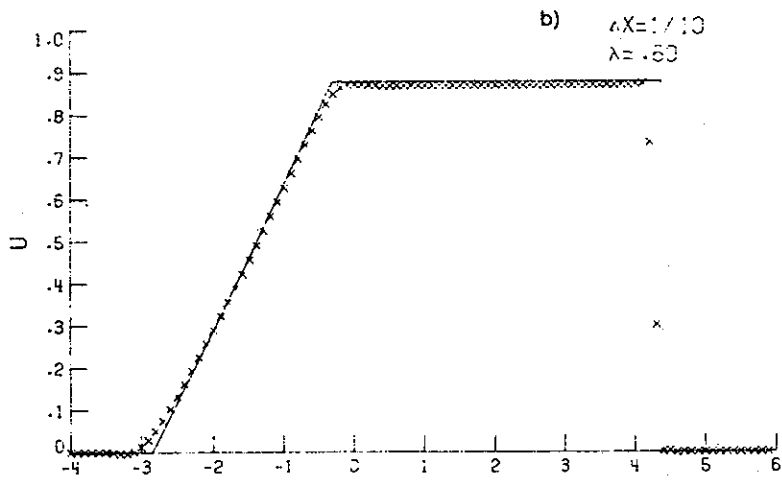
The 2D version is a three-stage method, in which the first two stages use the first stencil above separately in each of the two directions. The final stage then uses the second stencil in 2D form. Results for the shock tube problem are shown on the following page.

The second-order, two-stage MacCormack method (Ref. 135) has been widely used in compressible fluid dynamics. This scheme involves differences in opposite directions in the two stages with the typical stencils

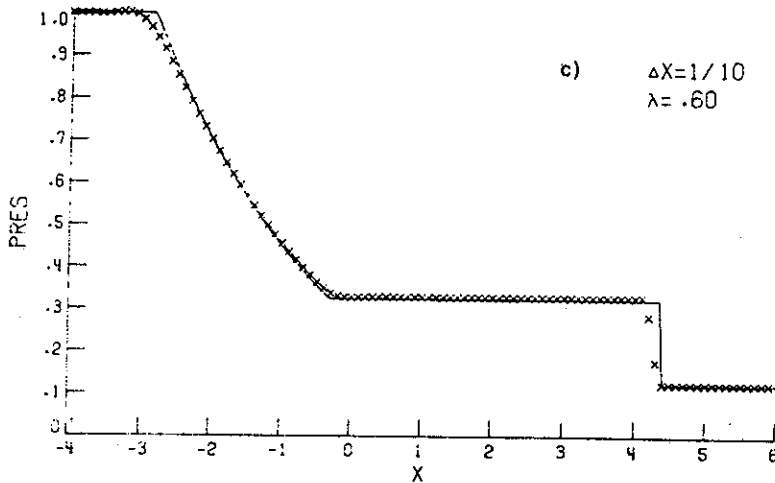




(Ref. 163)



(Ref. 163)



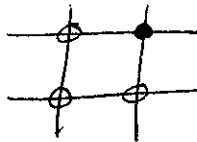
(Ref. 163)

Fig. 2. A comparison of the numerical and exact solution of a Riemann problem; the shock speed exhibits a relative error of 3% (Scheme 1.2).

Diffusion terms, if present, are represented by the same central difference expressions in each stage. Although each stage is first order, the result is second order, and, in fact, can be viewed as a two-stage implementation of the Lax-Wendroff method. The method is stable for Courant numbers less than unity.

In Ref. 136 MacCormack introduces a new version of the time-split MacCormack method which is still second order in time but also unconditionally stable. The new version is constructed by adding another stage to each

of the two stages of the original method. This additional stage is a Crank-Nicholson form with first-order, one-sided spatial differences, the stencil of which is



The overall method is still second order and remains explicit since the additional stages are applied with the differences opposite to the sweep direction. It was found necessary to add some artificial viscosity with strong transients.

McGuire and Morris (Ref. 144) give an implicit second-order Crank-Nicholson type two-stage method in 1D which is constructed by adding fourth-order dissipation to the Crank-Nicholson method. The stencils are



Boundary conditions are done explicitly in this implicit method.

The Arakawa second-order scheme (Ref. 15) in 2D uses the nine-point spatial stencil with leapfrog time differencing. Lilly (Ref. 133) has shown that the leapfrog scheme is subject to weak instability, where solutions at odd and even time steps become uncoupled. However, the use of Adams-Bashforth time differencing

$$\phi^{n+1} = \phi^n + \frac{\Delta t}{2} (3 \phi_t^n - \phi_t^{n-1}) \quad (1)$$

which is also three-level, removes the instability. However, Orszag

(Ref. 154) notes that the Adams-Bashforth form requires a time step that is half that of the leapfrog form for the same accuracy. The better approach then seems to be to use the leapfrog, and control the instability by averaging the solution at successive time steps at regular intervals. The stability of the Arakawa scheme is usually much greater than that of the conventional central difference form. The latter is a bit more accurate, however.

Chan (Ref. 40) constructs a second-order explicit method by a Taylor series expansion about the previous time level with the second time derivative determined from differentiation of the differential equations as usual. However, instead of then expressing the time derivatives in terms of space derivatives, the first time derivatives are considered additional dependent variables. This approach will expand the stencil in effect, since these first time derivatives, which depend on spatial differences of the function, will themselves be differenced in the equation for the new function value.

As noted in Turkel, Abarbanel, and Gottlieb (Ref. 216) second-order explicit methods in 2D that are not compact, i.e., that are not based on Hermite interpolation polynomials, require a minimum of seven points at the previous time level, while most schemes use nine for symmetry. For third-order the required number of points increases to 25. The method of lines, in which the equation is discretized in space and integrated as a system of ordinary differential equations in time, requires even more points, since equations for all points on an entire line (or plane in 3D) are integrated at once. Livine (Ref. 134) also shows that at least seven points must ultimately be involved in a second-order scheme in 2D. The Lax-Wendroff scheme (Ref. 121.) and several

others involve nine points, but the MacCormack scheme (Ref. 135), discussed later in this section, involves seven points. General seven-point schemes are given and are found to be twice as fast as nine-point schemes.

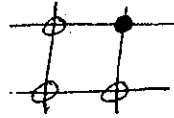
In Ref. 56, Cushman shows that several common finite difference schemes with uniform velocity can be obtained from a Galerkin finite element construction in space and time.

#### Spatial Oscillations

Siemieniuch and Gladwell, Ref. 188, analyzed several common lower-order methods for the convection-diffusion equation to determine conditions for oscillation-free solutions as well as stability. Those conditions place restriction on the cell Reynolds number. Khosla and Rubin (Ref. 115) note that nonlinear instability arises for cell Reynolds greater than 2 for conventional second-order methods, essentially independent of the Courant number. Fisk, in Ref. 69, notes that the spatial oscillations that occur with central difference schemes at larger cell Reynolds numbers in convection-diffusion equations appear even for approximation techniques in which time is continuous. Hirsh and Rudy (Ref. 102) show that the cell Reynolds number limit characteristic of explicit methods using central space differences appears also in tridiagonal implicit methods, making the tridiagonal algorithm fail due to the building of rounding error when diagonal dominance is lost. Griffiths (Ref. 91) determines that at least two points must be within a boundary layer to suppress oscillations with central differences.

In Ref. 120, Lam and Simpson analyze the Keller box scheme (Ref. 108) and conclude that this second-order scheme is superior to the second-order central difference scheme in both dispersion and dissipation, especially as convection dominates. The box scheme is constructed by

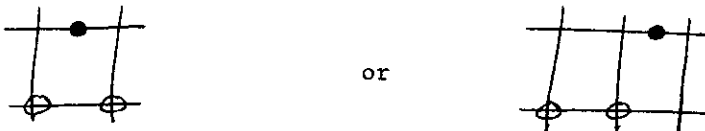
applying the difference equation in 1D at  $x + \frac{1}{2} \Delta x$  and  $t + \frac{1}{2} \Delta t$ . This amounts to a spatial averaging of the time derivative with central space differences, and the stencil is



This scheme has much more gradual breakdown at higher cell Reynolds numbers than does the central scheme because, unlike the latter, the various modes do not all begin to oscillate at once. In fact, the dominant modes are the last to go. The box scheme also retains its second-order accuracy on a nonuniform grid. Diffusion is included by considering the first derivatives to be additional dependent variables, so that a system of first-order equations is solved.

#### Upwind-Biased Methods

Cushman (Ref.57) obtains upwind schemes from a Galerkin finite element construction in space and time. The first-order versions of these schemes have stencils of the form



where the location of the point at the advanced time is a free parameter. Schemes with the location at the advanced time level to the right of the grid points at the previous level require that the Courant number be greater than 1 and less than 2 for stability. The second-order version, analogous to the two-stage Lax-Wendroff method, has one of the above

stencils for the first stage (but to the  $t + \frac{\Delta t}{2}$  level) and one of the following forms for the second.



However, the optimum location of the point at the advanced time was found to be at the mid-point for the first stage, thus reducing the stencil to the conventional Lax-Wendroff form. With nonuniform velocity, the present formulation replaces the velocity with a three-point spatial average.

Warming and Beam (Ref. 219) give a completely upwind version of the MacCormack method using the following stencils for the two stages:



The scheme is second order, as is the original MacCormack method, and is stable for Courant numbers less than 2. As with all upwind-biased schemes, it must be applied in the proper direction. Comparisons of dissipation and phase error for this and the original MacCormack methods are given on the following page. Both the dispersion and the dissipation are greatest for short wavelengths. The symmetric MacCormack method has a lagging phase error, while the upwind version has a leading error. The magnitude of the phase error increases as the Courant number decreases for each method. The dissipation, however, increases as the Courant number decreases for the upwind method, but decreases in the symmetric version. In fact, the dissipation for one method is the same as that of the other for a Courant

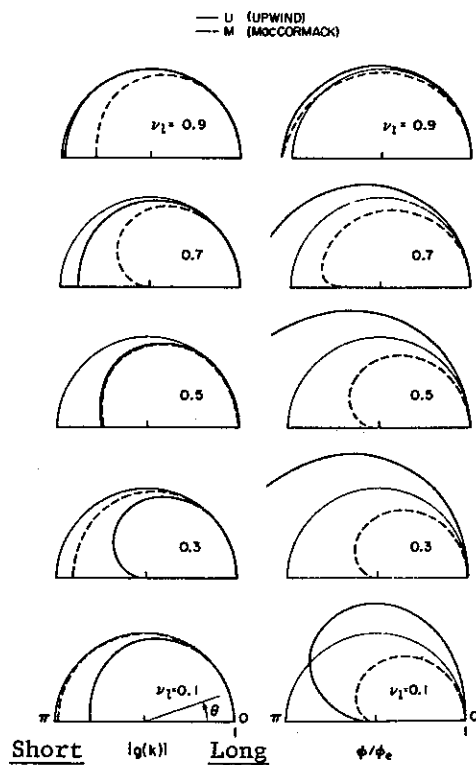


Fig. 3. Comparison of amplification factor modulus  $|g(k)|$  and phase error  $\phi/\phi_e$  for M and U schemes. (Ref. 219)

number symmetrically placed about  $\frac{1}{2}$ . Therefore, the upwind version has the more desirable dissipation properties, since the damping is greatest when the phase error is at its largest values. The dissipation and phase error of the upwind scheme for courant numbers above 1 are shown in the next figure.

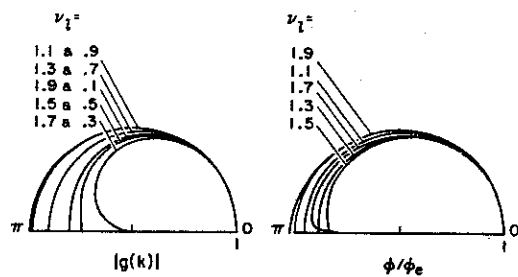
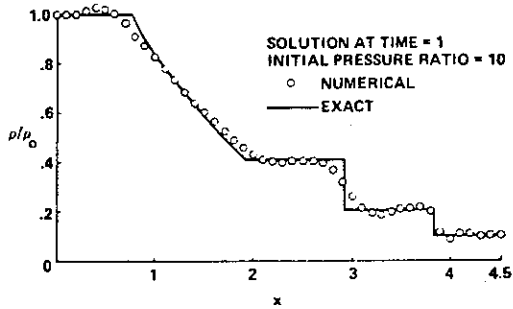


Fig. 4. Amplification factor modulus and phase error for U scheme with  $1 < \nu < 2$ . (Ref. 219)

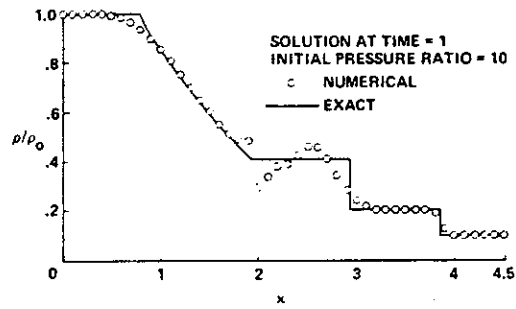
The phase error is lagging in this range, and is surprisingly lower. Since the present scheme and the original MacCormack scheme have opposite phase errors, there is some impetus to apply the two schemes in alternation at successive time steps.

In Ref. 197, Steger and Warming construct schemes for the gasdynamic equations that are based on splitting the flux vectors so that differencing can be done according to the signs of eigenvalues. For scalar equations this reduces simply to upwind differencing. It is noted that the conventional MacCormack method, being symmetric, has a lagging phase error, and that the completely upwind version given by Warming and Beam (Ref. 219), which is also second order, has a phase lead. Therefore the alternation of these two forms reduces the phase error. The effect of this alternation is shown below for the shock tube problem:



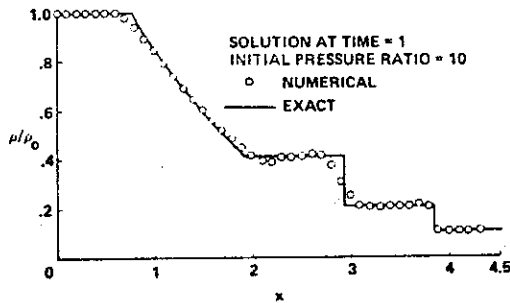
Shock-tube solution obtained using second-order explicit upwind

Fig. 5(Ref. 197)



Shock-tube solution obtained with explicit MacCormack.

Fig. 6(Ref. 197)



Shock-tube solution obtained by alternating explicit upwind and MacCormack schemes.

Fig.7(Ref. 197)

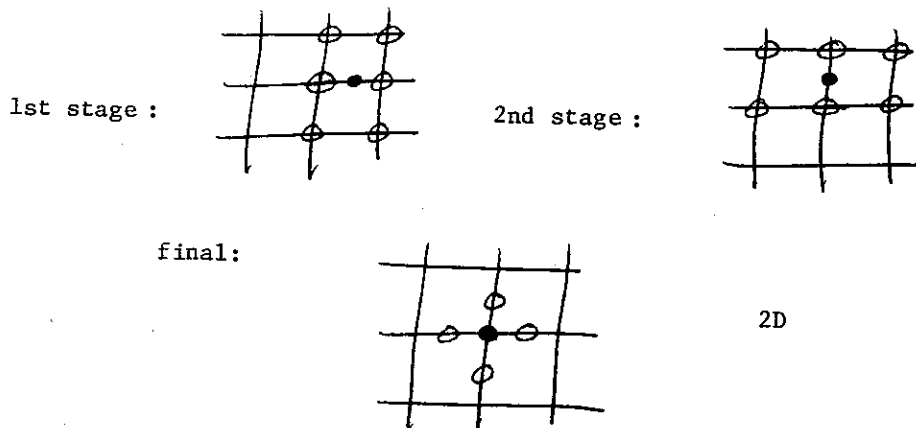
The alternating version is superior to either of its constituents.

Carver (Ref. 37) constructs an upwind-biased method based on the characteristics for a system of equations. This method evaluates different spatial differences in different ways according to eigenvalue signs and is related to the flux-vector splitting methods. For a single equation, conventional upwind methods result. The spatial differences are evaluated by either a four-point Lagrangian upwind formula or a three-point Hermite upwind formula, both of which are third order. Lower-order formulas of either type were found to give excessive phase error. The use of characteristic directions greatly increases the stability. The method is not significantly more difficult to implement than conventional methods. The time integration is by the method of lines, i.e., integrating a system of ordinary differential equations in time, the number of which is the product of the number of dependent variables and the number of field points.

Comparisons

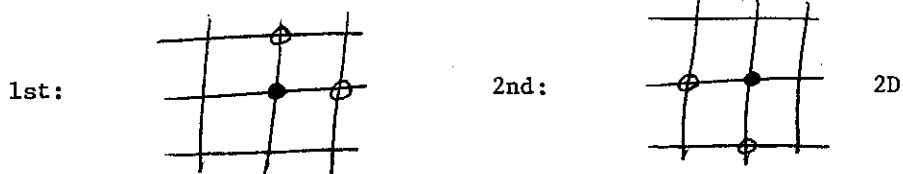
Turkel, in Ref. 214, analyzes a number of second-order schemes for phase error:

(1) The 2D Lax-Wendroff scheme (Ref. 121), a two-stage method with the stencil



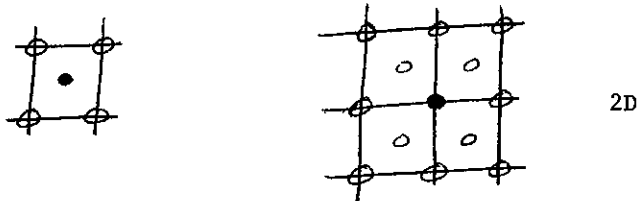
is stable for the individual Courant numbers less than  $\frac{1}{\sqrt{8}}$  and has a phase lag.

(2) The 2D MacCormack method (Ref. 135) is a two-stage method with four variations of the stencil



This method requires fewer operations than the Lax-Wendroff, but is weakly unstable in some cases. This instability may be localized, however, and can be controlled with some small viscosity if necessary, and the method is widely used. The phase lag is larger than that of the Lax-Wendroff method.

(3) The generalized two-stage 2D Burstein method (Ref. 36) has the stencil



and two free parameters. One of these parameters controls the inclusion of fourth-order dissipative terms. Without these terms the method is weakly unstable except for one value of the other parameter for which the scheme is stable for both Courant numbers less than unity. This version is known as the rotated Richtmyer method. As with the MacCormack method, the instability may be localized and controllable. Without the dissipation the phase lag is greater than that of the Lax-Wendroff scheme for all values of the second parameter. However, with the fourth-order dissipation

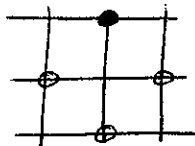
included, the phase error can be brought below that of the Lax-Wendroff method. The phase error decreases as the second parameter increases, but the stability limit on the time step decreases.

(4) The generalized Burstein scheme operated in a split mode (Ref. 145) uses the following 1D stencils



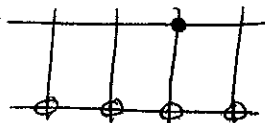
This split scheme seems to have phase error comparable to that of the 2D Lax-Wendroff scheme but allows larger time steps, since the stability is determined by the 1D schemes. The time-split version is stable for both Courant numbers less than unity.

(5) The leapfrog method is a single-stage 2D method using three time levels with the stencil



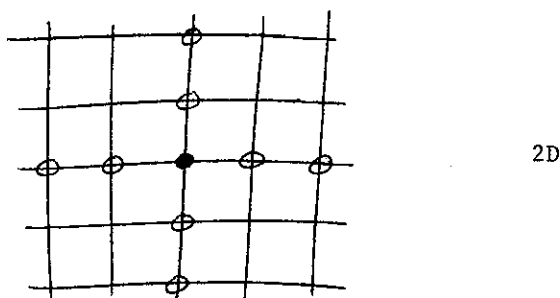
The phase error is the same as that of the Lax-Wendroff, and the stability is better, i.e., the sum of the Courant numbers is less than unity, but not as good as with time-splitting.

(6) The method of Fromm (Ref. 72) is an upwind-biased method with the 1D stencil



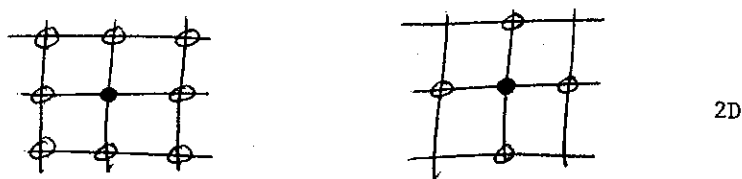
In the time-split mode this method is stable for the Courant numbers less than  $\frac{1}{2}$ . In contrast to the symmetric schemes this upwind-biased scheme has a phase lead, which is slightly smaller than the phase error of the other methods and vanishes for Courant number of  $\frac{1}{2}$ . The allowable time step is smaller, however, and the stencil extends beyond the immediate neighbors.

(7) The Kreiss-Oliger extension of the 2D leapfrog method to fourth order in space (Ref. 117) has the stencil



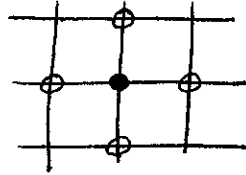
and involves three time levels as before. This scheme has a phase lead which decreases as a cubic in the time step, in contrast to the other methods for which the decrease is linear. This method should therefore be more competitive at smaller time steps. However, experience has shown that the errors accumulate if the step is too small. The optimal seems to be for Courant numbers around  $\frac{1}{4}$ .

(8) The two-stage method of Crowley (Ref. 55) has the stencil



However, there seems to be no advantage over the time-split methods, and this method is more complicated.

(9) The generalization of the two-stage Richtmyer scheme with one free parameter given by Courlay and Morris (Ref. 85) has the stencil



2D

for both stages. As with the Burstein generalization, the phase lag and the allowable time step decrease as the free parameter increases. The phase error is larger than that of the Burstein scheme, though.

Some comparisons of phase error from these schemes are given in the figures below for a Courant number of  $\frac{1}{4}$ . There the phase itself is plotted so that the error is indicated by the distance away from the diagonal line giving the true phase. Plots showing amplitude damping are also shown.

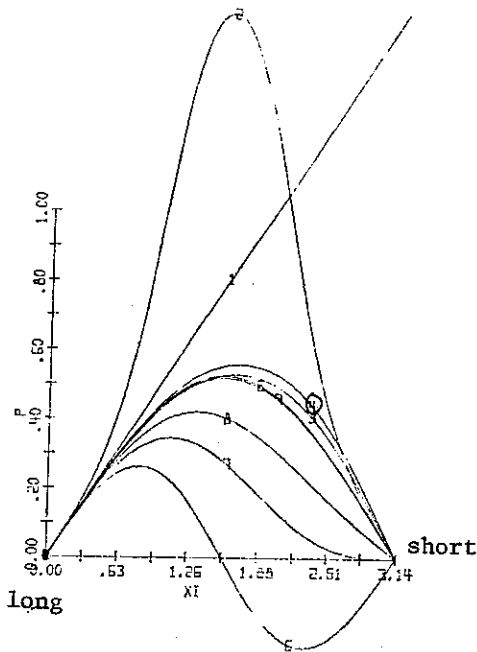


Fig. 8. Complete numerical phase of various nine-point schemes. (Ref. 214)

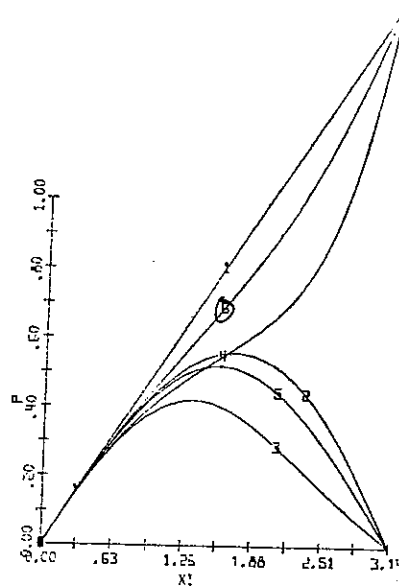


Fig. 9. Generalized Burstein scheme with a viscosity coefficient of 0.0625.

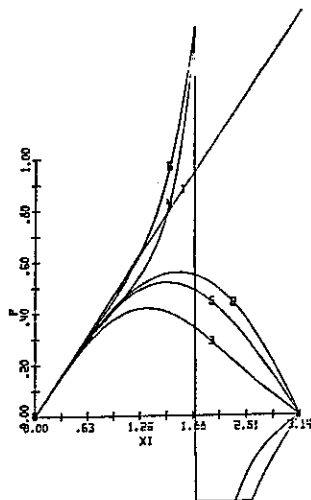
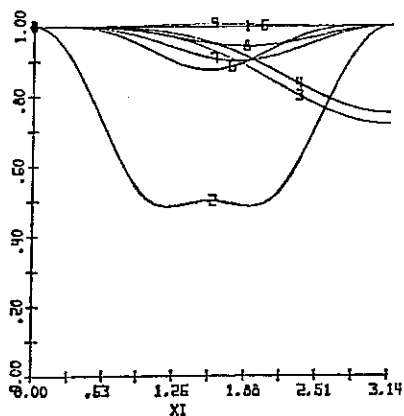


Fig. 10. Similar to Fig. 9 but with a viscosity coefficient of 0.125 for those schemes containing an artificial viscosity. (Ref. 214)



(Ref. 214)

Fig. 11. Norm of the amplification matrix for those schemes appearing in Fig. 8.

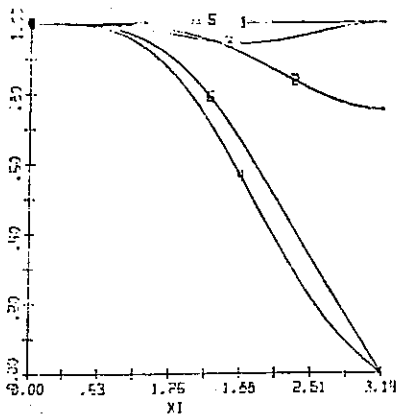


Fig. 12. Norm of the amplification matrix for those schemes appearing in Fig. 9. (Ref. 214)

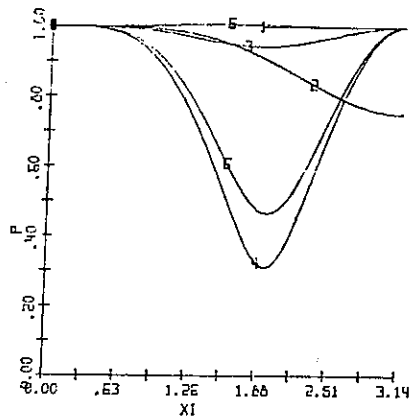


Fig. 13. Norm of the amplification matrix for those schemes appearing in Fig. 10. (Ref. 214)

All of the methods approximate the phase of the longest waves well. However, there are striking differences with short waves. Without artificial viscosity none of these schemes is superior in phase error to the Lax-Wendroff scheme, and some are very bad. The time-splitting, however, works well. The Burstein scheme clearly improves its phase quality with increasing values of the free parameter, but only approaches the quality of the Lax-Wendroff scheme. With some artificial viscosity added through the second free parameter, the Burstein scheme improves in phase quality dramatically and is superior to the Lax-Wendroff for short waves since the short waves are strongly damped. However, there is significant damping over a very large range of wavelengths as well.

As noted above, the short waves are not represented accurately anyway, so it may be best to damp out these components with some type of artificial viscosity or filter. The Lax-Wendroff and time-split methods do damp these short waves as desired, as is shown in the amplitude plots above. The Burstein scheme, however, has its maximum damping at intermediate wavelengths. The leapfrog method has no damping, and the

Burstein scheme approaches this scheme in phase and amplitude as the free parameter increases. Too large a value of the damping parameter in the Burstein scheme, however, degrades even the phase, as is evident in the last figure above. Here the damping is strongest at intermediate wavelengths.

The conclusions of this study are summarized as follows. Of the methods considered (second-order), the leapfrog, having no artificial dissipation, seems to be best for smooth problems. For more general problems time-splitting is more appropriate in regard to both stability and phase error. The Lax-Wendroff is the best of the schemes considered in regard to phase error, but this method requires a smaller time step than the time-split schemes. The Burstein methods without artificial viscosity and the generalization of the Richtmyer scheme have entirely too much phase error. In general the time-splitting approach is the most reasonable, followed by the leapfrog or the Lax-Wendroff scheme. However, all of these second-order schemes leave a lot to be desired in phase quality.

Runchal (Ref. 181) compares several common lower-order schemes in terms of dispersion and dissipation. The schemes compared are listed on the following page and the dispersion is shown in the next figure. The diagrams (a) and (b) represent pure convection, while the other two show the effect of including diffusion. The explicit upwind scheme has no dispersion at the Courant numbers shown, but such is not the case for other values. Of the upwind schemes, which are first order in space, the implicit has the greatest dispersion for pure convection.

The inclusion of diffusion in an explicit manner causes a significant increase in dispersion. Diffusion included in a Crank-Nicholson form

Table 1. Schematic representation of the FDFs. ---Transient link; —Conductive link; —Convective link (Ref. 181)

Conductive term	Explicit	Implicit	Crank-Nicolson(CN)
 Convective Term	 Explicit	 Implicit	 Crank-Nicolson(CN)
 Explicit central	I Fully explicit central		II Mixed CN central
 Implicit central		III Fully implicit central	
 CN central			IV Fully CN central
 Explicit upwind	V Fully explicit upwind		VI Mixed CN upwind
 Implicit upwind		VII Fully implicit upwind	
 CN upwind			VIII Fully CN upwind

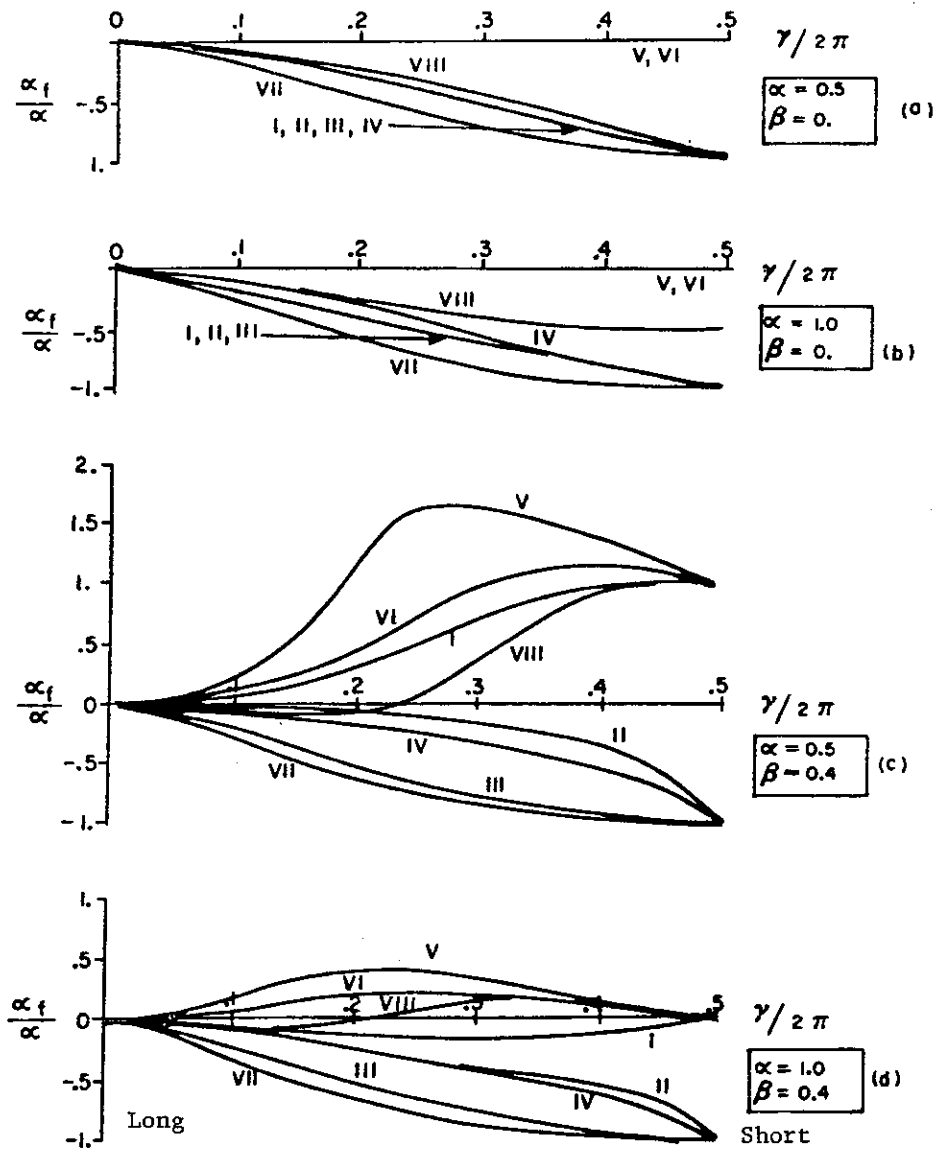


Fig. 14. "False" dispersion for the investigated finite-difference formulations (FDFs). (Ref. 181)

also causes a large increase with the upwind convective form, but not with the central. With the implicit forms, the inclusion of diffusion had less effect. The effect of diffusion on dispersion is more pronounced at the lower Courant number for all of these schemes.

The dissipation of these schemes is compared on the following page. The central schemes have no dissipation at the short wavelengths

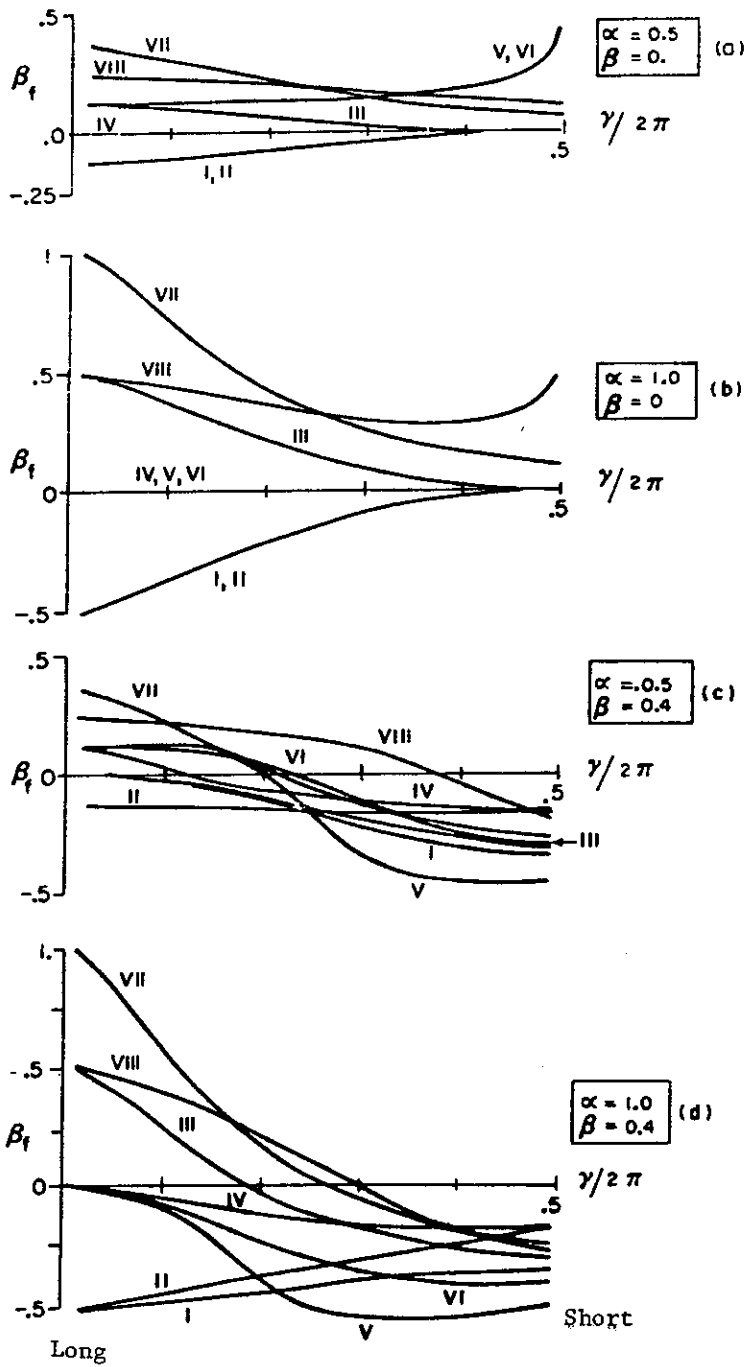


Fig. 15. "False" transient diffusion for the investigated FDFs. (Ref. 181)

where it is most needed, and the dissipation of the upwind scheme is excessive and generally has the undesirable feature of being greater at the longer wavelengths. The implicit schemes have more dissipation

than the explicit, as expected.

Several methods are compared by McRae, Goodin, and Seinfeld in Ref. 146. The seven methods considered are (1) the SHASTA algorithm using FCT (Refs. 28, 31, 32), (2) compact differencing methods with Crank-Nicholson time differencing (Refs. 5, 7, 50), (3) Galerkin finite element methods with linear elements (Refs. 150 and 204), (4) the zero-average phase error method of Fromm (Ref. 72), (5) upwind differencing (Ref. 172), (6) the Crowley second-order scheme (Ref. 55), and (7) the Price scheme (Ref. 167). Results for convection of a square wave, a triangular wave and a Gaussian are shown below:

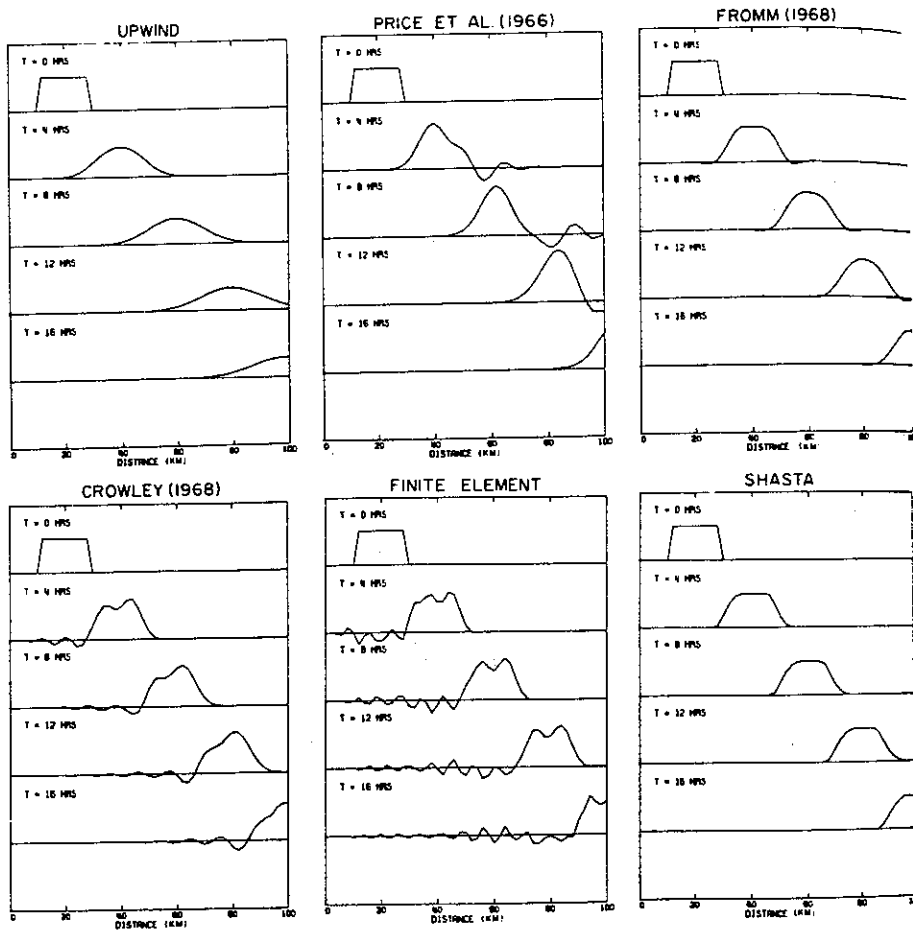


Fig. 16. Results of advection tests using square wave form. (Ref. 146)

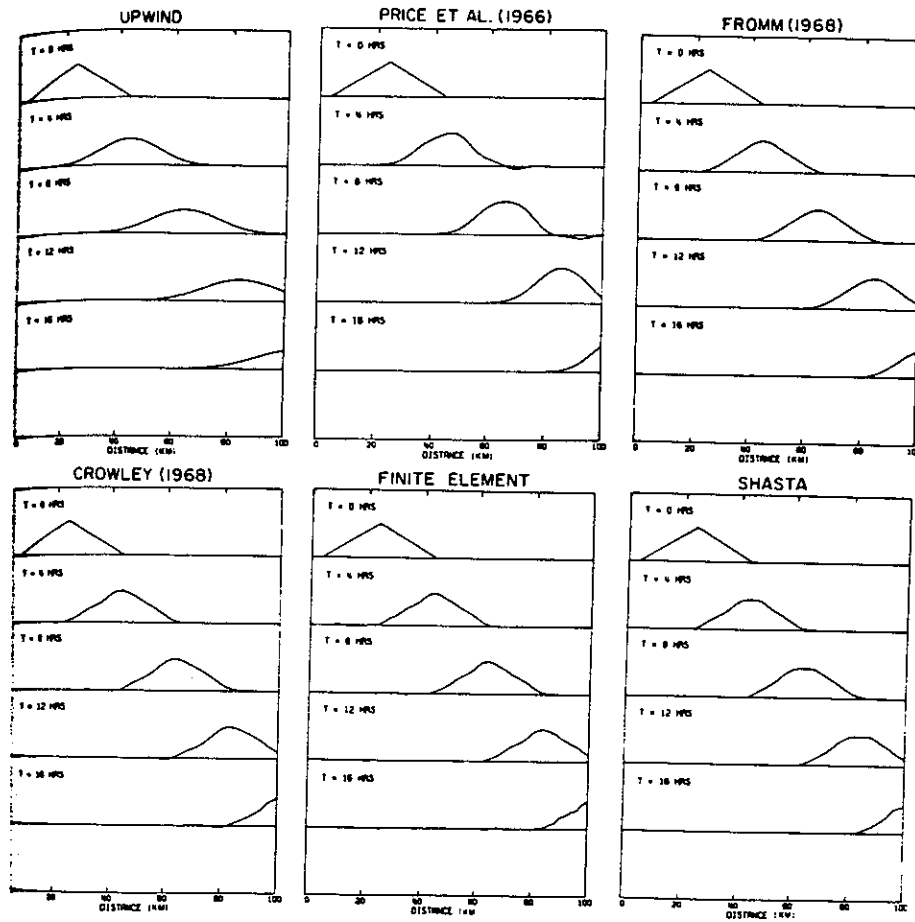


Fig. 17. Results of advection tests using triangular wave form. (Ref. 146)

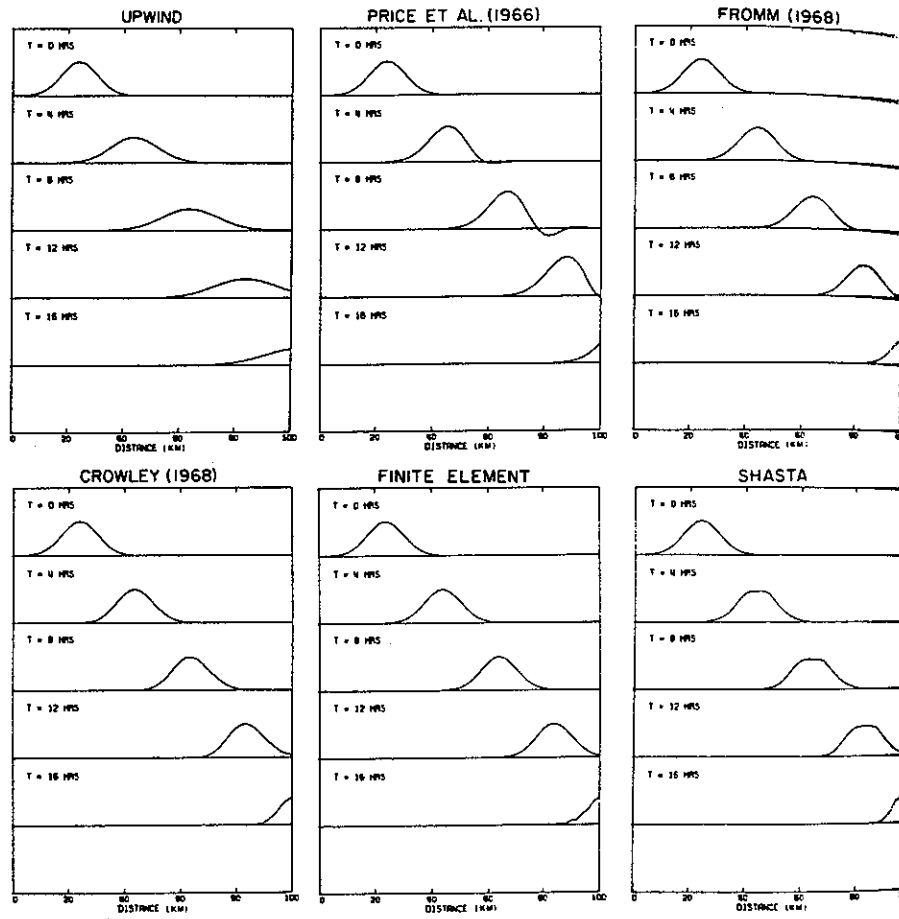


Fig. 18. Results of advection tests using Gaussian wave form. (Ref. 146)

The FCT algorithm does the best job on the square wave, and all the others are quite bad. The FCT flattens the peaks of the triangular and Gaussian waves, however. A comparison of the FCT method and the finite element method is given in the next figure for the revolving cone:

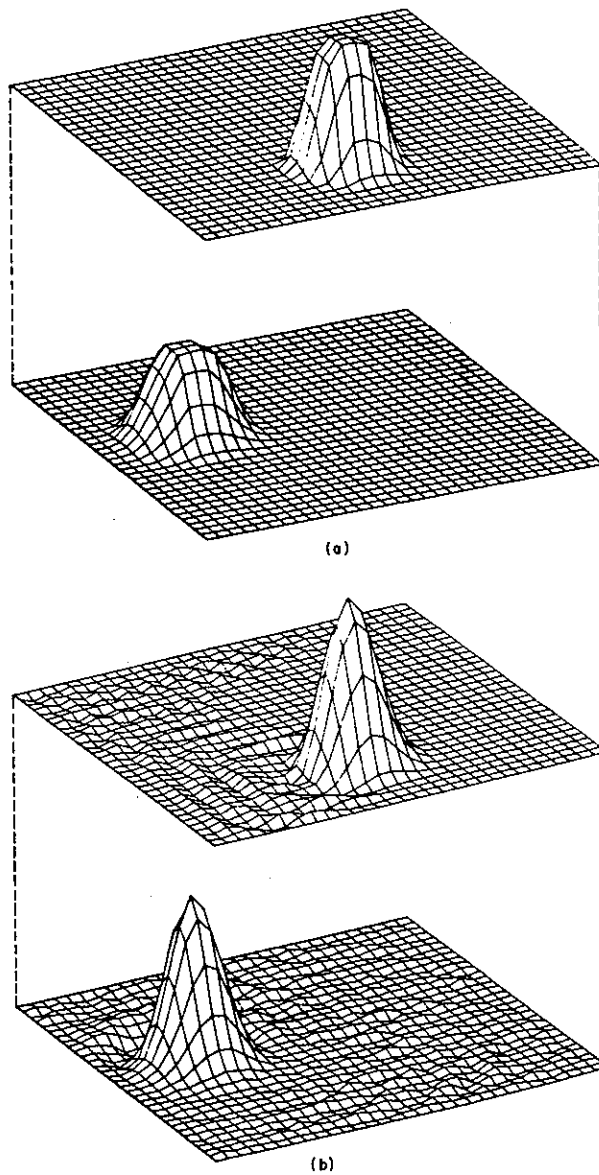


Fig. 19. Results of Crowley test problem for a quarter and complete revolution of a cone using (a) SHASTA method and (b) linear finite element scheme (without filtering step). (Ref. 146)

The strong dissipation of FCT and peak clippings are evident here.

Burstein and Mirin (Ref. 35) compared several methods for the revolving cone problem and found third-order methods to be significantly better than second-order, especially in regard to phase error.

Sasaki and Reddy (Ref. 186) compared several methods of convection of a vortex. The methods compared are the second-order leapfrog method (A), the second-order Arakawa method with leapfrog time differencing (Ref. 87)(B), and with Crank-Nicholson time differencing (E), the Arakawa scheme in two-stage modes, and a Galerkin finite element method using Crank-Nicholson time differencing (G). In one of the two-stage modes considered for the Arakawa scheme, the first stage is a forward-time predictor and the second is a backward-time corrector (Matsuno, Ref. 143). The other two-stage mode used has a forward-time predictor over half the time step, followed by a leapfrog corrector centered at the half-time level.

The second-order Arakawa scheme is designed for use with the stream-function vorticity formulation, and can be obtained from a Galerkin finite element approach using bilinear basis functions on a square element. For uniform velocity this scheme involves a weighted average of the second-order central difference expression at three adjacent points in the direction normal to the derivative. There are thus nine points involved, even though the representation is only second order.

Comparisons of the results of convection of the vorticity field are shown on the following pages. Of these schemes, the Crank-Nicholson form of the Arakawa method proved to be the best. The two-stage schemes had more damping than is desired.

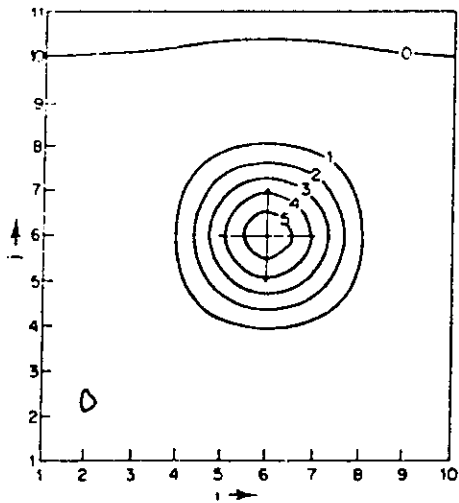


Fig. 20. Vorticity field,  $t = 0, 120, 240 \dots h$ . Analytical solution. (Ref. 186)

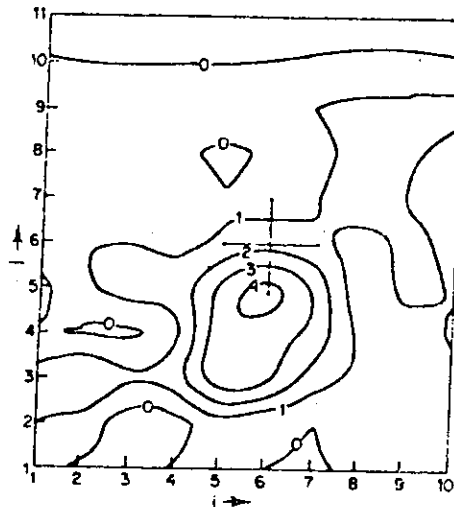


Fig. 21. Vorticity field,  $t = 120h$ ,  $\Delta t = 1h$ . Scheme A. (Ref. 186)

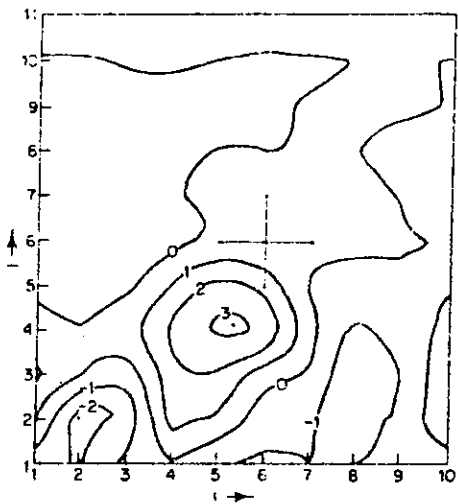


Fig. 22. Vorticity field,  $t = 120h$ ,  $\Delta t = 1h$ . Scheme B. (Ref. 186)

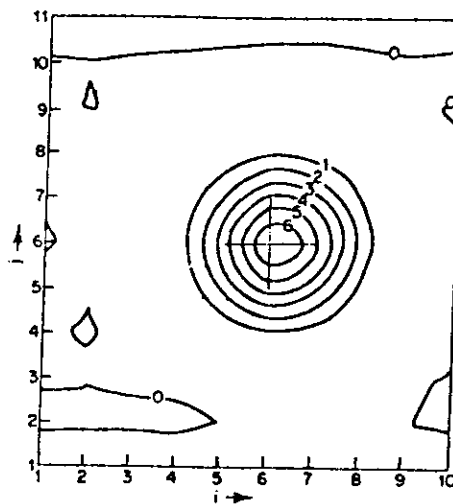


Fig. 23. Vorticity field,  $t = 120h$ ,  $\Delta t = 1h$ . Scheme E. (Ref. 186)

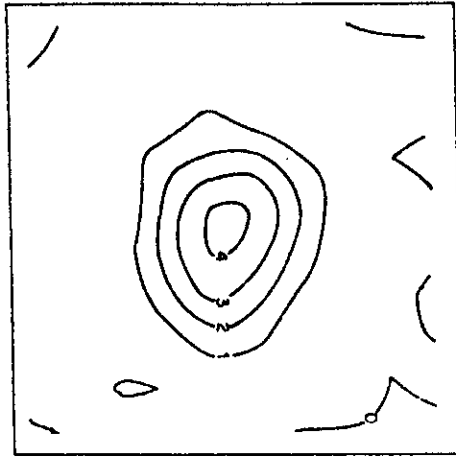


Fig. 24. Vorticity field at  $t = 120$  h. Scheme G. (Ref. 186)

Grammelvedt (Ref. 87) considered several methods for the dynamics of the atmosphere, most of which are delineated by the treatment of the momentum equation. The effects of various types of averaging, hence smoothing, of convective terms with a nonuniform velocity field may also be seen, however. All the schemes use second-order leapfrog time differencing. The fluxes formed by the product of the velocity and the concentration are written in the following forms at the mid-points between grid points: (1) average of product, where the velocity and concentration at the grid points are multiplied and then the product is averaged to produce the flux at the mid-point, (2) product of averaging, where the velocity and concentration are individually averaged and then these averages are multiplied, and (3) a combination in which the product of the averages is averaged in turn in the direction away from that of the derivative, hence using a nine-point stencil. Some staggered grid configurations are also included. The results show that the product of averages is better than the average of the product. The nine-point schemes

are more stable because of the smoothing accomplished by the additional average, but the phase error is increased.

It was also noted that more grid points per wavelength are required for longer-term integrations. Higher-order methods need fewer points, but may have to be averaged periodically between time steps to prevent aliasing errors.

Three multi-stage methods are compared by Anderson (Ref. 13) for shock problems. The schemes are (1) the conventional second-order MacCormack method (Ref. 135), (2) the third-order Rusanov method (Ref. 183), and (3) a third-order method due to Kutler, Lomax and Warming (Ref. 119). The Rusanov method is equivalent to that of Burstein and Mirin (Ref. 35) and is based on Runge-Kutta techniques. The third method is a variation of the Rusanov method, having the same third stage but using the MacCormack method for the first two stages. This method has two free parameters. Adjusting these parameters to minimize dispersion or dissipation improved the results but it did not matter greatly which was minimized. The MacCormack method was found to be superior with the Courant number near 1. However, the third-order methods performed better than the MacCormack method when the Courant number varied widely. Of these two methods, that of Kutler, Lomax and Warming is easier to program.

Srinivas, Gururaja, and Prasad (Ref. 195) compared five schemes for shock problems and found that different schemes modelled different aspects of the problem better. The results of some earlier comparisons are also summarized, the general conclusion of which is that the higher-order methods (Rusanov, Burstein and Mirin here) are best for general problems. In the present comparison the first-order van Leer scheme (Ref. 127) is considered preferable to the first-order Rusanov scheme (Ref. 184). The

second-order MacCormack (Ref. 135) was judged to be better than the Richtmyer scheme (Ref. 171) of the same order.

Taylor, Ndefo, and Masson (Ref. 207) compared four methods for shock problems and concluded that the third-order Rusanov (Ref. 183), also Burstein and Mirin (Ref. 35), is better than the Godunov, Richtmyer, or MacCormack methods. An older comparison of low-order methods for a shock problem is that of Emery (Ref. 67). Here a first-order method of Rusanov (Ref. 183) was preferred. Another older comparison of second-order schemes for shock problems is that of Rubin and Burstein (Ref. 177). A two-stage implementation of the Lax-Wendroff method was found to be best.

#### IV. HIGHER-ORDER METHODS

Baker (Ref. 17.) notes that the dispersive character of the discrete representation is the dominant error mechanism in convection-dominated problems. Williamson and Browning (Ref. 223) found that more efficient error reduction was possible by increasing the spatial order than by decreasing the grid size.

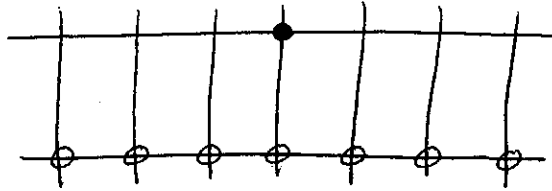
Gustafsson (Ref. 93) shows that representation of boundary conditions can be one order lower than that of the field method.

##### Symmetric Methods

Zwas and Abarbanel (Ref. 229) develop higher-order schemes by expanding the solution in a Taylor series about the previous time level and replacing the time derivatives with space derivatives obtained by repeated differentiation of the differential equation as discussed on p. 7. Third and fourth-order methods are given. It is noted that odd-order schemes are unstable unless modified by the addition of a term containing the next higher space derivative or by rewriting the central term as a spatial average of order equal to that of the method.

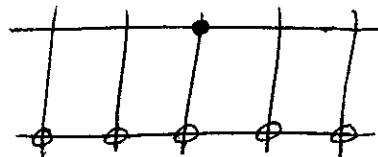
Oliger, in Ref. 153, uses fourth-order symmetric spatial differences with second-order leapfrog in time. Fourth-order was found to be far superior to second-order, and only slightly inferior to sixth-order. It is also noted that it is possible to use approximation of one order lower at boundaries without degrading the order of the solution. This was also noted by Gustafsson (Ref. 93).

Gerrity, McPherson, and Polger (Ref. 80) use a fourth-order representation of the first space derivative that involves six symmetric points about the point in question:



This is two more points than are necessary for a fourth-order expression. Fourth-order difference expressions are also used for the spatial derivatives by Takeo in Ref. 206.

Crowley (Ref. 55) constructs a fourth-order method using the characteristic equation, as discussed on p. 8, and an interpolation polynomial fitted to five symmetrically placed points at the previous time level. The stencil is



The method is fourth-order in space and time for uniform velocity, but only second-order in time for nonuniform velocity.

Conservative methods are also constructed by representing the flux through a cell side as time averaged, as discussed on p. 10. With a linear representation of the solution on the grid interval contacting the point of flux evaluation, this results in a second-order scheme. If the solution is represented by a cubic on the four grid points located symmetrically about the point of flux evaluation, the scheme will be fourth-order in space. With this symmetric placement of points about the point of flux evaluation, there is no upwind bias.

These methods have maximum phase error and dissipation at short

wavelengths. The phase error has a minimum and the dissipation a maximum for Courant number of  $\frac{1}{2}$ . The fourth-order conservation form has larger phase error than the non-conservation form of the same order. Extension at 2D is by time-splitting. The unsplit versions showed distortion not present in the split version.

Results for the revolving cone problem are shown below:

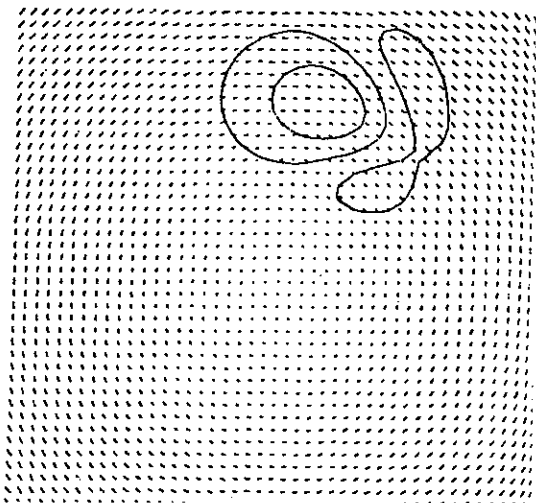


Fig. 25. Second-order solution at cycle 475. (Ref. 55)

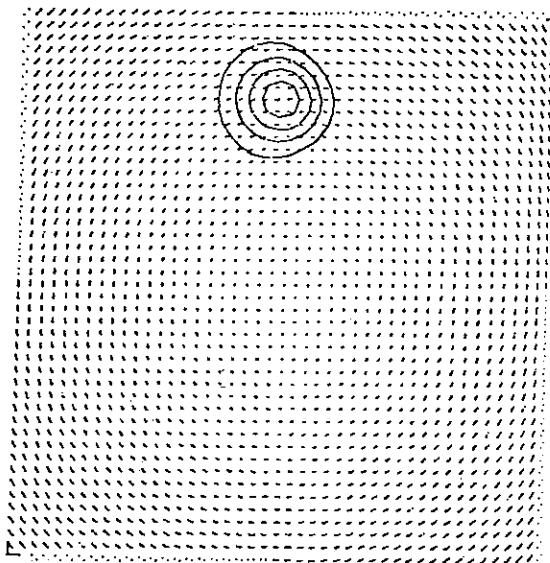


Fig. 26. Fourth-order solution at cycle 475. (Ref. 55)

The improvement with order is evident.

Fromm (Ref. 73) shows that the Crowley fourth-order scheme (Ref. 55) can be written in a two-stage form with the stencils



### Upwind-Biased Methods

Davies in Ref. 58, with uniform velocity and one dimension, takes the approach of expressing the solution at the advanced time level in terms of the value at the previous time at an upstream point determined by the characteristic backward to the previous level, as discussed on p. 8 :

$$\phi(x, t + \Delta t) = \phi(x - u\Delta t, t) \quad (1)$$

The value at the point  $(x - u\Delta t)$  at the previous time level is determined by polynomial interpolation among the grid points at this level. This approach produces methods that are of the same order in space and time (for uniform velocity). Linear interpolation using the points  $(i - 1, i)$  produces the familiar first-order upwind scheme, while quadratic interpolation over the points  $(i - 1, i, i + 1)$  yields the second-order Lax-Wendroff scheme.

Symmetric even-order central schemes are obtained by using polynomials of even degree, with the points placed symmetrically about the grid point  $i$ . Odd-order schemes with upwind bias are obtained with polynomials of odd degree, using points placed symmetrically about a point one-half cell upstream of the grid point  $i$ , assuming positive velocity. The odd-order schemes have zero phase error at Courant numbers of  $0, \frac{1}{2},$  and  $1.$

Particular schemes up to fifth order are given, the stencils for the third and fifth-order versions being respectively, or the form



(This third-order scheme is also discussed by Huffenus and Khaletzky in Ref. 106, where it is mislabeled first order in time.)

The damping and phase error of schemes of this type are illustrated below for two Courant numbers:

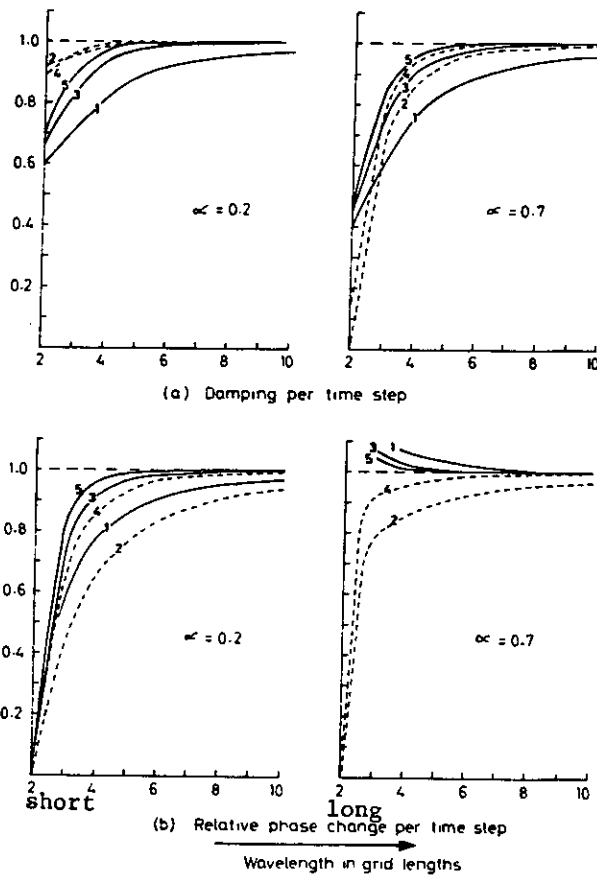


Fig. 27. (a) Damping per time step and (b) relative phase change per time step plotted as a function of the wavelength (in grid lengths) for both  $\alpha = 0.2$  and  $\alpha = 0.7$ . The numerals on the curves refer respectively to the order of the interpolation scheme (e.g., 5 denotes the quintic scheme). (Ref. 58)

As expected, the odd-order schemes have lower phase error, but more damping. Also the phase error of the odd-order schemes reverses sign at Courant number  $\frac{1}{2}$ , leading for the lower numbers and lagging for the higher. For the even-order schemes the phase error is leading over all Courant numbers. Phase error generally decreases with increasing Courant number for the even-order methods, while extrema occur on either side of Courant  $\frac{1}{2}$  for the odd-order schemes. Both phase error and damping decrease with increasing order for all the schemes.

Damping generally increases with the Courant number, and the increase is more marked for the even-order methods, which have very low damping at low Courant number. Both the greatest damping and the largest phase errors occur at the shortest wavelengths.

Comparison of the third and fifth-order schemes with the schemes of Gadd, Ref. 76, and Mahrer and Phiki, Ref 139 are given below:

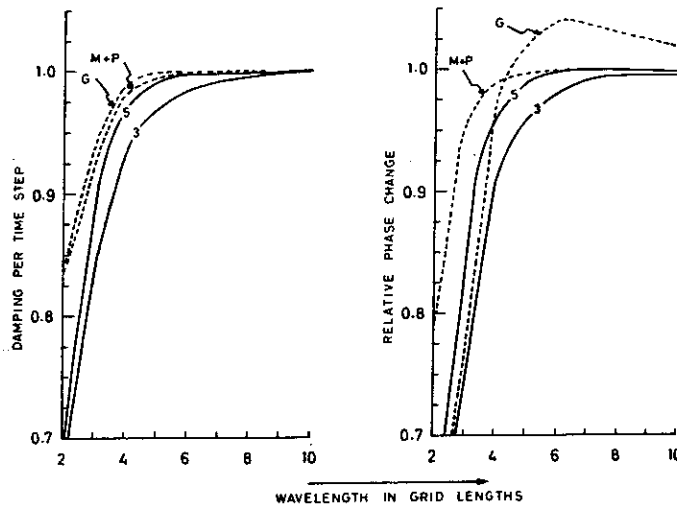
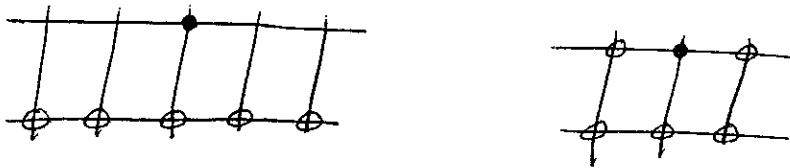


Fig. 28. (a) Damping per time step and (b) relative phase change per time step plotted as a function of the wavelength (in grid lengths) with  $\alpha = 0.2$ , for the cubic and quintic pseudo-upstream schemes and for the schemes of Gadd (G), and Mahrer and Phiki (M + P). (Ref. 58)

Of these schemes, that of Mahrer and Phiki is superior in regard to phase error and damping. The Gadd scheme is not satisfactory in that it has an extremum in the phase error at a wavelength where the damping is very low.

Although these upwind-biased, odd-order schemes of order greater than one are not monotonic in general, they are able to handle spikes of an order of greater than can be handled by the second-order Lax-Wendroff or leapfrog schemes without loss of monotonicity. The maximum spike amplitude for which the scheme remains monotonic decreases with increasing order.

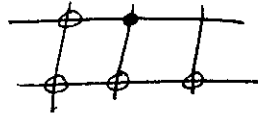
Kholodov, in Ref. 112, develops a measure of the non-monotonicity of schemes. This measure is then used to select the free parameters in second and third-order schemes to obtain the schemes of that order which are most monotonic. The stencils of the general explicit and implicit forms considered are, respectively,



These forms give a two-parameter family of second-order schemes, and a one-parameter family of third-order schemes. Oscillations, i.e., non-monotonicity, can occur when some of the difference coefficients are negative. The most monotonic schemes of a given order are obtained by selecting the free parameter to minimize the least-square difference between the coefficients and those of the monotonic scheme with lowest

numerical dissipation.

Second-order explicit schemes with stability limits requiring the Courant number to be less than 1, and schemes requiring the Courant number to be between 1 and 2, are obtained with the explicit stencil given above, and with the stencil formed by deleting the right-most point from the advanced time level of the implicit stencil:



A third-order scheme with stability for Courant number less than 1 is also obtained.

These schemes can be interpreted as being constructed from the characteristic equation (p. 8) using the interpolation polynomials of the given order that has the smallest deviation from the first-order interpolation polynomial in the least-square sense.

Comparisons for a shock problem are given below for several third-order explicit schemes with the first stencil above:

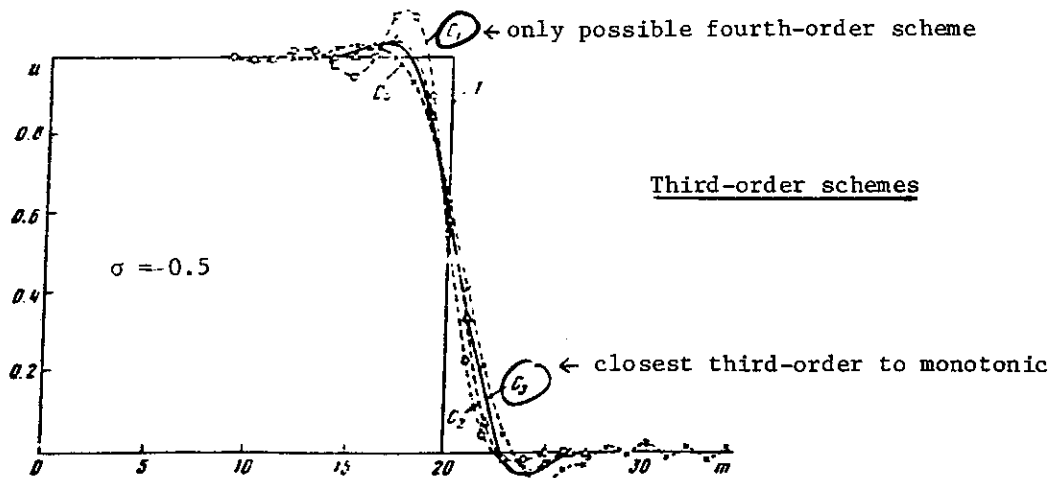


Fig. 29. (Ref. 112)

The scheme designed to have the greatest monotonicity has the least oscillation as expected. The next figure compares second-order methods with this same stencil.

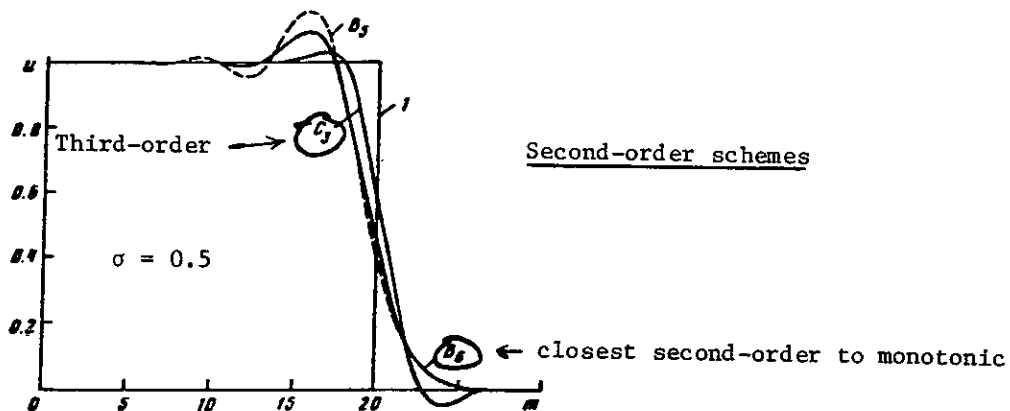


Fig. 30. (Ref. 112)

Second-order explicit schemes with the five-point stencil given above are compared in the next figure:

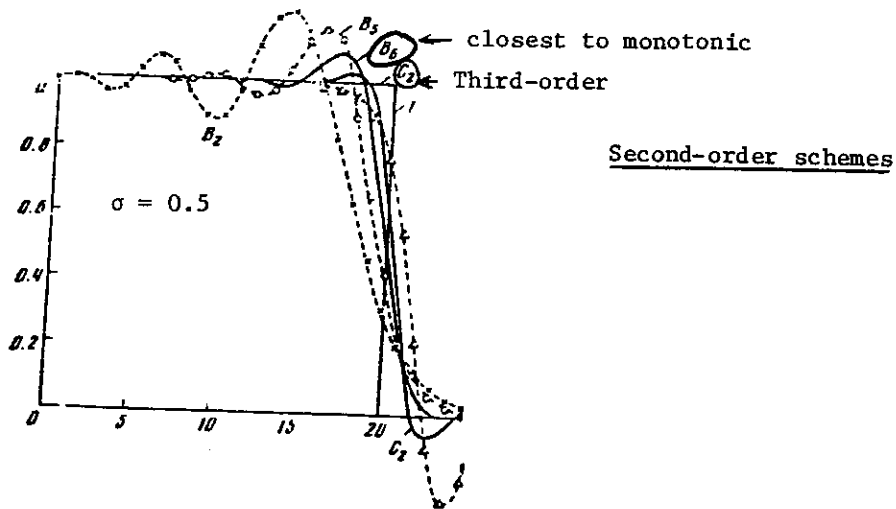


Fig. 31.  
(Ref. 112)

Differences are more noticeable with this stencil. Finally second-order methods with this last stencil with Courant numbers between 1 and 2 are compared below:

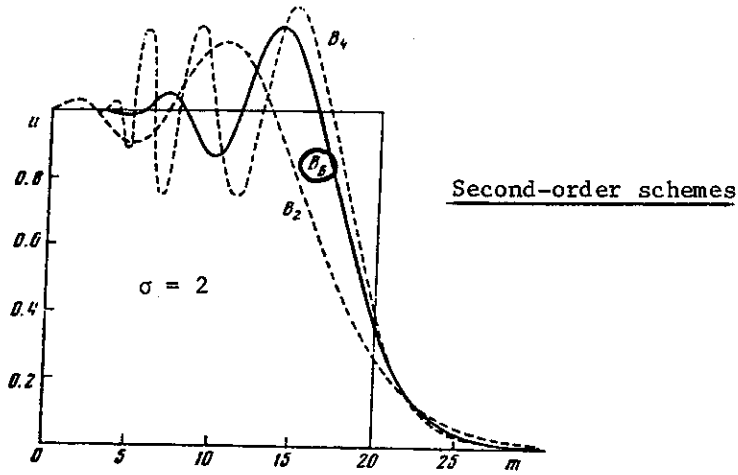


Fig. 32. (Ref. 112)

The schemes designed for Courant numbers less than 1 are better. Extensions to nonlinear cases are also given.

Higher-order, multi-level schemes with an upwind bias are constructed in one dimension by Chan in Ref. 39 using Taylor series expansions of the solution at the previous time step at about a point one-half mesh width upstream of the point of solution evaluation. These schemes are of equal order in space and time. These schemes are based on uniform velocity, however, and the points are placed on the previous time line either at grid points or at the intersection of characteristics from grid points on adjacent time lines, using the relation (cf. p. 8 )

$$\phi(x, t + \Delta t) = \phi(x - u\Delta t, t) \quad (2a)$$

$$\phi(x + u\Delta t, t) = \phi(x, t - \Delta t) \quad (2b)$$

The same results could have been reached by expanding the function at grid points at the adjacent times, differentiating the differential equation to obtain expressions for the time derivatives in terms of space derivatives.

The stencils and the symmetrically placed points are shown below for three fourth-order methods and one sixth-order method.

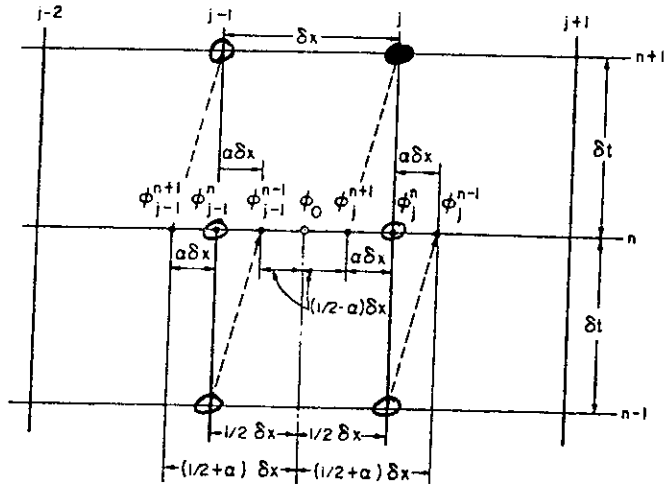


Fig. 33. Definition of the variables used in A1 scheme. (Ref. 39)

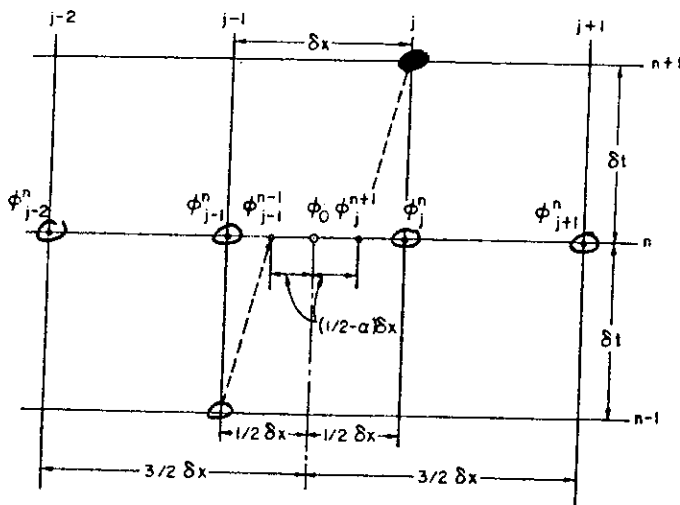


Fig. 34. Definition of the variables used in A2 scheme. (Ref. 39)

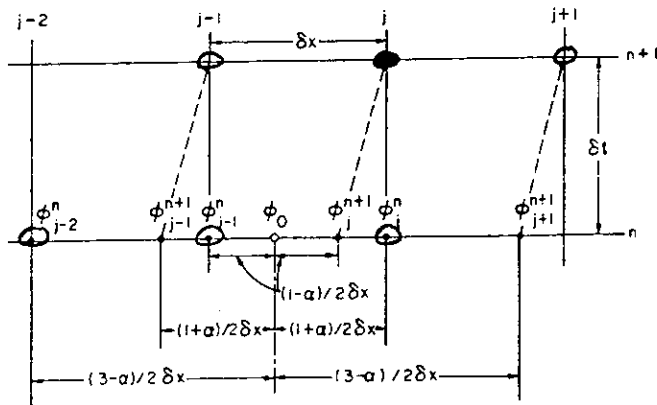
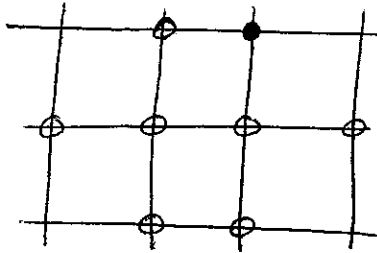


Fig. 35. Definition of the variables used in A3 scheme. (Ref. 39)

The stencil for the sixth-order scheme, A4, is as follows:



The last of the fourth-order methods is implicit, but all the other methods are explicit if the field is swept downstream. All of these methods except the implicit one use three time levels.

This use of symmetrically placed points eliminates all even derivatives in the truncation error, and hence schemes of this type are non-dissipative even though there is an upwind bias. The phase

error for schemes 1 and 2 vanishes for Courant numbers of 0,  $\frac{1}{2}$ , and 1 and is leading for the lower Courant numbers and lagging for the higher.

This behavior is clear in the figure below:

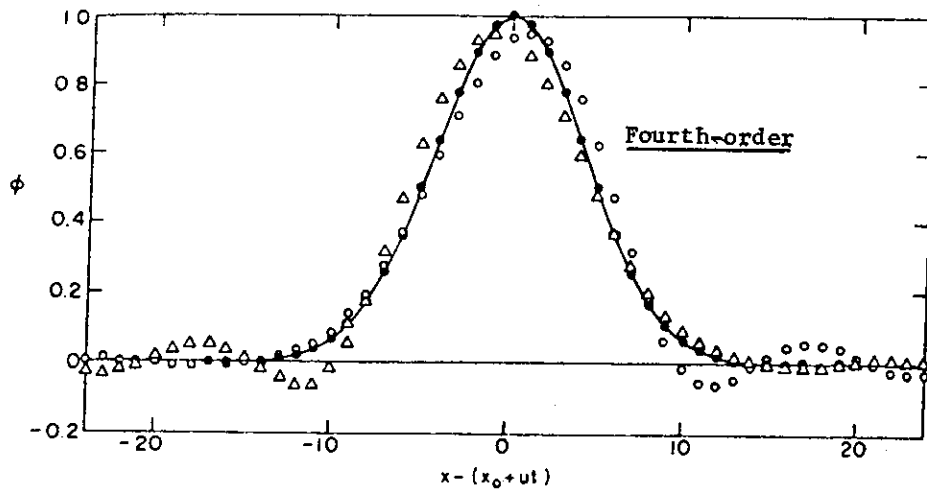


Fig. 36. A2 results at NCYC = 50,000 ( $\circ \alpha = 0.25$ ;  $\bullet \alpha = 0.50$ ;  $\Delta \alpha = 0.75$ ). (Ref. 39)

That the phase error decreases as the order increases is evident in comparison of the figure above with the following figure:

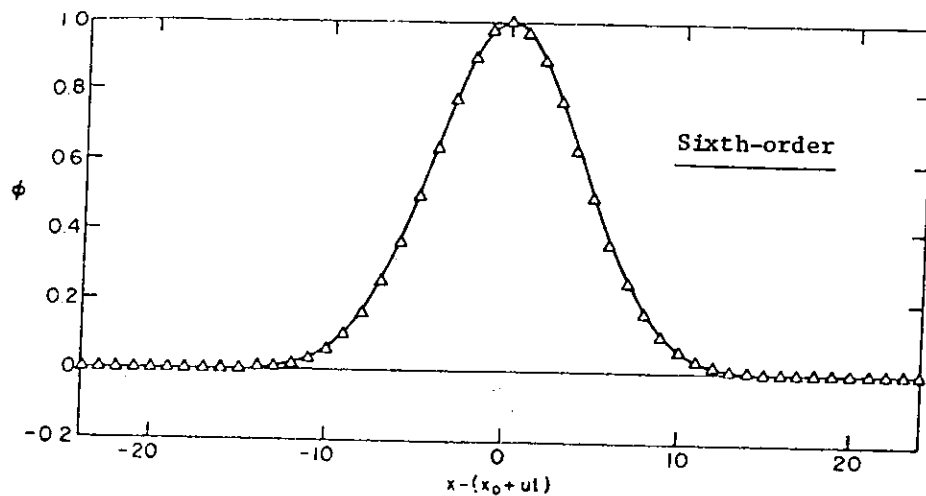


Fig. 37. Results using A2 once as predictor and A4 twice as correctors ( $\alpha = 0.75$  and  $\Delta$  represents NCYC = 50,000 and NCYC = 100,000)- (Ref. 39)

Performance with a triangular wave is shown in the next figure:

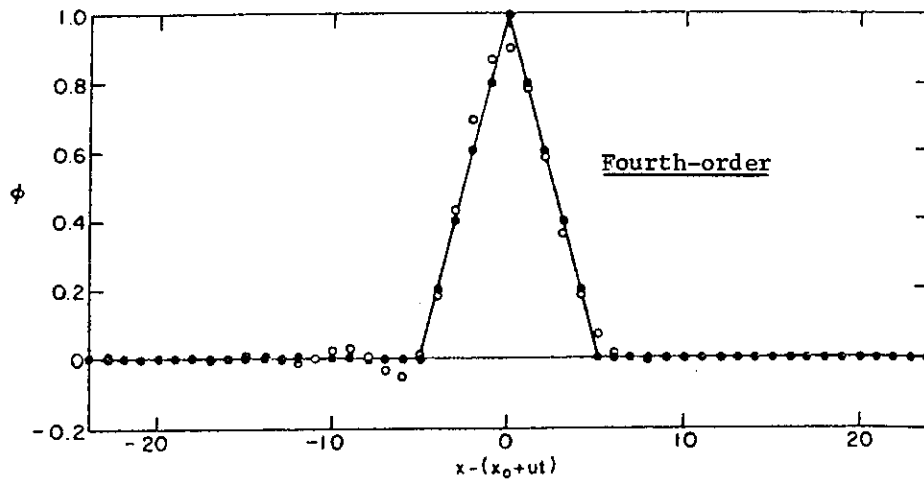


Fig. 38. A2 results for triangular wave at NCYC = 1,400 ( $\bullet$   $\alpha = 0.50$ ;  $\circ$   $\alpha = 0.75$ ). (Ref. 39)

A procedure for including diffusion is also given, using a time-split approach in which the function is essentially convected along the characteristics and then diffused at a fixed time.

If the velocity is nonuniform, the points will no longer be symmetrically placed on the present time line, so that even though analogous schemes using the same grid points could be derived which would preserve the order, these schemes would not be nondissipative, since not all of the even derivatives in the truncation error would be eliminated. In this case the derivation would proceed using Taylor series expansion of the function at the grid points at each time without using the characteristic relations to relate these values to values on the present time line.

This use of expansions about an upstream point to introduce an upwind bias is attractive even in the case of nonuniform velocity, especially since such a scheme will become nondissipative when the

velocity is uniform. The upwind bias allowed stable solutions to be obtained without a cell Reynolds number limitation in Ref. 39.

The QUICKEST method of Leonard, Ref. 129, uses individual quadratic interpolation polynomials to evaluate the fluxes through the sides of a cell (Cells contain one grid point and are bounded by sides located mid-way to the adjacent grid points.) in 1D, with the three grid points fitted by the interpolation polynomials being chosen to extend upstream, i.e., with the cell side located between the two most downstream points, as diagrammed below (cf. p. 11).

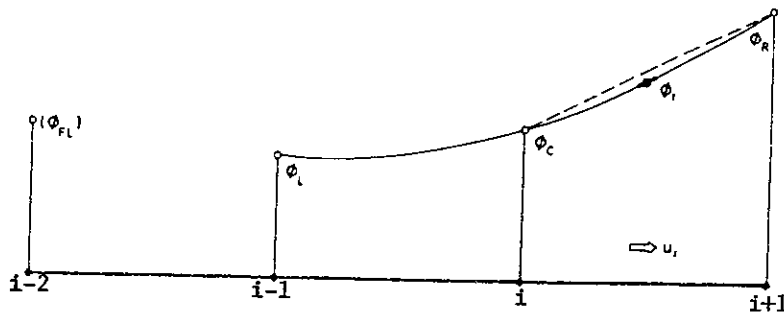


Fig. 39. Quadratic upstream interpolation for  $\phi_r$  and  $(\partial\phi/\partial x)_r$ . (Ref. 129)

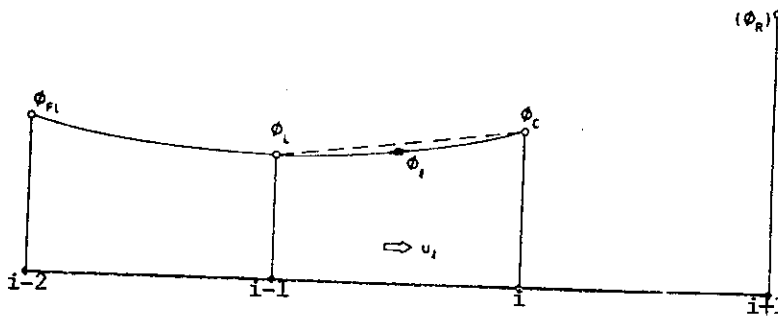
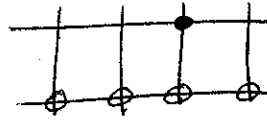


Fig. 40. Quadratic upstream interpolation for  $\phi_l$  and  $(\partial\phi/\partial x)_l$ . (Ref. 129)

This results in a third-order upwind biased method for convection with the stencil



This scheme is constructed by first integrating the differential equation  $\phi_t + (u\phi)_x = 0$ , over space and time, as in Eq. (II-26), to produce the exact relation

$$\int_{-\frac{\Delta x_\ell}{2}}^{\frac{\Delta x_r}{2}} (\phi^{n+1} - \phi^n) dx = - \int_0^{\Delta t} (u_r \phi_r - u_\ell \phi_\ell) dt$$

$$= - \int_0^{\Delta \zeta_\ell} \phi_r(x_r - \zeta) d\zeta + \int_0^{\Delta \zeta_r} \phi_\ell(x_\ell - \zeta) d\zeta \quad (3)$$

where  $\Delta \zeta_r = \int_0^{\Delta t} u_r dt$ , etc. Here the subscripts,  $r$  and  $\ell$ , refer to the right and left sides of the cell, respectively. The integrals on the right are the time-average fluxes through the cell sides. With the solution given by the characteristic relation,  $\phi(x, t_0 + t) = \phi(x - ut, t_0)$ , the  $\phi$  passing through a cell side during time will be all that is located up to a distance  $x_r - \Delta \zeta_r$  to the left of the side, hence the form of the integrals on the far right. These average fluxes are evaluated by replacing  $\phi$  in the integrals on the far right with the interpolation polynomial corresponding to the cell side in question. The integral on the left is a spatial average of the time change of the solution and is evaluated from the interpolation polynomial fitted to the points  $(i-1, i, i+1)$ .

With the uniform velocity and spacing, the QUICKEST method is equivalent to the third-order upwind biased method of Davies (Ref. 58), which uses a cubic interpolation function on four points biased to the upstream side. The Fromm method (Ref. 72) uses these same four points, but averages two quadratics, one through  $(i - 2, i - 1, i)$  and the other through  $(i - 1, i, i + 1)$ , to represent the solution on the interval  $[i - 1, i]$ . That the present method is truly third order with nonuniform velocity is unfortunately not demonstrated and no reference is cited for such a demonstration.

Diffusion is included in a second-order central difference form. A second-order version, called QUICK, is given also using the same stencil. In the second-order version, the integrands in the time-average fluxes in Eq. (3) are simply evaluated at the cell sides from the corresponding interpolation polynomial, instead of being functions of  $\zeta$ . Long waves are unstable in the second-order version.

This method reduces to the second-order Leith method (Ref. 128 and 129) if the quadratic interpolation is replaced by linear interpolation, and further to the Lax-Wendroff method for uniform velocity. The method is stable for Courant numbers less than unity in the pure convection case, and has some stable ranges for Courant numbers greater than unity for some values of the diffusion coefficient. This method is shown to produce much less oscillation near a shock than does the lower-order Leith method, and the results are relatively insensitive to the Courant number within the stable range. A comparison for convective and diffusion of a step function is shown in the next figure.

The extension to multiple dimensions, except for cases in which convection dominates in a single direction, is not straightforward. The 1D scheme can, however, be applied in a time-splitting mode to

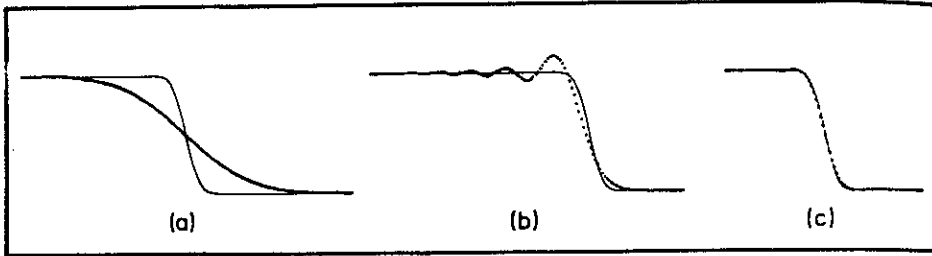


Fig. 41. Convection and diffusion of a step ( $P_{\Delta} = 50$ ): (a) upstream differencing, (b) Leith's method, (c) QUICKEST method (in each case the exact (error-function) solution is shown for reference). (Ref. 129)

treat higher dimensions, but the third-order in time would be lost.

The QUICKEST method is extended by Leonard in Ref. 130 to use exponential, rather than polynomial, interpolation in regions of strong gradients. A continuous change from polynomial to exponential interpolation is made as the region of high gradient is entered. Examples of convection of a step and a Gaussian wave are shown below. Significant dissipation is still present.

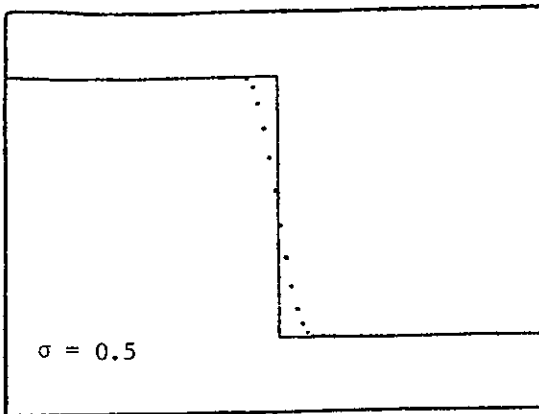


Fig. 42. Monotonic step profile predicted by the adjusted QUICKEST algorithm under conditions of pure convection. (Ref. 130)

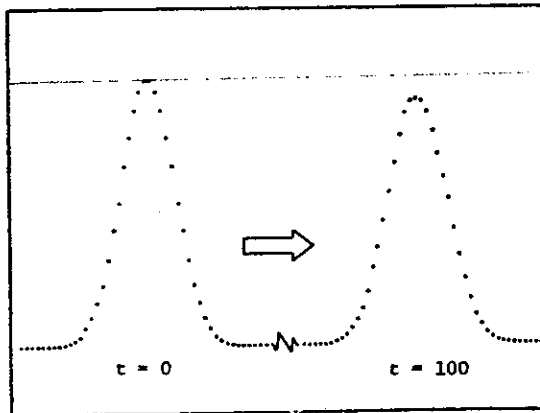


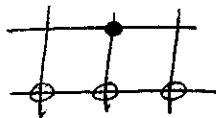
Fig. 43. Pure convection of an initial Gaussian profile using the adjusted QUICKEST algorithm (Ref. 130)

Han, Humphrey, and Launder (Ref. 95 ) found the QUICK scheme to be markedly superior to the first-order hybrid scheme. Leschziner and Rodi (Ref. 131) found the QUICK scheme to exhibit some over- and undershoots. Both of these applications were to turbulent confined recirculating flows.

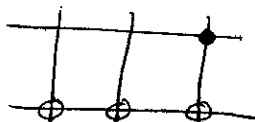
MacCracken and Bornstein (Ref. 137) also represent the flux as a time-average using the characteristic equation for the solution. Use of a linear interpolation polynomial on each grid interval produces the flux expression used by Leonard (Ref. 129) without the curvature term, which is equivalent to the Leith method (Ref. 128).

As in Fromm, Ref. 72, the Lax-Wendroff method in 1D with uniform velocity can be constructed from the characteristic relation (1), as also noted on p. 9 .

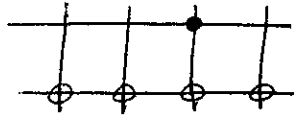
The scheme results from fitting a quadratic to the three points  $(i - 1, i, i + 1)$  and evaluating the polynomial at  $x - u\Delta t$ . The stencil then is



This scheme has dissipation and a lagging phase error, both of which are greatest for small wavelengths. If the quadratic is fitted to the point  $(i - 2, i - 1, i)$ , however, the stencil is



and this method has a leading phase error. A scheme with a phase error an order of magnitude lower can be constructed by averaging these two schemes, and the stencil then is



The improvement is greatest at the short wavelengths.

In Ref. 124, van Leer generalizes the Fromm scheme to a one-parameter family of second-order upwind-biased schemes. A third-order scheme results for one value of the parameter. Another value minimizes the dispersive and dissipative errors. A two-stage version of this family of schemes is also given. These schemes, including the original Fromm methods, involve many more operations than does the Lax-Wendroff scheme.

In Ref. 125, van Leer constructs several second and third-order schemes that have upwind bias. These schemes are formed by approximating the solution between each pair of mid-points by a polynomial which matches the average value of the solution, and perhaps some average derivatives also, on the interval between the mid-points. This interval between mid-points, containing one grid point, is called a cell. The solution is thus represented by separate polynomials within each interval, and is not necessarily even piecewise continuous. (In Ref. 125, the scheme is actually formulated to produce new average values of the solution on the intervals between grid points, so the polynomials are applied between the grid points. The present interpolation is used for compatibility with other schemes in this survey.)

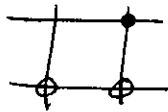
The construction is based on the same exact integral over space and time given in Eq.(3) and discussed on p.11. In the present development,

the time-averaged fluxes are evaluated from the integrals on the far right as in the construction discussed in connection with this equation. Here, however, the interpolation polynomial used to evaluate the flux through each side of the cell is the one formed on the cell to the left of the side in question.

The basic difference between the present approach and that of Ref. 129 is the use of a compact representation in the present case, i.e., interpolation polynomials defined on intervals between two points instead of over several points. Order is increased in the present case by matching derivatives, as well as the function, on the same interval, while in Ref. 129 order is increased by expanding the interval, i.e., fitting the polynomial to more points. The present approach also interprets the solution values obtained at the grid points to be averages over the cell. In all schemes based on flux evaluations from interpolation functions, the interpolation used can be of one order less than the order of the method since it is the difference of the fluxes that enters the equation.

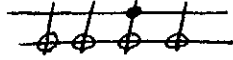
The first-order version of the present scheme, formed with a zero-degree polynomial, is equivalent to the Godunov method (Ref. 172), which is labeled the best first-order method by van Leer in Ref. 124.

The stencil is



With linear interpolation, which fits some average of the first space derivatives as well as the solution, several second-order versions of the scheme result, depending on the representation used for this average

of the first derivative. If this average is represented as a central difference of the average solution values in adjacent cells, then the method of Fromm (Ref. 71) results (Scheme I here), with the stencil



Another possibility (II) is to represent the first derivative as a central difference between the solution values on the cell sides, these values being equal to the solution values at a distance  $u\Delta t$  to the left of the side at the previous time level by the characteristic relation, Eq. (1). This value, for each side, can be evaluated from the interpolation polynomial on the cell to the left of the side. This results in a difference equation for the average first derivative, so that this quantity becomes an additional dependent variable, with both stencils of the form

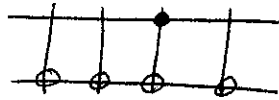


This scheme unfortunately has dissipation even at zero Courant numbers.

Still another possibility (III) is to define the average derivative such that the solution and the interpolation polynomial have the same first moment in each cell, i.e., so that the difference between the solution and the interpolation polynomial is minimized in the least-squares sense over the cell. Again the derivative becomes an additional dependent variable with the same stencils given above for scheme II.

Third-order methods are obtained by using a quadratic interpolation polynomial fitting some average of the second space derivative as well. One third-order scheme (IV) is obtained by representing this average second derivative by a central difference using the average solution values in the adjacent cells, with a similar representation for the first derivative as usual above.

This scheme has the stencil



In another scheme (V) the second derivative is chosen such that the interpolation polynomial matches the solution at the cell sides. In this case the polynomial representation of the solution is piecewise continuous. In this form the solution at the cell sides becomes an additional dependent variable, the difference equation for which is obtained from the characteristic relation as done above in connection with the representation of the first derivative in terms of solution values on the cell sides. This representation of the first derivative is, in fact, again used in this form. The stencils are



Finally, in analogy with Scheme III above, the second derivative can be chosen so that the solution and the interpolation polynomial have the same second moment over the cell, with the first derivative chosen as in Scheme III. Here both derivatives become additional dependent variables (VI).

Since upwind-biased methods have maximum dissipation for Courant number  $\frac{1}{2}$ , the dissipation of these schemes is compared here at that Courant number in the figure on the following page.

In this and the next figure the semi-circle is the ideal. The phase error vanishes for a Courant number of  $\frac{1}{2}$ , and therefore the

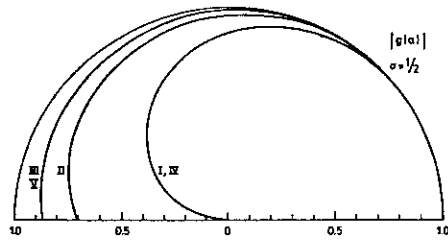


Fig. 44. Dissipation in schemes I-V. Polar plots of the damping factors per time step  $|g_1^{I,IV}|$ ,  $|g_1^{II}|$  and  $|g_1^{III,V}|$  as a function of the wavenumber  $\alpha = 2\pi\Delta x\ell$  of the wave, for Courant number  $\frac{1}{2}$ . (Ref. 125)

schemes are compared in this regard at a Courant number of zero in the next figure.

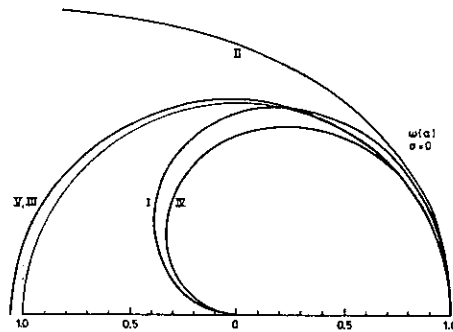


Fig. 45. Dispersion in schemes I - V. Polar plots of the ratios  $\omega_1^I$ ,  $\omega_1^{II}$ ,  $\omega_1^{III,V}$  and  $\omega_1^{IV}$  of numerical and exact convection speeds as a function of  $\alpha$ , for vanishing Courant number. (Ref. 125)

These figures show that the second-order schemes I and II, and the third-order scheme IV, have very large dispersion. In fact, this third-order scheme is worse than the two second-order schemes. Schemes I and IV also have large dissipation which would damp out much of the dispersion, so that these schemes might be fairly smooth but inaccurate. These two schemes are also the least compact of the six schemes considered. Scheme II has less dissipation, but the large dispersion would render it

inaccurate. As noted above, this scheme has some dissipation even for zero Courant number. These three schemes are thus unsatisfactory. The second-order scheme III, however, approaches the third-order scheme V in accuracy, and both of these schemes have small dispersion and dissipation.

These comparisons show that order alone is not a complete measure of accuracy. Scheme V is somewhat more accurate than scheme III and requires about the same number of operations. Scheme VI is somewhat more accurate but is more complicated as well. Therefore scheme V is the best of the six schemes. A comparison of the convection of a triangular wave by schemes I and III is given in the figure below

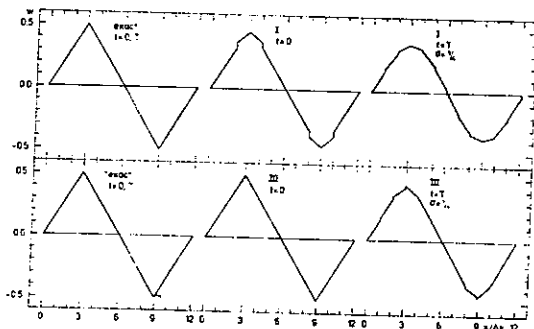


Fig. 46. Convection of a triangular wave by Scheme I (top row) and Scheme III (bottom row). No monotonicity enforced. (Ref 125)

Scheme II is applied by van Leer in Ref. 124 to a system of equations, in what may be regarded as a second-order sequel to the Godunov method. This code is named MUSCL, for Monotonic Upstream-central Scheme for Conservation Laws. The results of this code for the shock tube problem are shown on the following page.

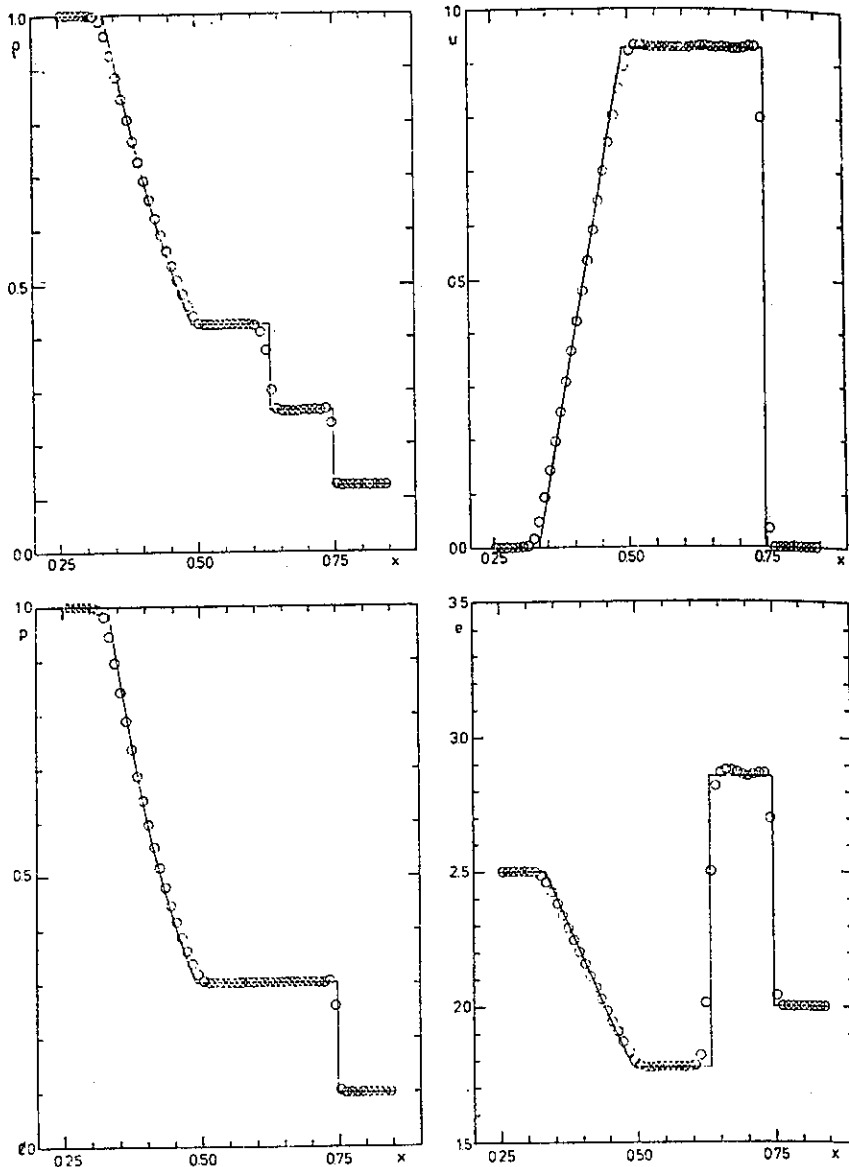
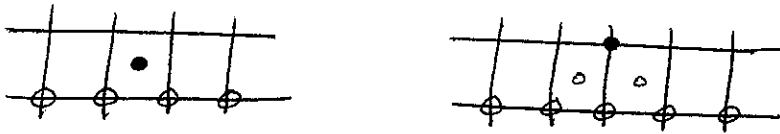


Fig. 47. Exact solution (line) and cell averages (circles) of  $\rho$ ,  $u$ ,  $p$  and  $e$  obtained with MUSCL (Eulerian) for the same exploding diaphragm problem as used by Sod. Initial values:  $u \equiv 0$ ;  $\rho = p = 1$  for  $x < 0.5$ ;  $\rho = 0.125$ ,  $p = 0.1$  for  $x > 0.5$ ;  $\gamma = 1.4$ . Courant number 0.9;  $\Delta x = 0.01$ . Output after 34 time steps at  $t = 0.14154$ . (Ref. 124)

### Multi-Stage Methods

Gottlieb and Turkel, Ref. 84, construct two two-parameter generalizations of the two-stage Lax-Wendroff method which are fourth-order in space and second-order in time. The largest Courant number allowed for any value of the free parameters is about 0.731, which is only slightly larger than that of the Kreiss-Oliger scheme (Ref. 118) of the same order. One of these schemes is of the Richtmyer form with the 1D stencil



and the other is of the MacCormack form:



This form is fourth-order when the directions of the differences are alternated at successive time levels.

These fourth-order space methods have about the same amount of dissipation as the analogous second-order methods, but the phase error is significantly reduced for sufficiently small time steps. Some direction is given as to the choice of the free parameters to increase the stability limits or to decrease the dissipation and/or phase error. With these schemes the phase error decreases with the time step.

The dissipation can be reduced to sixth order by alternating these schemes with the Kreiss-Oliger fourth-order space scheme (Ref. 118). This alternation of schemes can be considered to be a three-stage scheme, with the Kreiss-Oliger third stage having the same stencil as the second

stage shown above.

Some results for a sine wave are shown below:

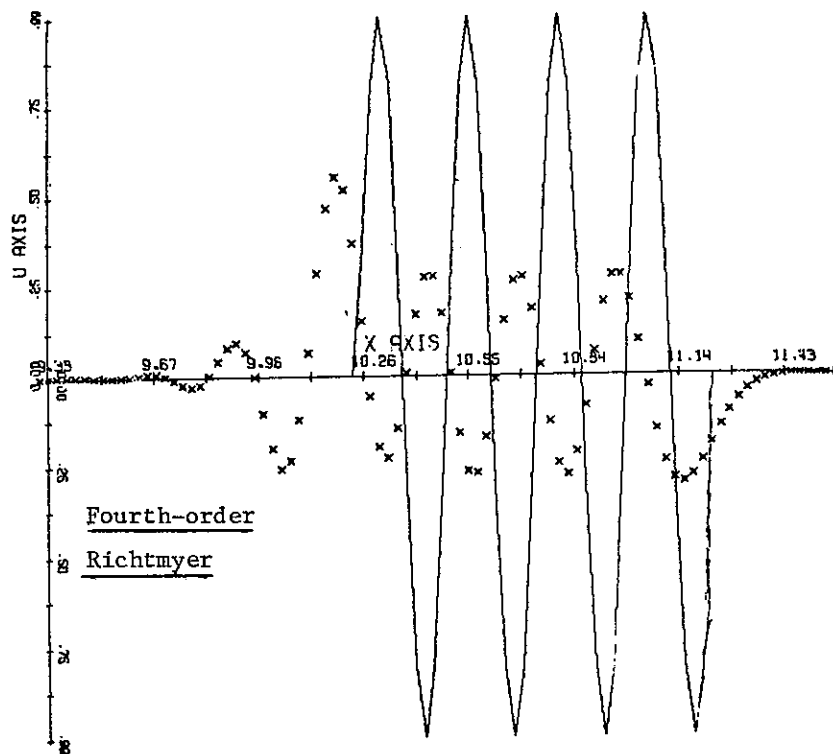


Fig. 48.  
(Ref. 84)

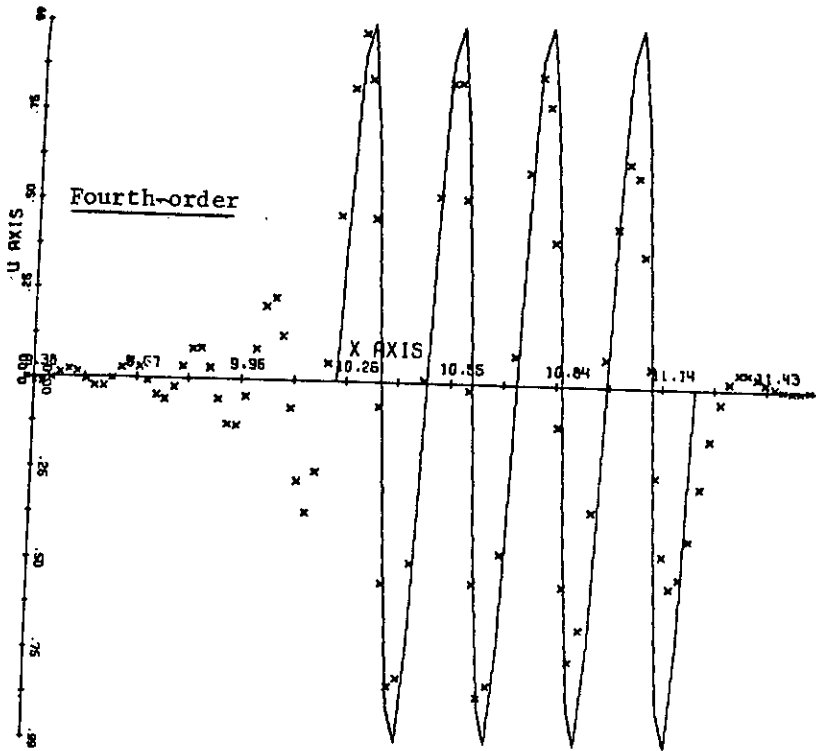


Fig. 49. (Ref. 84)

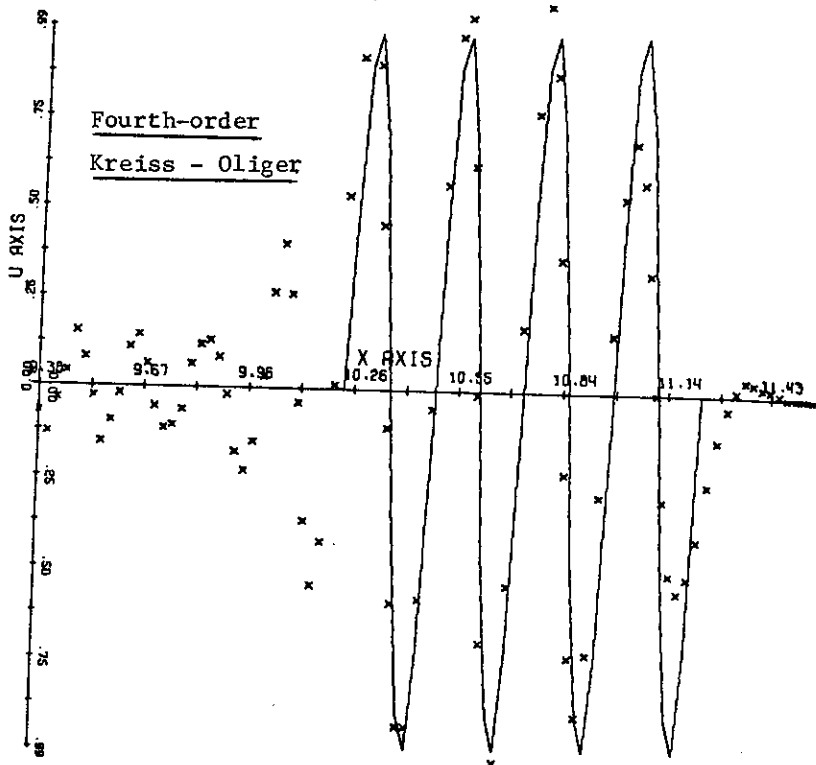
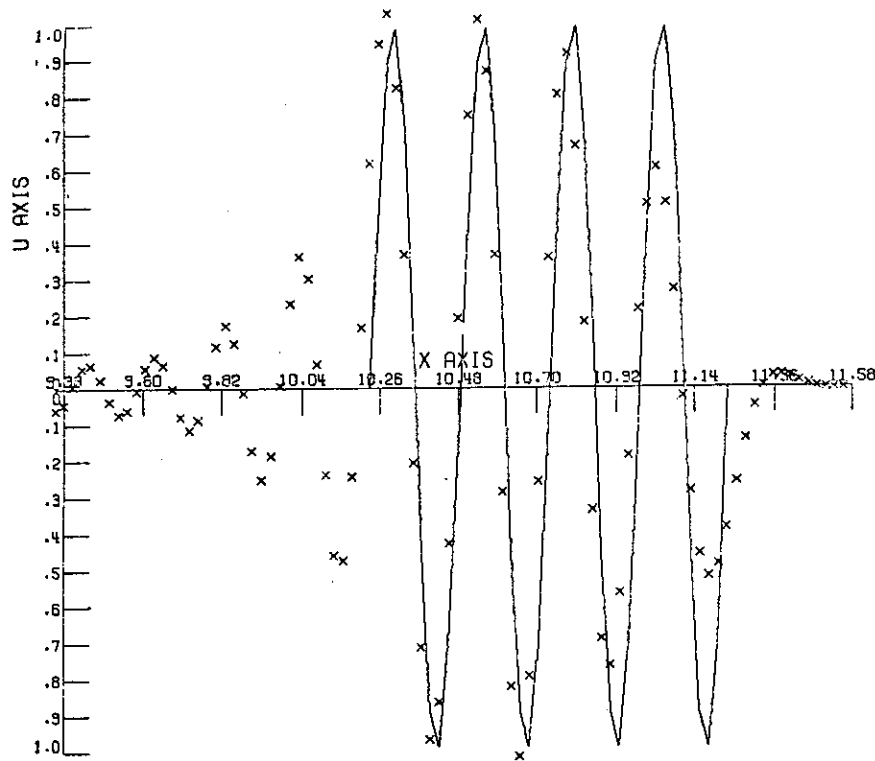


Fig. 50. (Ref. 84)

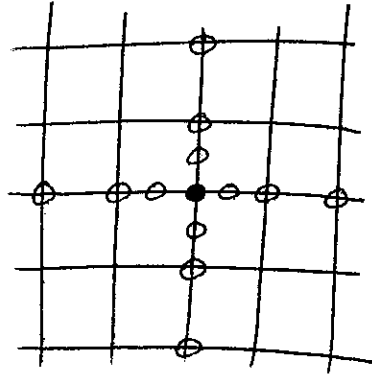
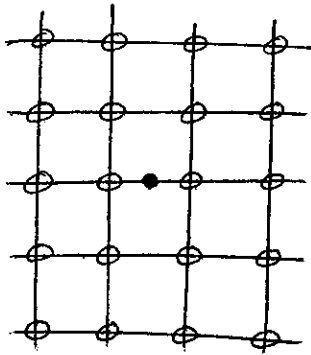


Alteration of previous two schemes.

Fig. 51. (Ref. 84)

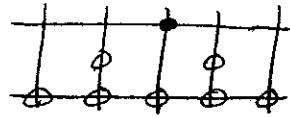
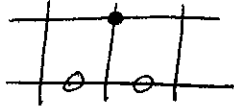
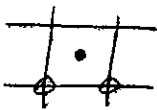
The phase error of this scheme is considerably better than second-order methods and is comparable with Kreiss-Oliger. The dissipation is also much less than with the lower-order methods.

A 2D form is also constructed but as a three-stage method with the stencils shown on the following page. This scheme has nine free parameters, and no complete choice is given.

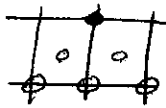
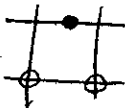


2D

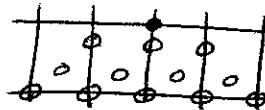
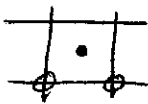
Burstein and Mirin (Ref.35) note that the multi-stage methods involving successive evaluations of the flux vectors at intermediate levels are of the Runge-Kutta class. Such a third-order method is given, having one free parameter. Each stage here is a consistent approximation to the time-dependent equations. One three-stage version has the stencils



Another is a two-stage method with the stencils



Rusanov (Ref. 183) gives a third-order scheme using three stages with the stencils



Here each stage is a consistent approximation, to first, second, and third order. The method has two free parameters. A 2D version is also given. This scheme is equivalent to that of Burstein and Mirin (Ref. 35).

Abarbanel and Gottlieb, Ref. 3, give a general formulation for constructing schemes of order  $p + 1$  and  $p + 2$  in space and time for the equation,  $w_t + f_x = 0$ , if a scheme of order  $p$  is known. From this result, a general multi-stage scheme of any desired order is constructed for  $N$  dimensions. Both explicit and implicit schemes are included in the general formulation. This general scheme is said to include all finite difference schemes presented thus far for one and two dimensions, and several examples are given. The number of stages is equal to the order. Written as a one-stage method the even order schemes would involve  $2M + 1$  symmetrically placed grid points, where  $M$  is the order, and  $2M + 2$  symmetrically placed mid-points for odd order. Extensions to higher dimensions are also given. For the explicit schemes, stability requires that the Courant number not exceed  $1/N$ , where  $N$  is the number of dimensions, for even order, and  $1/2N$  for odd order. A significant feature of this multi-stage formulation is that each stage is a valid approximation to the solution.

Reddy in Ref. 169 follows a similar approach to construct a scheme of order  $p + 1$  in space and time if a scheme of order  $p$  is known, but involves the Jacobian matrix of the flux as well, while Abarbanel and Gottlieb (Ref. 3) used only the flux itself. The stability criteria, number of points and stages required are the same as that in the formulation of Abarbanel and Gottlieb, but fewer flux evaluations are required. One specific third-order scheme and two fourth-order schemes are given. The convection of a sine wave by these three schemes and a fourth-order

scheme of Abarbanel, Gottlieb, and Turkel (Ref. 4) is compared in the figures below.

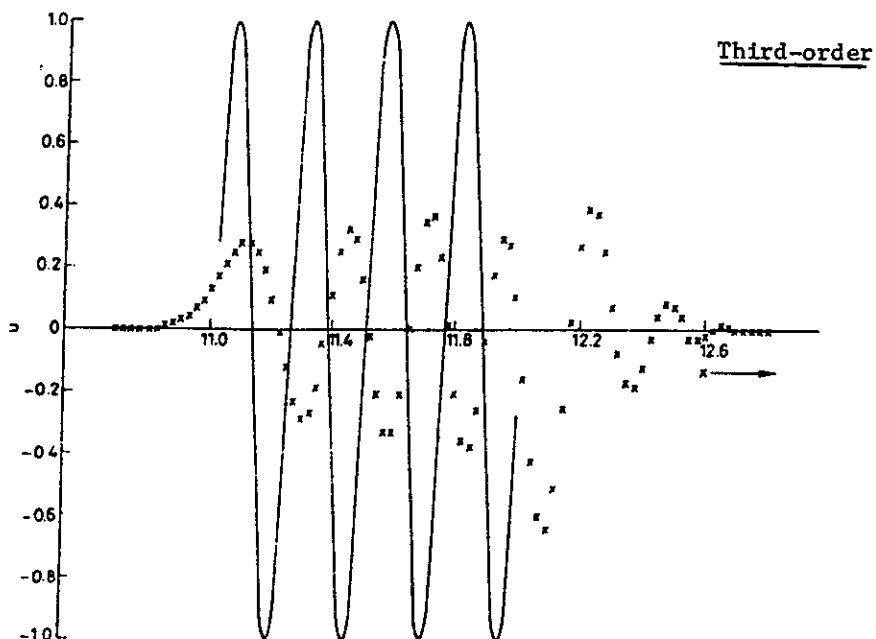


Fig. 52. Solution to Problem 3, using scheme I, at  $t = 10.0125$ ,  $\Delta x = 1/40$ ,  $\Delta t/\Delta x = 0.45$ . (Ref. 169)

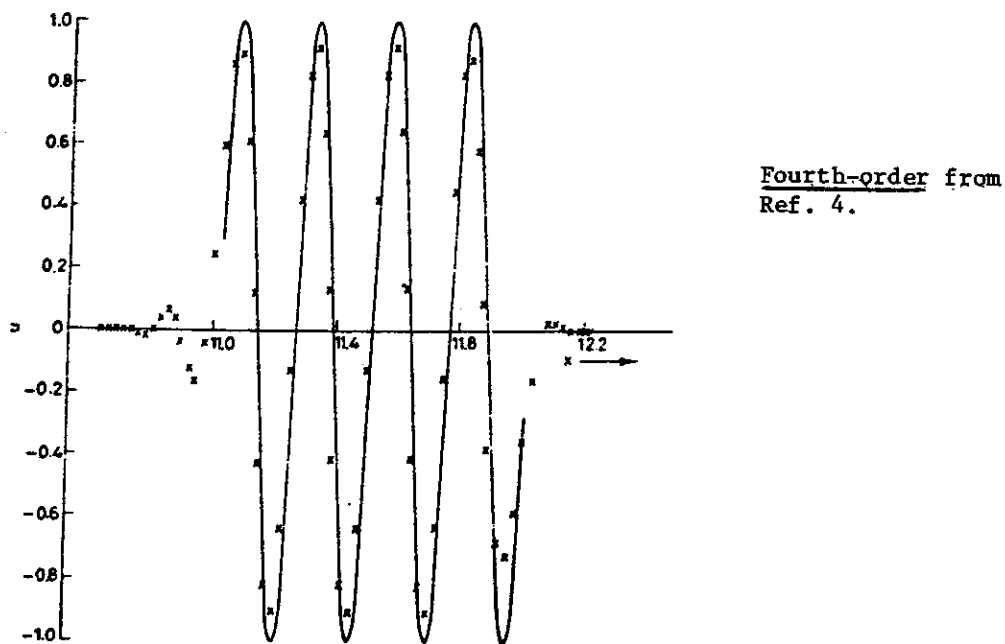


Fig. 53. Solution to Problem 3, using AGT scheme, at  $t = 10.0125$ ,  $\Delta x = 1/40$ ,  $\Delta t/\Delta x = 0.9$ . (Ref. 169)

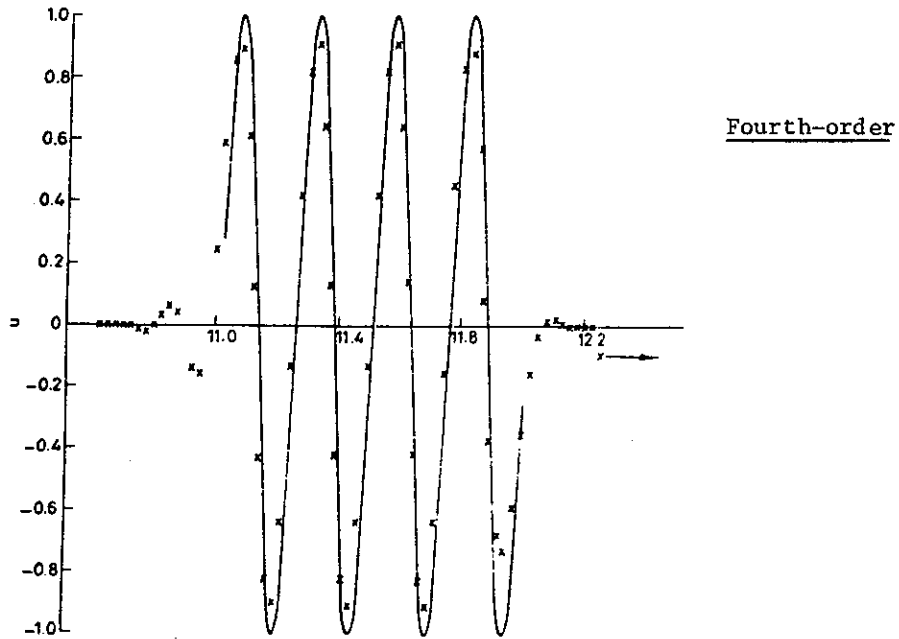


Fig. 54. Solution to Problem 3, using scheme II (a), at  $t = 10.0125$ ,  $\Delta x = 1/40$ ,  $\Delta t/\Delta x = 0.9$ . (Ref. 169)

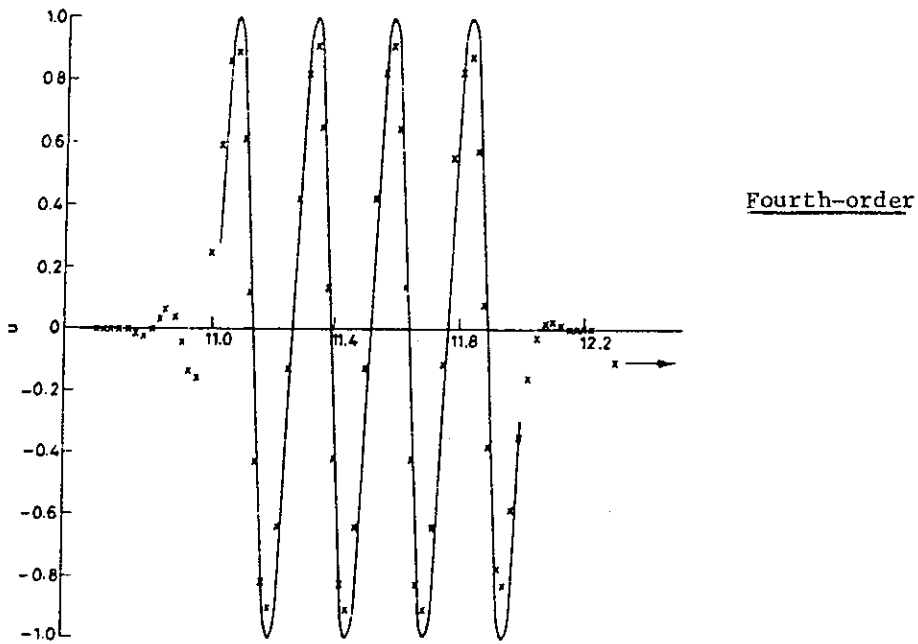
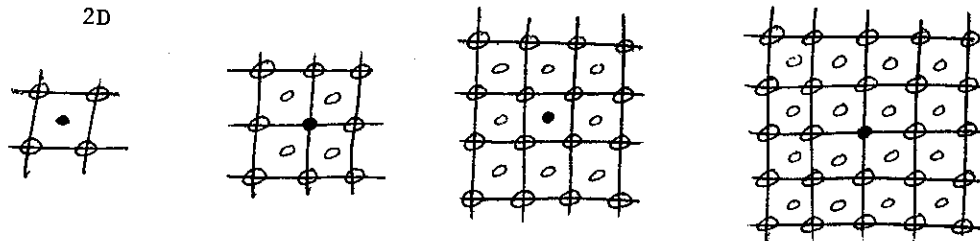


Fig. 55. Solution to Problem 3, using scheme II(b), at  $t = 10.0125$ ,  $\Delta x = 1/40$ ,  $\Delta t/\Delta x = 0.9$ . (Ref. 169)

The improvement of the quality with order is evident in a reduction of both dissipation and dispersion. The results for the three fourth-order schemes are nearly the same.

Turkel, Abarbanel, and Gottlieb (Ref. 216.) give a four-stage scheme that is fourth order in both space and time, with the stencils



Here the first three stages are first order. This scheme contains eleven free parameters, and no procedure for selection is given.

This fourth-order scheme was found to give accuracy equal to that of second-order schemes, while using only about 1/25 as many points for the 2D wave equation. The fourth-order scheme is twice as fast as the leapfrog scheme for the same accuracy, and 60 times as fast, with less storage, than the rotated Richtmyer scheme (Ref. 224). This advantage is expected to even improve for more complicated equations, as the time required for evaluation of the fluxes increases. This occurs because fluxes calculated in the early stages are used in all the remaining stages. For the same accuracy, the present scheme requires fewer flux evaluations than the Kreiss-Oliger scheme (Ref. 117), that is fourth order in space but only second order in time, and about the same number as pseudospectral methods. The latter, however, require Fourier expansion. The fourth-order scheme is more efficient also as the error tolerance decreases or

at higher frequencies. This present method was more efficient than the Kreiss-Oliger fourth-order space, second-order time scheme (Ref. 117) in each of these situations. An advantage of equal order in space and time is that the error decreases as the time step increases, while in schemes with unequal order the error has a minimum at some time step. Time step selection is thus more simple with equal order. This method does have dissipation, and decreased the amplitude of a rotating cone by about the same amount as did the Arakawa fourth-order space, second-order time scheme, and less than second-order schemes, though more than do pseudospectral methods. Both the phase error and dissipation decrease with the present method as the time step increases.

Khaliq and Twizell (Ref. 111) construct higher-order methods in time by combining the results of a lower-order scheme applied twice over two time steps and once over a double time step to eliminate the leading term in the truncation error of each.

#### Compact Methods

Compact methods are based on interpolation polynomials which match solution derivatives, as well as solution values, at certain points. Within this category are methods based directly on Hermite interpolation polynomials, methods using Pade difference approximations, and spline methods. All of these approaches are ultimately equivalent.

#### Hermite Methods

Fischer, Ref. 68, also uses the characteristic approach (p. 8) with uniform velocity, but with a cubic Hermite interpolation polynomial fitted to each grid interval, thus fitting both the solution and its gradient at the end points of the interval. Again the schemes have the same temporal and spatial order with uniform velocity. Here the gradient

is treated as an additional dependent variable. With uniform velocity, we have

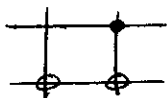
$$(\phi_x)_t + u(\phi_x)_x = 0 \quad (4)$$

so that the gradient is convected in the same manner as is the solution and, therefore,

$$\phi_x(x, t + \Delta t) = \phi_x(x - u\Delta t, t) \quad (5)$$

Thus the gradient at each grid point at the new time is equal to the value at the upstream point  $(x - u\Delta t)$  at the previous time level, as is the function itself.

This upwind-biased scheme is constructed by expanding the function, and its gradient, at this upstream point in a Taylor series about the grid point  $i$  at time  $t$ . Second and third derivatives in this expansion are evaluated by differentiating the interpolation polynomial. This is equivalent to evaluating the solution from the interpolation polynomial evaluated at this upstream point, and the derivative from the derivative of the polynomial evaluated there. Schemes up to third-order can be obtained using the cubic polynomial. These schemes are compact, with the stencil



Results for convection of a triangular wave are shown on the following page for first, second, and third-order versions in comparison with the Fromm scheme, Ref. 71.

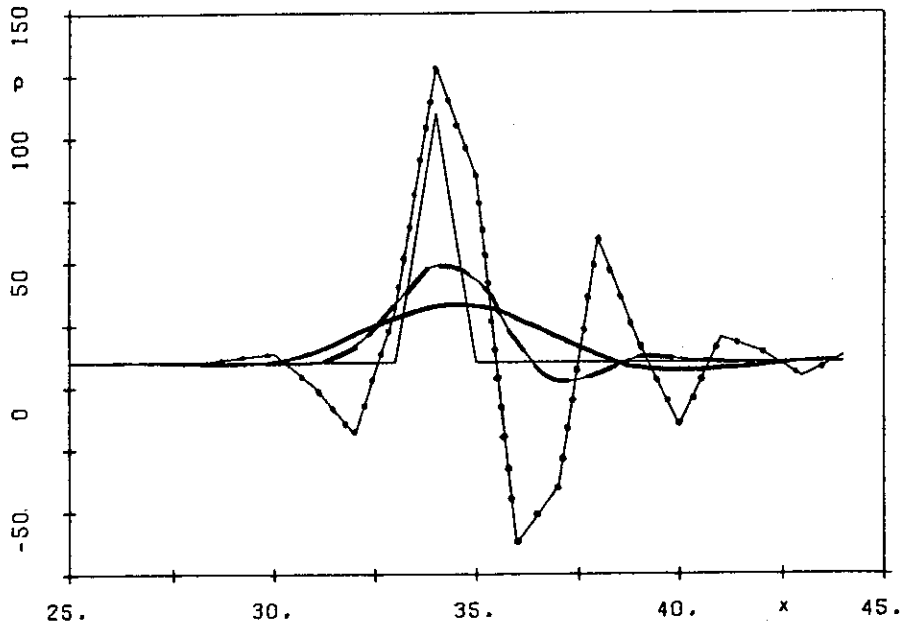


Fig. 56. Numerical convection results,  $C = 0.1$ , 240 steps. Peak at  $x = 34$ : exact solution. Bold: Fromm's method. Dotted: present method; second-order. (Ref. 68)

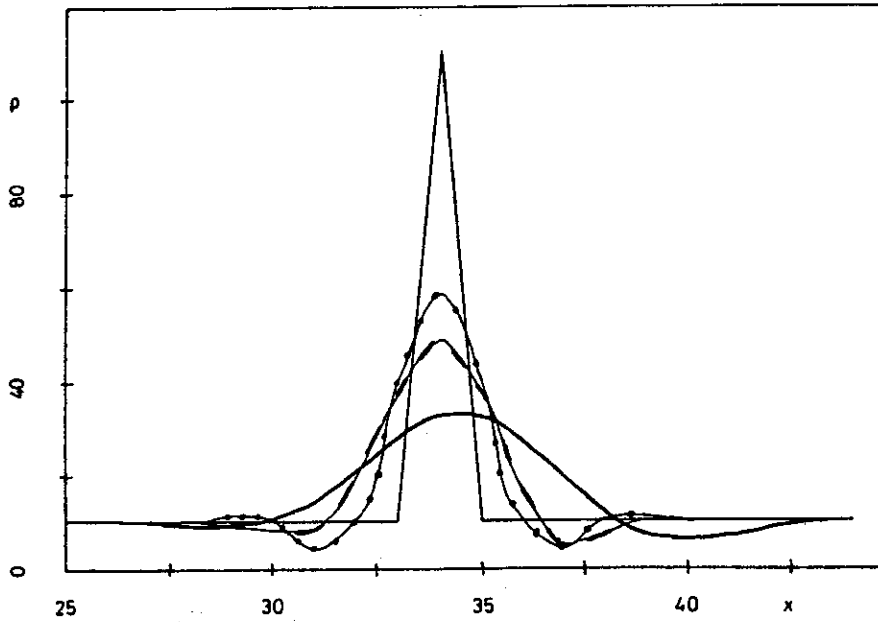


Fig. 57. Numerical convection results.  $C = 0.1$ , 240 steps. Peak at  $x = 34$ ; exact solution. Bold: Fromm's method. Dotted: present method, third-order. (Ref. 68)

The conservative version of the present scheme referred to in the above figure involves an ad hoc correction that is applied to the solution at each time step to bring the change in a cell into exact balance with the net flux into the cell. The improvement with order is evident, and these schemes are less dissipative than the Fromm scheme. However, the dissipation is still significant and some oscillations are present due to phase error. The results for the third-order scheme improve with increasing Courant number, as do those of the Fromm scheme, as is seen by comparison of the following figure with that above. (The first- and second-order versions are unstable at this Courant number.)

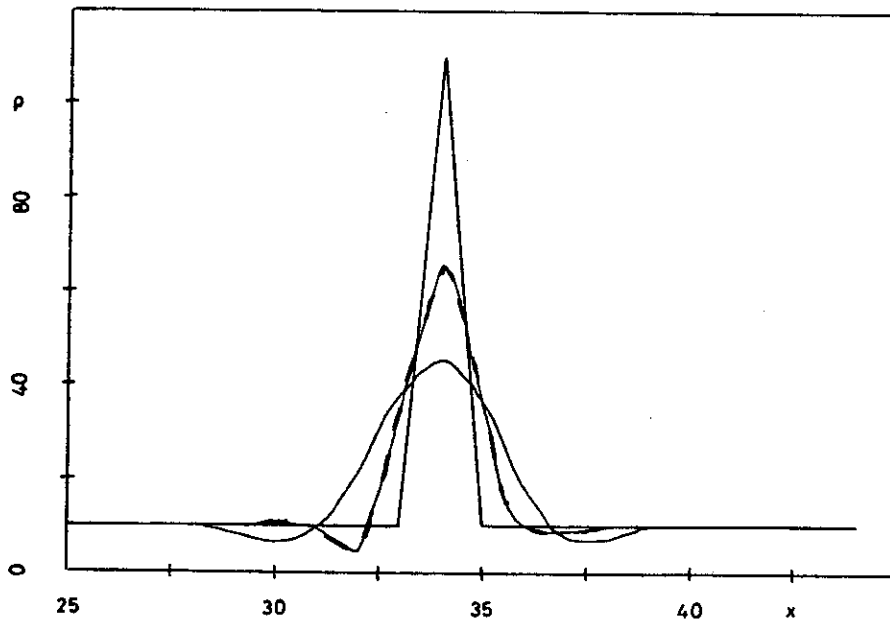


Fig. 58. Numerical convection results,  $C = 0.8$ , 30 steps. Peak at  $x = 34$ ; exact solution. Thin: Fromm's method. Dashed: present method, third-order. (Ref. 68)

Essentially this same approach was used by Holly and Preissman, Ref. 104, but the method is mislabeled fourth order, when it is actually third order in space and time for uniform velocity. Comparisons of representation of convection of a Gaussian by this and other methods are seen in the figure below.

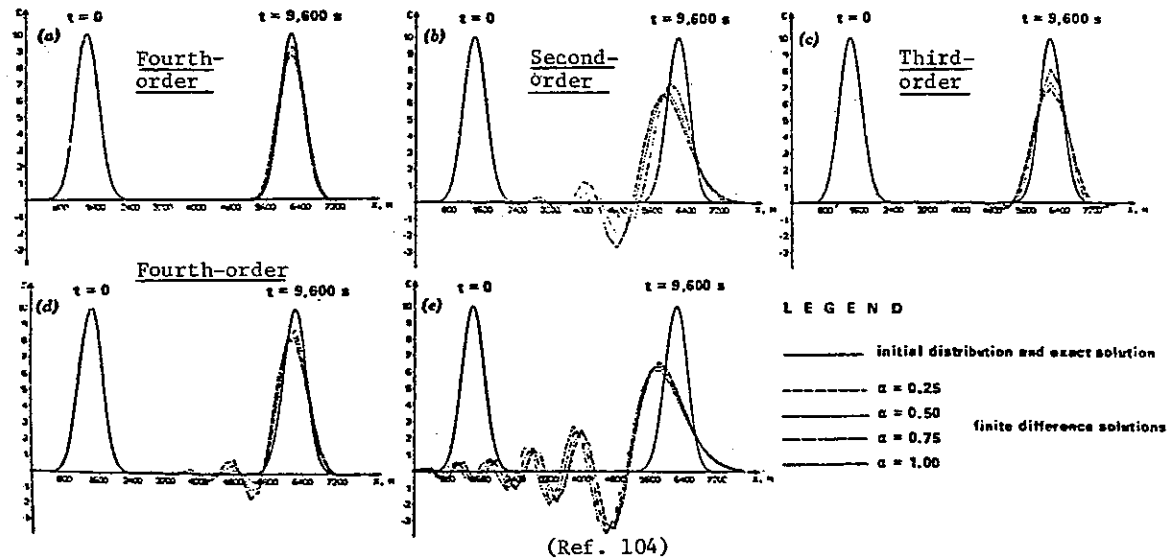


Fig. 59. Calculations of one-dimensional advection of Gaussian distribution using several methods: (a) Two-point fourth-order; (b) Martin (3)  $n = 2$ ; (c) Martin (3)  $n = 3$ ; (d) Martin (3)  $n = 4$ ; (e) Leendertse (2).

The Martin schemes (Ref. 141) used here are second, third, and fourth-order schemes in space, which for pure convection are formed simply by using the appropriate order representation of the spatial derivative. The superior phase quality of the present compact scheme is evident, even in comparison with the third and fourth-order non-compact schemes. Also evident here is the general superior phase representations of schemes with an upwind bias, i.e., the Martin third-order as well as the present

scheme.

An extension to nonuniform velocity is also given as follows:

With nonuniform velocity, the velocity appearing in Eq. (1) is taken as the average of the velocity,  $u$ , at the point  $(x,t)$  and that evaluated from the interpolation polynomial at the point  $(x - u\Delta t, t)$ . Also Eq. (4) is replaced by

$$(\phi_x)_t + u(\phi_x)_x + \phi_x u_x = 0 \quad (6)$$

and the last term is approximated by  $\phi_x \left( \frac{u_i - u_{i-1}}{x_i - x_{i-1}} \right)$ , where  $\phi_x$  is evaluated from Eq. (5), but using the average velocity obtained above.

This procedure amounts to a single iteration of a complete representation of the effect of the nonuniform velocity. An example of convection of a Gaussian through a nonuniform velocity field is given below.

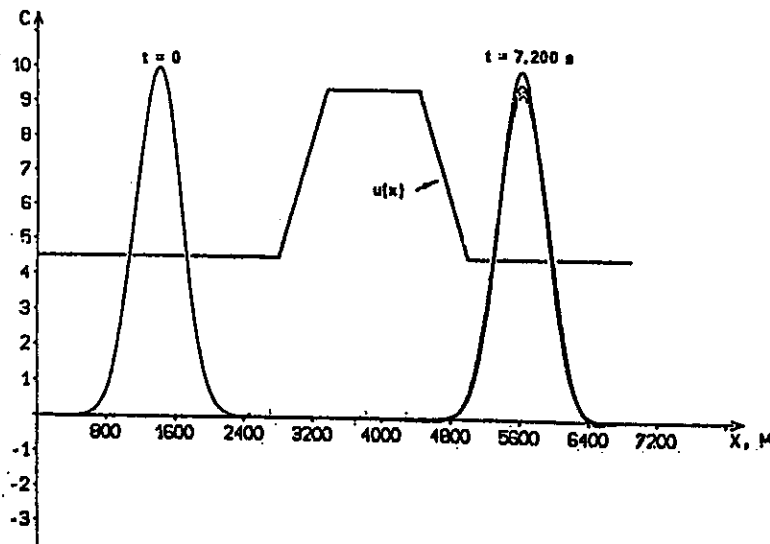


Fig. 60. Calculation of one-dimensional advection of Gaussian distribution through zone of nonconstant velocity, two-point fourth-order method. (Ref. 104)

Diffusion is added in a time-split manner, the solution being first convected and then diffused. An extension to a fifth-order scheme (mis-labeled sixth-order) is also cited, using a quintic Hermite interpolation polynomial on the interval  $[i - 1, i]$ , fitting the second derivative at the end points as well. In this case the second derivative is added as a third dependent variable. An extension to 2D is also noted using the solution, its two first derivatives, and the cross-derivative at each point on a cell as the dependent variables.

Huffenus and Khaletzky (Ref. 106) note that the simple addition of 1D methods is not consistent. Bad results for 2D convection of a trapezoid with this approach are shown below for two schemes that perform very well in 1D:

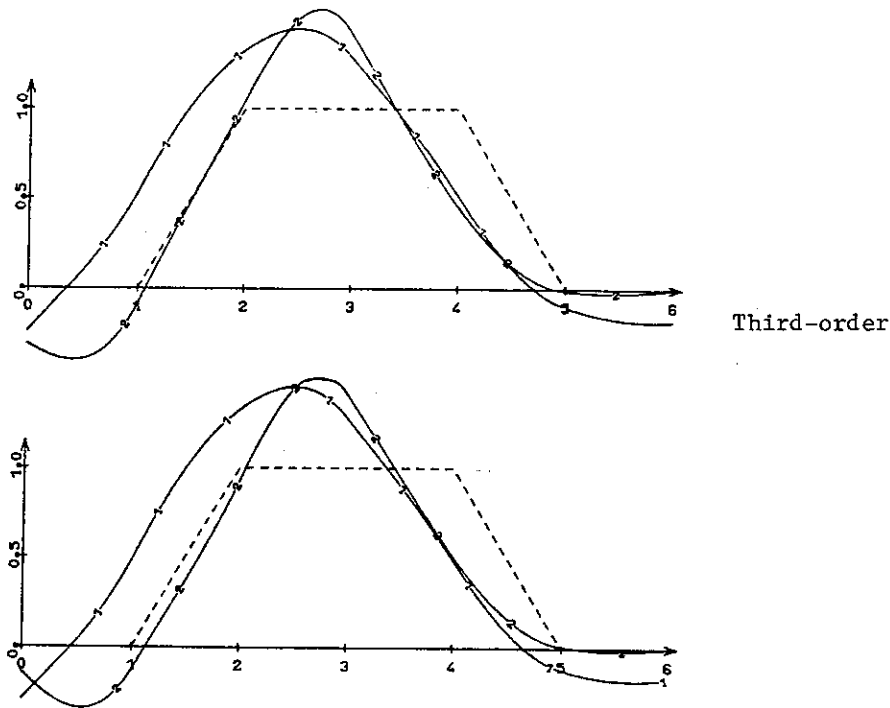


Fig. 61. Two-dimensional test problem: 1 - FTUS3 uncoupled. 2 - Akima uncoupled. (Ref. 106)

The improvement gained by using 2D interpolation polynomials analogous to those used in 1D versions is evident in the figure below for the 2D extensions of the methods of Holly and Preissman (Ref. 104), Akima (Ref. 10), and the third-order method of Davies (Ref. 58):

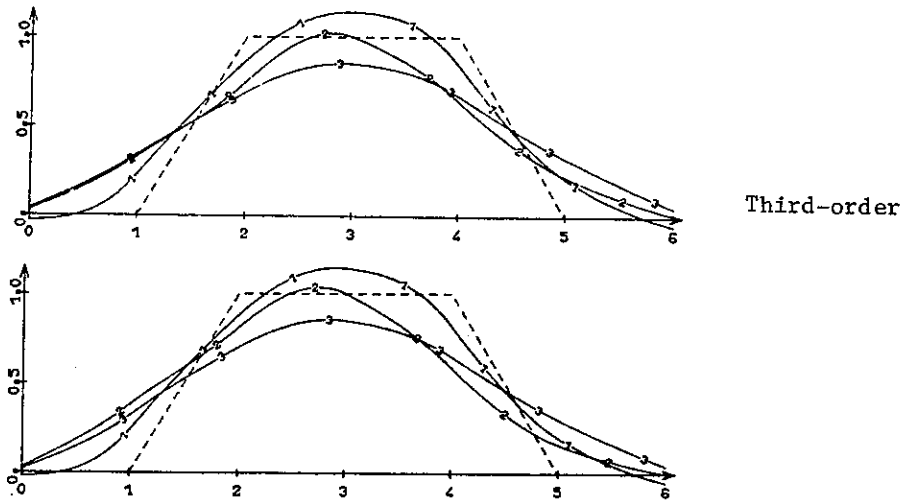


Fig. 62. Two-dimensional test problem: 1 - Transport of the derivatives, 2 - Akima, 3 - FTUS3. (Ref. 106)

These extensions are expensive, however, because of the large number of coefficients in the polynomials. Also the extension is not complete, in that not all of the features of the 1D version are analogously transferred to the 2D version. For instance the 2D version of Holly and Preissman uses the two first derivatives and the cross-derivative in the interpolation polynomial, but not the two second derivatives.

The present reference proposes a polynomial fitted to the x-derivative at  $i$  and  $i - 1$ , the y-derivative at  $j$  and  $j - 1$ , and the solution at the four corners of the cell formed by these points (and the point  $i - 1, j - 1$ ). The polynomial is a bi-cubic without the cubic cross term. Results are shown in the figure on the following page.

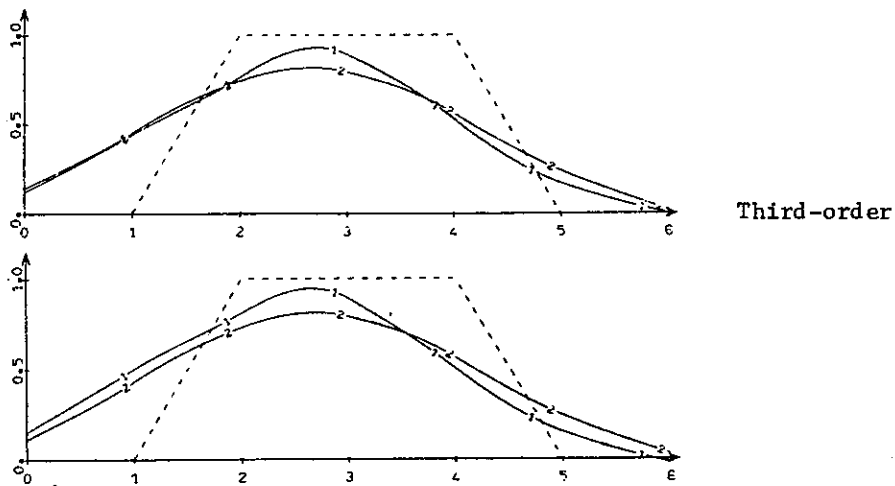


Fig. 63. Two-dimensional test problem: 1 - Akima simplified, 2 - FTUS3 simplified. (Ref. 106)

This scheme requires fewer operations than the more complete 2D schemes cited above.

Hermite interpolation polynomials were used in a finite element approach by Sobey, Ref. 190, using rectangular space-time elements. It is argued that increased nodal continuity gives better results than does more nodes. It is anticipated that the extension to the continuity of second derivatives also is beyond the point of diminishing returns in regard to accuracy and complexity, since such higher-order representation increases the operations by an order of magnitude. Results for phase and for elements including (1) only the solution values and (2) the first space derivative, (3) the first and second space derivatives, (4) the first time derivative, or (5) the first space and time derivatives are compared in the figures on the following pages.

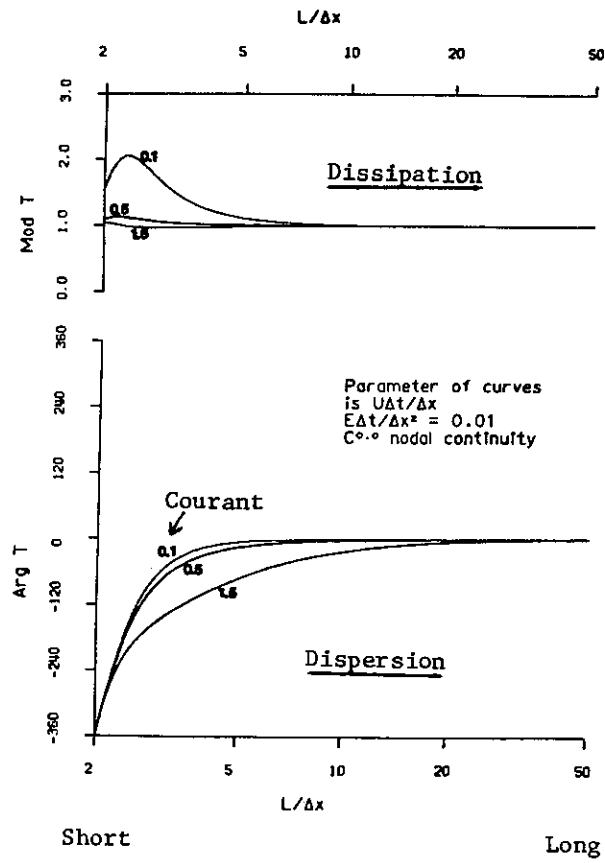


Fig. 64. Wave deformation for Element 1. (Ref. 190)

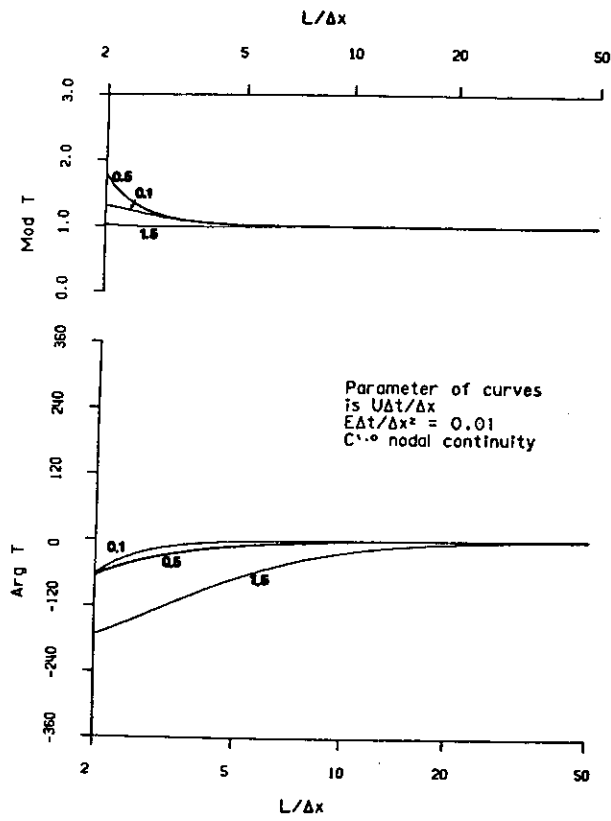


Fig. 65. Wave deformation for Element 2. (Ref. 190)

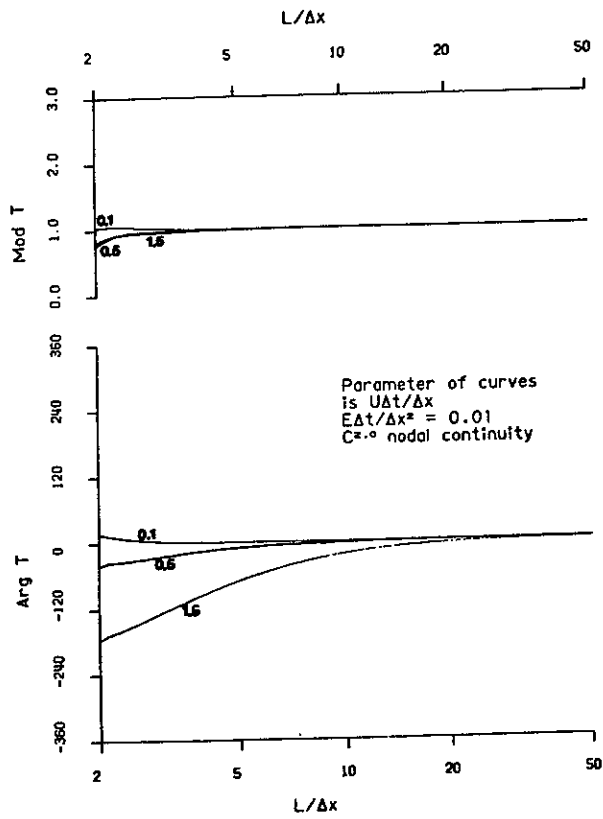


Fig. 66. Wave deformation for Element 3. (Ref. 190)

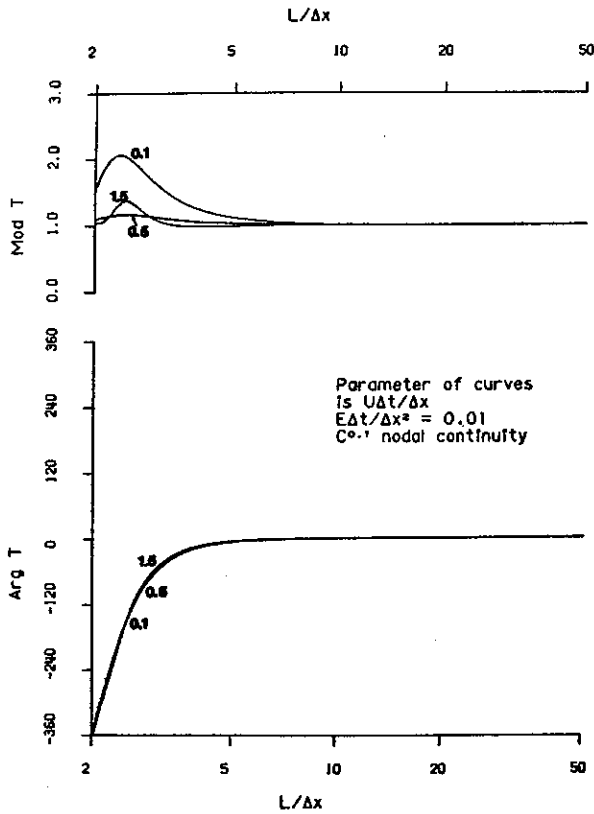


Fig. 67. Wave deformation for Element 4. (Ref. 190)

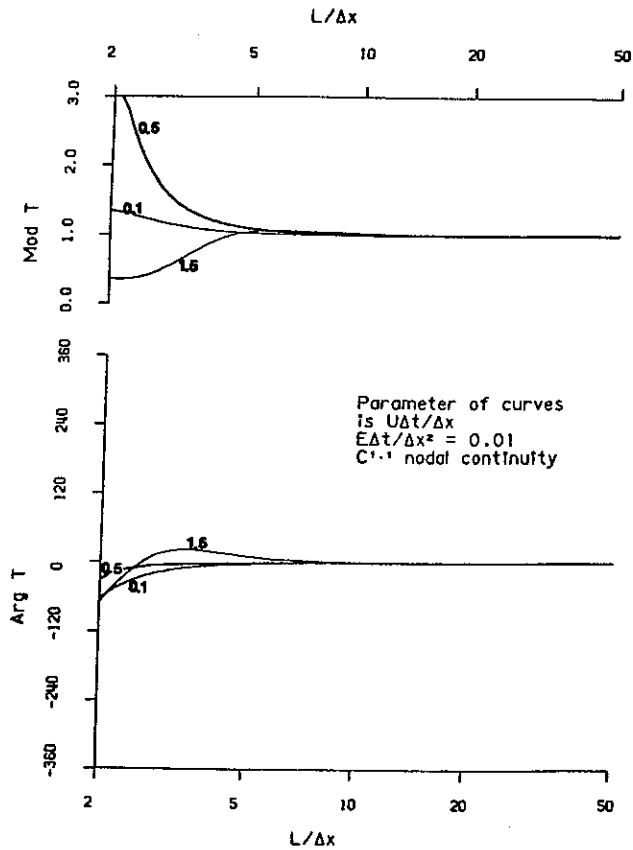
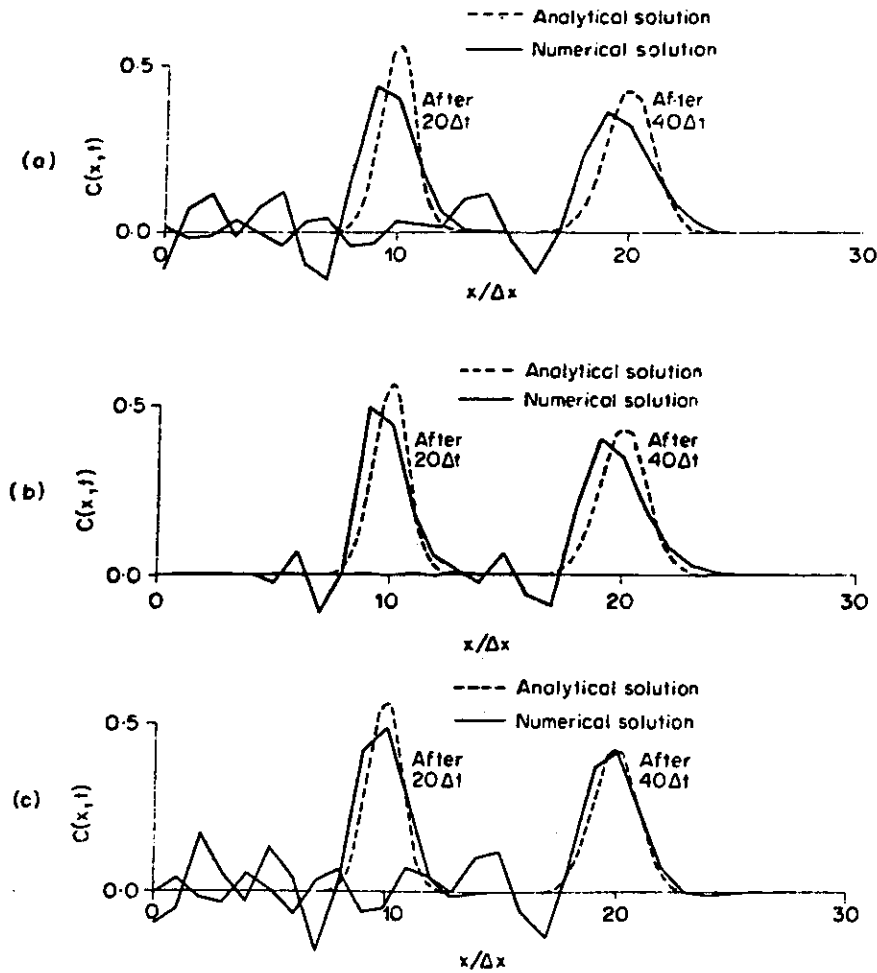


Fig. 68. Wave deformation for Element 5. (Ref. 190)

The phase error increases with the Courant number except when the time derivative is included. The complete Hermitian element (5) using both the space and time derivatives clearly has the least dispersion, and the dispersion is relatively insensitive to the Courant number. The dispersion of the elements using only the spatial derivatives is moderate for Courant number of 1/2, but excessive for larger values. The element using both of these derivatives has the lowest dissipation. The dispersion is greatest with the elements that do not use any space derivatives. These elements also have the greatest dissipation for the five-cell wavelength, thus indicating the importance of spatial order in reducing dispersion. The inclusion of the time derivative alone has little effect on the phase error.

The inclusion of the second space derivative as well reduces the dissipation but has less effect on the dispersion, while the inclusion of the first derivative evoked a marked change from the linear case. Inclusion of only the first time derivative, however, had little effect except to remove the dependence of the dispersion on the Courant number, but the inclusion of the time derivative was much more effective when the first space derivative was already in use. It appears that all of these schemes, except that using both space derivatives, would have stability problems with short wavelengths.

These schemes are compared in regard to convection of a Gaussian wave in the figure below:



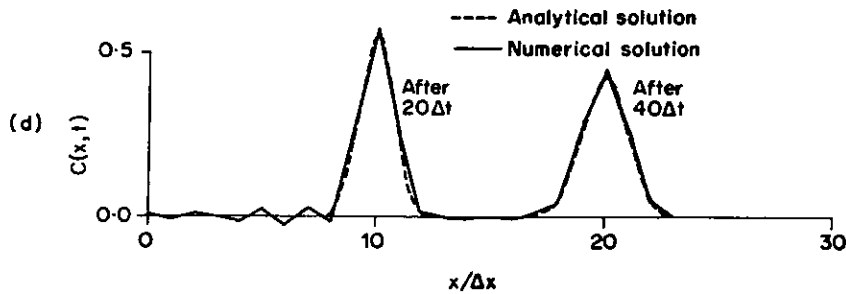


Fig. 69. Comparison of numerical experiments: (a) Element 1 ( $C^{0.0}$  nodal continuity); (b) Element 2 ( $C^{1.0}$  nodal continuity); (c) Element 4 ( $C^{0.1}$  nodal continuity) (d) Element 5 ( $C^{1.1}$  nodal continuity) (Ref. 190)

The element using both the space and time derivatives is clearly superior. Adding the time derivative alone has little beneficial effect, but adding the time derivative to the space derivative has a significant effect. Adding the second space derivative had little effect.

Agarwal (Ref. 8) uses a symmetric compact fourth-order expression for the first derivatives, which amounts to fitting the solution and its derivatives on three points with a Hermite quintic polynomial. The derivative then becomes an additional dependent variable. Adam (Ref. 6) constructs fourth-order methods using Hermite interpolation. Although both of the derivatives become additional dependent variables, the second derivative is analytically eliminated to reduce the size of the system. Krause, Hirschel, and Kordulla (Ref. 116) give a fourth-order method based on Hermite interpolation. Application is made to 3D turbulent boundary layers. Hermitian polynomials are used by Thiele in Ref. 208 for boundary-layer equations.

Watanabe and Flood (Ref. 220) use fourth-order central expressions for the spatial derivatives. The method is formed from Eq. (II-23) using

Simpson's rule for the integration, i.e., using a quadratic to represent the integrand on the interval  $\Delta t$ . This introduces the value at the intermediate time level,  $n + 1/2$ , which is obtained from a cubic Hermite polynomial on the interval over  $\Delta t$ . The resulting implicit scheme has two stages with the stencils



and is fourth order in time and space. Being implicit, the method is unconditionally stable.

Chin, Hedstrom, and Karlsson (Ref. 45) construct higher-order schemes of the method-of-lines type by integrating the differential equation in space as on p. 11. Representation of the integration by Simpson's rule gives a fourth-order three-point method. Methods of higher order are obtained by expanding the range of points in the interpolation for the integrand. Sixth and eight-order forms, involving five and seven points, respectively, are given.

In a series of papers, Ref. 198-200, Steppeler constructs second and third-order symmetric schemes based on polynomials that match some derivatives as well as the solution. The procedure is somewhat complicated in both construction and operation and produces the solution alternately at grid points and at mid-points between grid points at successive time levels. Time advancement is by the usual Taylor series expression of the solution at the new time level about that at the previous level, with the time derivatives in the series replaced by space derivatives through repeated differentiation of the differential equation. Similar Taylor series are

used to give the first three spatial derivatives at the new time level in terms of derivatives at the previous level.

To start with, the solution is represented on each interval bounded by grid points by a polynomial fitted to the solution at the grid points and to the second and third derivatives at the mid-point. The values of the solution and the first derivative at the mid-point are calculated from this polynomial and its derivative. The solution and its first three derivatives are then calculated at the mid-point at the new time level from the Taylor expansions. A spatial Taylor series expansion of the solution at the new time level about the mid-point is then given in terms of the new solution and first three derivative values obtained at this point. The solution at the new time level is also represented on the intervals bounded by mid-points as a polynomial fitting the new solution values at the mid-points and the as yet unknown new second and third derivative values at the grid points. These new derivative values at the grid points are then determined to minimize the least squares integrals of the difference between this polynomial and that from the spatial Taylor series about the mid-points on the intervals bounded by the mid-points, and similarly to minimize the integral of the difference between the first derivatives. This completes one time cycle, with the solution now represented on each interval bounded by mid-points by a polynomial fitted to the solution at the mid-points and to the second and third derivatives at the grid points. Successive time steps then alternate from intervals between the mid-points to intervals between the grid points. This alternation introduces a smoothing into the solution.

The stability limitation is to Courant numbers less than 0.5 in the first-order case, 0.24 for second-order and 0.22 for third-order. A

major disadvantage of this approach is that dissipation occurs even for zero velocity. In fact, the dissipation increases as the Courant number decreases, and is largest for a Courant number of zero. The second-order scheme exhibits an extremum in the phase error at a wavelength for which the dissipation is less than its maximum. The phase error at the larger wavelengths increases as the Courant number decreases.

These trends are illustrated in the figures below:

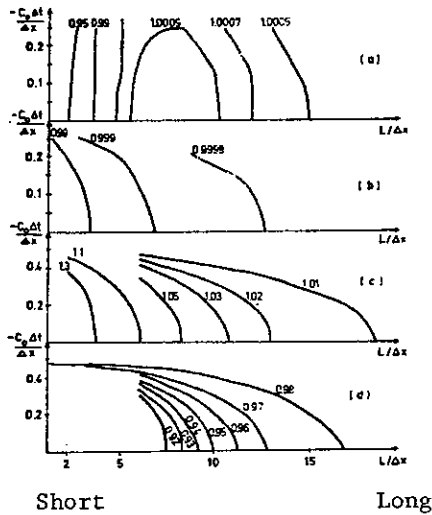


Fig. 70. Relative phase velocity and damping factors for first- and second-degree method. (a) Relative phase velocity  $C/C_0$  of second-degree method. (b) Damping factor  $A_{n+1}/A_n$  of second-degree method. (c) Relative phase velocity  $C/C_0$  of first-degree method. (d) Damping factor  $A_{n+1}/A_n$  of first-degree method. (Ref. 200)

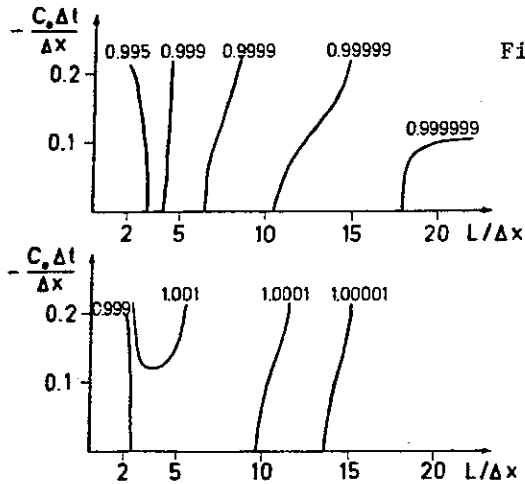


Fig 71. Damping factors (above) and relative phase velocities (below) for the third-degree method, corresponding to the first eigen-value. (Ref. 199)

Both the phase error and the dissipation decrease as order increases, and with the third-order scheme the extremum in the phase error is shifted to lower wavelengths where there is more dissipation. Also, the phase error and the dissipation both decrease with the Courant number at larger wavelengths with third order. There remains some dissipation at zero velocity, however. The third-order scheme is twice as expensive as the second. That the dissipation in these schemes is significant is illustrated in the next figure showing convection of a triangular wave.

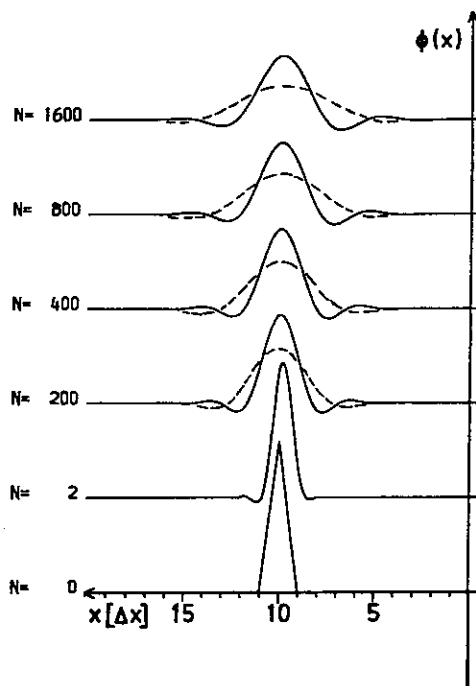


Fig. 72. Solution of the linear advection equation with positive initial values,  $N$ , number of timesteps; -----, second-degree method; ———, third-degree method. (Ref. 199)

The dramatic improvement obtained with the third-order method is evident in the figures on the following pages, showing convection of a two-cell wavelength wave train.

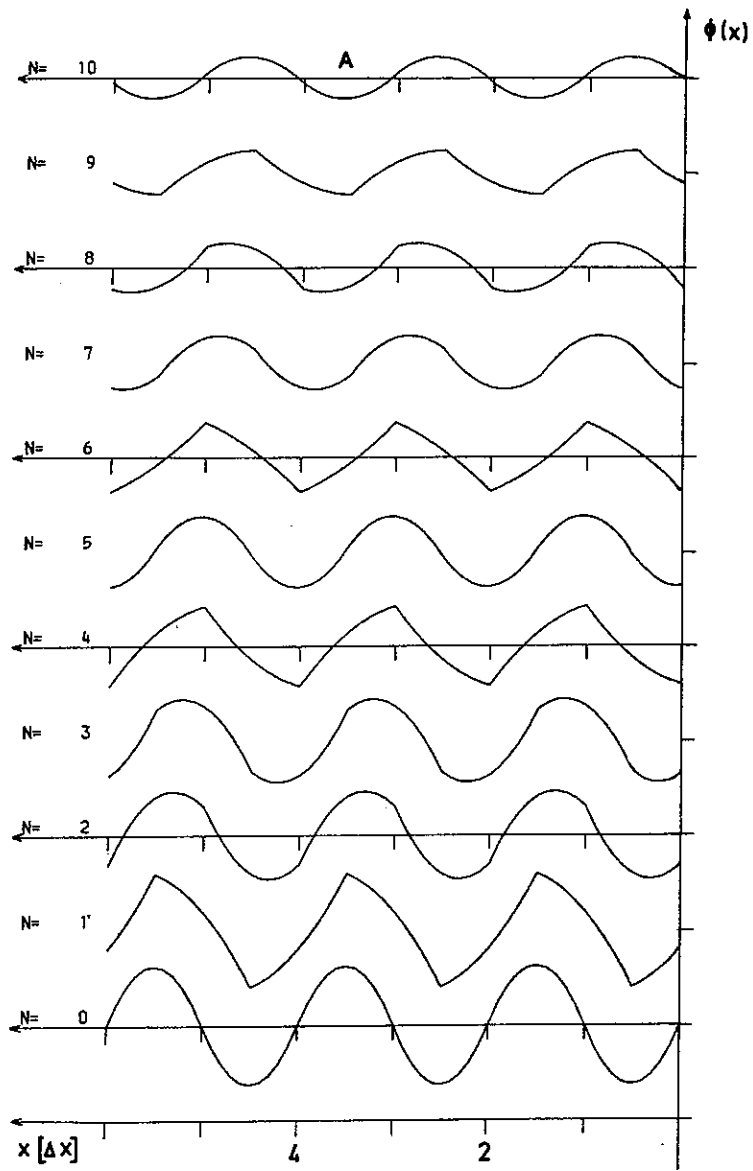


Fig. 73. The time development of the  $2\Delta x$  wave. (A) Second-degree method. (Ref. 199)

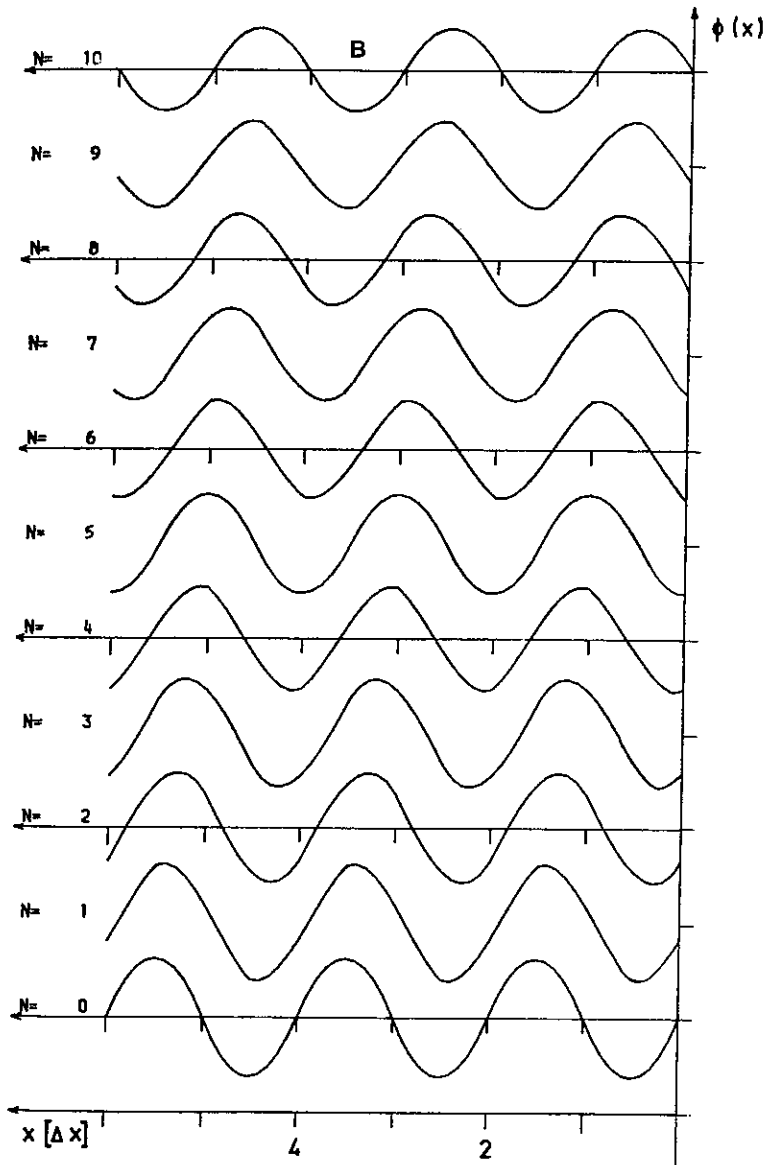


Fig. 73b. Third-degree method.

The 2D case is treated in Ref. 199 by alternating between cells with grid points for corners and cells with center points of the original cells for corners. Certain terms are neglected in 2D.

The dissipation is reduced in Ref. 198 by alternating the third-order time advancement procedure between the Taylor expansion used in Ref. 199 and a third-order leapfrog procedure. This latter procedure uses three time levels, and eliminates one averaging of the solution

between grid points that occurs in the former procedure. The stability limitation is now Courant of 0.3, and the phase error is slightly greater than the original third-order scheme of Ref. 199. With this scheme the dissipation has, unfortunately, also been reduced at the small wavelengths where it is needed. It was, in fact, necessary to introduce some additional smoothing by using the original form once in each five time steps in a 2D shallow water wave problem.

On the whole, these schemes seem to be too cumbersome to be considered for general codes.

#### Pade Difference Methods

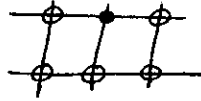
Harten and Tal-Ezer, Ref. 97, give higher-order generalizations of the Crank-Nicholson implicit method, based on the time integration on p. 10, that are nondissipative and unconditionally stable in the linear sense. The usual Crank-Nicholson scheme is constructed from Eq. (II-23) by approximating the integrand with a linear function. Spatially second and fourth-order schemes can be obtained using the following difference representation of  $f_x$ :

$$f_x = \frac{1}{\Delta x} \mu \delta f + O(\Delta x^2) \quad (7a)$$

$$f_x = \frac{1}{x} \frac{\mu \delta}{I + \frac{\delta^2}{6}} f + O(\Delta x^4) \quad (7b)$$

Both of these expressions can be obtained by differentiation of interpolation polynomials - a quadratic fitted to the function at the points  $(i - 1, i, i + 1)$  in the first case, and a quartic fitted to the function at these three points and to the derivative of the function at the points  $(i - 1, i + 1)$  in the second case. The stencil for both schemes is of

the form



The schemes are linearized to second order in time by expanding  $f^{n+1}$  about  $f^n$  as

$$f^{n+1} = f^n + A(\phi^{n+1} - \phi^n) + O(\Delta t^2)$$

where  $A$  is the Jacobian matrix of  $f$  with respect to  $\phi$ . Both schemes remain second order in time under this linearization. The difference equations then are linear and are block tridiagonal in form. The first scheme is second order in space, while the second scheme is fourth order. Both are second order in time.

A scheme that is fourth order in both space and time is obtained by using a Hermite polynomial (cubic in this case) for the integrand. The fourth-order expression of (7b) is used for  $f_x$ , and the second-order expression

$$(u\phi_x)_x = \frac{1}{\Delta x^2} \delta(u\delta\phi) + O(\Delta x^2) \quad (8)$$

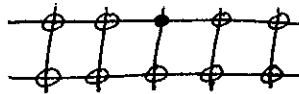
is used for the product derivative. The stencil is again as given above. In order to preserve the fourth order in time, the linearization must be done about some second-order accurate approximation of the new time solution instead of about the old time solution as in the previous case. The result is again a linear block-tridiagonal system of difference equations. The linear stability and order of accuracy do not depend on the intermediate second-order approximations of the solution, which may even be calculated from a scheme that is unstable in itself.

In contrast to the above two second-order time schemes, which are unconditionally stable, this fourth-order time scheme is stable only for

Courant numbers less than unity. It was found that the expansion of the difference representation of the product derivative in (8) to five points, i.e.,

$$(u\phi_x)_x = \frac{1}{\Delta x^2} \mu\delta(u\mu\delta\phi) + O(\Delta x^2) \quad (9)$$

improved the stability, but at the cost of a pentadiagonal, rather than tridiagonal, matrix so that no real gain in efficiency is realized. The stencil is now of the form



This form also has a larger truncation error, though still of fourth order. A two-step version is also given in which the derivative,  $f_x$ , is evaluated in the first step from a tridiagonal solution of (7b), and then is used directly in the solution of the difference equation, which, with this derivative known, is also tridiagonal. This is essentially a spline approach. Hirsh (Ref. 101) uses the Pade forms to construct higher-order three-point spatial approximations, each derivative becoming an additional dependent variable.

### Spline Methods

The spline approach is taken by Rubin and Khosla in Ref. 179 to construct compact methods. Here the solution is represented by cubic splines on each grid interval, with the effect that the higher derivatives become additional dependent variables. The scheme is fourth order on uniform grids and third order on nonuniform. It is noted that the approaches based on splines, Hermitian interpolation polynomials, and Pade approximants are all equivalent.

Rubin and Khosla (Ref. 180) give a number of spline representations

and discuss the relationship with Hermite forms. It is noted that all of the results obtained by the Hermite (Pade, Mehrstellen) development can also be reached with appropriate spline forms. Some of the Hermite forms are equivalent to representations using different spline forms for different derivatives. Others require spline-on-spline representations. Although the overall representations are equivalent, the spline approach provides certain relationships between derivatives that are not shown by the other developments. The spline representations also carry over to nonuniform grids while the others do not.

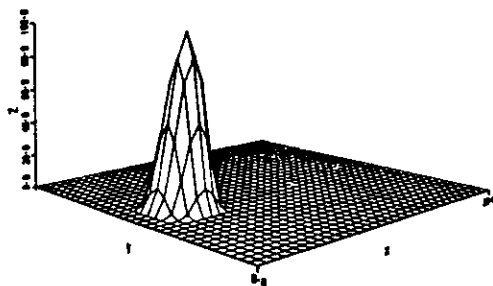
Rubin and Graves ( Ref. 178) construct spatially fourth-order schemes, with second-order time, using cubic splines. The spatial order drops to third for nonuniform grids. The inclusion of diffusion also drops the spatial order by two. The oscillations due to large cell Reynolds numbers were reduced. Cubic splines were used by Price and MacPherson in Ref. 166.

Holla and Jain (Ref. 103) use cubic splines as the interpolation function to construct compact implicit schemes that are second order with three free parameters or third order with one free parameter. These schemes involve a weighted average of the fluxes between true time steps and hence include a scheme of the Crank-Nicholson type. Also included is the scheme of McGuire and Morris (Ref. 144). The schemes are dissipative of order four. The schemes operate in two stages with the 1D stencils



Extension to 2D is by time-splitting.

Pepper, Kern, and Long (Ref. 160) compare a compact fourth-order scheme based on cubic splines with a Galerkin linear finite element scheme. Both schemes use second-order Crank-Nicholson time differencing. The results for rotation of a cosine hill are shown below:



b. Isometric View

Fig. 74. Cosine hill distribution of concentration. (Ref. 160)

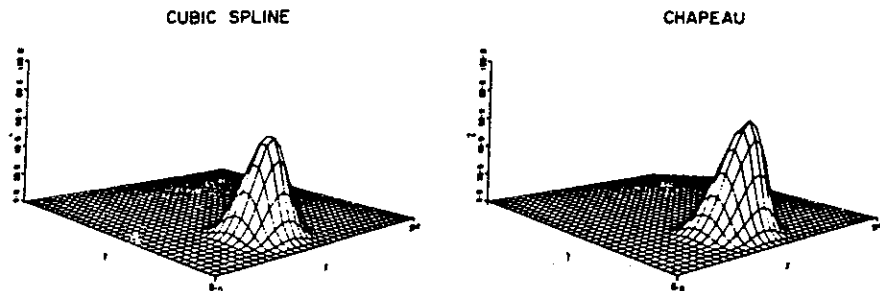
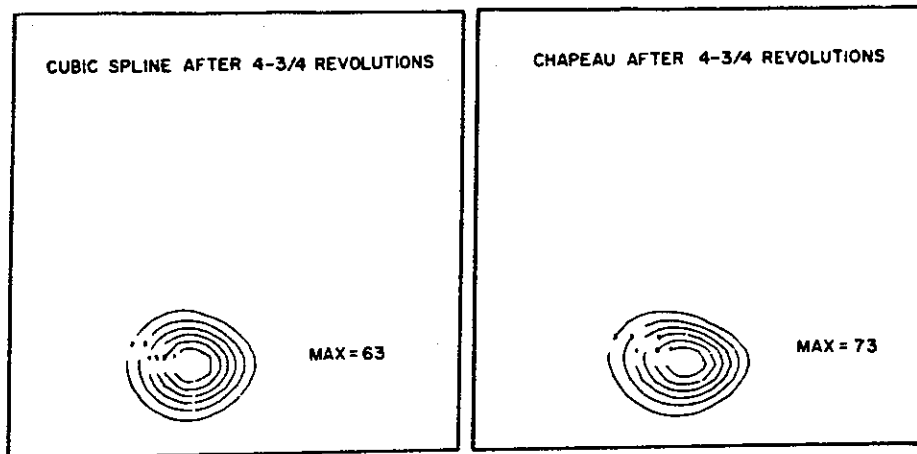


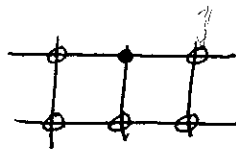
Fig. 75. Concentration after 4-3/4 revolutions using (a) cubic splines (b) chapeau functions with  $\Delta X = \Delta Y = 2500$  m. (Ref. 160)

With nonuniform grids, the noise was greater with the finite element scheme. The noise oscillations are more localized near the cosine hill with the spline scheme. The finite element scheme tends to spread the noise over the entire field. The methods were also applied to a pollution dispersion problem.

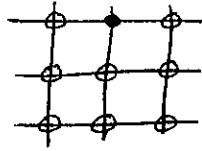
Operator Compact Methods

In Ref. 50, Ciment, Leventhal and Weinberg construct implicit schemes based on a tridiagonal relationship between the solution and the spatial operator at three adjacent points in each direction. Such schemes are referred to as "operator compact implicit" methods. The use of the entire spatial operator, rather than the separate derivatives, in the construction produces schemes which are point-tridiagonal, rather than block-tridiagonal as results from schemes constructed simply by replacing the individual derivatives with compact difference expressions based on Hermite polynomials. The boundary conditions are more easily represented also using the full operator, since values of the individual derivatives are not required. The schemes are fourth-order in space on a uniform grid, and third-order on a nonuniform grid. The schemes given by Peters (Ref. 162) and Krause, Hirschel, and Kordulla (Ref. 116) are of this class, as are the "mehrstellen" methods of Collatz (Ref. 52).

Two second-order time discretizations are given, the Crank-Nicholson form with the stencil



and the three-level Lees form with the stencil



Both of these forms are stable for all time steps provided the cell Reynolds number does not exceed  $\sqrt{12}$ . The Crank-Nicholson form is nonlinear, but the Lees form is linear since the coefficients in that form are evaluated at the previous time step. The nonlinear Crank-Nicholson form is solved by approximate factorization. Both forms were found to converge to a steady state at about the same speed for the parabolic problems considered.

It is noted that the block-tridiagonal compact schemes referred to above do not satisfy a reasonable stability requirement, but at low cell Reynolds numbers no ~~dominate~~ oscillations occur. This is a potential problem for such methods, though.

Leventhal (Ref. 132) derives an integral identity relating the solution values and the values of the inhomogeneous term of the convection-diffusion equation on the points  $(i - 1, i, i + 1)$ . This tridiagonal relationship is

$$r_i^+ u_{i+1} + r_i^c u_i + r_i^- u_{i-1} = q_i^+ f_{i+1} + q_i^c f_i + q_i^- f_{i-1} \quad (9)$$

Schemes with nonzero  $q_i^+$  and  $q_i^-$  are implicit. The expressions for the coefficients involve exponentials of integrals of the functions  $a(x)$  and  $b(x)$ , and integrals of  $f(x)$ , on the interval  $[x_{i-1}, x_{i+1}]$ . If the functions  $a(x)$  and  $b(x)$  are approximated as constants,  $a_i$  and  $b_i$ , on this interval, and the integrals of  $f(x)$  are evaluated by the mid-point rule, the explicit first-order method of Allen and Southwell (Ref. 11) results. If  $a$ ,  $b$ , and

$f$  are taken to be piecewise constant in  $[x_{i-1}, x_{i+1}]$ , with the values in  $[x_{i-1}, x_i]$  represented by the averages of the grid values, etc., the second-order implicit method of El-Mistakawy and Werle (Ref. 66) is obtained.

The present scheme is developed by taking  $a$  and  $b$  to be piecewise quadratic on  $[x_{i-1}, x_{i+1}]$ , i.e., in  $[x_{i-1}, x_i]$ ,  $a(x)$  is represented by a quadratic fitted to the values  $a_{i-1}, a_{i-1/2}, a_i$ , etc. The integrals are evaluated by Simpson's rule. The resulting implicit scheme is fourth order in smooth regions and second order at shocks. This scheme can be extended to conservative form, i.e.,  $(bu)_x$  instead of  $bu_x$ , to time-dependent equations, and to two dimensions. The time-dependent form is constructed using conventional differencing in time, and the version given is in the second-order Crank-Nicholson form. This scheme is in the class of operator compact implicit methods, and is expensive because of the evaluation of exponentials in each of the coefficients. The scheme is being applied to reservoir simulation.

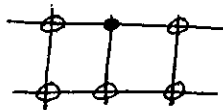
#### Local Solution Methods

Although most methods use interpolation functions of some general type in the construction of difference representations, some schemes use functions obtained as local solutions of the partial differential equation. These local solutions are derived by holding certain quantities locally constant to obtain a form that can be integrated. The use of such functions that have a close relationship to the solution naturally leads to greater accuracy, but these functions often involve exponentials or the like which are expensive to evaluate.

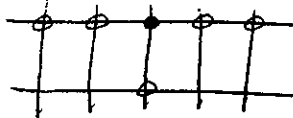
Khaliq and Twizell (Ref. 111) use a local solution in time, assuming constant velocity, and approximate the exponential of the spatial difference operator by Pade approximants. The spatial difference operator was taken to be the second-order central difference in all cases considered. The (1,0) Pade approximant produces the familiar first-order time implicit scheme:



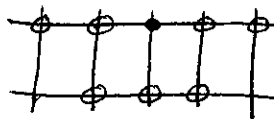
while the (1,1) Pade gives the second-order Crank-Nicholson scheme



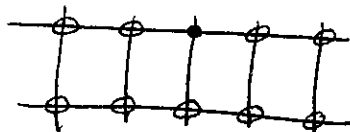
The (2,0) approximant gives the following scheme also with temporal second order:



and the (2,1) Pade gives the second-order scheme



Finally, the (2,2) Pade approximant yields the temporal fourth-order scheme;



In this work these schemes were formulated to be extrapolated to higher temporal order by combining the results of a scheme applied twice over two time steps, and once over a double time step, to eliminate the leading term in the truncation error. This process yields a second-order method from the first-order method with the (1,0) Pade approximant above. From the three second-order schemes above, i.e., the schemes using the (1,1), (2,0) and (2,1) approximants, this process produces fourth, third, and fourth-order methods in time, respectively. The fourth-order scheme above from the (2,2) Pade, leads to a sixth-order time method.

Local solutions are also used by Roscoe, Ref. 176, for a convection-diffusion equation. Here the difference representation of the differential operator

$$aD_{xx} + bD_x$$

is taken as

$$\frac{b}{\Delta x(1 - e^{-\frac{b\Delta x}{a}})} [E - (1 + e^{-\frac{b\Delta x}{a}})I + e^{-\frac{b\Delta x}{a}} E^{-1}]$$

where E is the shift operator. An analogous operator is applied in each direction with multiple dimensions. This difference representation is expensive, because of the exponentials, but it can eliminate the oscillations that occur with covention representation, as is illustrated in the figure on the following page.

The exponential operator compact schemes of Leventhal, Ref. 132, are also based on local solutions in space through the integral idêntity formed from the differential operator.

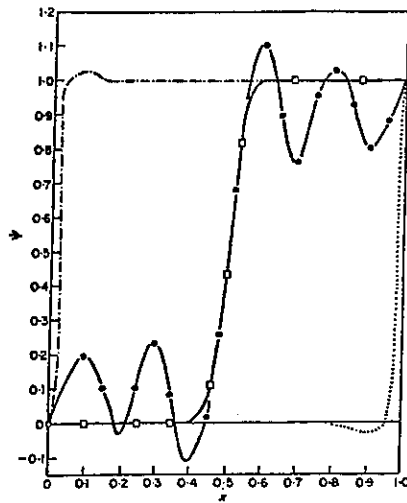


Fig. 76. Solution of equation (4.1) with  $\epsilon = 750$  and  $\psi(0) = 0$ ,  $\psi(1) = 1$ . The BDR and FDR are extremely poor, the CDR is good about  $x = 0.5$ , and very poor elsewhere. The UDR gives excellent results everywhere: ●, Central difference solution; ◻, true solution and the UDR solution: ---, backward difference solution; -·-·-, forward difference solution. (Ref. 176)

Chien, in Ref.43, includes a coefficient in the overall spatial difference expression for a 1D convection-diffusion equation, and evaluates this coefficient such that the difference expression will be exact when the velocity is constant on the interval spanned by the differences. In a similar fashion, a coefficient affixed to the first-order forward time difference expression is evaluated to make the difference equation be exactly satisfied by the analytical solution of an approximation of differential equations in which all of the off-center terms in the spatial difference expression are included in source term, which is considered constant in time.

In actual computation, approximate truncated expansions of the exponentials are used to avoid the computation time required to evaluate the exponentials. The use of such difference expressions based on locally exact solutions removes the stability limitation normally associated with explicit methods. In the case of nonuniform velocity the accuracy remains

only second-order, however, and second-order artificial diffusion is introduced that is proportional to the velocity gradient.

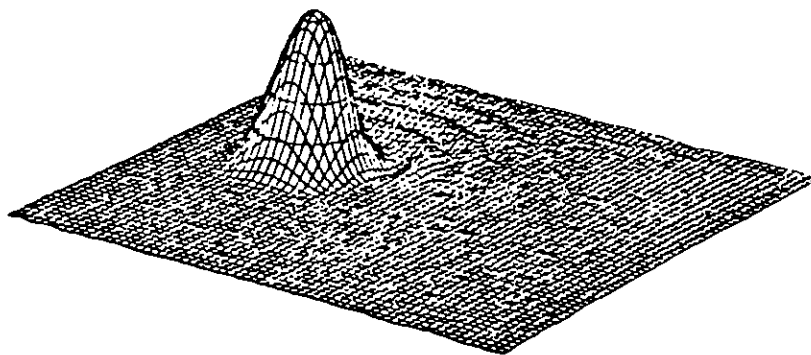
In higher dimensions, with no cross-derivatives, the above 1D spatial difference expression is applied in each direction using the corresponding velocity component and spacing interval. Results are given for several 2D flow problems which show that Courant numbers in excess of unity can, in fact, be used. There is no improvement in accuracy, however, so that the use of locally exact solutions is primarily a device to improve stability of explicit methods.

A type of local solution is given by Kellogg, Shubin, and Stephens in Ref. 109 for a convection-diffusion equation. This scheme incorporates the local solution in the difference coefficients of the diffusion term and hence is not relevant to pure convection. Like the first-order upwind scheme, and unlike the central scheme, this second-order scheme does not have a cell Reynolds number restriction.

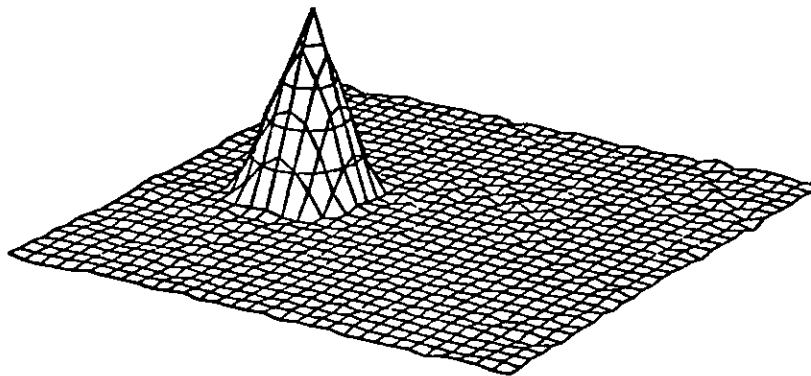
#### Spectral and Pseudospectral Methods

Orszag (Ref. 154) notes that the principal source of inaccurate results with finite difference schemes is phase error, and that accurate spatial differencing is the prime requirement. In spectral methods, the solution is expanded in Fourier series, and the Galerkin approach is used to solve the equations numerically. These methods are essentially of infinite order in space, and thus have essentially no phase error.

Comparisons are made with the second and fourth-order Arakawa finite-difference methods on the revolving cone problem:



(c)



(d)

Fig. 77. Three-dimensional  $(x_1, x_2, A)$  perspective plot of the  $A(x,t)$  field obtained after revolution using (a) second-order Arakawa scheme on  $32 \times 32$  space grid; (b) fourth-order Arakawa scheme on  $32 \times 32$  space grid; (c) fourth-order Arakawa scheme on  $64 \times 64$  space grid; (d) cut-off Fourier-expansion scheme  $32 \times 32$  space grid. (Ref. 154)

The spectral method here used second-order leapfrog differencing in time.

The reduction that occurs in both phase error and dissipation with

increased order is clearly evident here. The spectral method is superior

to the fourth-order finite difference method on twice as many grid points

in each direction. Second-order methods require twice as many points again.

The stability limit of the spectral method is  $\frac{1}{\pi}$  for the Courant number,

whereas those of the second and fourth-order methods are 1.0 and 0.73,

respectively. The spectral methods thus require more time steps and more

work per time step.

Pseudospectral and spectral methods are compared by Fox and Orszag in Ref. 75. Pseudospectral approximation uses truncated spectral series to obtain approximations to derivatives and imposes the differential equation at selected discrete points. Spectral approximation attempts to distribute the error more uniformly by making the error in the differential equation orthogonal to the retained spectral functions.

Gazdag (Ref. 77) constructs a pseudospectral scheme of very high order in space by expressing the spatial derivatives in terms of Fourier transforms of the solution. The explicit method is based on the usual Taylor series expansion of the solution at the new time level about that at the previous level, with the time derivatives expressed in terms of space derivatives through repeated differentiation of the differential equation. In this scheme the velocity is not assumed to be uniform, so that spatial derivatives of the velocity appear as well. The time order is determined by the extent to which the Taylor series is taken. The spatial order is essentially infinite.

The dissipation and the phase error generally decrease as the temporal order increases. Convection of a Gaussian through one complete rotation reduced the peak by 0.18% for the third-order method and by 0.11% for the fourth. In neither case were the trailing oscillations greater than 0.005% of the peak in amplitude, as seen in the figure on the following page.

Diffusion can be included either by time-splitting, where the solution is first convected and then diffused, or directly, with the diffusion terms being included in the differential equation when expressions of the time derivatives are obtained by repeated differentiation. The latter procedure is more accurate, especially for large diffusion coefficients.

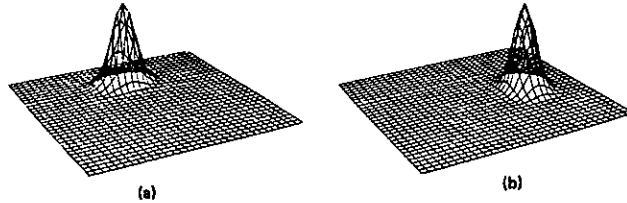


Fig. 78. Perspective view of the Gaussian distribution in Experiment 1 of Table I. (a) At  $\pi/2$ , (b) At  $\pi$  turn from its initial position. The mesh size is  $32 \times 32$ . (Ref. 77)

The Fourier transforms naturally increase the computing time, but the one-dimensional fourth-order version was found to be only about twice as expensive as conventional fourth-order methods. This comparison is expected to improve in higher dimensions.

A pseudospectral method for convection-diffusion based on an expansion in exponential functions is given by Christensen and Prahm in Ref. 48. This expansion takes advantage of the fast Fourier transform. Boundaries are included by specifying exponential decay of the solution thereon. This generates some aliasing which is suppressed with a selective filter passing only wavelengths greater than a certain value. The filter was applied at regular intervals after a certain number of time steps. The scheme is operative only for velocity fields that do not vary rapidly. The time discretization was leapfrog.

Comparison of the results of a number of schemes for revolution of a cone is given in the table following:

TABLE I  
Uniform Rotations of the Gaussian Distribution

Experiment	Order of scheme $p$	Rotations		$\phi_{\max}$ in degrees (approx.)	$\frac{2\pi}{\Omega\Delta t}$	Maximum at a meshpoint	Minimum at a meshpoint
		Clockwise	Counter Clockwise				
1	3	0	0	80	400	1.0000	0.0000
		$\pi/2$	0			0.9996	0.0000
		$\pi$	0			0.9991	0.0000
		$3\pi/2$	0			0.9987	0.0000
		$2\pi$	0			0.9982	0.0000
		$2\pi$	$\pi$			0.9973	0.0000
		$2\pi$	$2\pi$			0.9964	0.0000
2	4	0	0	80	400	1.0000	0.0000
		$\pi/2$	0			0.9997	0.0000
		$\pi$	0			0.9995	0.0000
		$3\pi/2$	0			0.9992	0.0000
		$2\pi$	0			0.9989	0.0000
		$2\pi$	$\pi$			0.9984	0.0000
		$2\pi$	$2\pi$			0.9979	0.0000

(Ref. 77)

The maximum error after one revolution with the present method was 2%. This small error was achieved only by the spectral or pseudospectral methods in this comparison. Pseudospectral methods are about a factor of 2 faster than spectral methods.

#### Moment Methods

Egan and Mahoney (Ref. 64) construct a method based on conserving the zeroth, first and second moments of the distribution within each grid interval so as to conserve the moments. This scheme will convect a square wave exactly without distortion in a uniform velocity field, but will deform all other waveforms into a square wave. Diffusion is included in a separate stage of a time-split process. An extension to 2D is also given.

Pepper and Baker, Ref. 159, use the method of moments, given by Egan and Mahoney (Ref. 64), in which the first three moments of the concentration within a cell are preserved during the convection. In this method a single cell of concentration is convected without dispersion or dissipation:

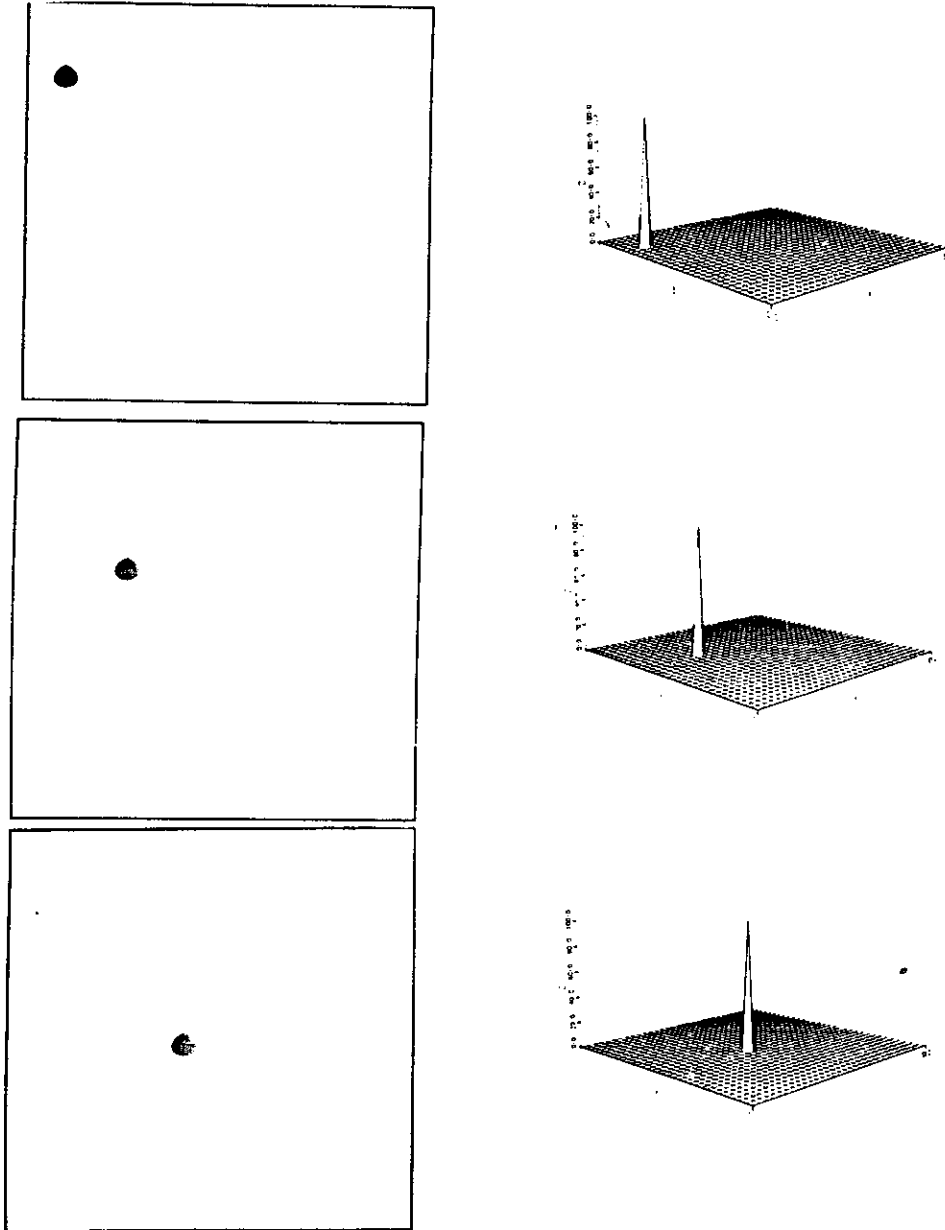


Fig. 79. Advection of concentration ( $C=100$ ) in two-dimensions;  $V=(1,1,0)$ ;  $\Delta X = \Delta Y = 1$ ;  $\Delta t = 0.5$ . (Ref. 159)

A width correction procedure due to Pederson and Prahm (Ref. 158) is used to check the lateral spread of concentration within each cell. This correction is also discussed by Pepper and Long (Ref. (16)). Diffusion is added through time-splitting. Application is made to atmospheric pollutant transport.

Pederson and Prahm also used a different form for the second moment designed to reduce the dissipation, and Pepper and Long found this form to give better results than the original form used by Egan and Mahoney when the velocity was uniform. However, with nonuniform velocity, the Pedersen-Prahm form can be very inaccurate. A comparison of the two forms for convection of a revolving cosine distribution is shown below:

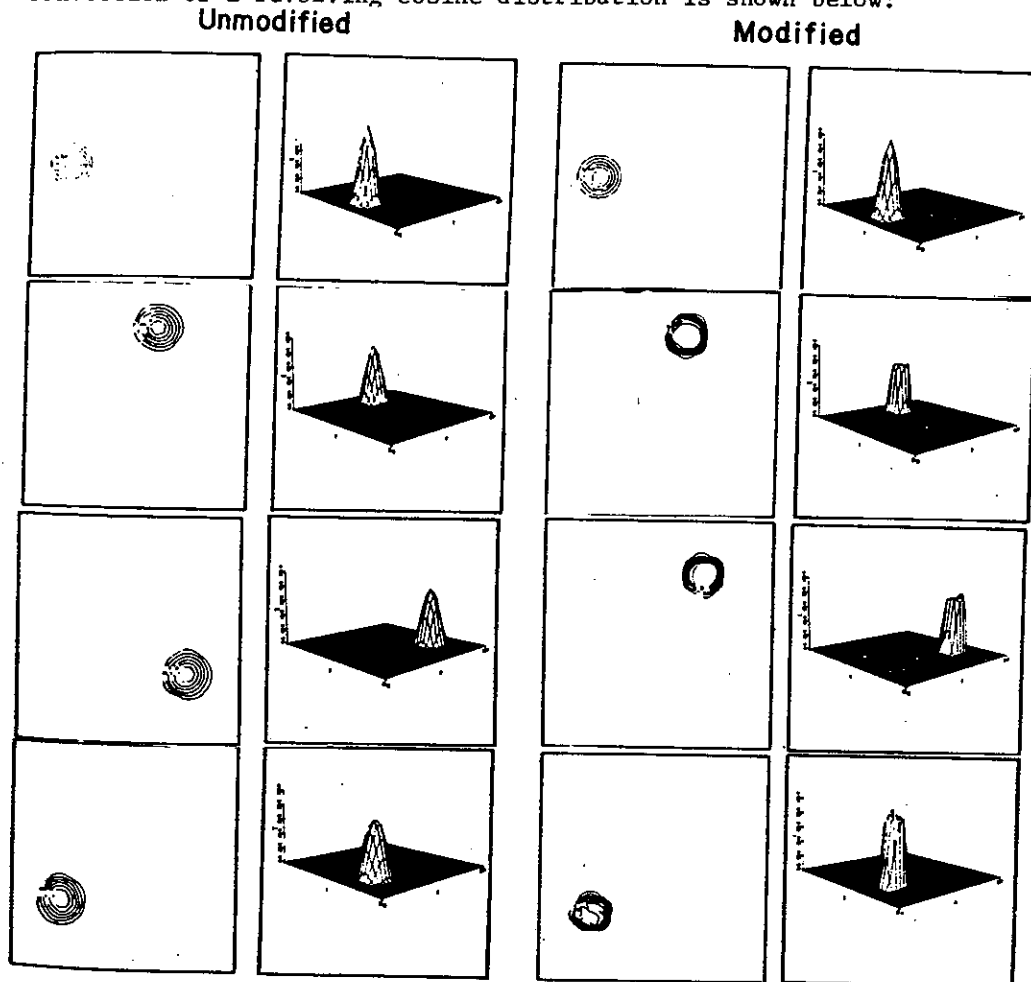


Fig. 80. Concentration contours after  $3/4$  revolution for unmodified/modified methods. (Ref.159)

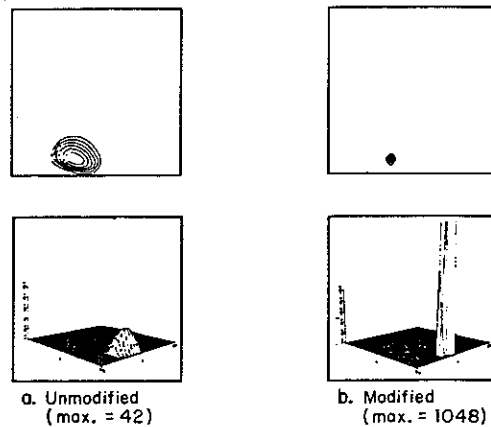
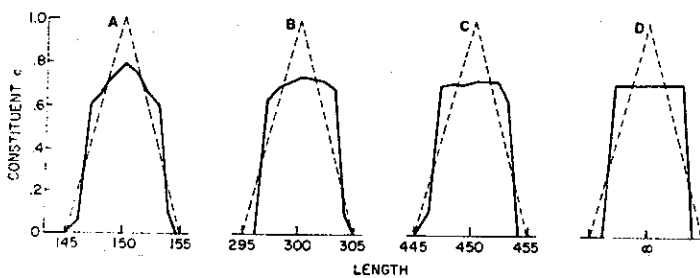


Fig. 81. Concentration contours for unmodified and modified methods after 4-3/4 revolutions. (Ref. 159)

The original form is clearly superior, but does have noticeably more dissipation than the modified form. The width-correction term can also degrade the accuracy with a non-uniform velocity.

The second-moment conserving method of Egan and Mahoney (Ref. 64), as extended by Pederson and Prahm (Ref. 158), is analyzed by Kerr and Blumberg in Ref. 110 for uniform velocity. Results for the convection of a triangular wave are shown below:



(Ref. 110)

	INITIAL CONDITIONS	A 15 WIDTHS	B 30 WIDTHS	C 45 WIDTHS	D ∞ WIDTHS
$\int c^2 dx$	• 3.4000	3.3490	3.4470	3.4480	3.5287
$\int c^3 dx$	• 2.1330	1.6440	1.7010	1.7020	1.7788
$\int \left(\frac{\partial c}{\partial x}\right)^2 dx$	• 0.4000	0.5597	0.7710	0.7640	1.0082
$\int \left(\frac{\partial c}{\partial x^2}\right)^2 dx$	• 0.2400	0.7853	1.3320	1.2730	2.064

Fig. 82. A comparison between the analytical and numerical distributions for advection intervals of 15, 30, 45 and ∞ wedge-widths with  $\sigma = 0.3125$ .

Although there are no dispersion effects, the wave is eventually deformed into a rectangle. This effect is more pronounced at lower Courant number. The scheme preserves the long waves but amplifies certain short waves, a property that may lead to instability in nonlinear problems. This scheme is compared with second and fourth-order leapfrog methods and another method that is fourth-order in time but second in space:

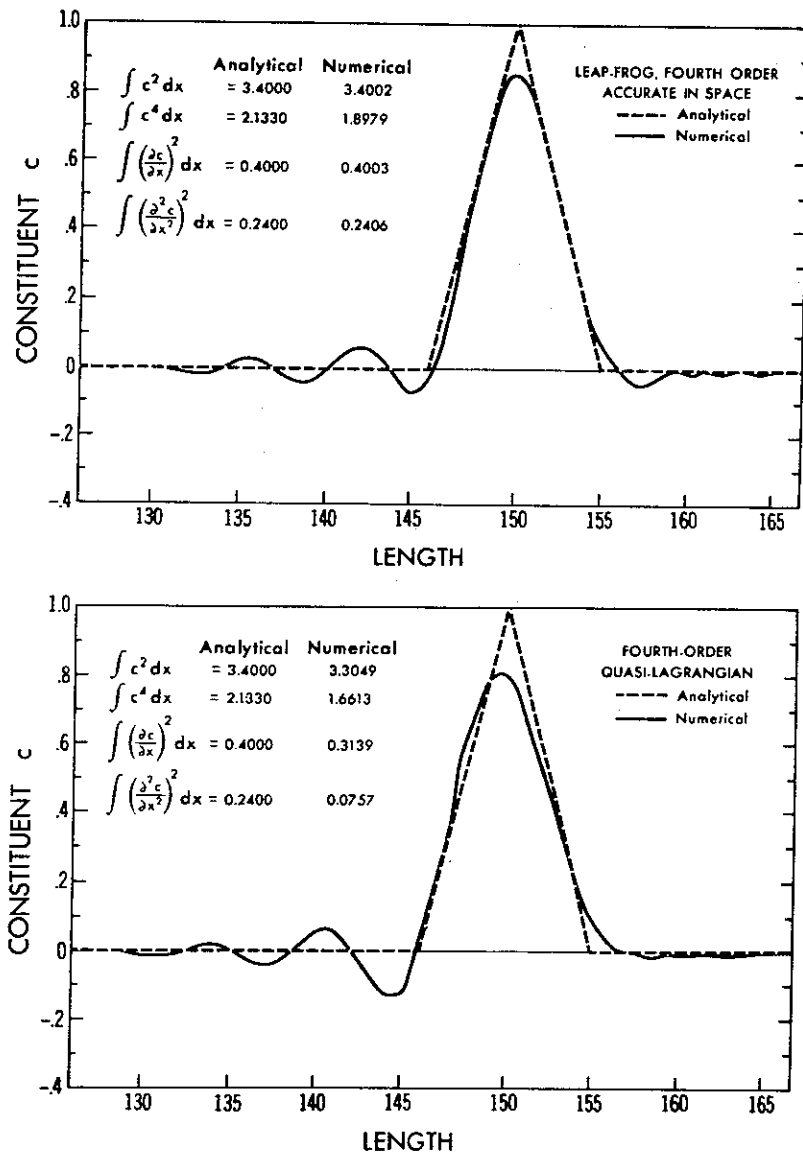
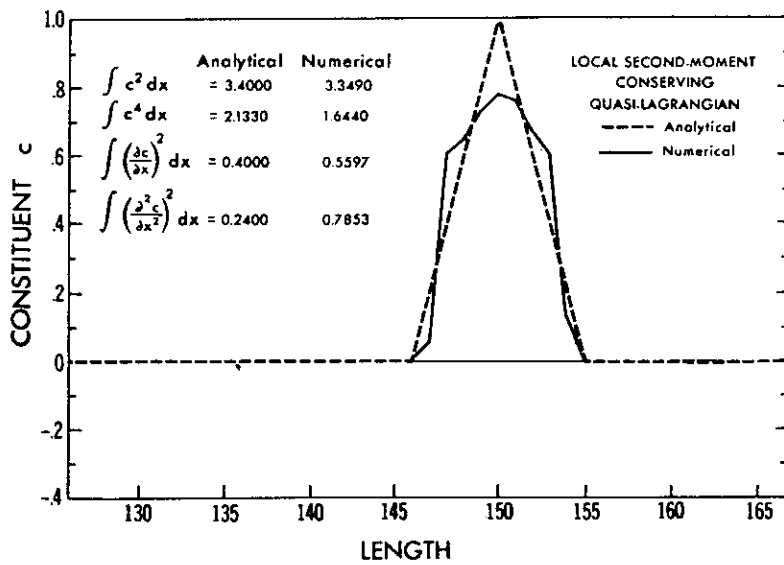
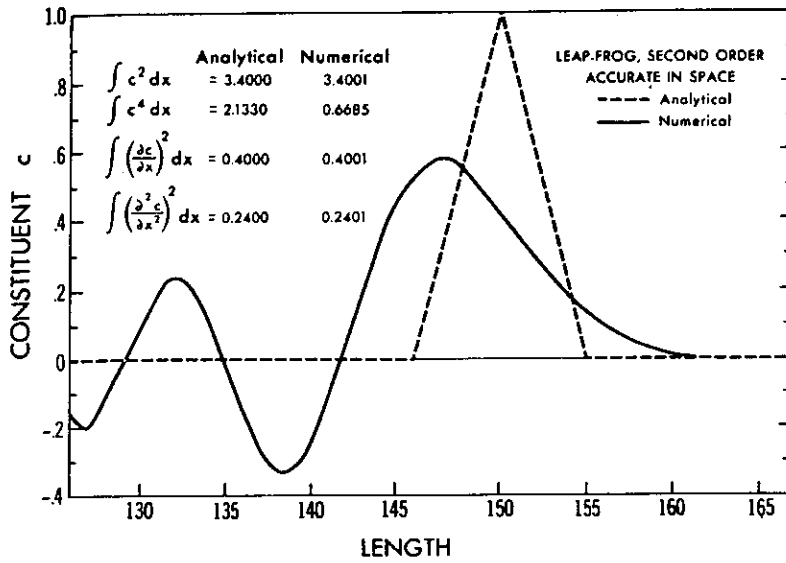


Fig. 83. A comparison between the analytical distribution and several numerically obtained distributions after an advection interval of 15 wedge-widths with  $\sigma = 0.3125$ . (Ref. 110)

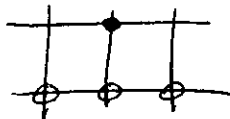


(Fig. 83 continued)

The improvement in both dispersion and dissipation to be gained with higher order is evident upon comparison of the two leapfrog results here. The present method eliminates the trailing oscillations due to dispersion but badly deforms the wave.

Wesseling (Ref. 222) constructs difference schemes by choosing a free parameter in a scheme of given order of consistency so as to minimize the weighted deviation of the difference solution from the analytical solution for a harmonic wave in the least square sense. This minimization and the requirements for order determine the coefficients in the difference expression. The weight function depends on the wave number of the wave, and ideally should be the square of the modulus of the Fourier transform of the exact solution at time  $t$ . The use of this ideal form of the weight function would require the exact solution and hence is not reasonable. Difference schemes can be developed, however, using weight functions corresponding to certain specified forms of the solution. Four forms are considered: (1) harmonic wave, (2) step function, (3)  $2\Delta x$  wave, and (4)  $2n\Delta x$  wave with  $n = 2, 3$ . Each of these will convect the solution form on which it is based exactly. The harmonic wave form produces the conventional schemes. The last two forms lead to schemes which will model the shorter waves well.

With the stencil



and only first-order required, the first of the above forms produces the Lax-Wendroff scheme (Ref. 121), while the second gives the upwind scheme of Courant, Isaacson, and Rees (Ref. 54). This latter scheme is first order in space, but the other three are second-order. The temporal order is the same as the spatial for uniform velocity, but becomes first order with nonuniform velocity. The last two lead to schemes with cosine functions of the Courant number for coefficients.

Dispersion and dissipation for the first and last of these schemes are compared below:

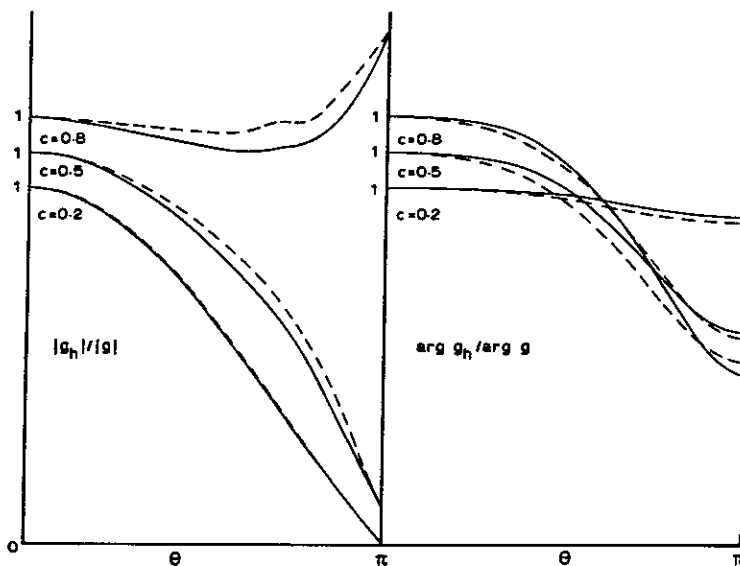


Fig. 84. Dispersion and dissipation: —, Lax-Wendroff; ----, scheme 4. (Ref. 222)

Although the results are not greatly different, the Lax-Wendroff scheme does have more dispersion, but less dissipation, than the other scheme. These two schemes are compared for convection of a Gaussian distribution in the next figure.

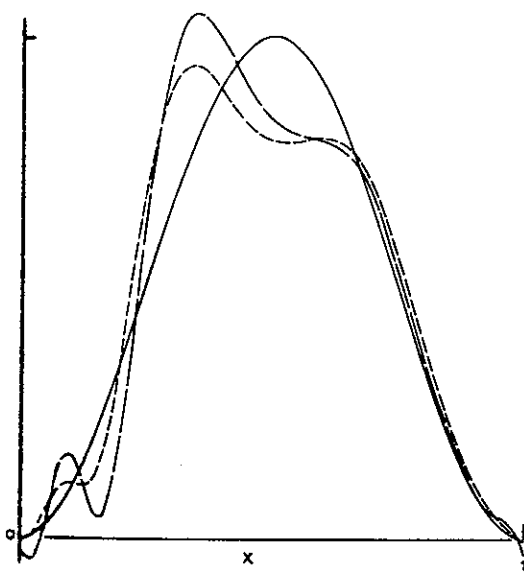
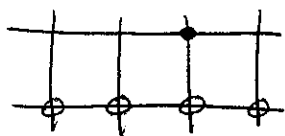


Fig. 85. Results for test-case 4: —, exact solution; — —, Lax-Wendroff; - · - ·, scheme 4. (Ref. 222)

Neither is very good, but scheme 4 has less oscillation. The increased dissipation is evident also, however.

Higher order schemes are obtained with the stencil



The scheme produced by the step-function form is identical to the zero average phase error of Fromm (Ref. '71). The first scheme is the classical third-order scheme. The other three are second order. Again the temporal order drops to one with nonuniform velocity. Three of these schemes are compared for dispersion and dissipation below

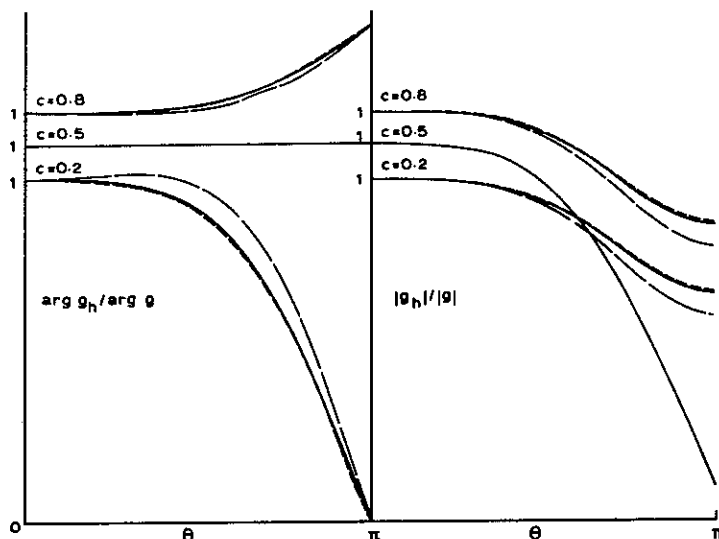


Fig. 86. Dispersion and dissipation: —, scheme 5; - - -, scheme 6 (Fromm); - · - ·, scheme 8. (Ref. 222)

The only noticeable difference here is the somewhat improved phase error of the Fromm scheme, again accompanied by more dissipation, however. The scheme designed for  $2\Delta x$  waves was worse than the others with both stencils.

The multi-stage third-order Burstein and Mirin scheme (Ref. 35, also Rusanov, Ref. 183) was also included in the comparison and found to be slightly more accurate than the present schemes using the second stencil with free parameter in the former scheme chosen so that the scheme is fourth-order in space though still third in time. Other choices make this scheme significantly worse than the present schemes as shown on the following page.

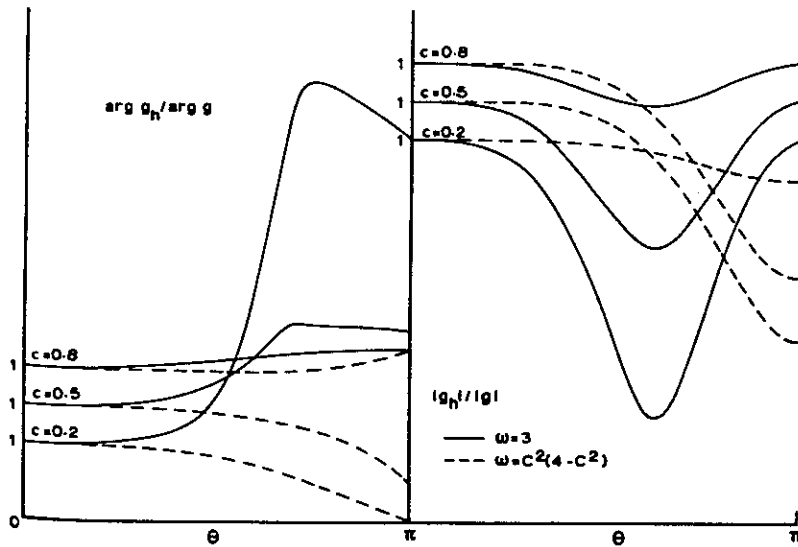


Fig. 87. Dispersion and dissipation of the Rusanov-Burstein-Mirin scheme. (Ref. 222)

Of all these schemes the conventional forms, i.e., those based on convecting the harmonic wave form, are best. The special forms designed to enhance the short wave accuracy are more time-consuming because of the cosine functions involved at each point and did not show significant improvement over the conventional forms.

#### Finite Element Methods

Baker, Soliman, and Pepper (Ref. 23) give a Galerkin finite element algorithm using quadrilateral elements and linear basis functions. For 2D the use of bi-linear basis functions and 1D time-splitting through approximate factoring is compared. Some comparisons for the revolving cone problem are shown on the following page. The second and last figures here are for the finite element solution in the unsplit and split 2D forms. The accuracy is virtually the same with the two forms, but the split form requires one-fourth the time and one-fifth the storage of the unsplit form. The third figure is from a finite difference (second-order Crank-Nicholson)

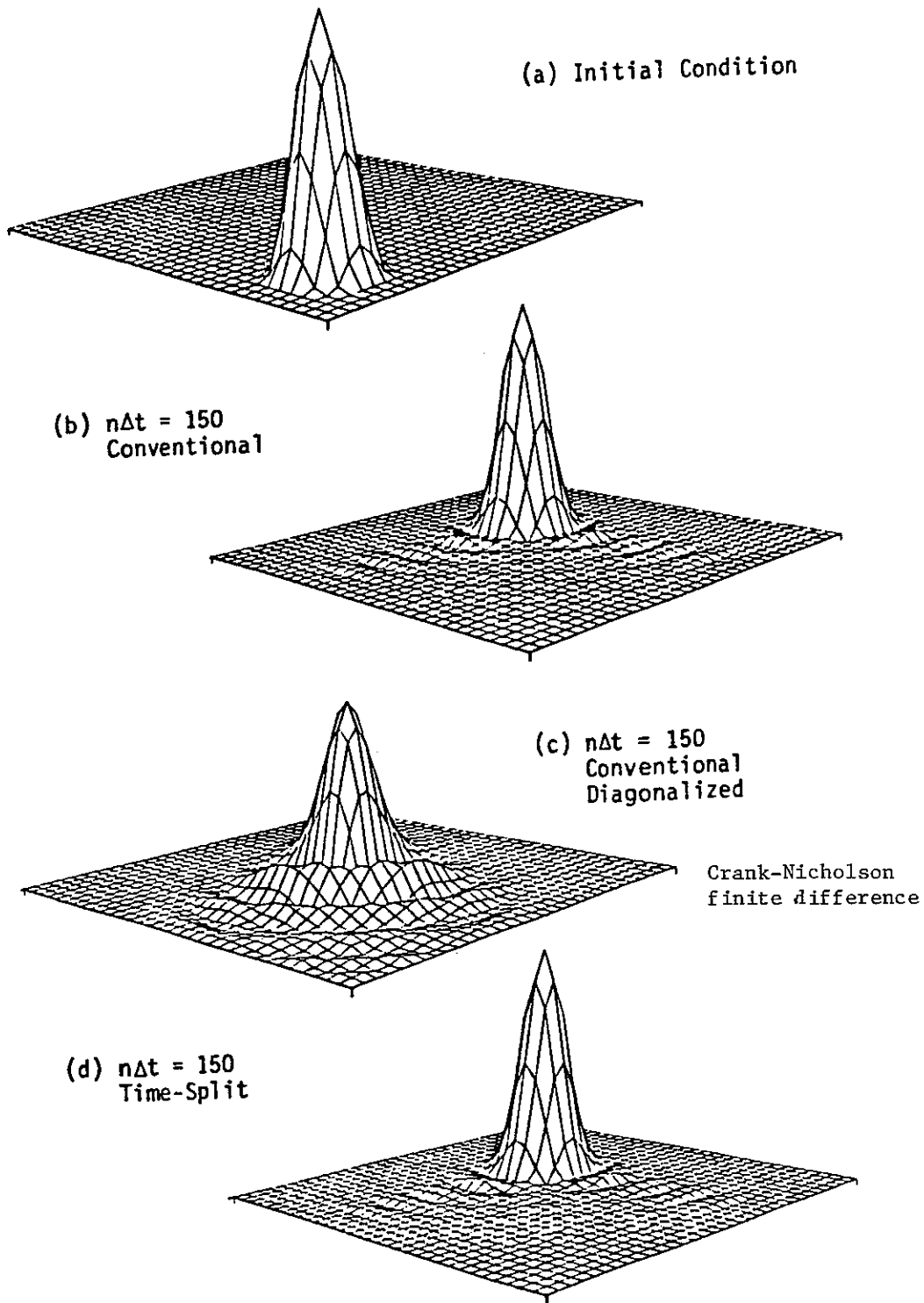


Fig. 88. Advection of environmental release in constant velocity field  $\vec{U}_1$ .  
 $C = 0.1$ . (Ref. 23)

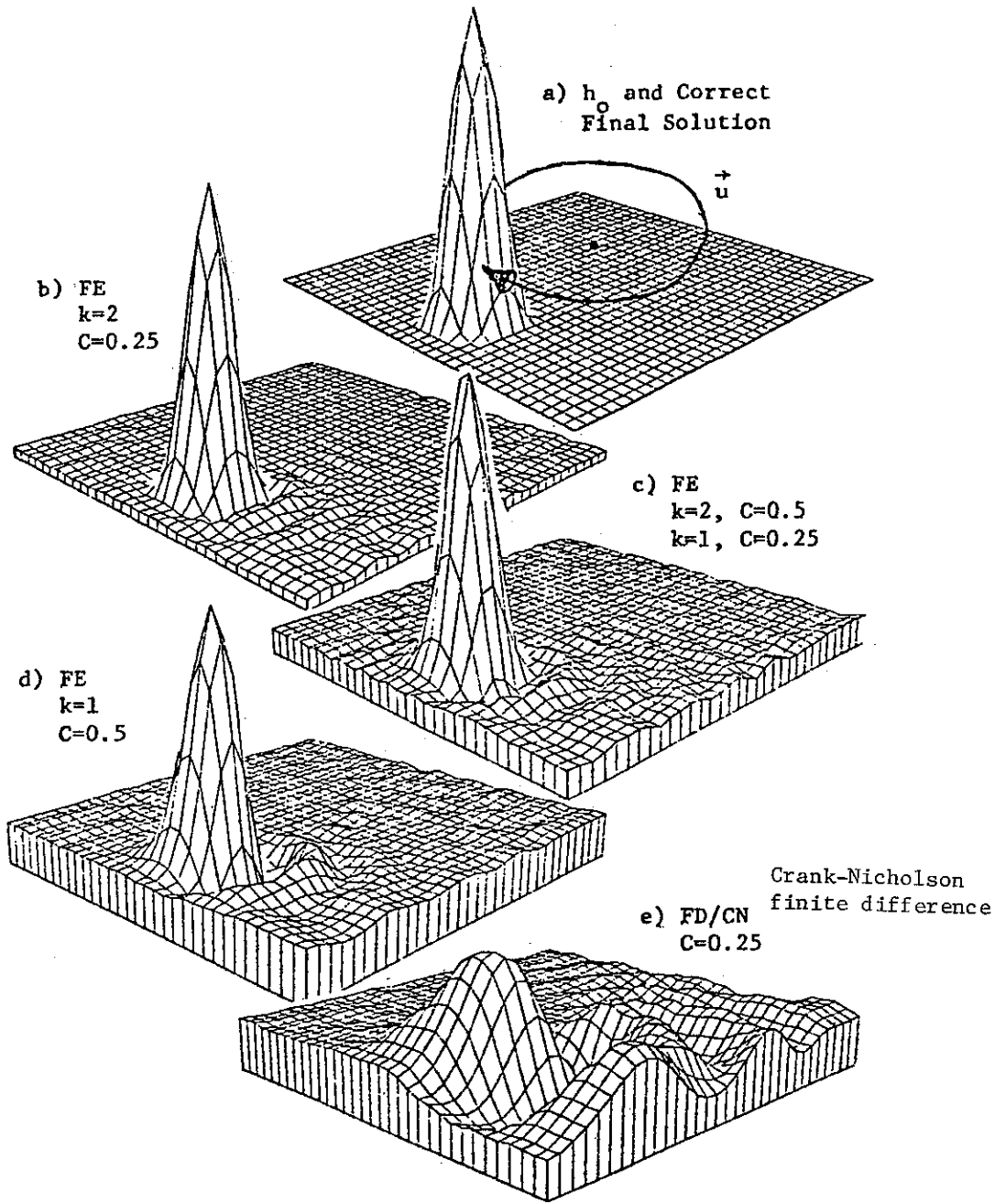


Fig. 89. Rotational convection of a symmetric surface  $h_0$ . (Ref. 23)

type of approach. The reduced dispersion and dissipation with the present form are evident.

This procedure is further developed by Baker in Ref. 18. Here a dissipative mechanism is added by requiring the gradient of the residual to be orthogonal to the basis functions also. The procedure is extended to quadratic basis functions, and the time-splitting factorization is further developed for multiple dimensions. With quadratic elements the time-split factorization is to pentadiagonal matrices, rather than tridiagonal as in the linear case. The scheme based on the linear element is shown to have sixth-order phase error for one value of a free parameter associated with the added dissipation and fourth-order otherwise. The dissipation is fourth order. Without the dissipation this scheme is thus fourth order and neutrally stable. The improvement using the quadratic element was found to be significant, at a cost of about 1% in storage and 16% in time. Less dissipation is required with the higher-order version.

In Ref. 21, Baker and Soliman extend the algorithm to treat free surfaces. Further comparisons for the revolving cone are also given in the figure on the following page. The improvement gained with the higher-order element ( $k = 2$ ) is clear here. The dispersion and dissipation decrease with the Courant number.

Further amplification of this scheme is given by Baker in Ref. 17, by Baker and Soliman (Ref. 20) and by Baker (Ref. 16). Here extension is made to general curved-sided elements for use with curvilinear coordinate systems. The cartesian coordinates within each element are given by the same type of interpolation from nodal point values used for the solution. A differential constraint to enhance satisfaction of continuity is also added. The dissipation mechanism is expanded to include two free parameters.

The scheme based on the linear element is second order in phase error and first order in dissipation for arbitrary values of these parameters, but can be made sixth order in phase error for a particular choice, with the dissipation at third order. Without the dissipation the scheme is fourth order.

With the quadratic element, the scheme is only second-order without the dissipation, and is zero order for arbitrary values. The scheme can be made fourth order in phase for a particular choice of parameters. The formal accuracy of the quadratic element is less than that of the linear, but the performance of the former seems to be somewhat better. Application is made to the shallow water equations.

Further results from the finite element method of Baker and Soliman, these from Ref. 22 for convection of a cone, are given below.

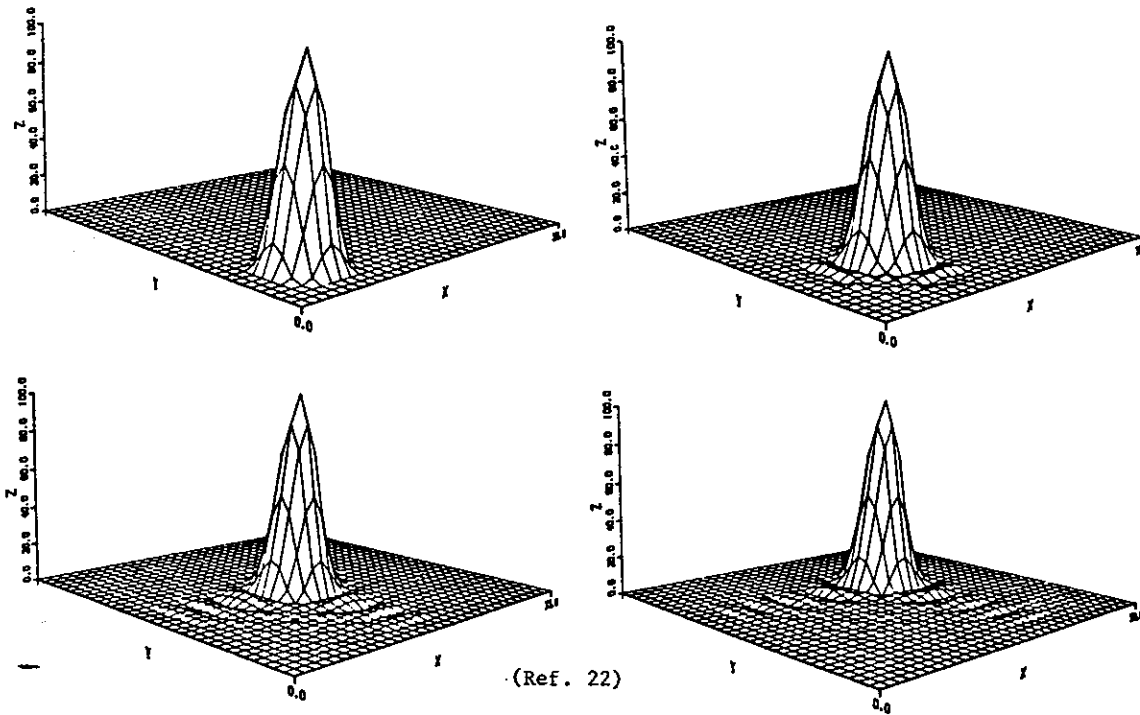


Fig. 90. Advection of concentration cone.  $C = 0.1$ ,  $n\Delta t = 0, 50, 100, 150$ .

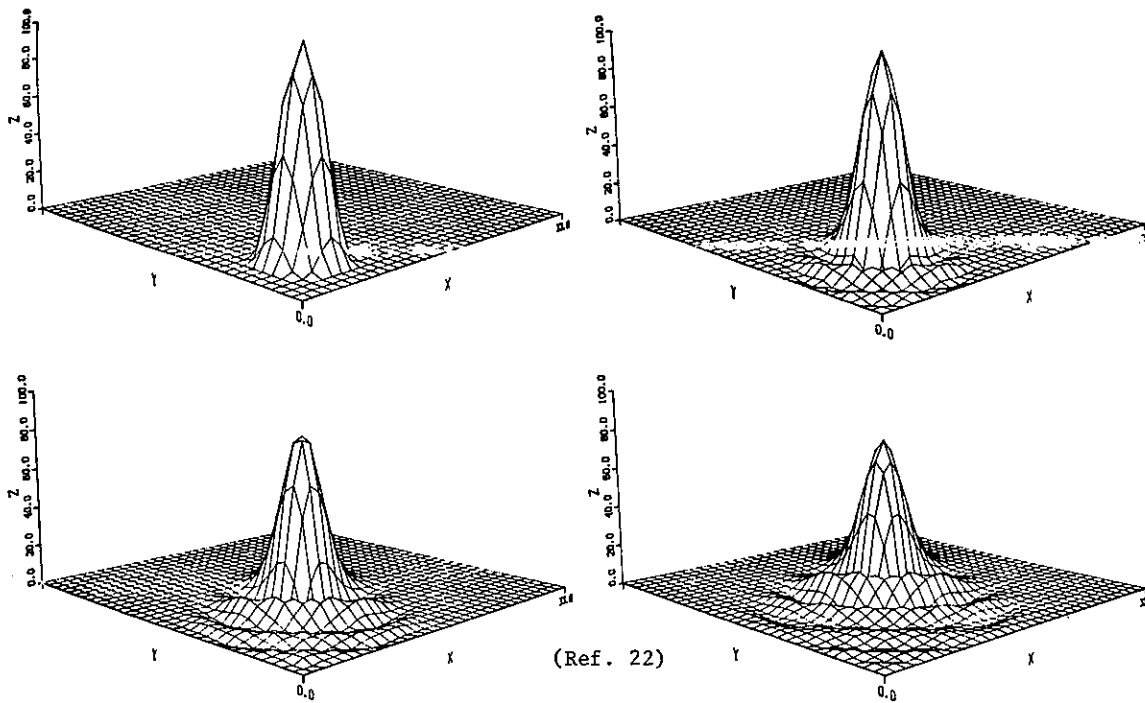


Fig. 91. Advection of concentration cone.  $C = 0.1$ , diagonal transient matrix,  $n\Delta t = 0, 50, 100, 150$ . Crank-Nicholson finite difference.

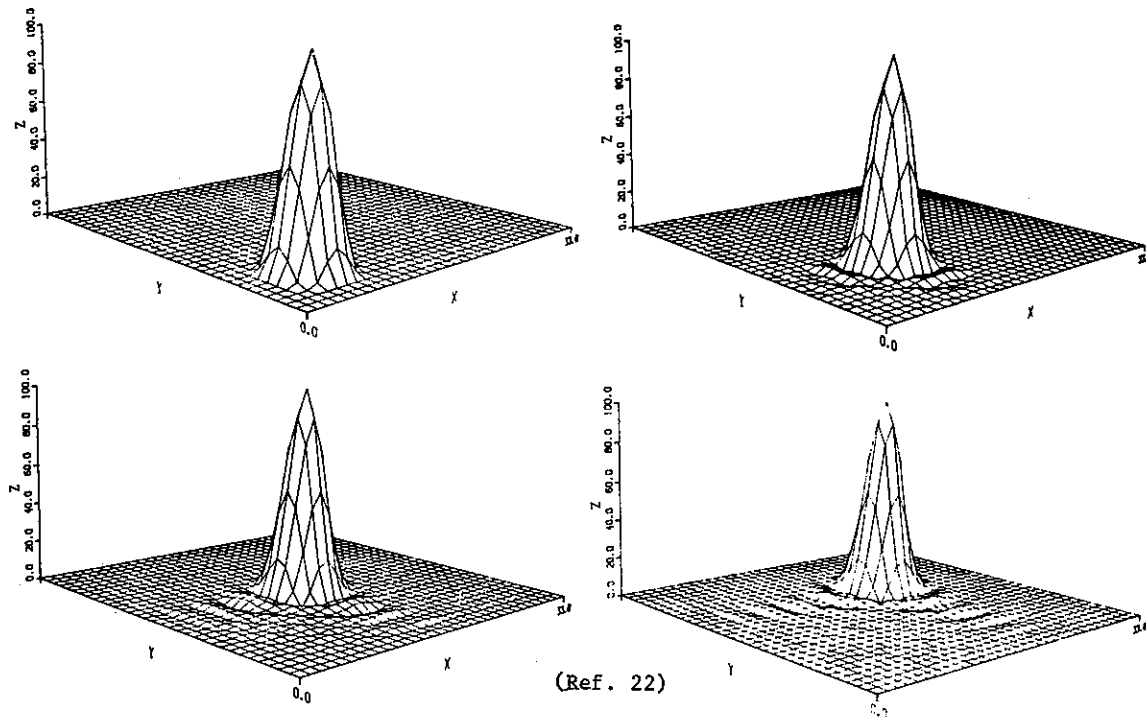


Fig. 92. Advection of concentration cone.  $C = 0.2$ ,  $n\Delta t = 0, 50, 100, 150$ .

Here the first and third sets of figures are the finite element method. The Courant number here has little effect. The second set is for a second-order finite difference Crank-Nicholson scheme. The higher-order of the finite element scheme clearly leads to a reduction in phase error.

Further comparisons are given in the next figure

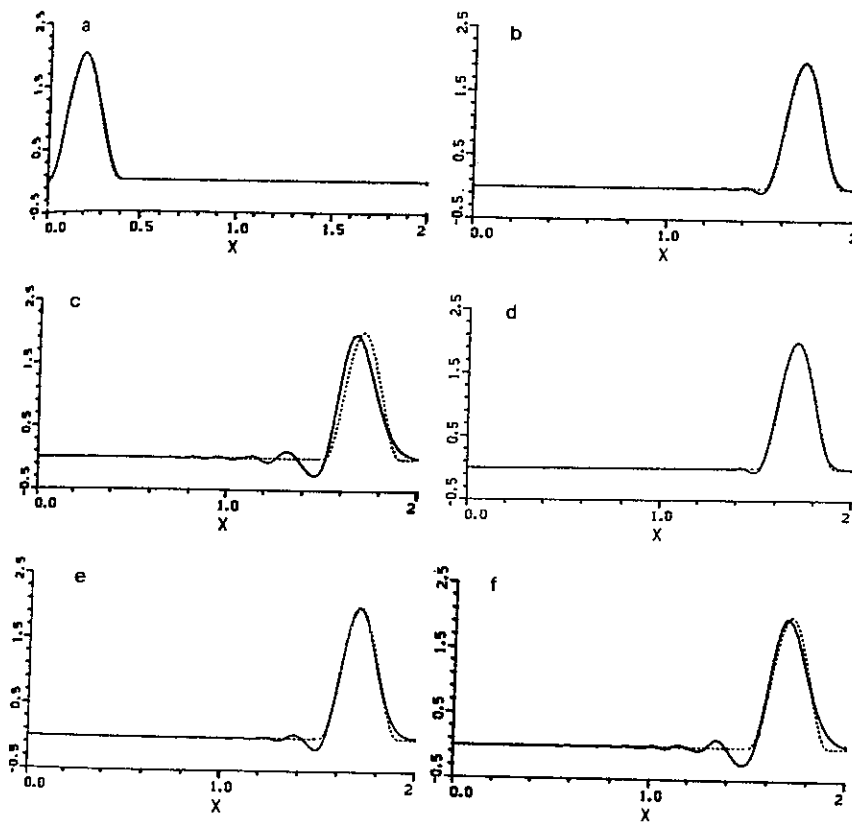
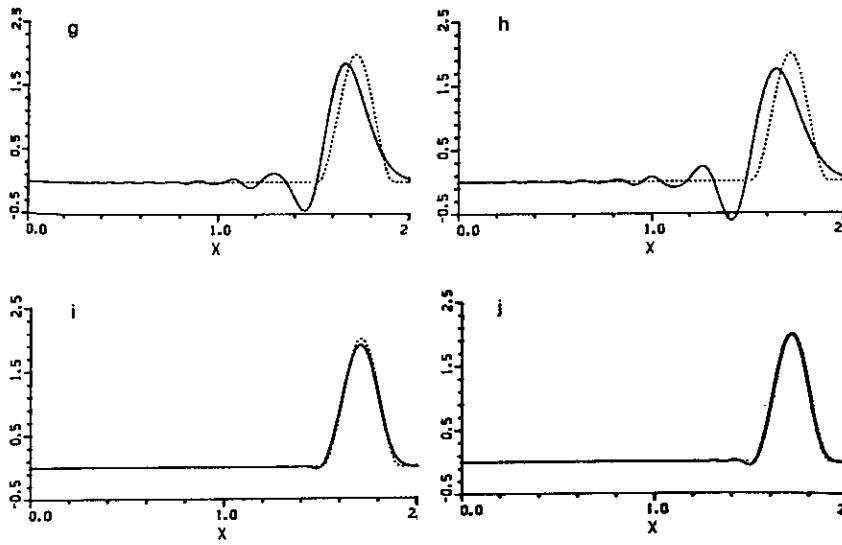


Fig. 93. Advection of a concentration packet. (a) Initial condition, dashed line is analytical solution. (b) Finite element,  $k = 1$ ,  $C = 0.4$ ,  $Re = \infty$ . (c) Crank-Nicholson,  $C = 0.4$ ,  $Re = \infty$ . (d) Finite element  $k = 2$ ,  $C = 0.4$ ,  $Re = \infty$ . (e) Finite element,  $k = 1$ ,  $C = 0.8$ ,  $Re = \infty$ . (f) Finite element,  $k = 1$ ,  $C = 1.2$ ,  $Re = \infty$ . (g) Finite element  $k = 1$ ,  $C = 1.6$ ,  $Re = \infty$ . (h) Crank-Nicholson,  $C = 1.6$ ,  $Re = \infty$ . (i) Finite element,  $k = 1$ ,  $C = 0.4$ ,  $Re = 10^2$ . (j) Finite element,  $k = 1$ ,  $C = 0.4$ ,  $Re = 10^4$ . (Ref. 22)



(Fig. 93 continued)

The small oscillations in the finite element scheme increase with the Courant number. Only a small effect of the element order is evident here. Related to the finite element methods is the least squares approach of Chattot, Guiu-Roux and Lamine (Ref. 42).

### Ordinary Differential Equation Methods

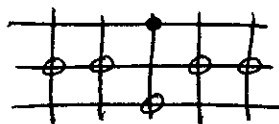
In Ref. 152, Oey reduces the partial differential equation in space and time to a set of ordinary differential equations in space by using difference representation in time only. The ordinary differential equations are then solved numerically by high-accuracy methods. Multiple dimensions are treated by approximate factorization, i.e., time-splitting, which reduces the equation to a multi-stage set of ordinary differential equations. A third-order split form is given. The number of ordinary differential equations to be solved at each stage is equal to the number of dependent variables. In contrast, with the method of lines, where spatial discretization is used to produce ordinary differential equations in time, the number of equations in the set to be solved is equal to the number of points in the field.

Bellman, Kashef, and Casti (Ref. 25) represent the first derivative in terms of the solution values at neighboring points to obtain a system of ordinary differential equations in time. The spatial order is determined by the number of points used in the representation of the derivative.

### Comparisons

Turkel (Ref. 215) compares several methods that are fourth order in space and second order in time.

(1) The Kreiss-Oliger scheme (Ref. 118) is the fourth-order extension of the leapfrog three-time level method and has the 1D stencil



Stability requires that the Courant number be less than 0.72. This scheme is nondissipative.

(2) The fourth-order extension of the MacCormack method (Ref. 135) is

a two stage method with the stencils



with four obvious variations of implementation of these stages. It is necessary to alternate the succession of difference directions at successive time steps to achieve fourth order. Here the stability limitation on the Courant number is  $2/3$ . A compact version of the MacCormack method is also given based on the Pade approximation of the derivative. This method has the stencils:



The stability criterion is that the Courant number not exceed 0.57. The compact version thus has a more restrictive stability criterion than the version using wider stencils.

(3) The fourth-order version of the implicit Crank-Nicholson method (Ref. 107 and 155) has the stencil:



This implicit method is unconditionally stable in the linear sense, so that the short waves will not destabilize the solution even though they are still not computed accurately.

In addition to these methods, pseudospectral methods are also considered. Here the spatial order is effectively infinite. For unbounded regions Fourier series expansions are used, while with boundaries Chebyshev expansions are more appropriate (Ref. 83). These methods are also unconditionally stable

in the linear sense.

The fourth-order MacCormack scheme was about twice as fast as the second-order version and required less than half the storage for moderate accuracy in 1D problems. The fourth-order implicit Crank-Nicholson form was about 30% more efficient than the second-order version and required about a quarter of the storage. The fourth-order version was most effective with smaller time steps than those used in the second-order version, since for larger steps the temporal error dominates and the fourth-order accuracy in space is not being utilized. The time step should be chosen so that the temporal and spatial errors are about equal.

These advantages of fourth order increase dramatically when greater accuracy is required and for stiffer problems. Although the fourth-order accuracy is lost at shocks, overshoots and oscillations are not aggravated by the higher-order methods.

Multiple dimensions are treated by time-splitting, which if done symmetrically preserves the second order in time and does not disturb the spatial order. The stability condition is simply the most restrictive of the 1D criteria. The fourth-order version of the MacCormack method was found to give smaller phase error and similar accuracy with half the points in each direction required by the second-order version.

The spectral method allowed a reduction in storage but was not more efficient than the fourth-order method. Spectral methods may be more efficient, however, if the solution contains the small wavelengths which are not resolved accurately by the finite-order method. The speed of the spectral method is highly dependent on the fast Fourier transform used.

In general the fourth-order methods were about three to five times faster at 5% accuracy than the second-order versions, and required half the points in each direction. These advantages increase in higher dimensions

or with smaller error tolerances. In some cases especially sensitive to boundary treatment, the fourth-order methods may be less stable. Fourth-order schemes are most appropriate for stiff equations, where the higher frequency components are of less physical significance. Higher order in space than in time is also more appropriate with stretched meshes, since the time step is limited to small values by the minimum spacing. The fourth-order extension of the MacCormack method has been found to be robust in several applications.

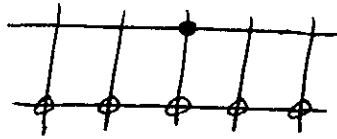
The time step of the fourth-order space, second-order time methods should be chosen small enough that the temporal errors are not larger than the spatial errors. Too large a time step severely degraded the solution. In general it was better to choose the time step too small than too large. In many problems, e.g., stiff equations or stretched meshes, the largest time step allowed by the stability criteria is small enough that the second order in time is comparable to fourth in space. Higher-order methods usually require more computer time per time step, so efficiency is improved only if a coarser grid can be used. Methods for which only the spatial order is increased are not significantly more complicated than the lower order version.

Fromm, Ref. 71, states that the variations in relative quality among second-order methods are too small to warrant efforts toward selecting a best method. Fourth-order methods have much better phase properties and much less dissipation. First-order methods are monotonic but have massive dissipation and large phase error.

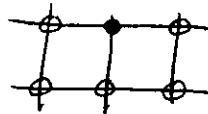
Central difference representations generally have lagging phase error. All second-order methods generally have the property that the phase error decreases as the wavelength increase. It is thus desirable that the dissipation be greatest at shorter wavelengths. Some methods, however, have the greatest damping at intermediate wavelengths. In this class are the Richtmyer two-stage method, with the stencils:



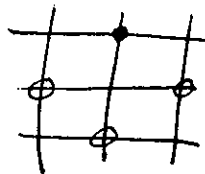
which is equivalent to the Lax-Wendroff method written over points that are twice as widely spaced. The  $4\Delta x$  mode is nonpropagating in this scheme, as well as the  $2\Delta x$  mode. Also in this category are the Burstein method (Ref. 36), discussed elsewhere, and the Crowley fourth-order method (Ref. 55), formed by simply adding another term to the Taylor expansion, for which the stencil is



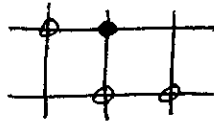
The time-centered methods have no dissipation. Among such second-order methods are the implicit Crank-Nicholson with the stencil



the leapfrog:



and the method of Roberts and Weiss (Ref. 174):



The figure below gives a comparison of the phase error for some of these methods for a wavelength of  $4\Delta x$  and a range of Courant numbers.

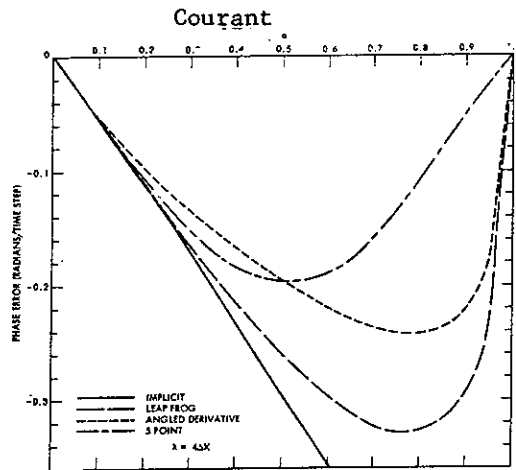


Fig. 94. Phase lag curves for  $\lambda = 4\Delta X$  for typical second-order schemes.  $[\partial(\Delta\phi)/\partial\alpha]_0 \approx -0.5$ . (Ref. 71)

For small Courant numbers there is little difference among the methods, but the methods vary widely at larger Courant numbers.

Phase properties can be dramatically improved by fourth-order methods. Here time centering is less important since the dissipation is

greatly reduced. A comparison analogous to that given above appears in the next figure for three different wavelengths for the fourth-order methods of Roberts and Weiss (Ref. 174) and Crowley (Ref. 55). Again there is a phase lag, but much reduced in magnitude.

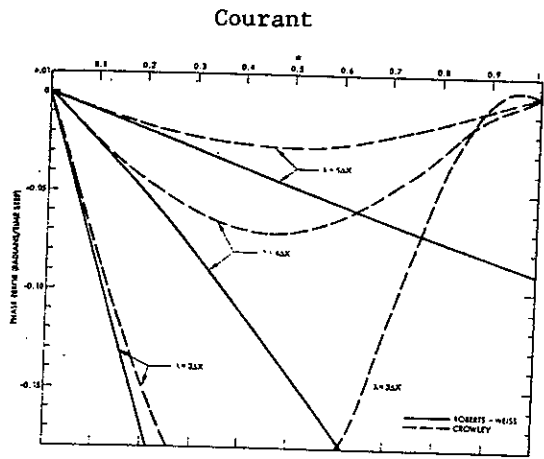


Fig. 95. Fourth-order methods compared for phase error. For  $\lambda = 4\Delta X$ ,  $[\partial(\Delta\phi)/\partial\alpha]_0 \approx -0.25$ . Compare Figure 94. (Ref. 71)

A composite fourth-order method is formed by averaging schemes with lagging and leading phase errors. The scheme with the phase lag it taken to be one formed from a quartic interpolation polynomial fitted to five symmetrically located points. The new time value is formed by

evaluating the polynomial at the point  $x - u\Delta t$ . The scheme with a phase lead is formed in the same way, but with the five points shifted one point upstream. The phase error of the combined schemes is shown below, together with that of a similar second-order combination.

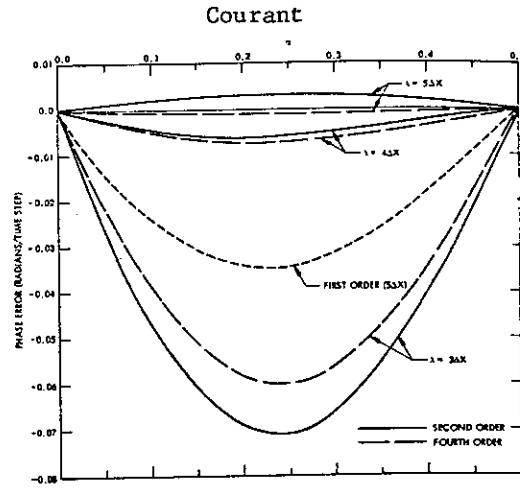


Fig. 96. Comparison of phase errors of various orders of upstream difference methods where the second- and fourth-order forms are combined forms [Eq. (21) for fourth order]. For  $\lambda = 4\Delta X$ ,  $[\partial(\Delta\phi)/\partial\alpha]_0 \approx -0.05$  in both second and fourth order. Compare Figure 95. (Ref. 71)

The phase error clearly drops rapidly with increasing wavelength. The dissipation is also reduced in the combination except for the shortest wavelength, where it is desirable anyway.

Huffenus and Khaletzky (Ref. 106) compare several methods on the basis of convection of a Gaussian. The excessive dissipation of the simple first-order upwind method is clear in the figure below:

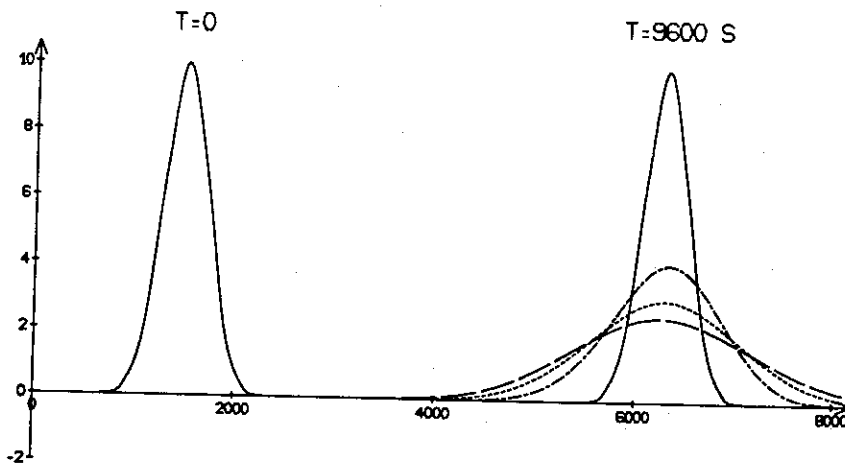


Fig. 97. Upwind differencing scheme (FTUS1) (Ref. 106)

The Lax-Wendroff scheme, also called the Leith scheme, is second order and consequently has less dissipation but more dispersion:

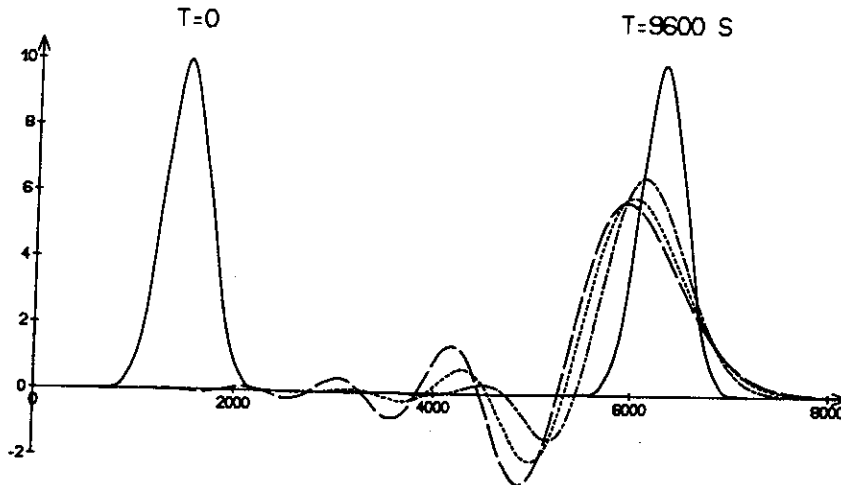


Fig. 98. Leith scheme.

The second-order Crank-Nicholson scheme, which is time centered and implicit, has even more dispersion:

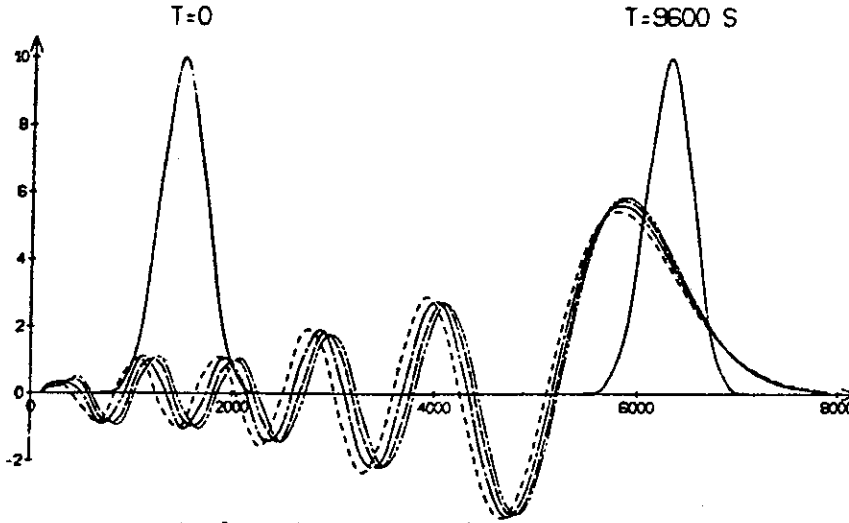


Fig. 99. Euler's modified method.  
(Ref. 106)

This time-centered scheme is less dependent on the Courant number and, being implicit, is unconditionally stable. Another implicit scheme is the simple first-order backward-time, second-order central space scheme. This scheme is more dissipative than the Crank-Nicholson method, however, because of the low time order:

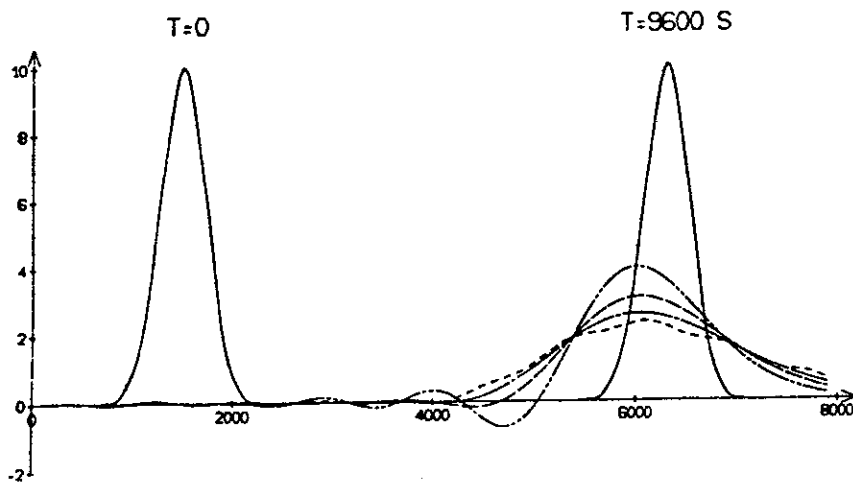


Fig. 100. Implicit centered space scheme.  
(Ref. 106)

The third-order upwind-biased scheme given by Davies in Ref. 58 has much less dissipation and better phase properties than the second-order methods:

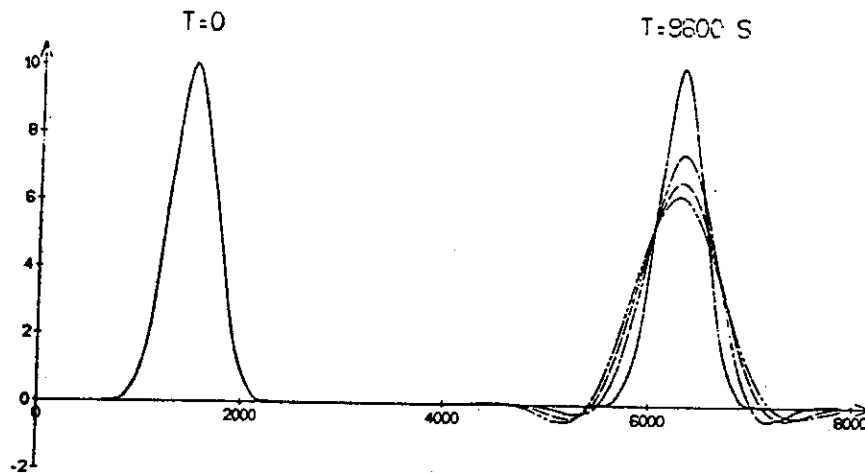


Fig. 101. Polynomial fitting of degree 3 (FTUS3). (Ref. 106)

The third-order compact method of Holly and Preissman (Ref. 104) has even better phase properties and less dissipation:

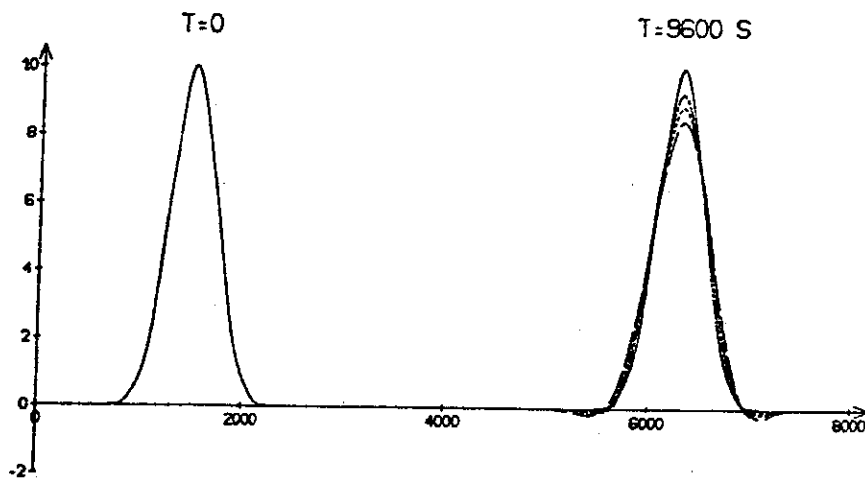


Fig. 102. Transport of the derivatives. (Ref. 106)

Akima's method (Ref. 10) is not compact and involves six points from  $i - 3$  to  $i + 2$ . This scheme has a built-in filter for W and N waves as discussed elsewhere. The dispersion and dissipation are slightly greater than that of the compact method above:

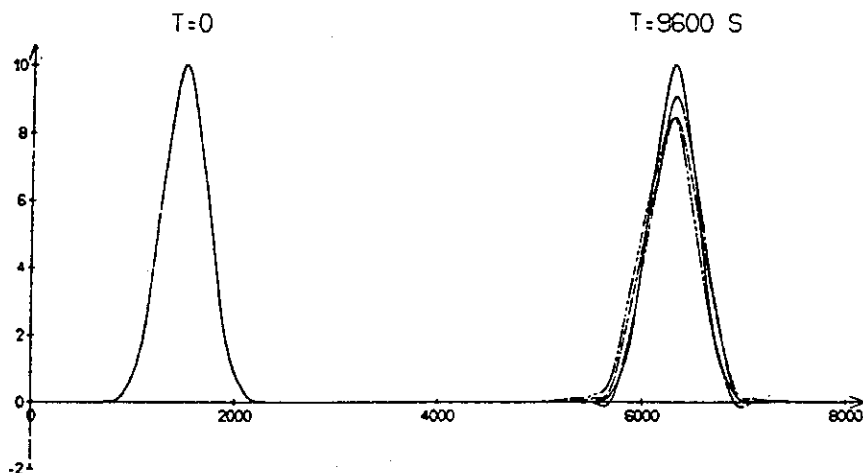


Fig. 103. Akima interpolation method.  
(Ref. 106)

Overall the authors favor the Davies third-order scheme because of its simplicity for the accuracy given.

Forester compares a number of higher-order schemes in Ref. 74 for convection of several waveforms. The schemes considered were:

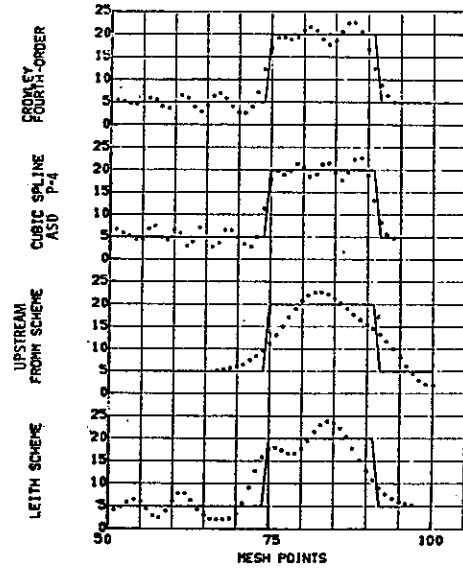
- (1) the original FCT scheme of Boris and Book (Ref. 31 and 32),
- (2) the monotonic van Leer scheme (Ref. 123), which consists of the application of a flux limiter to the second-order averaged phase error scheme of Fromm (Ref. 71),
- (3) the second-order Leith scheme (Ref. 71), to which the Lax-Wendroff scheme reduces for uniform velocity,
- (4) the second-order upstream-biased form of the Leith scheme given by Fromm (Ref. 71),

- (5) the second-order Crank-Nicholson scheme,
- (6) the fourth-order space Crowley scheme (Ref. 55) using second-order Crank-Nicholson time differencing,
- (7) the one-flux version of the Crowley scheme given by Fromm (Ref. 71),
- (8) the two-flux version of the Crowley as given by Fromm (Ref. 71),
- (9) a symmetric spatial sixth-order scheme with second-order Crank-Nicholson time differencing,
- (10) the spatial eighth-order form of the previous scheme, and finally,
- (11-13) schemes based, respectively, on determination of the derivative by cubic, quintic, and septemic splines.

In the spline schemes higher derivatives are obtained by splining the lower derivatives in turn. This requires a tridiagonal solution for each derivative. Thus all the required derivatives are obtained on the entire field from the solution at the previous time level. Substitution of these derivatives in the Taylor series expansion then produces the solution at the next time level, all time derivatives in the series being replaced by spatial derivatives obtained by repeated differential equation. These spline schemes follow the same approach used by Gazdag (Ref. 77) except for the method of determination of the derivatives. The order of these spline schemes is more than twice the spline degree with Courant number less than about  $1/4$  and more than two time derivatives retained in the Taylor series. For larger Courant numbers, the order depends on both the spline degree and the number of derivatives retained in the Taylor series. The quintic spline method has order about midway between a spatial fourth-order method and the pseudospectral methods. A ninth-degree spline method would have order approaching that of the pseudospectral methods.

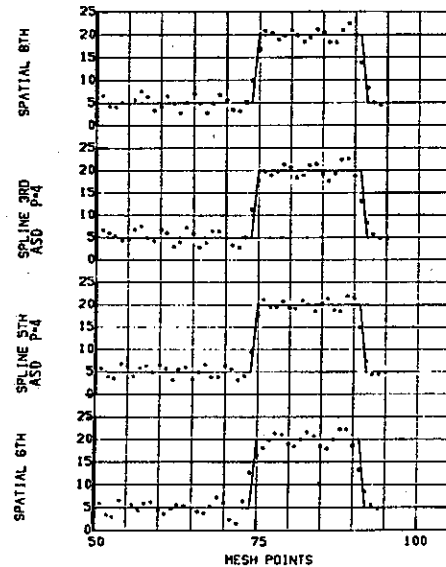
These spline schemes are applicable to arbitrary numbers of grid points while the Gazdag method, using fast Fourier transform, is not.

Results are compared with low Courant number for a square wave below:



(Ref. 74)

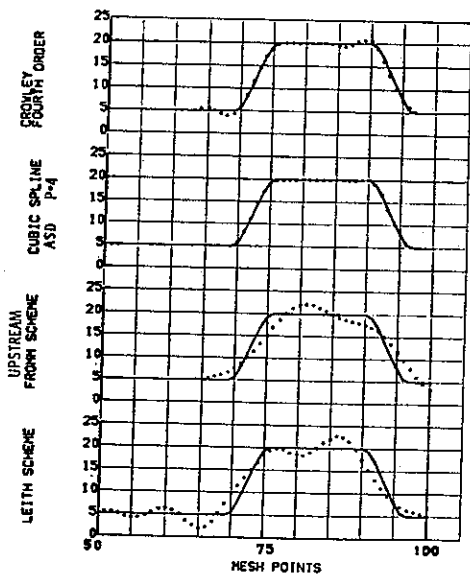
Fig. 104. The dots indicate the numerical representation of the linear wave shown which has been propagated 60 mesh intervals with 600 time cycles by a second, second, sixth, and fourth-order convective scheme. Note the significant increase in the frequency of the computational noise as the order of the convective scheme is increased.  $\sigma = 0.1$ ; exact solution (—); approximate solution (\*\*\*\*).



(Ref. 74)

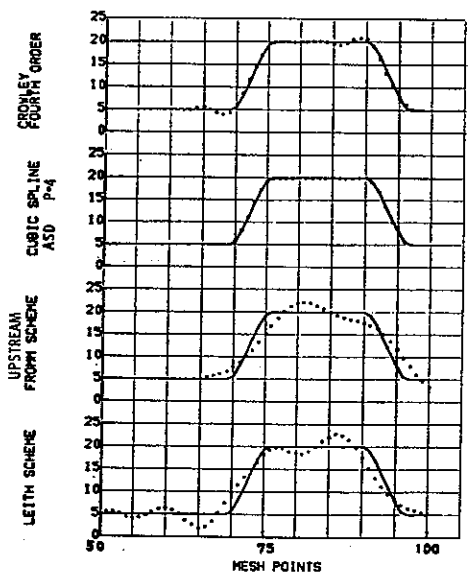
Fig. 105. Same comments as Fig. 104, except for sixth, tenth, sixth and eighth-order schemes.

and for such a wave with rounded corners in the next figures:



(Ref. 74)

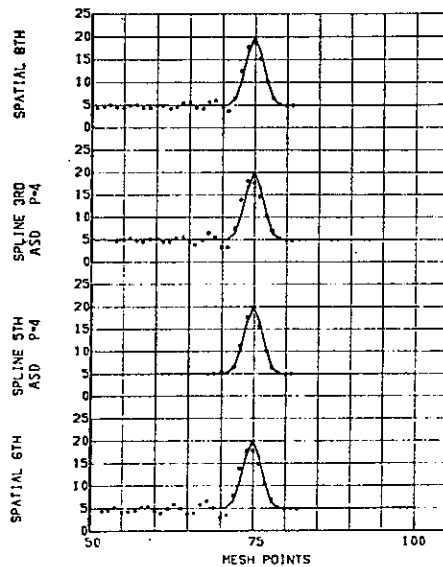
Fig. 106. Same as comments in Fig. 104 with the following additional consideration. Compare Fig. 104 with Fig. 106 and note the significant increase in the amplitude but not the frequency of the computational noise by decreasing the number of mesh intervals over which the steep gradient regions are distributed.



(Ref. 74)

Fig. 107. Same comments as in Fig. 105 with the same additional comment as in Fig. 106, except compare Fig. 105 with Fig. 107.

and for a Gaussian wave next.

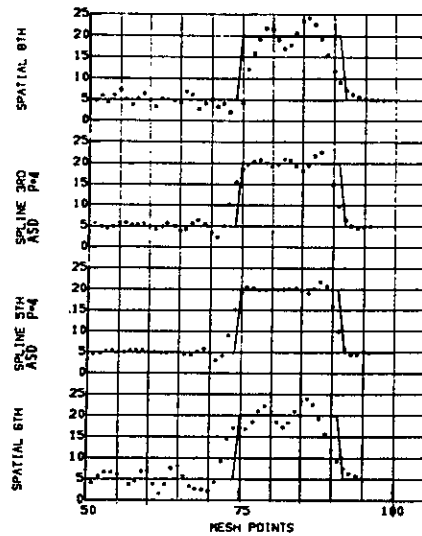


(Ref. 74)

Fig. 108. Same as the comments in Fig. 105 with the same additional comment as in Fig. 106, except compare Figs. 107 and 108.

The frequency of the noise increases with the order of the scheme but the amplitude decreases. Rounding of the corners of the wave significantly reduces the error with the high-order schemes, but the effect is less pronounced for the lower-order methods. Higher-order schemes thus can handle steeper gradients with a fixed grid point distribution, or can handle the same gradient with fewer points, than can the lower-order methods. The frequency of the noise is not affected by the steepness of the gradient.

The figure on the following page illustrates the effect of the Courant number. The noise frequency decreases as the Courant number increases, especially for the schemes that are lower-order in time. The amplitude also increases with the Courant number for these methods, but not for the higher-order time methods.

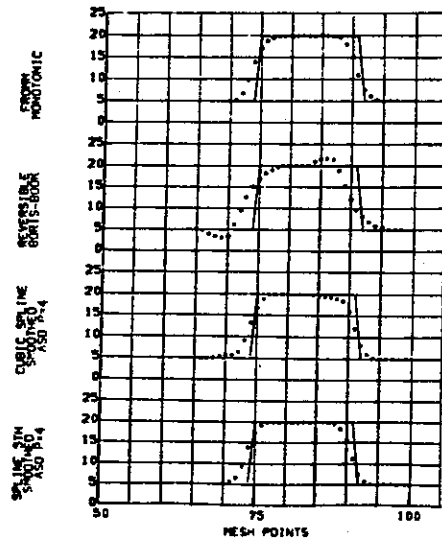


(Ref. 74)

Fig. 109. Same as the comments in Fig. 105 except for 75 time cycles. Compare Fig. 105 with 109 and note the reduction in frequency of the computational noise associated with the increase of Courant number.  $\sigma = 0.8$ .

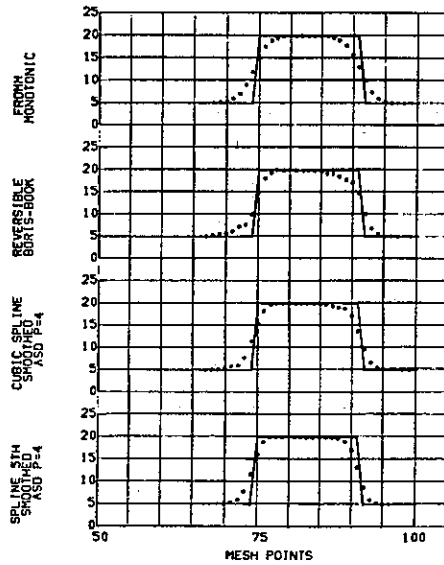
Though reduced, the noise persists even in the higher-order schemes when the wave form has sharp corners. The tenth-order spline method, though, has virtually eliminated the oscillations with the Gaussian.

Results for the square wave using the present and other methods of fitting are shown in the figure below:



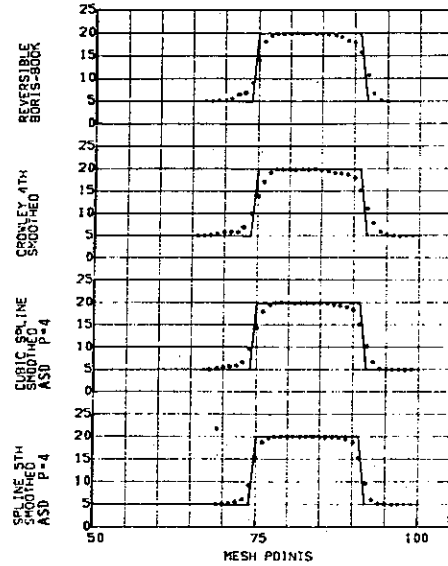
(Ref. 74)

Fig. 110. The same test computation as shown in Fig. 109 except the application of the filter of Section 2 has been used to remove the computational noise in the splined ASD convective schemes.  $\sigma = 0.8$ ; filter constants:  $c = 0.1$ ;  $K = 1$ .



(Ref. 74)

Fig. 111.  $\sigma = 0.4$ . Filter constants:  $c = 0.1$ ;  $K = 1$ .



(Ref. 74)

Fig. 112. The comparison of Figs. 110, 111, and 112 shows that the phase errors of the Fromm monotonic and filtered splined ASD methods are reduced as the Courant number is reduced. However, the acuity of the steep gradient regions improves upon reducing the Courant number for filtered splined ASD computations, whereas the opposite result occurs in the Fromm monotonic scheme. Notice the fine results of the Boris-Book scheme for the Courant number range represented in Figs. 110 and 112. A comparison of the results of Leith's scheme in Fig. 104 with the results of Boris-Book scheme in Fig. 112 shows dramatically the power of the Boris-Book filter to improve the solution accuracy in phase and amplitude properties.  $\sigma = 0.1$ . Filter constants:  $c = 0.1$ ;  $K = 1$ .

The lower-order FCT and van Leer filtering of the Fromm method deform the wave badly. From the earlier figures, wavelengths below about  $8\Delta x$  must be filtered in general, though with higher-order and lower Courant numbers the filtering may be limited to shorter waves.

Results from the filtered schemes for the Gaussian wave are shown next.

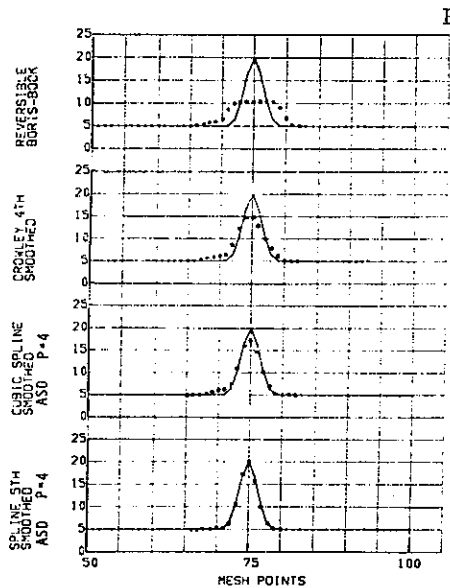


Fig. 113. The Gaussian wave distribution is propagated 60 mesh intervals for 600 time cycles. Note the excellent phase but poor amplitude properties of the Boris-Book algorithm for this problem. Also note the substantial improvement in amplitude response as the order of the filtered algorithms is increased. Compare Figs. 108 and 113 and observe the small amount of amplitude damping of the peak of the wave which the filter of Section 2 produces.  $\sigma = 0.1$ ; Filter constants  $c = 0.1$ ;  $K = 1$ . (Ref. 74)

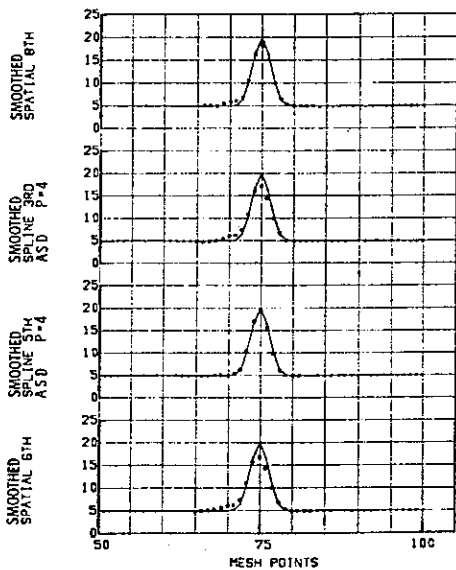
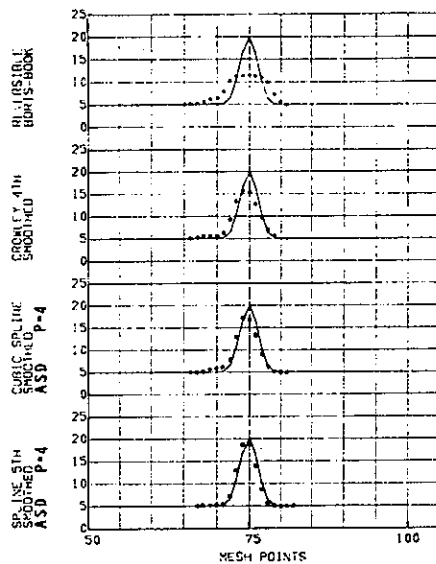


Fig. 114. Same as the comments in Fig. 113, except compare Figs. 108 and 114. (Ref. 74)



(Ref. 74)

Fig. 115. Compare Figs. 113 and 115 and note the increase in phase errors of various filtered solutions with increased Courant number. In spite of this, note the monotonic response of the solutions.  $\sigma = 0.4$ . Filter constants:  $c = 0.1$ ;  $K = 1$ .

While the effect of order on the filtered schemes is small when the solution has sharp corners, it is clear that higher-order methods are far superior with the Gaussian. The lower-order methods require at least three times more points than are needed by the fourth and higher-order schemes. Phase error tends to increase with Courant number, and decrease with increasing order, for the filtered schemes. The strength of the filter must increase with the Courant number.

General recommendations for use of the filter are given. It is generally better to keep the strength of the filter at  $1/5$  and to restrict the Courant number sufficiently that only a few repetitive filter applications are necessary to bring the error to within tolerances.

Zalesak (Ref. 226) compares several higher-order leapfrog schemes having second order in time. These are two-stage schemes formed of a leapfrog predictor and a trapezoidal corrector, both of which are of the same high order in space and second order in time. Actually the corrector

is not applied at each time step. Results of these schemes for convection of a square wave are shown below; together with results of a pseudospectral scheme.

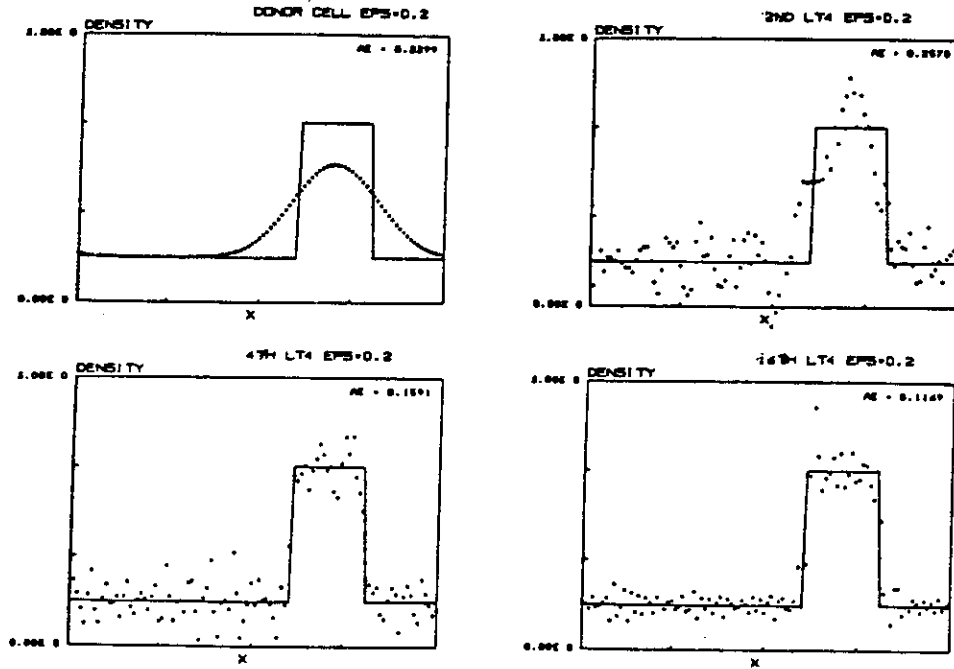


Fig. 116. Tests of various schemes applied to the linear advection (Eq. 1.3) of a square wave, using periodic boundary conditions. This is the same problem originally used by Boris and Book, and subsequently many others, to test advection schemes. The standard output time (shown here) is after 800 time steps using a Courant number  $v\Delta t/\Delta x$  of 0.2. The analytic solution is shown as a solid line. In the upper left plot we show results using the first-order donor cell scheme, followed by results for the leapfrog-trapezoidal scheme using spatial derivatives of second, fourth and sixteenth-order accuracy. Note the "ripples" in the high-order schemes and the monotone but excessively dissipative performance of the donor cell scheme. (Ref. 226)

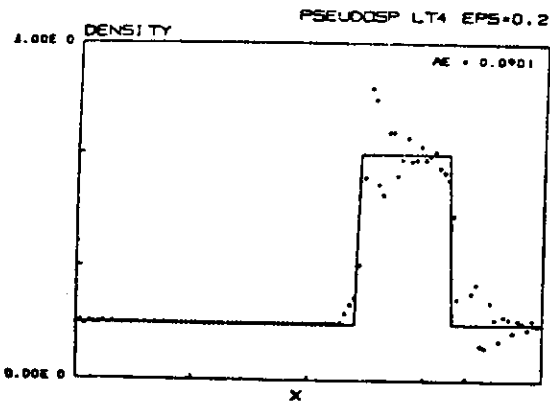


Fig. 117. Tests of the linear advection of a square wave, as in Fig. 116, but using the Fourier pseudospectral approximation of spatial derivatives together with the leapfrog-trapezoidal temporal discretization as the "high-order" scheme. Shown is the result of using just the pseudospectral scheme alone (no FCT). (Ref. 226)

As seen in other comparisons, the amplitude of the oscillating error decreases, and the frequency increases, with increasing order. However, even the pseudospectral method, which is essentially infinite in spatial order, is not able to handle this problem satisfactorily.

In Ref. 213, Trefethen discusses the group speed of difference schemes and its relation to numerical dispersion. The analysis is strictly applicable only to non-dissipative schemes. It is noted that the error in the group speed is typically three times the error in the phase speed. Wave fronts and wave packets travel at the group speed. Numerical dispersion arises when the group speed is dependent on the wave number. Short wavelength parasitic waves may be generated at interfaces, shocks, or other discontinuities and also from sudden changes in grid spacing.

Haidvogel, Robinson and Schulman (Ref. 94) compare three methods for vorticity convection. The first method is the second-order Arakawa scheme (Ref. 15) for the convective terms with leapfrog time differencing. The second is a Galerkin finite element scheme using linear rectangular elements and second-order centered time differences or second-order Adams-Bashforth time differencing, both of which are three-time level schemes. Here the matrices are factored into a tridiagonal matrix for each direction. The method is fourth order in phase error.

The final scheme is a pseudospectral method based on Chebyshev polynomials. The pseudospectral method was found to be the most accurate, and the finite difference the least accurate. It should be recalled that the finite difference method considered was only second order. However, nonlinear instability is more of a problem with the pseudospectral and finite element methods. Periodic smoothing can maintain stability, however.

Harten and Tal-Ezer (Ref. 97) found that the accuracy advantage of fourth-order spatial differences over second-order differences decreased with increasing Courant numbers above unity in implicit schemes of the Crank-Nicholson form. Fourth-order differences gave an order of magnitude improvement in accuracy over second order for Courant number of unity, but negligible improvement for Courant above 4. The use of fourth-order in time gave about two orders of magnitude improvement in accuracy for all Courant numbers considered (up to 8) over second order in time, both with fourth order in space. With fourth order in space only, the optimal Courant number for accuracy was around 0.25, while with fourth order in space and time the optimal was around 2.5. At Courant numbers near unity, fourth order gave considerably less oscillation with shocks (using a switched Shuman filter) than did second order, while at Courant numbers around 2 no such improvement was seen.

It was concluded that with shocks present, the Courant number should not be much larger than unity.

Sod, in Ref. 191, compares a number of schemes for the shock tube problem. The methods considered were the following:

- (1) the two-stage first-order Godunov with the stencils



- (2) the two-stage second-order Richtmyer rendering of the Lax-Wendroff method (Ref. 171),

- (3) the MacGormack two-stage second-order method (Ref. 135),

- (4) the first-order Rusanov method (Ref. 183),
- (5) the first-order upwind scheme,
- (6) the random choice two-stage, first-order method of Glimm (Ref. 81) rendered by Chorin (Ref. 46), which builds the solution by sampling Riemann solutions, i.e., propagation of step functions,
- (7) Harten's artificial compression method (Ref. 96), which is inherently first order,
- (8) the hybrid scheme of Harten and Zwas (Ref. 98), which combines low and higher order schemes, using the former only when necessary to suppress oscillations,
- (9) FCT of Boris and Book (Ref. 31) applied to the two-stage Richtmyer version of the Lax-Wendroff method,
- (10) Hyman's two-stage predictor-corrector method using a first-order explicit predictor for a half time step followed by a second-order leapfrog correction, with fourth-order spatial differencing in each, the stencils being



First and second-order artificial viscosity, respectively, was added to the two stages, lowering the order to that of the artificial viscosity.

The lower-order method used in the hybrid method above was the second-order MacCormack method with first-order artificial viscosity added, and the higher-order was the second-order MacCormack method without the artificial viscosity. Some type of artificial viscosity was added to the methods of Godunov and MacCormack and to the Lax-Wendroff methods. The results are shown on the following pages:

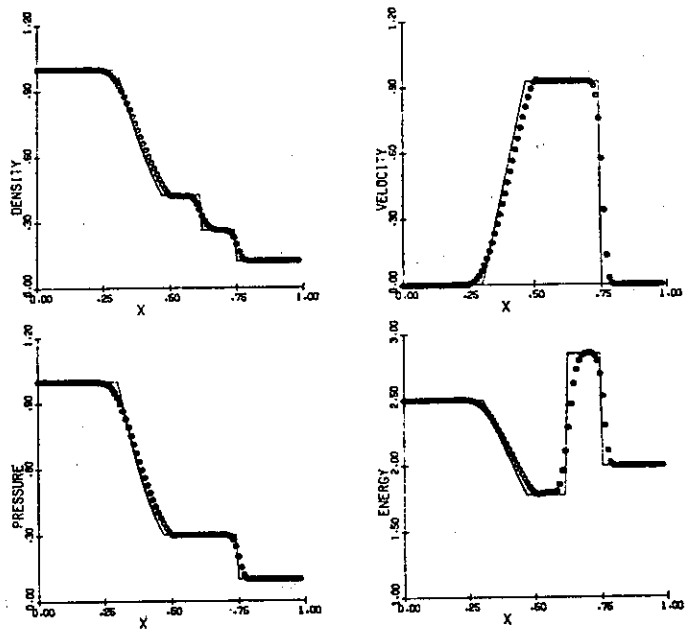


Fig. 118. Godunov's method. (Ref. 191)

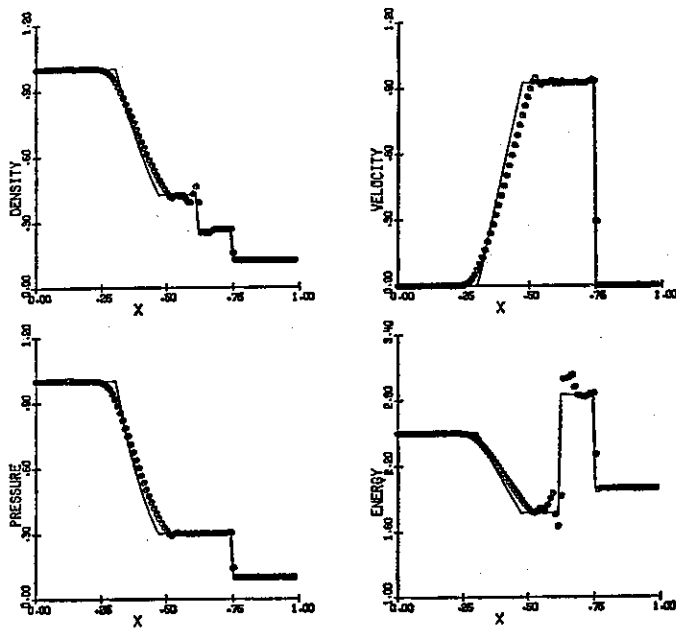


Fig. 119. Godunov's method with ACM. (Ref. 191)

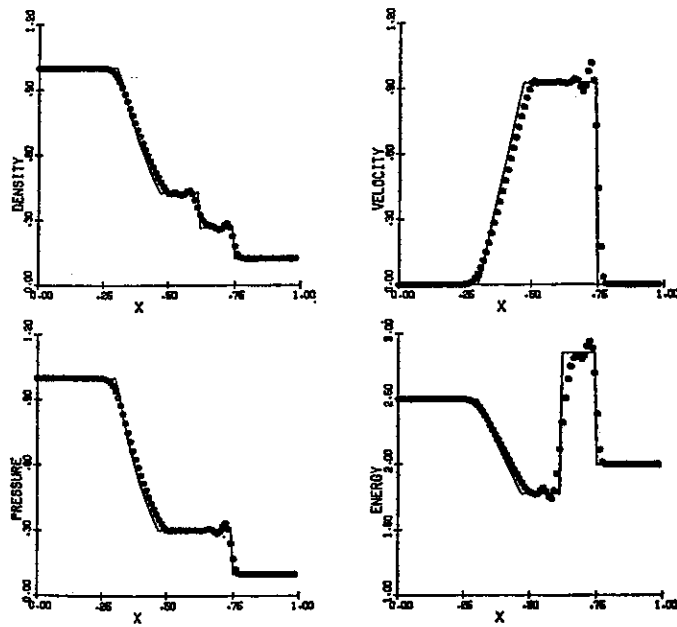


Fig. 120. Two-step Lax-Wendroff method. (Ref. 191)

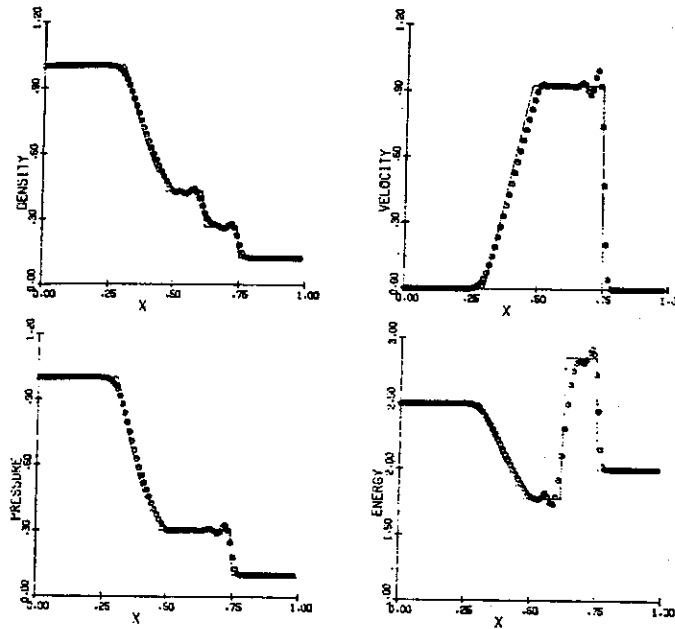


Fig. 121. MacCormack's method. (Ref. 191)

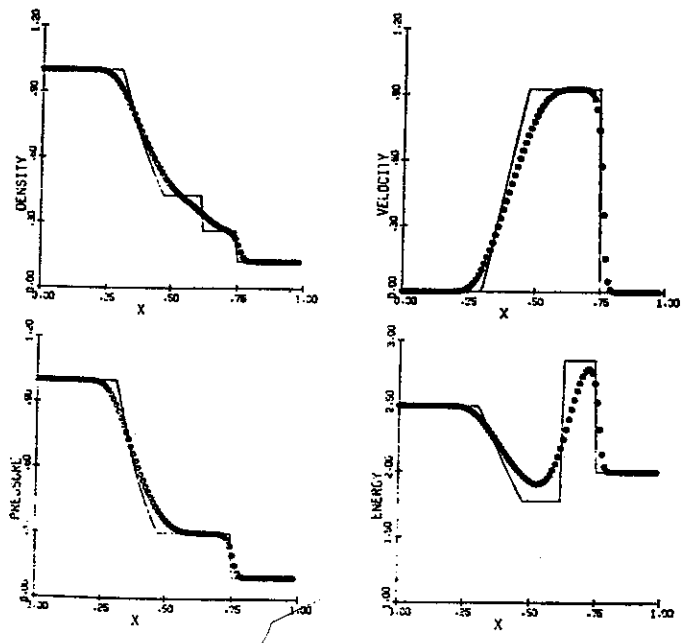


Fig. 122. Rusanov's first-order method. (Ref. 191)

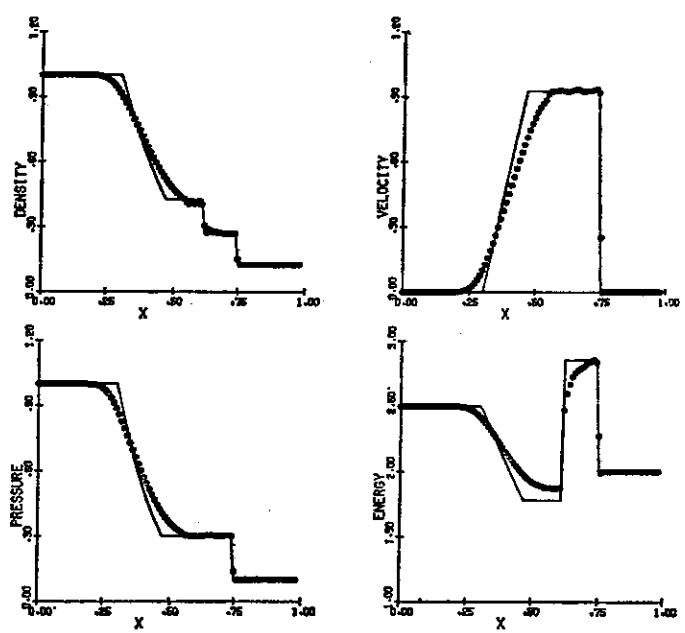


Fig. 123. Rusanov's first-order method with ACM. (Ref. 191)

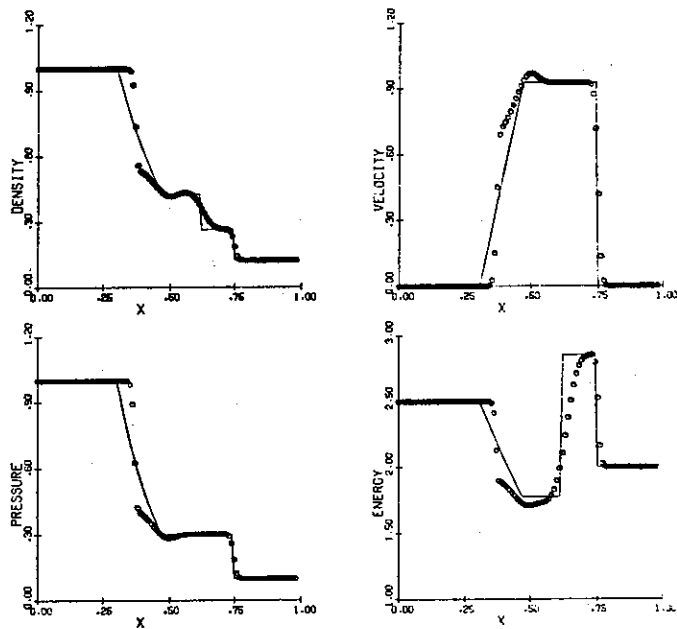


Fig. 124. Upwind difference method. (Ref. 191)

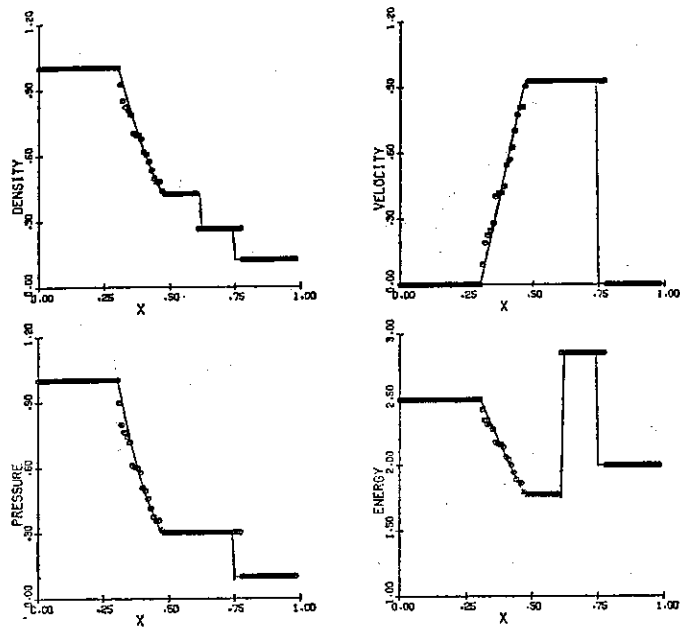


Fig. 125. Glimm's method. (Ref. 191)

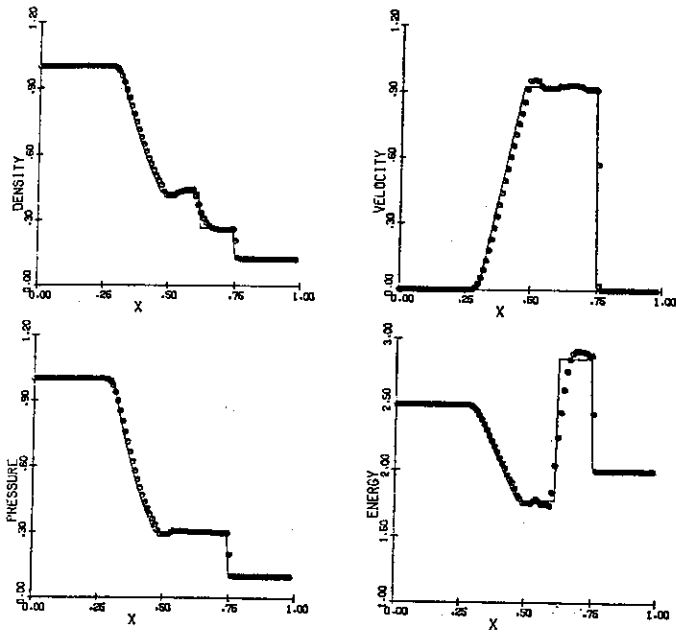


Fig. 126. Antidiffusion method. (Ref. 191)

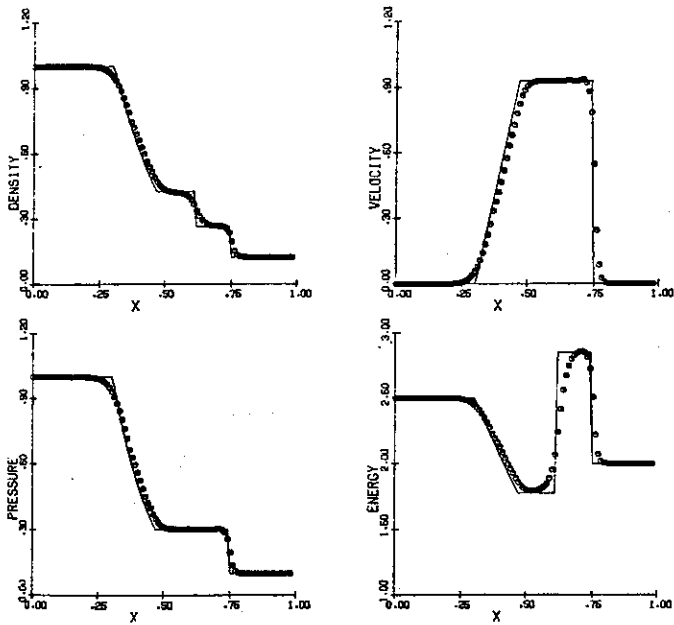


Fig. 127. Hybrid method. (Ref. 191)

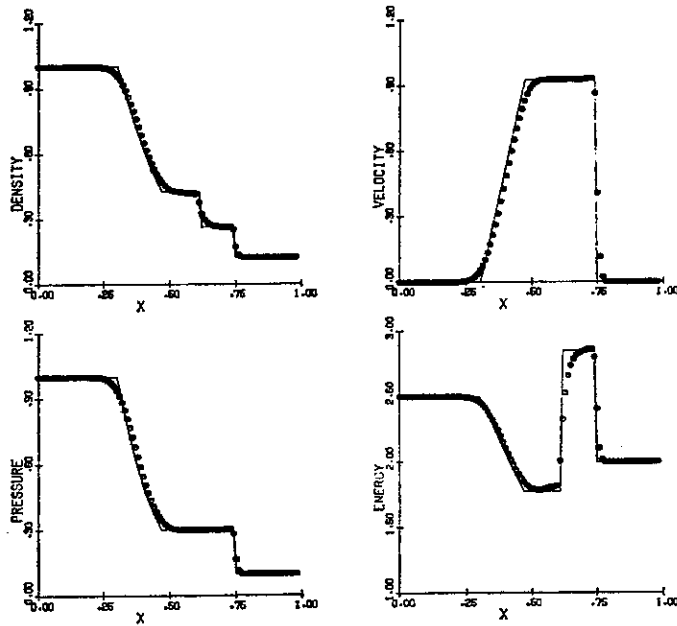


Fig. 128. Hybrid method with ACM. (Ref. 191)

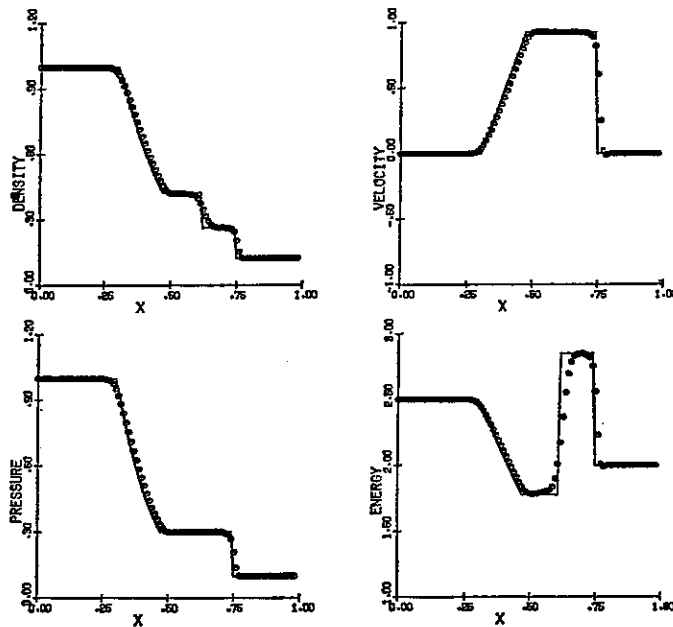


Fig. 129. Hyman's predictor-corrector method. (Ref. 191)

The artificial compression cannot be applied in the presence of oscillations. The Glimm scheme required three times as much time but far less grid points. Without corrective procedures, the Godunov and Hyman methods gave the best results. The Glimm scheme gave the best shock resolution. The shock tube problem, however, is the type of problem to which Riemann solvers are particularly well suited. The higher-order schemes gave better approximations to the smooth parts of the flow.

Raithby and Torrance (Ref. 168) note that order may be misleading in cases with strong convection when higher-order derivatives in the Taylor expansion may be larger than those of lower order. These authors also found that the use of variable time steps over the field speeded up convergence to the steady state considerably, though true time representation is lost.

Orszag and Jayne (Ref. 156) note that order is degraded at solution discontinuities, but even then the higher-order methods are superior. Second and fourth-order schemes are examined. It is stated that spectral schemes require at least a factor of two less resolution to achieve the same accuracy as fourth-order schemes, while fourth-order schemes require a factor of two less than second-order schemes. The amplitude and wavelength of phase error-induced oscillations decreases as the order of the scheme increases. Necessary dissipation can therefore be smaller and more localized with higher-order schemes.

## V. FILTERS

The computational noise, i.e., short wavelength spatial oscillations that occur near strong gradients, can be controlled by filters which smooth out the oscillations by selectively applying large local dissipation.

### Switched Shuman Filter

An older form of filter, usually called the Shuman filter, simply applies large dissipation everywhere in the form of the addition of a second derivative term to the equation. The artificial diffusion coefficient is such as to produce the effect of replacing the solution value at each point by the average of the present value and the average of the neighboring values. The Shuman filter was used by Vliegenthart (Ref. 218). This filter applies too much dissipation for realistic use.

A better approach is the switched Shuman filter, in which the artificial diffusion coefficient is made space-dependent, being large only near large gradients and being of the order of the difference scheme elsewhere. This coefficient, i.e., the switch, is usually made proportional to a power of the gradient of importance. A related approach is the switched hybrid schemes, which are constructed of a weighted average of low and high-order methods, discussed later in this section. Here the switch favors the low-order scheme in regions of large gradient.

The switched Shuman filter was applied by Harten and Zwas in Ref. 99. The switched Shuman filter was used by Harten and Tal-Ezer, Ref. 97, in second and fourth-order schemes of the Crank-Nicholson type to control oscillations occurring with shocks. This type of filter was also used by Holla and Jain, Ref. 103. The effects of the Shuman switch (Ref. 99) were investigated by Srinivas, Gururaja, and Prasad

in Ref. 195 for several shock problems. This filter was found to be effective against oscillations, but it did smear the shock considerably.

Srinivas and Gururaja (Ref. 193) make the coefficient on the Shuman switch filter (Ref. 99), or in the switch used for hybrid methods (Ref. 98), locally dependent on the Courant number, such that maximum filtering effect occurs for values of  $1/2$ , with no filter at 0 or 1. This type of switch was used by Sod (Ref. 191) for the Harten and Zwas hybrid scheme (Ref. 98). A switch was also used by Sod to reduce added artificial viscosity in a predictor-corrector method. Results for these schemes are shown on p. 171-176.

#### Flux-Corrected Transport

Flux-corrected transport (FCT) is basically a procedure for adding artificial diffusion to an algorithm and then removing diffusion, i.e., adding anti-diffusion, whenever possible without allowing the solution to assume new local extrema. This procedure involves three stages-- convection, diffusion, and anti-diffusion. (Diffusion here is understood to be artificial. Physical diffusion would be included in the convection stage or applied separately in a time-split mode.) Some testing procedure, called a flux limiter, is also necessary to locally limit the anti-diffusion so that its application will not push the solution beyond its values at neighboring points to form new local extrema.

There are two free parameters in FCT, the diffusion and anti-diffusion coefficients, which may be uniform or variable over the field. There are also the choices of what provisional solution to base the anti-diffusion on, and how to construct the flux limiter. The original form given by Boris and Book in Ref. 32 had both the diffusion and anti-diffusion coefficients equal to  $1/8$ , with the anti-diffusion based on a convected and diffused provisional solution.

With the convection, diffusion and anti-diffusion operations represented by C, D, and A, respectively, the overall operation in this case is given by

$$\phi^{n+1} = (1 + A)(1 + C + D)\phi^n \quad (1)$$

and the provisional solution from which the anti-diffusion is calculated is

$$\phi^* = (1 + C + D)\phi^n \quad (2)$$

The flux limiter used was the limitation of the anti-diffusion flux at each point to the minimum of (1) the diffusion flux at this point and (2) the anti-diffusion flux which would push the provisional solution at either of the two points affected by this anti-diffusion flux beyond its value at the adjacent points.

The results of this version of FCT applied to the second-order Lax-Wendroff scheme is shown below.

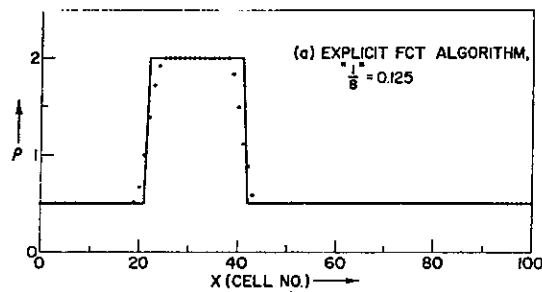


Fig. 130. Simple explicit ("1/8" = 0.125) version of FCT antidiffusion using the SHASTA Transport algorithm. The velocity is unity and  $\epsilon = 0.2$ . The time is  $t = 20$  (cycle = 100). The explicit version is far better than the standard schemes. (Ref. 32)

This early form was used by Book and Ott (Ref. 29) for a shallow water problem, and is also discussed by Boris in Ref. 30. In Ref. 28 the diffusion and anti-diffusion coefficients were kept uniform and equal, but were determined as the minimum necessary to make the combined convection and transport stages monotonic. The uniform value then depends on the maximum Courant number.

An implicit anti-diffusion version is also given in Ref. 32. Here the overall operation is represented as

$$(1 - A)\phi^{n+1} = (1 + C + D)\phi^n \quad (3)$$

and a tridiagonal solution is required. The flux limiter is based on the same provisional solution as used for the explicit case. The implicit version is not significantly better than the explicit in general but does eliminate the residual diffusion that remains with zero velocity in the explicit version, as shown below:

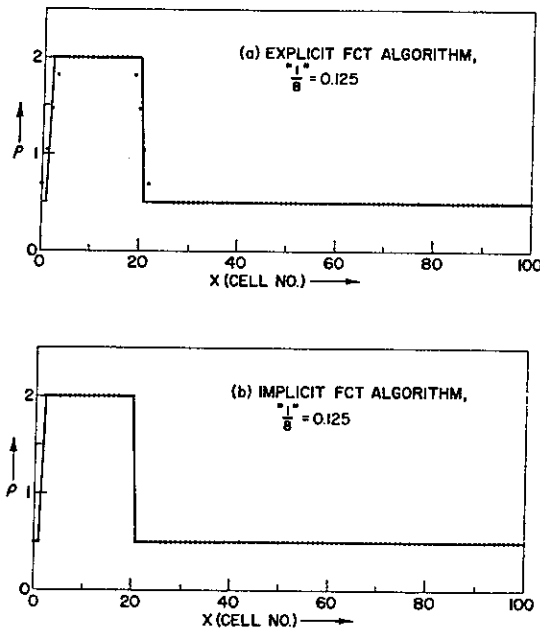


Fig. 131. Same as in Fig. 130 except the flow velocity is zero. The solid line again shows the correct solution. Here the implicit FCT algorithm (b) gives the exact answer whereas the somewhat simpler explicit method still has a small residual smoothing. (Ref. 32)

In Ref. 31, a "zero residual damping" version of the implicit form is used. In this case the diffusion and anti-diffusion coefficients are again equal but are determined as functions of the local Courant number such that the anti-diffusion (when not limited) exactly equals the

diffusion. The results, however, are not as good as the original explicit version with uniform coefficients because this choice of the coefficients increases the phase error by about a factor of 2:

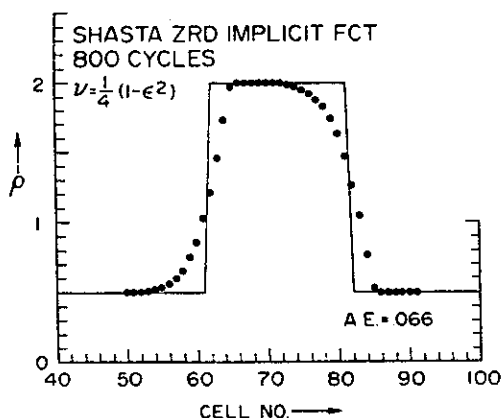


Fig. 132. Result of using Shasta ZRD on the square wave test. Implicit anti-diffusion is required for zero residual damping and  $\nu$  is chosen to complete the square in the squared amplification factor so that two equal implicit anti-diffusion steps can exactly cancel the damping. The Shasta ZRD result, A.E. = 0.66, is worse than simple FCT algorithm because even though the residual damping is zero, the phase properties are much worse than in the simpler Shasta algorithms. (Ref. 31)

The residual damping remains with zero velocity in the original explicit form because the anti-diffusion operator acts on the diffusion operator as well as on the convection operator. Thus from Eq. (1) with  $C = 0$  we have  $\phi^{n+1} = (1 + A)(1 + D)\phi^n$ , so that even if the anti-diffusion has exactly the opposite effect of the diffusion, i.e.,  $A = -D$ , we still have  $\phi^{n+1} = (1 - D^2)\phi^n$  at zero velocity. The implicit version avoids this, since Eq. (3) reduces to

$$(1 + D)\phi^{n+1} = (1 + D)\phi^n \quad (4)$$

for zero velocity and  $A = -D$ .

It is also possible to construct an explicit form without residual diffusion at zero velocity simply by basing the provisional solution on only the convection stage. Thus Eq. (1) is replaced by

$$\phi^{n+1} = [(1 + A)(1 + C) + D]\phi^n \quad (5)$$

with the provisional solution now given by

$$\phi^* = (1 + C)^n \quad (6)$$

Clearly,  $\phi^{n+1} = \phi^n$  if  $C = 0$  and  $A = -D$  in this version. This form was introduced by Book, Boris, and Hain in Ref. 28, and given the name "phoenical FCT." Implementation is by first calculating the provisional solution from convection only. Then the anti-diffusion fluxes are calculated and limited, all based on the provisional solution. The diffusion flux is calculated from the previous time level solution. Finally, both the diffusion and anti-diffusion fluxes are added to the provisional solution to produce the solution at the new time level. Here again the coefficients of the diffusion and anti-diffusion must be taken to be equal else residual diffusion will still remain at zero velocity. The coefficients do not have to be uniform, however.

Results for several uniform diffusion strengths are shown below:

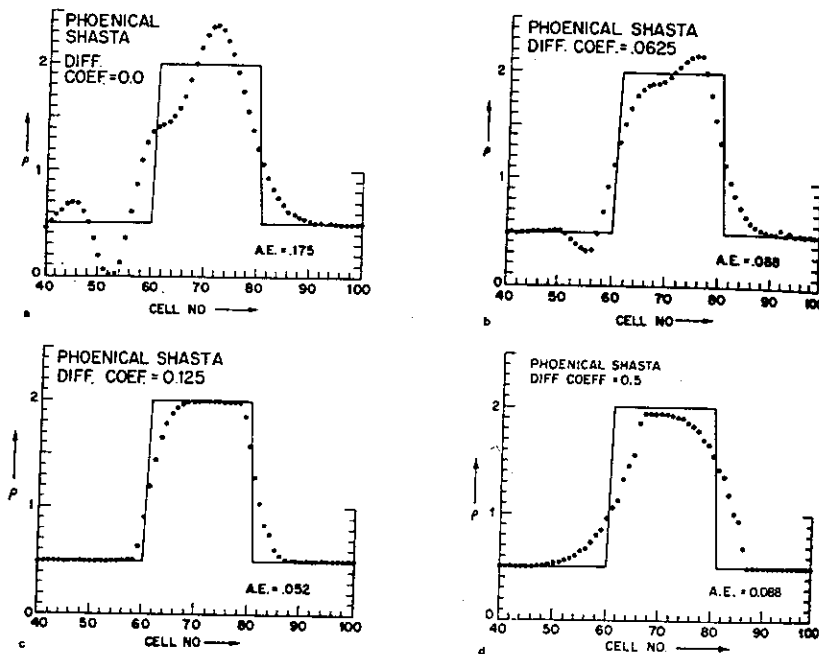


Fig. 133. Phoenical SHASTA (or Lax-Wendroff) with diffusion/antidiffusion coefficient (a)  $\eta = 0.0$ ; (b)  $\eta = 1/16$ ; (c)  $\eta = 1/8$ ; (d)  $\eta = 1/2$ . (Ref. 28)

Ref. 28 also gives results for phoenical FCT applied to the second-order leapfrog scheme and the first-order upwind scheme. However, with equal and uniform coefficients of diffusion and anti-diffusion set at 1/8 the results do not differ significantly among these schemes for convection of a square wave.

Convection of a square wave is a problem to which FCT is particularly well suited since the flux limiter clips sharp peaks as shown below:

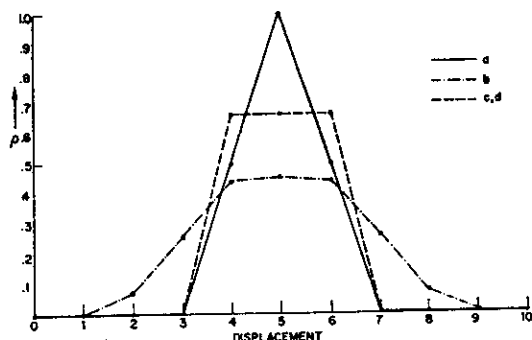


Fig. 134. Results of successively diffusing and antidiffusing the sharply peaked profile (a) 20 cycles with diffusion/antidiffusion coefficient  $\eta = 0.2$ . Curve (b) is produced by explicit antidiffusion, curves (c) and (d) (indistinguishable on the scale of the plot) by phoenical and implicit antidiffusion. (Ref. 28)

The clipping is less pronounced, but still significant, for the phoenical version. Terraces can also be formed on the sides of steep gradients when local extrema occur due to phase error and thus activate the flux limiter.

The phase error of FCT applied to second-order schemes is second order. This order can be increased to fourth by making the equal diffusion and anti-diffusion coefficients functions of the local Courant number as in Ref. 31. The results of this "low phase error" phoenical version are considerably better, as shown in the following figure:

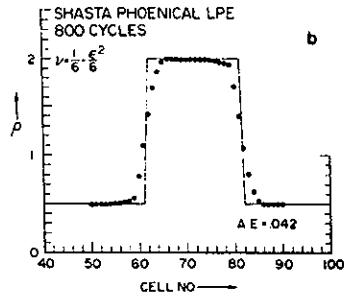


Fig. 135. Implicit and phoenical low phase error Shasta on the square wave test problem. Using  $\nu = \frac{1}{6}(1 - \epsilon^2)$  in each case reduces phase errors from second order to fourth order in  $kx$ , and hence, dispersive ripples are minimized, making the work on the flux corrector much easier. Phoenical antidiffusion is not quite accurate. It does have the advantage of being local and not requiring the solution of a tridiagonal system of equations and is more accurate than the simplest FCT algorithms. (Ref. 28)

It is also possible to go one step further, of course, and construct an implicit phoenical low phase error form, with the overall operation represented

as

$$\phi^{n+1} = [(1 - A)^{-1}(1 + C) + D]\phi^n \quad (7)$$

with the provisional solution

$$(1 - A)\phi^* = (1 + C)\phi^n \quad (8)$$

The results are shown below:

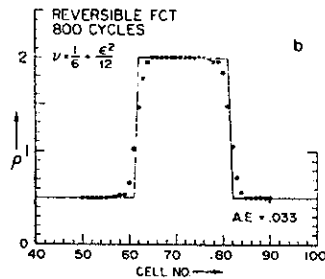


Fig. 136. Reversible FCT algorithm on the square wave test. The reversible FCT algorithm, here with the diffusion coefficient  $\nu$  chosen to minimize phase errors, gives the lowest error of any finite-difference algorithm tested to date. A.E. = 0.033 is within 50% of optimum and 8 times smaller than the donor cell value A.E. = 0.260. (Ref. 28)

but the improvement is not worth the extra work.

The FCT filtering was applied in the ALFVEN code of Weber, Boris, and Gardner (Ref. 221) using the original flux limiter. This code will therefore clip peaks badly. The SHASTA formulation using FCT was used by Anderson in Ref. 14 in a time-split mode.

In Ref. 125, van Leer gives a flux limiter that is more compact than that used in the original FCT algorithm (Ref. 32). A comparison with the FCT limiter is given for convection of a triangular wave below:

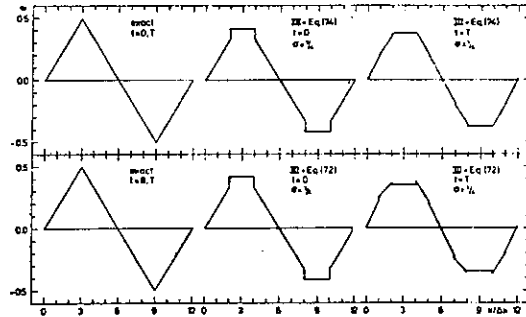


Fig. 137. Convection of a triangular wave by Scheme III, using the monotonicity algorithm (74) (top) and the FCT algorithm (72) (bottom). (Ref. 125)

The clipping phenomenon characteristic of monotonicity algorithms is still present but the present limiter does give a somewhat smoother solution. This limiter is used with a system of equations by van Leer in Ref. 126. A flux limiter which takes account of the solution's history is given by Zalesak in Ref. 227, as discussed below in connection with the hybrid methods form of FCT.

#### Hybrid Methods

The hybrid method of Harten and Zwas (Ref. 98) is formed by taking the algorithm to be a weighted average of a low-order method and one of higher order. The weight is designed to be  $O(1)$  near discontinuities, and in smooth regions of order at least equal to the difference between the order of the high and low-order methods. The weight (switch) is incorporated with the fluxes in such a manner that the scheme is in conservative form. This weight can be taken to be the ratio of a first-derivative magnitude to the average thereof over the field raised to a power equal to the difference in order between the high and low-order methods. In the 2D version separate switches can be used in the two directions, basing each on the derivative in the

given direction.

Zalesak (Ref. 227) redefines FCT in a form which is essentially the same as the hybrid method of Harten and Zwas (Ref. 98). This form is as follows: First, the fluxes are computed on the entire field independently from a low-order scheme and a high-order scheme. An "anti-diffusive" flux is defined to be the difference between these two fluxes. A low-order provisional solution is computed by applying the low-order flux to the solution at the previous time level. The anti-diffusive flux is then limited at each point such that the solution at the new time level, formed by the application of this anti-diffusive flux to the provisional solution, will not be beyond the combined ranges of neighboring values in both the provisional solution and the solution at the previous time level. Finally, the new time-level solution is formed by applying the limited anti-diffusion fluxes to the provisional solution. If the anti-diffusion fluxes were not limited, the final result would be simply that of the high-order scheme. The differences that arise between the schemes of Ref. 227 and Ref. 98 are due only to different construction of the flux limiter.

The extension of these steps to 2D is straightforward. Some care must be exercised in the construction of the flux limiter, however.

The present flux limiter differs from that used in the earlier version of FCT in two significant ways. In the first place, the original form did not allow the new solution to move beyond the range of neighboring values in the provisional solution, thus, the range of neighboring values at the previous time level was not considered. Even more significant, the original version limited the flux at a point based

entirely on its individual effect, not in concert with the other member of the pair (in 1D) of fluxes that affects the solution at each grid point.

In 1D the lack of consideration of fluxes acting in concert errs on the conservative side by cancelling each member of the pair in the cases when they would push the solution in the same direction. This does not carry over into 2D, however.

The present limiter considers the cumulative effect of all fluxes affecting the solution at a point. With a maximum and minimum permissible values defined for the solution, least upper bounds on the fractions which must multiply all anti-diffusive fluxes into and away from each grid point to guarantee that the solution there does not move beyond the maximum or minimum are determined. At each point this defines the fraction of the combined flux that can be allowed. Each individual flux is then multiplied by the minimum of the fractions determined for all the points affected by this flux.

This is, in a way, the reverse of the philosophy followed in the original form. In that case a fraction was assigned directly to a flux, dependent on how this one flux affected the solution at the relevant points. In the present case the fraction is assigned to the points, dependent on the combined effect of all relevant fluxes. The difference is subtle, and irrelevant in 1D, but important in higher dimensions.

There remains the choice of definition of the maximum and minimum solution values to be allowed. A conservative choice is to take the maximum to be the maximum of the provisional solution at the point in question and at the adjacent points, with an analogous definition of the minimum. However, this choice is essentially that used in the original

FCT and results in the clipping phenomenon characteristic of the original limiter. A less restrictive choice is to include the solution values from the previous time level at the same three points in the determination of the extrema. This allows the new solution to exceed the range of the low-order provisional solution provided that it remains within the range of the solution at the previous time level.

That the new limiter reduces the clipping phenomenon is evident in the figure below:

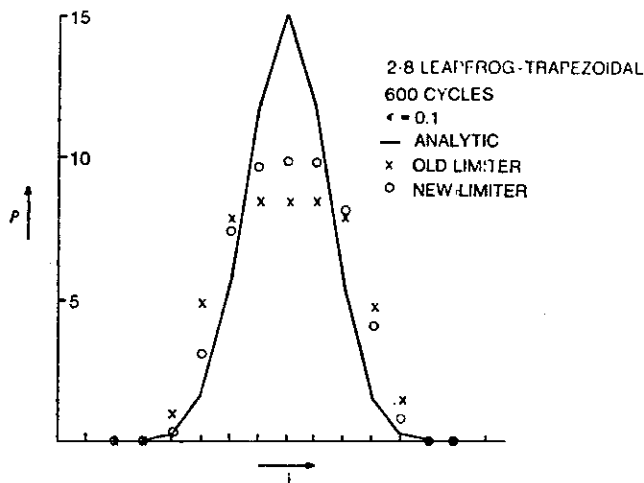


Fig. 138. Same comparison as in Fig. 5, but with more accurate transport algorithm (2-8 leapfrog-trapezoidal). Again note the reduced clipping with the new flux limiter. (Ref. 227)

Here the high-order solution was a leapfrog-trapezoidal scheme with second order in time and eighth order in space (Ref. 117). The low-order scheme was the donor-cell procedure with zero-order diffusion added, as was common in the original FCT. Some clipping is still present, however.

A further reduction is possible in 1D by projecting the provisional solution values to form peaks between grid points and including these peaks on either side of the point in question in the determination of the

extrema, as illustrated below:

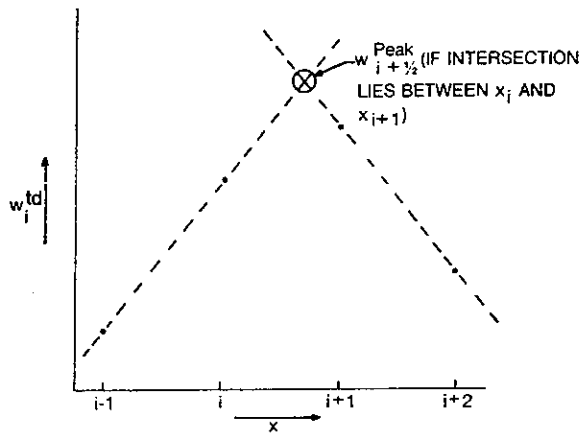


Fig. 139. A possible scheme for extracting information about extrema which exist between grid points at a given point in time. An extremum is assumed to exist between grid points  $i$  and  $i+1$  if the intersection of the right- and left-sided extrapolations of  $w^{td}$  has an  $x_i$  and  $x_{i+1}$ . The  $w$  coordinate of the intersection is then used in the computation of  $w^{\max}$  and  $w^{\min}$ . (Ref. 227)

The results below show considerable improvement, with clipping virtually eliminated.

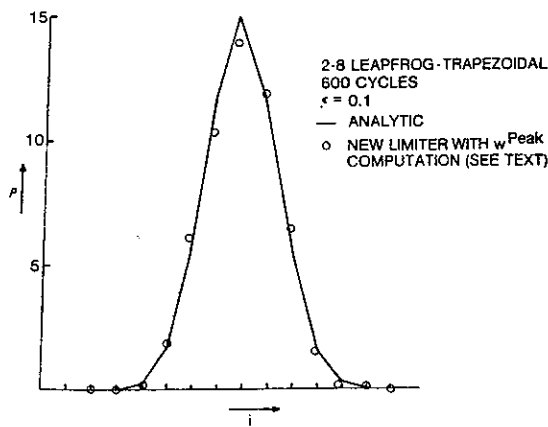


Fig. 140. Same as Fig. 138, except that Eq. (19) and (2), which utilize the  $w^{\text{peak}}$  computation illustrated in Fig. 139, are used to compute  $w^{\max}$  and  $w^{\min}$  in the new flux limiter. Values for the old flux limiter since they are identical to those shown in Fig. 138, are not shown. Note that the clipping has been virtually eliminated. (Ref. 227)

It is clear that, in order to eliminate clipping, some past history of the solution extending to the sub-grid level must be included in the limiter.

The new flux limiter generalizes directly to higher dimensions. The figures below show results obtained for rotation of a cylinder with a cut-out using a leapfrog scheme that is second order in time and fourth order in space (Ref. 117) as the high-order scheme. The low-order scheme was the same as that used above. (The new limiter here did not include the sub-grid peaks).

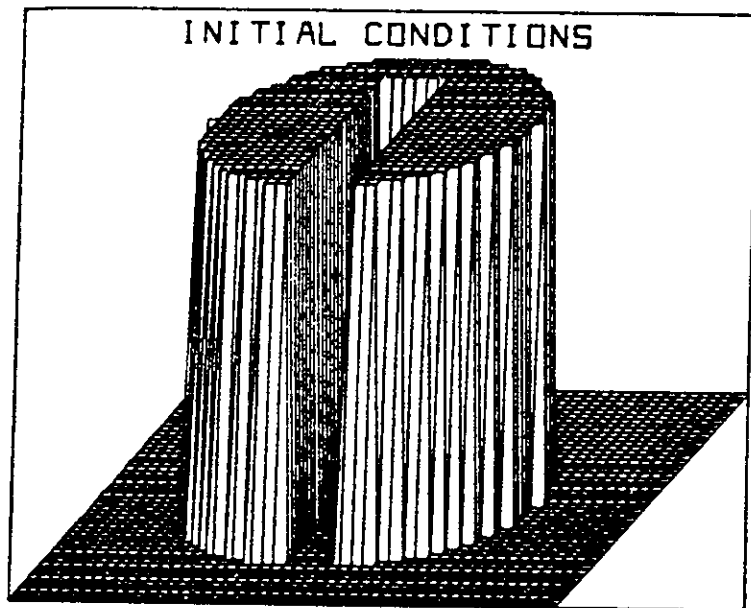


Fig. 141. Perspective view of initial conditions for the two-dimensional solid body rotation problem. Note that only a 50 x 50 portion of the mesh centered on the cylinder is displayed. Grid points inside the cylinder have  $w_{ij} = 3.0$ . All others have  $w_{ij} = 1.0$ . (Ref. 227)

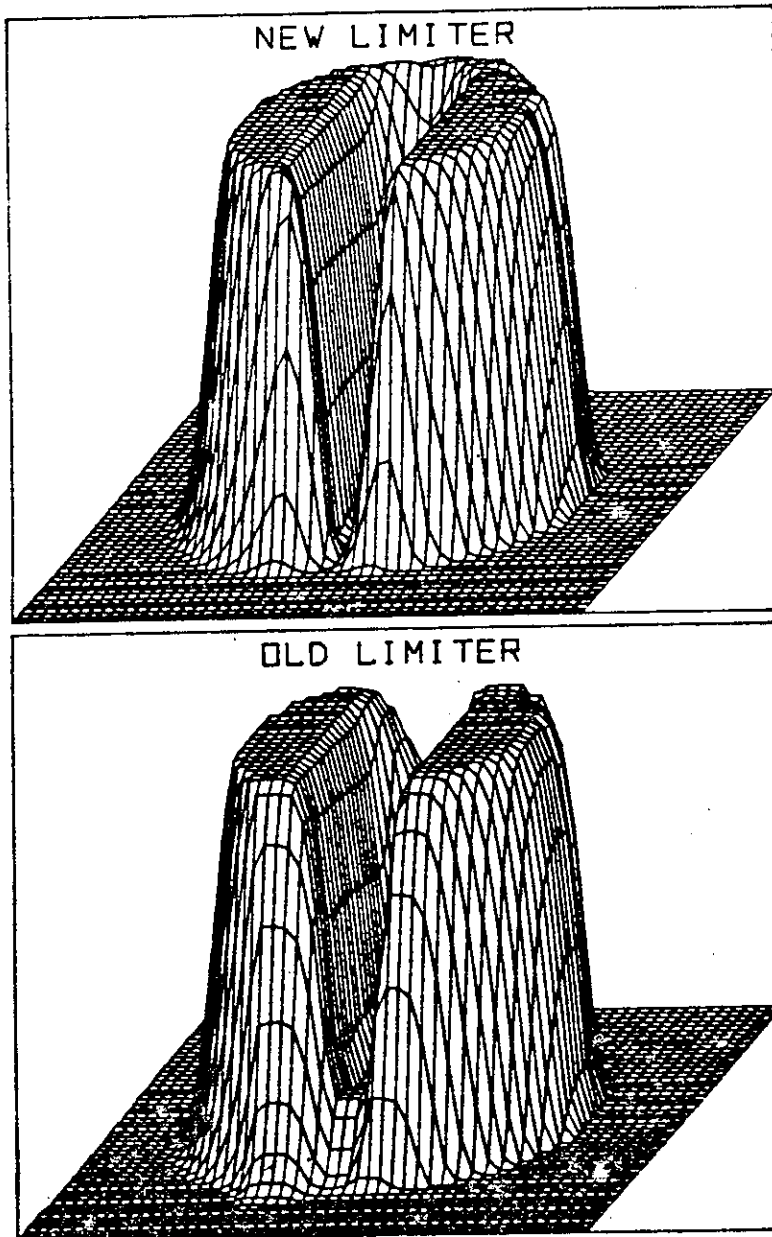


Fig. 142. Comparison of perspective views of the w profile after 157 iterations ( $1/4$  revolution) with both the old and new flux limiters. The perspective view has been rotated with the cylinder, so that direct comparison with Fig. 141 can be made. Again we plot the  $50 \times 50$  grid centered on the analytic center of the cylinder. Features to compare are the filling-in of the gap, erosion of the "bridge," and the relative sharpness of the profiles defining the front surface of the cylinder. (Ref. 227)

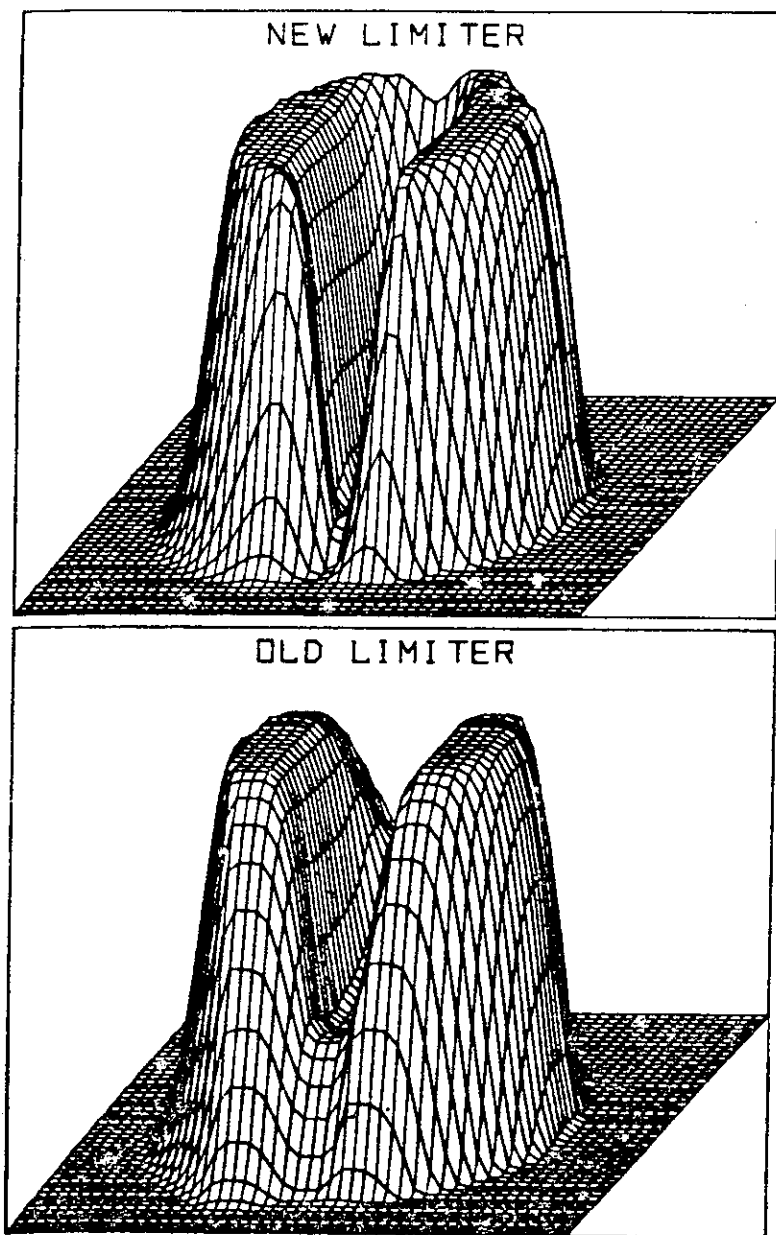


Fig. 143. Same as Fig. 142, but after 628 iterations (one full revolution).  
Again note decreased diffusion with new flux limiter.  
(Ref. 227)

The superiority of the new flux limiter is apparent.

Zalesak (Ref. 226) states that with FCT in the form given in Ref. 227, involving a combination of higher and low-order methods, higher order of resolution as obtained in smooth regions and sharper representation of discontinuities, such as shocks, are also obtained. No linear scheme of order higher than first will preserve the monotonicity of a step function.

Comparisons of several high-order schemes in this FCT framework are given below for convection of a square wave. The low-order scheme was the donor cell first-order upwind method in each case:

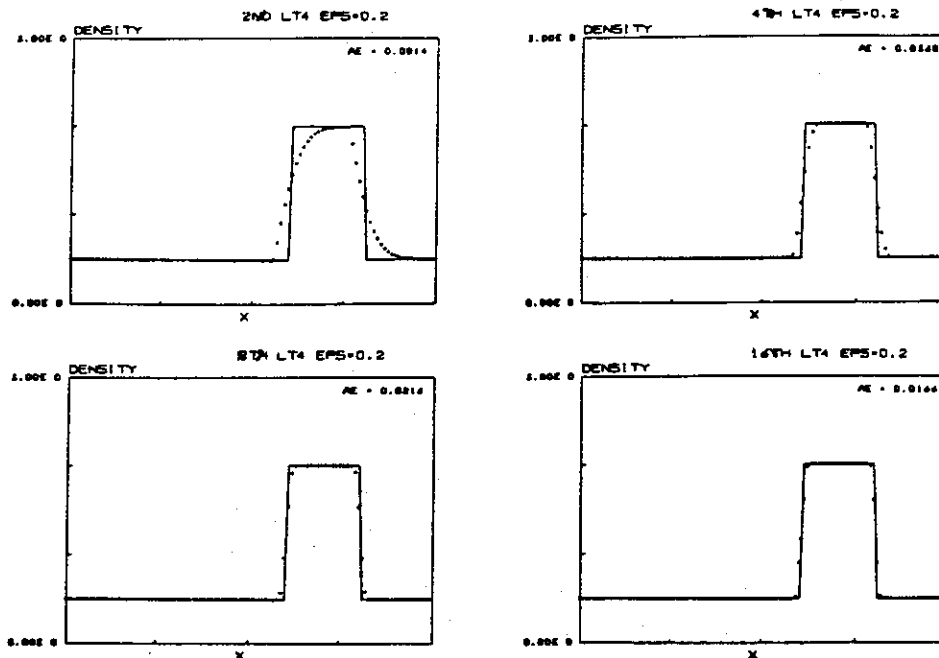


Fig. 144. The same test as in Fig. 117, but using FCT algorithms. The "low-order" and "high-order" components were selected from the schemes shown in Fig. 117. Results are shown using the donor cell scheme as the low-order scheme and leapfrog-trapezoidal schemes utilizing spatial derivatives of second, fourth, eighth, and sixteenth-order accuracy, respectively as the high-order schemes. Note that the monotonicity of the analytic solution is preserved in all cases, and that there is a marked increase in the sharpness of the profile as the order of the spatial derivatives is increased. (Ref. 226)

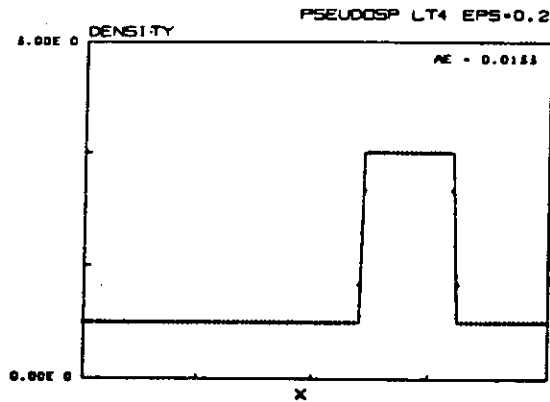


Fig. 145. Tests of the linear advection of a square wave, as in Fig. 117, but using the Fourier pseudo-spectral approximation of spatial derivatives together with the leapfrog-trapezoidal temporal discretization as the "high-order" scheme. Shown are results for our pseudospectral-FCT scheme. The  $L_1$  error of 0.0133 is the lowest ever seen by this author for this problem. (Ref. 226)

Similar comparisons for a Gaussian are shown next:

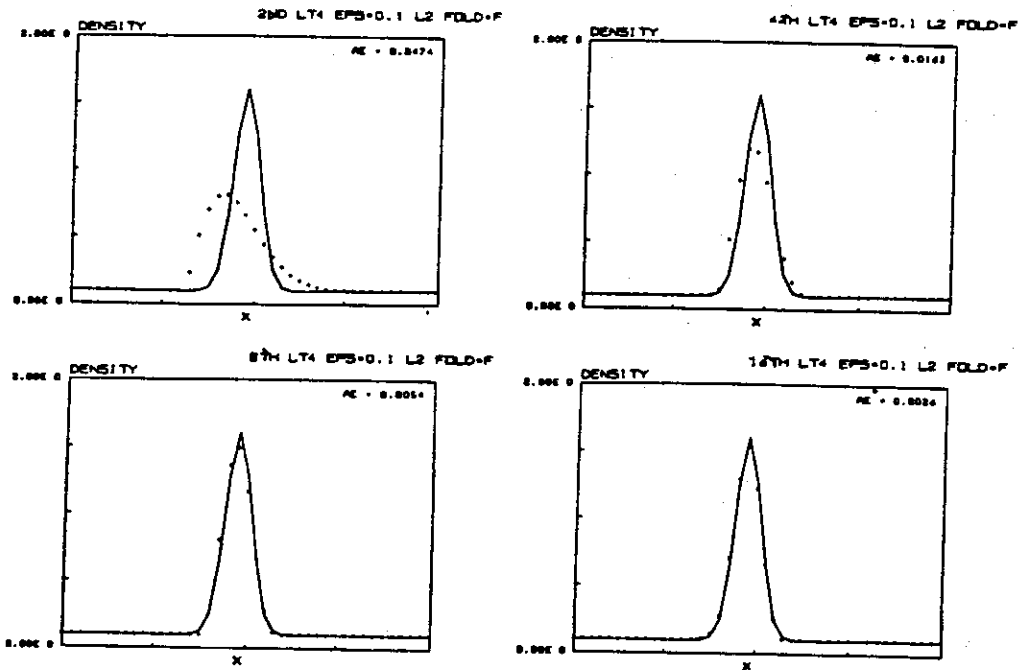


Fig. 146. Tests of linear advection using FCT algorithms, but this time using the sharply peaked Gaussian of half-width  $2\Delta x$  used by Forester. The standard output time (shown here) is after 600 time steps using a Courant number  $v\Delta t/\Delta x$  of 0.1. We have used exactly the same four FCT algorithms as in Fig. 144. Again note the increase in accuracy as the order of the spatial derivatives is increased. (Ref. 226)

Clearly the combination of this form of FCT with higher-order schemes in space is effective in reducing the dispersive error without introducing significant dissipation.

Zalesak (Ref. 225) again suggests that the ultimate convection scheme may be a very high-order scheme operating in the FCT framework.

Chapman (Ref. 41) first calculates provisional values using a higher-order method, and then uses these values to determine the diffusion coefficients of first-order diffusion terms to be added to these provisional values. The diffusion coefficients are set to 0 or 1 according to whether the provisional values are beyond the range of the local Lagrangian solution, modified by the effect of nonuniform velocity. This is accomplished as follows. By the characteristic equation, the solution value one grid point at  $i - 1$  will appear at some point between this point and point  $i$  at the next time level if the velocity is uniform. With nonuniform velocity this value is modified by the term,  $-\phi u_x$ , which is here expressed by a central difference. Similarly, the solution value at point  $i$  at the previous time level will appear at some point between this point and the point  $i + 1$  at the next level, subject to the nonuniform velocity modification. Therefore, the maximum allowed for the provisional value at point  $i$  is  $\max(\phi_{i-1}^*, \phi_i^*, \phi_{i+1}^*)$ , where

$$\phi_k^* = \phi_k^n - \phi_k^n \left( \frac{u_{k+1}^n - u_{k-1}^n}{2\Delta x} \right) \Delta t \quad k = i-1, i, i+1$$

The lower limit is just the minimum of these three values.

Results for this type of switched dissipation applied to the Crowley second-order scheme (Ref. 55, same as the Lax-Wendroff) are shown on the following page for convection of a square wave.

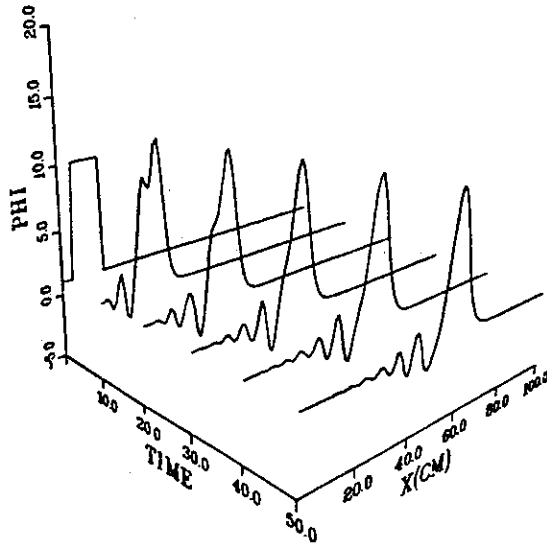


Fig. 147. Crowley second-order convection of square pulse.  $\phi_{\max}$  at  $t = 50 = 12.2$ . (Ref. 41)

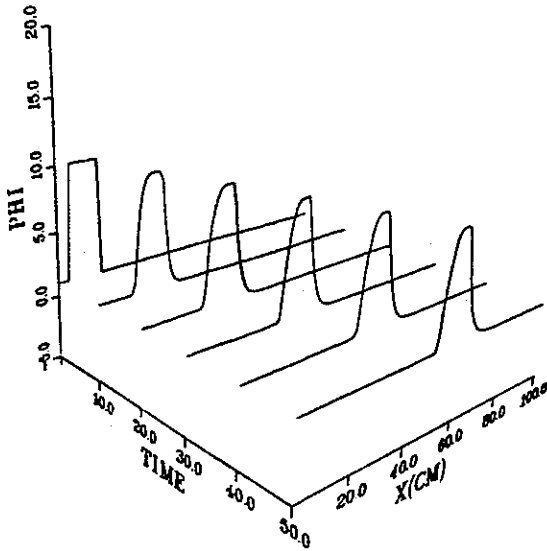


Fig. 148. Filtered Crowley second order,  $\phi_{\max}$  at  $t = 50 = 9.6$ . (Ref. 41)

Next a comparison is given for convection of a Gaussian of  $2\Delta x$  half-width by the Crowley scheme using (a) the Forester filter (Ref. 74) set to filter  $2\Delta x$  wavelengths, (b) the generalized form of FCT given by Zalesak (Ref. 227) using upwind with zero-order diffusion as the lower-order method and the original FCT limiter of Refs. 32, 28, and 31, (c) FCT as above but with the new limiter of Ref. 227, and (d) the present filter.

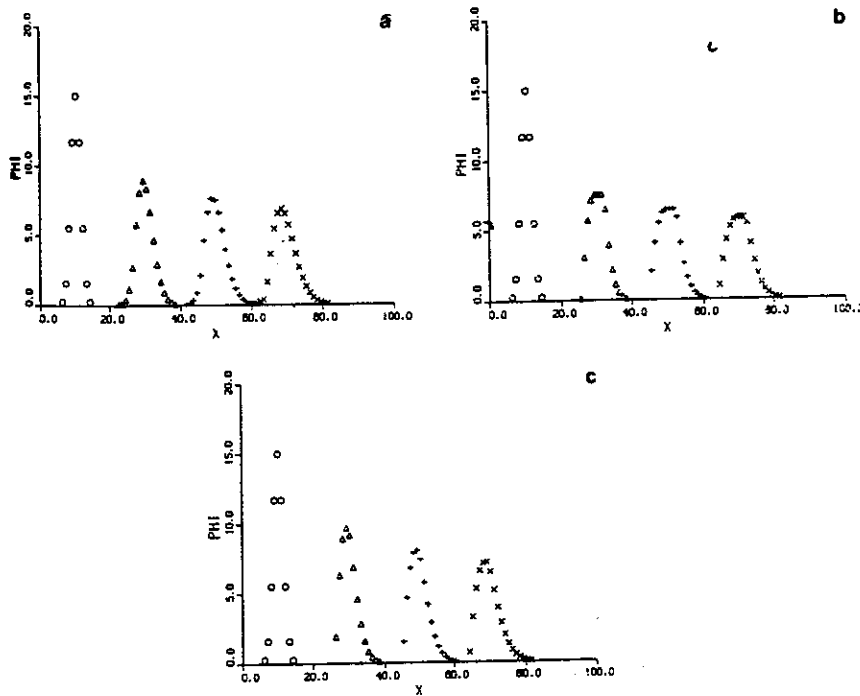


Fig. 149. Gaussian test probe. (a) Filter of Forester; (b) FCT, old limiter; (c) FCT, new limiter. (Ref. 41)

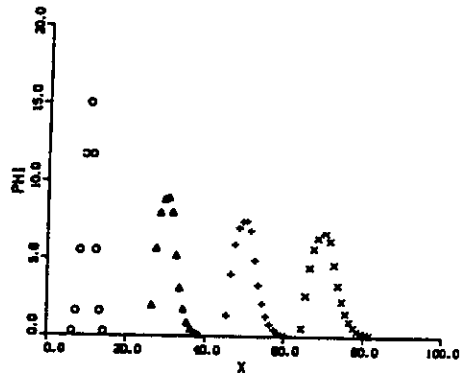


Fig. 150. Gaussian test problem. Crowley second order plus FRAM. (Ref. 41)

Of these, FCT with the new limiter is the best, and FCT with the old limiter is the worst.

The present scheme for uniform velocity is equivalent to the generalized version of FCT using the upwind scheme as the low-order method, but with the present form of the limiter.

The next figure shows a comparison of the schemes mentioned above for a square wave in a nonuniform velocity field. Also shown is FCT with the new limiter and using the upwind scheme as the low-order method.

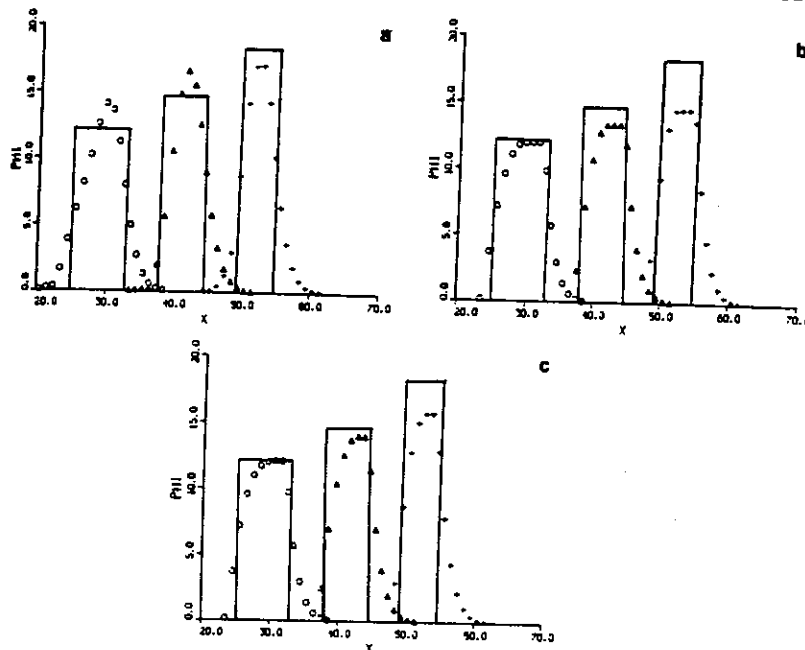


Fig. 151. Test problem 2. (a)Forester's algorithm; (b) FCT algorithm, low-order upwind +1/8; (c)FRAM plus Crowley. (Ref. 41)

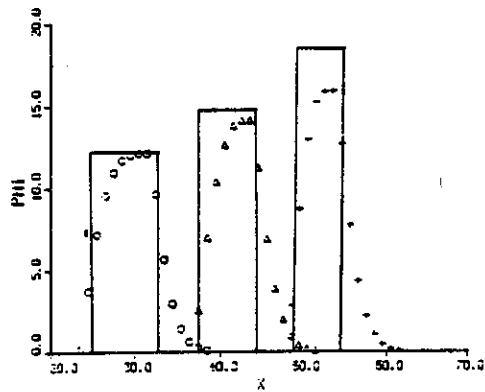


Fig. 152. Test case 2. FCT new limiter, low-order flux upwind. (Ref. 41)

The upwind scheme is a better choice for use with FCT, and the present scheme gives essentially the same results as this form of FCT. The peak amplitude for the distribution of this problem as given by the numerical solution is shown next.

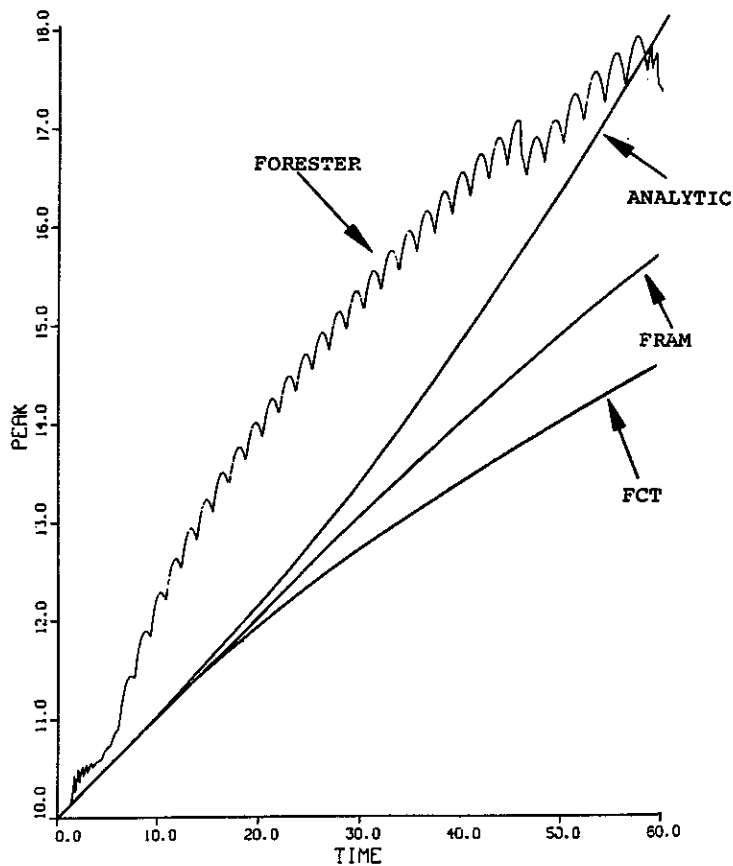


Fig. 153. Peak pulse amplitude as a function of time for  $\partial u / \partial x < 0$ . (Ref. 41)

Here FCT with upwind for the lower-order method was essentially coincident with the results of the present scheme.

The construction of the present filter in 2D is similar to that in 1D, with  $\nabla \cdot \underline{u}$  replacing  $u_x$  in the modification of the Lagrangian velocities used to set the limits. Five points are now used to form the limits. In the figure below the unfiltered results are compared with those of the present scheme and FCT using upwind as the low-order method for a square wave. Here the FCT was applied separately in each direction.

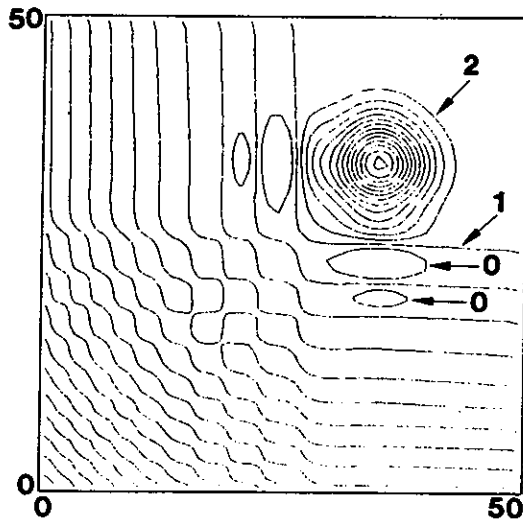


Fig. 154. Contour plot for second-order convective scheme,  $\phi_{\max} = 14.5$ ,  $\phi_{\min} = -1.94$ . (Ref. 41)

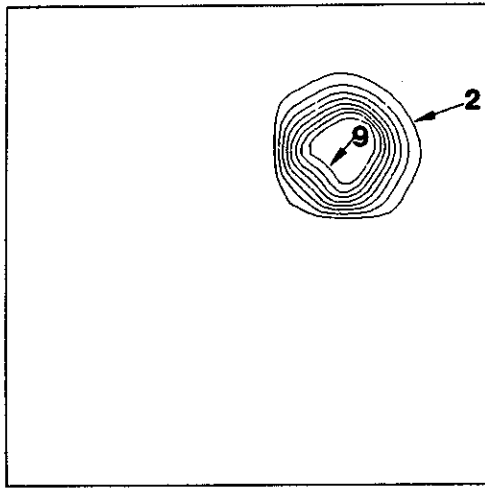


Fig. 155. Second-order with damping,  $\phi = 9.81$ . (Ref. 41)

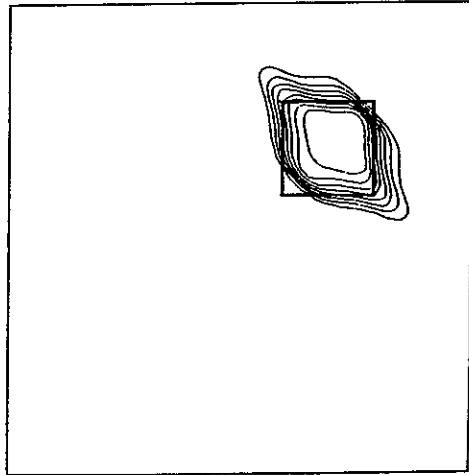


Fig. 156. Operator split FCT upwind,  $\phi_{\max} = 9.99$ . (Ref. 41)

The FCT applied in this split manner clearly shows a skewness.

With fourth-order method the results are much sharper as shown below:

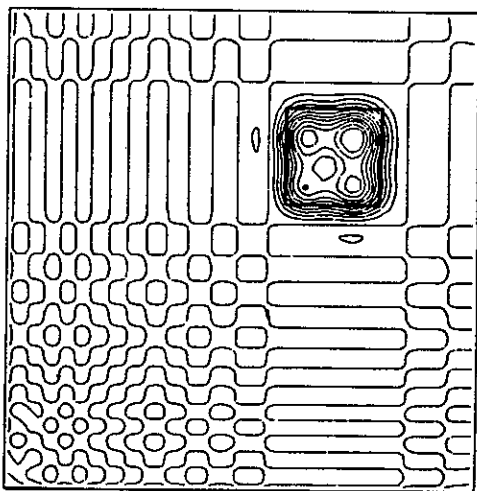


Fig. 157. Fourth-order unfiltered,  $\phi_{\max} = 13.6$ . (Ref. 41)

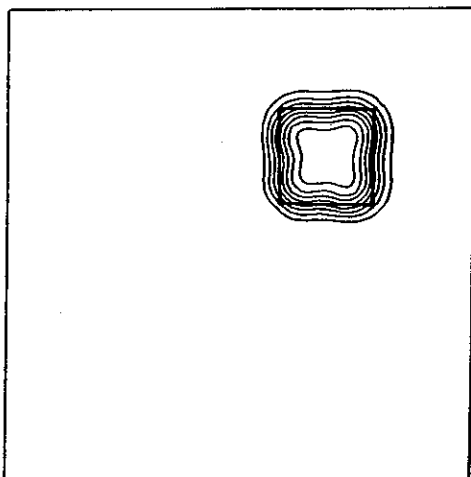


Fig. 158. Fourth-order filtered,  $\phi_{\max} = 9.50$ . (Ref. 41)

The fourth-order scheme used was that of Fromm (Ref. 72), which is a two-stage method with the stencils



and the flux at  $i + 1/2, j$ , for example, evaluated on the stencil



The present scheme is said to require fewer operations than FCT.

#### Waveform Filters

In Ref. 74, Forester constructs a nonlinear filter based on the addition of second-order artificial diffusion with the diffusion coefficients set to 0 or 1 according to a test for slope sign continuity on either side of a point. At each point where the sign of the slope (the difference in the solution between grid points) changes, a range of  $N$  points on either side is examined for additional slope changes. If any are found, the coefficients are set to 1 at the central point and at  $M$  points on each side. Here  $N$  is chosen to span one-half of the wavelength of the longest waves to be filtered. Thus  $2\Delta x$  waves are filtered for  $N = 1$ ,  $4\Delta x$  and shorter waves for  $N = 2$ , etc. The value of  $M$  is taken to be less than that of  $N$ , half the largest even integer equal to or less than  $N$  being a typical choice. The filter can be extended to longer

wavelengths also by repetitive application, and this was found to be more effective than increasing  $N$  for waves longer than  $10\Delta x$  when higher-order algorithms are used. Repetition until none of the diffusion coefficients is set to 1 will produce a monotonic scheme. Several comparisons of results using this filter have been given on p. 163-166.

Zhmakin and Fursenko (Ref.228 ) use a selective filter that operates by setting a diffusion coefficient different from zero at mid-points located in an  $N$  wave to produce a monotonic method. A comparison with other methods is shown below for a triangular wave:

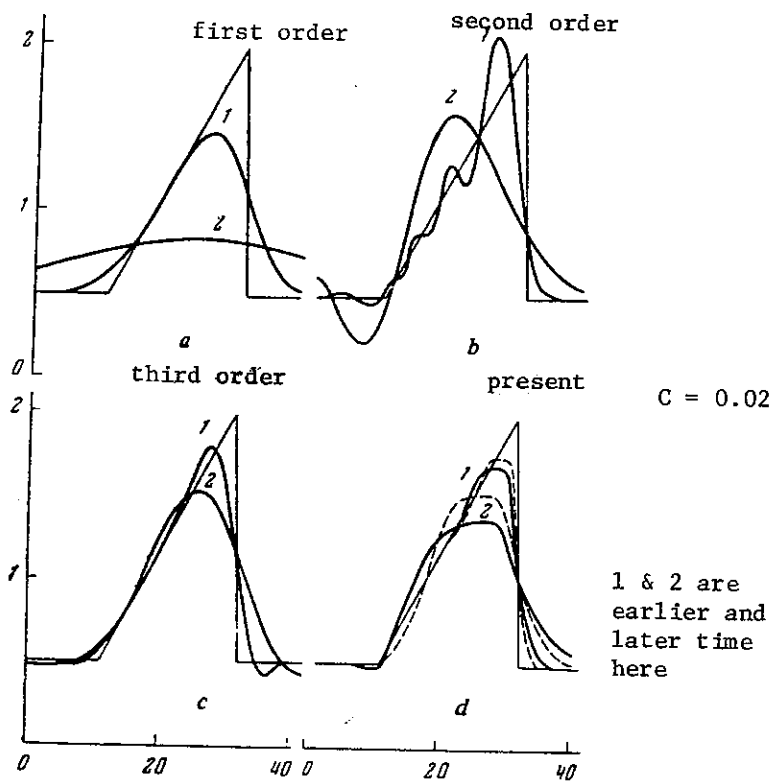


Fig. 159. Note that unlike algorithms (1.4) - (1.7) with smoothing by (1.8) - (1.10) the solution is not distorted at all in regions of monotonic variation of the parameters. (Ref.228)

Dispersion is reduced, but there is considerable dissipation.

Shapiro (Ref. 187) gives a filter based on repetitive applications of the basic smoothing operator,  $\delta_{xx}$ , with the coefficient used at each repetition chosen so that wavelengths below a certain value are strongly damped while longer waves are hardly damped at all. This filter is shown to be equivalent to adding an artificial viscosity of order  $2N$  given by

$$F_N = (-1)^{N-1} \left(\frac{\Delta x}{2}\right)^{2N} \delta_{xx}^N$$

The 2D form is

$$F_{NM} = (-1)^{N-1} \left(\frac{\Delta x}{2}\right)^{2N} \delta_{xx}^N + (-1)^{M-1} \left(\frac{\Delta y}{2}\right)^{2M} \delta_{yy}^M \\ + (-1)^{M+N} \left(\frac{\Delta y}{2}\right)^{2N} \left(\frac{\Delta x}{2}\right)^{2M} \delta_{xx}^N \delta_{yy}^M$$

The cross-terms are necessary to preserve the highly selective character of the filter.

McRae, Goodin, and Seinfeld (Ref. 146) discuss several types of filters designed to prevent negative concentration. The simplest approach is simply to reset any negative concentration to zero. This procedure will violate mass conservation, however. Mahlman and Sinclair (Ref. 138) take the concentration to zero from the downstream cell. A comparison of these two filters with the Forester filter (Ref. 74) set to filter all wavelengths less than  $8\Delta x$  is given for a squarewave on the page following. The Forester filter is clearly superior.

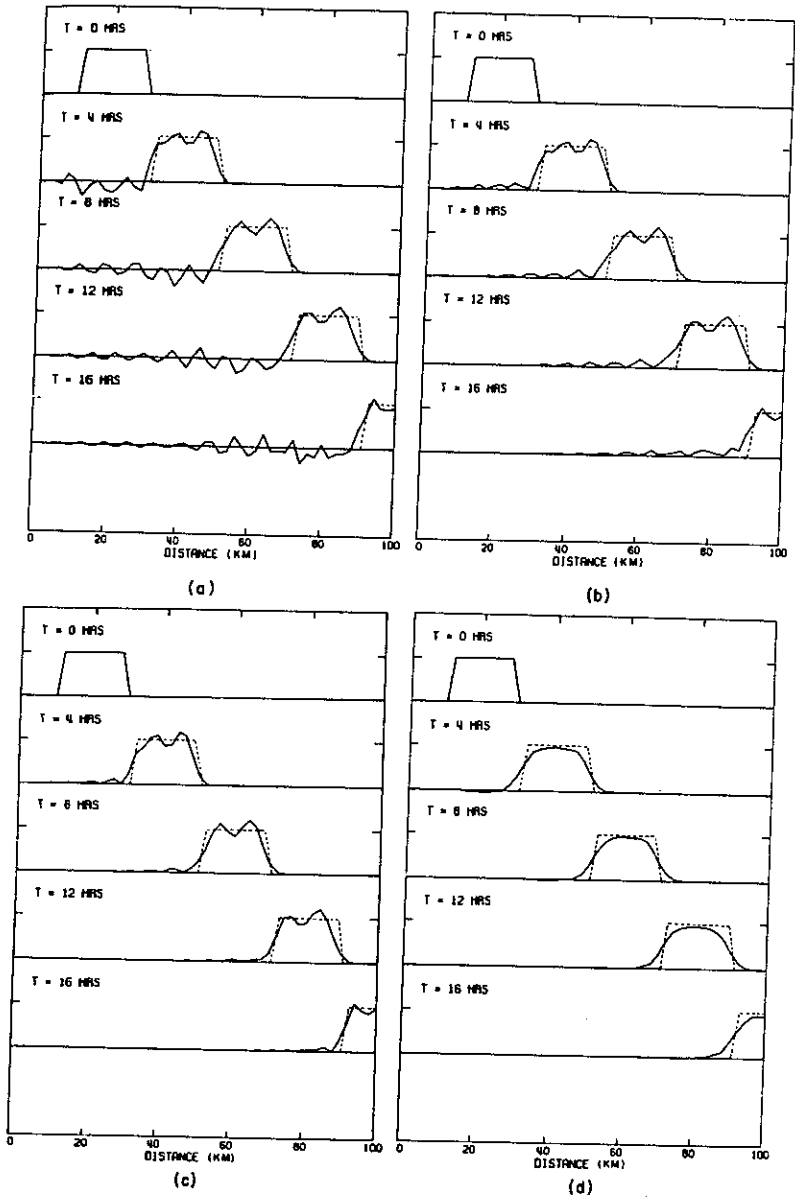


Fig. 160. Application of difference schemes to maintain concentration positivity. (a) Original linear finite element solution. (b) Absolute value  $|c|$ . (c) Downstream borrowing. (d) Nonlinear filter. (Ref. 146)

### Implicit Filters

Pepper, Kern and Long (Ref. 160) use an implicit filter of the form  $(4\mu_X^2 - \alpha\delta_X^2)\phi = 4\mu_X^2\bar{\phi}$ , where  $\bar{\phi}$  is the solution being filtered and  $\alpha$  is a parameter to be set. The  $2\Delta x$  waves will always be damped out completely, and the range of filtering extends to higher wavelengths as the parameter  $\alpha$  increases. Typical operation is to apply the filter after a certain number of time steps. Results from application to convection to a rotating cosine hill are shown below:

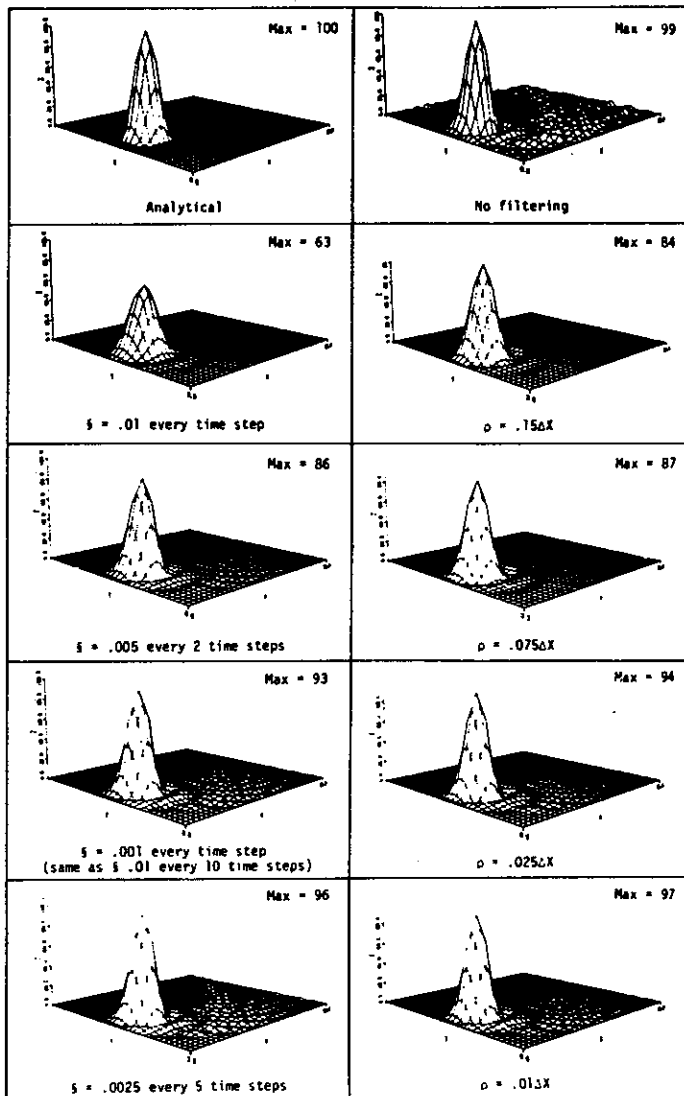


Fig. 161. Effects of filtering on a cosine hill distribution at  $2\pi$  revolutions by using chapeau functions with  $\Delta X = \Delta Y = 2500$  m. (Ref. 160)

Alpert (Ref. 12) gives an implicit filter requiring a tridiagonal solution:

$$(1 - \alpha)\bar{\phi}_{j-1} + 2(1 + \alpha)\bar{\phi}_j + (1 - \alpha)\bar{\phi}_{j+1} = \phi_{j-1} + 2\phi_j + \phi_{j+1}$$

The  $2\Delta x$  waves are completely eliminated and the smoothing of longer waves is determined by  $\alpha$ . This filter has somewhat less damping than the explicit filter at the lower wavelengths and a bit more at the higher. However, this implicit filter is sharper than the explicit.

The implicit filter is made sharper by reducing  $\alpha$ , while it is necessary to add more points to sharpen the explicit filter. It is possible to set the implicit filter such that there is less damping than the explicit for all waves of interest, while still completely removing the  $2\Delta x$  waves.

Khosla and Rubin (Ref. 115) replace the convective velocity with a three-point weighted average of the form

$$u_i = \frac{u_{i+1} + u_{i-1} + ku_i}{2 + k}$$

which is of order  $\frac{\Delta x^2}{2+k} u_{xx}$ . In general  $k$  can assume any value greater than  $-2$ . The filtering effect decreases to zero as  $k$  becomes very large.

#### Artificial Viscosity

In Ref. 127, van Leer determines the minimum artificial diffusion necessary to stabilize some second-order methods. This artificial diffusion is found to be proportional to the square of the Courant number. This topic is continued by van Leer in Ref. 122 where it is noted that the minimum artificial diffusion for second-order methods corresponds to that in the Lax-Wendroff method. Also determined is the minimum amount for monotonicity, this corresponding to the first-order Godunov method

There are no linear monotonic schemes higher than first order.

The question of monotonicity is further pursued by van Leer in Ref. 123, and Fromm's second-order composite scheme (Ref. 72), formed as an average of schemes with lagging and leading phase error, is made monotonic through the inclusion of nonlinear feed-back terms. The dissipation is naturally increased, but oscillations are eliminated in the monotonic form. The scheme retains its formal second order, however.

Sirinivas, Gururaja, and Prasad (Ref. 194) give a first-order scheme based on the addition of the local minimum amount of first-order artificial viscosity to a second-order central difference scheme required to ensure stability locally. This scheme is related to the first-order van Leer scheme of Ref. 72 and the first-order Rusanov scheme (Ref. 184). The scheme does not guarantee monotonicity, and extra viscosity must be added near shocks. The Lapidus form of third-order artificial viscosity was used by Sod in Ref. 191.

Strauss (Ref. 205) notes that the use of second-order artificial viscosity based on the difference of the diagonal averages across a square cell in 2D, as given by Chan, is equivalent to using  $2\delta_{xx} - \delta_{dd}$ , instead of  $\delta_{xx}$ , for the artificial viscosity, where  $\delta_{dd}$  has the same form of  $\delta_{xx}$  but rotated  $45^\circ$ . This nine-point form has less damping for long waves than the usual five-point form, while still eliminating the  $2\Delta x$  mode.

Dukowicz and Ramshaw (Ref. 62) introduce a multiple-dimension tensor artificial viscosity based on representation of the second time derivative in the Taylor series expansion in terms of spatial derivatives through differentiation of the differential equation without assuming uniform velocity. Actually only the part of this term involving second derivatives

of the concentration is used. The resulting scheme is first order.

Chin and Hedstrom (Ref. 44) show that it is better to add an artificial viscosity to a nondissipative scheme than to use a scheme with built-in dissipation.

Sod (Ref. 191) found that with high-order methods using the appropriate high-order artificial viscosity term, the coefficient of numerical diffusion was so large that the time step was limited to prohibitively small values. A third-order artificial viscosity was the largest that could be used.

## VI. TIME-SPLITTING

One-dimensional schemes can be applied to higher dimensions in a sequence of properly factored steps. It is also possible to include physical diffusion in succession to convection in this manner.

### Multiple Dimensions

Since time-split methods operate as a sequence of 1D methods, this approach achieves maximal stability properties because the amplification matrix is a product of matrices each of which is derived from a 1D scheme, so that the stability requirements are those of the individual 1D scheme.

Strang introduced the symmetric product form of time-splitting which preserves the order of second-order methods in Ref. 203, in the form

$L_x(\frac{\Delta t}{2}) L_y(\Delta t) L_x(\frac{\Delta t}{2})$ . Earlier, Strang (Ref. 201) had proposed the sum of products form,  $\frac{1}{2}[L_x(\Delta t)L_y(\Delta t) + L_y(\Delta t)L_x(\Delta t)]$ . The symmetric product form requires fewer operations than the earlier form.

Several generalizations and extensions of Strang-type splittings are given by Gottlieb in Ref. 82 for any number of dimensions. All of these schemes are symmetric in some sense and preserve the second order of the component 1D schemes. For ease of understanding, these schemes are given below for three dimensions, the generalizations to higher dimensions and the specialization to 2D being easily inferred.

The first scheme was originally given by Strang (Ref. 201) and has the form

$$L_1 = \frac{1}{3!} \sum_i L_i L_j L_k$$

where  $i, j, k$  represent cyclic permutations of the indices  $x, y, z$ , and the summation extends over all permutations (six terms).

The new generalizations introduced by Gottlieb follow. In each case obvious variations are possible:

$$L_2 = L_x^{\frac{1}{2}} L_y^{\frac{1}{2}} L_z L_y^{\frac{1}{2}} L_x^{\frac{1}{2}}$$

where the superscript indicates the use of  $\frac{\Delta t}{2}$  in the 1D operator.

$$L_3 = \frac{1}{2}(L_x L_y L_z + L_z L_y L_x)$$

The 2D forms of both of the above two schemes were also introduced by Strang, in Ref. 203 and Ref. 201, respectively. The 3D versions of both of these schemes were originally given by Gourlay and Morris (Ref. 86). Finally any symmetric combination of portions of the above two schemes is also a valid second-order scheme. For example, the following scheme was considered:

$$L_4 = \frac{1}{2} L_x^{\frac{1}{2}} (L_y L_z + L_z L_y) L_x^{\frac{1}{2}}$$

Other possibilities are easily inferred.

The first scheme,  $L_1$ , is grossly inefficient compared with the others, requiring about 1/3 more operations in 2D and three times as many in 3D. The second scheme,  $L_2$ , is the most efficient, requiring 3/4 as many operations as the other two in 2D, and 5/6 as many in 3D. The stability of all the schemes is that of the individual 1D components, a feature characteristic of splitting methods. Implementations of the schemes  $L_2$  and  $L_3$  in 3D were given by Gourlay and Morris (Ref. 86) and are repeated by Gottlieb. An implementation of the scheme  $L_4$  is also given by Gottlieb.

Eilon, Gottlieb, and Zwas (Ref. 65) found the Strang symmetric

splitting (Ref. 201, 203) of the form  $L_x^{\frac{1}{2}} L_y L_x^{\frac{1}{2}}$  to be more efficient than several split and unsplit methods for 2D.

Burstein and Mirin (Ref. 35) give another second-order symmetric splitting based on combination of splittings given by Strang:

$$\frac{2}{3}(L_x^{\frac{1}{2}} L_y L_x^{\frac{1}{2}} + L_y^{\frac{1}{2}} L_x L_y^{\frac{1}{2}}) - \frac{1}{6}(L_x L_y + L_y L_x)$$

Of more interest, a third-order splitting is given:

$$\frac{9}{8} L_x^{\frac{1}{3}} L_y L_x^{\frac{2}{3}} L_y L_x^{\frac{1}{3}} - \frac{1}{8} L_x L_y$$

where each 1D operation is third order. It is also shown that any third-order splitting must involve six 1D operations.

Morchoisn, Ref. 149, uses the time-split approximate factorization procedure with the residual evaluated in a pseudospectral manner, while using difference expressions in the matrices multiplying the solution change in the delta form. Approximate factorization time-split forms are given by Beam and Warming in Ref. 24 which are second order in time, and in space are second or fourth-order central or second-order one-sided.

#### Multiple Processes

The use of convection followed by diffusion is considered in some detail by Pironneau in Ref. 165. McRae, Goodin, and Seinfeld (Ref. 146) use symmetric time-splitting for a reacting flow, with the chemical step in the middle.

#### Numerical Considerations

Some forms of time-splitting can introduce error either because the combined steps do not reproduce the difference equations exactly or because the intermediate steps are not consistent approximations of the

difference equations. Error of the first sort occurs, for instance, when terms of the order of the temporal truncation error are added to the difference equations in order to factor the equations into a product of 1D difference operators. This type of error is no real problem with the small time steps of explicit methods, since the formal order of the difference approximation is not altered. It can be significant, however, with the large time steps allowed in implicit methods. The other kind of error results from the fact that the proper expression of the boundary conditions is not clear if the intermediate steps are not consistent approximations of the time-dependent equations. Both of these types of error in splitting methods are discussed by Dwoyer and Thames in Ref. 63, and procedures for removing these sources of error are given.

Gourlay and Morris (Ref. 85) discuss the formulation of immediate boundary condition for the time-split methods given by Strang (Ref. 203). The use of explicit boundary conditions in implicit schemes was found to be satisfactory.

Abarbanel and Gottlieb (Ref. 2) note that the locally one-dimensional splittings that have been in common use in explicit methods, such as the MacCormack method, are not optimal in stability when mixed derivatives are involved. They show that the optimal splitting involves a split into a hyperbolic part (convective terms), a parabolic part (double second derivatives) in each direction and a mixed-derivative part. In 2D there are thus five distinct factors in the split. A symmetric product of these factors then preserves second order in space and time. This has no bearing on pure convection problems, of course, since the mixed derivatives arise from the diffusion terms.

In Ref. 105, van der Houwen discusses general multi-stage splittings

to construct iterative solutions for implicit methods. In particular, the increase in order from that of the initial guess toward that of the difference approximation is covered. It is shown that the formal order of the difference approximation can be reached in finite number of iterations but stability considerations, and accuracy at finite  $\Delta t$ , may require tighter convergence.

## VII. VARIOUS CONSIDERATIONS

### Stability

Stability in the linear sense is analyzed by substitution of elementary waveforms into the difference equation, as has been mentioned earlier. Explicit methods will have limitations on the Courant number, which become more restrictive as the number of dimensions increases. This decrease in stability in multiple dimensions can be circumvented by time-splitting as noted above. Some other considerations follow in this section.

Gerrity (Ref. 79) shows that the second-order Lax-Wendroff method can exhibit a nonlinear instability which is associated with the separation of solutions on alternate grid points. Robert, Shuman, and Gerrity (Ref. 173) discuss nonlinear instability and recommend time-averaging as a control.

Griffiths, Christie, and Mitchell (Ref. 92) show that error can become arbitrarily large after a finite number of time steps even though it ultimately decays to zero. Thus the accuracy of the steady-state solution may not necessarily be a good indication of that of the transient solution. It is also noted that the von Neumann method of stability analysis is more indicative of stability at finite time than is the spectral radius approach.

Piacsek and Williams (Ref. 164) show that the difference form

$$(u\phi)_x = (u_{i+\frac{1}{2}} \phi_{i+1} - u_{i-\frac{1}{2}} \phi_{i-\frac{1}{2}} \phi_{i-1}) / 2\Delta x \quad (1)$$

is more stable than the form

$$(u\phi)_x = [u_{i+\frac{1}{2}}(\phi_{i+1} + \phi_i) - u_{i-\frac{1}{2}}(\phi_i + \phi_{i-1})] / 2\Delta x \quad (2)$$

The first of these differs from the second by subtraction of the term  $\phi_i(u_{i+\frac{1}{2}} - u_{i-\frac{1}{2}}) / 2\Delta x$ , which is a type of mass residual correction (being

zero when continuity is satisfied in the 2D case).

Zalesak (Ref. 225) notes that ZIP differencing of fluxes, i.e., representing  $(u\phi)_x$  as

$$(u\phi)_x = [(u\phi)_{i+\frac{1}{2}} - (u\phi)_{i-\frac{1}{2}}]/\Delta x \quad (3)$$

with

$$(u\phi)_{i+\frac{1}{2}} = \frac{1}{2}(u_i\phi_{i+1} + u_{i+1}\phi_i) \quad (4)$$

is equivalent to expanding the product derivative and then representing each of the derivatives by central differences:

$$\begin{aligned} (u\phi)_x &= u\phi_x + u_x\phi \\ &= u_i(\phi_{i+1} - \phi_{i-1})/2\Delta x \\ &\quad + \phi_i(u_{i+1} - u_{i-1})/2\Delta x \end{aligned} \quad (5)$$

An alternate representation uses averages of the product:

$$(u\phi)_{i+\frac{1}{2}} = \frac{1}{2}(u_i\phi_i + u_{i+1}\phi_{i+1}) \quad (6)$$

The truncation error of the average-of-product form contains both odd and even derivatives, while that of the ZIP form has only odd derivatives. The formal order is the same in each case. The presence of the even derivatives in the truncation error of the average-of-product form results in numerical diffusion which may be negative and hence destabilizing.

A third form, product-of-average, is given below:

$$(u\phi)_{i+\frac{1}{2}} = \frac{1}{4}(u_i + u_{i+1})(\phi_i + \phi_{i+1}) \quad (7)$$

This form is actually the average of the above two forms, and hence also has the even derivatives in its truncation error, though half those of the average-of-product form. Thus the ZIP form can be expected to be

the most stable of the three, and the average-of-product the least stable. The greater stability of the product-of-average form relative to that of the average-of-product form was noted by MacCormack (Ref. 136) and by Grammelvedt (Ref. 87).

Higher-order ZIP representations require only higher-order representation of the derivatives in the expanded product derivative. Specific versions up to sixth order are given by Zalesak in Ref. 225.

MacCracken and Bornstein (Ref. 137) show that flux is better represented on nonuniform grids by averaging the contravariant velocity, i.e., averaging the product of the geometric term and the velocity, than by using the product of the individual averages.

Gresho and Lee (Ref. 90) argue that the answer to oscillations, often called wiggles, that result from dispersion errors and are induced by boundary conditions and at discontinuities in the solution or grid, is to refine the grid, rather than to use methods with large numerical dissipation. The use of centered time forms, i.e. Crank-Nicholson, is also suggested. Oscillations in time are said to be indicative that the time step is too large. The oscillations that occur with central differences for all Reynolds numbers above 2 can be suppressed by going to upwind differencing. However, in that case the solution becomes essentially independent of the cell Reynolds number for the larger values thereof and hence only represents a solution with an effectively increased diffusion, i.e., that injected by the numerical method rather than the physical diffusion.

### Curvilinear Coordinate Systems

Numerical grid generation has now become a fairly common tool for use in the numerical solution of partial differential equations on arbitrarily shaped regions. This is especially true in computational fluid dynamics, from which came much of the impetus for the development of this technique, but the procedures are equally applicable to all physical problems that involve field solutions.

Numerical grid generation is basically a procedure for the orderly distribution of observers over a physical field in a way that efficient communication among the observers is possible and all physical phenomena on the entire continuous field may be represented with sufficient accuracy by this finite collection of observations. This technique frees the computational simulation from restriction to certain boundary shapes and allows general codes to be written in which the boundary shape is specified simply by input. The boundaries may also be in motion, either as specified externally or in response to the developing physical solution. Similarly, the observers may adjust their positions to follow gradients developing in the evolving physical solution. In any case the numerically generated grid allows all computation to be done on a fixed square grid in the computational field. (Computational field refers to the space of the curvilinear coordinates, i.e., where these coordinates serve as independent variables, rather than the cartesian coordinates. This field is always rectangular by construction as explained in Ref. 209.)

The area of numerical grid generation is relatively young in widespread practice, although its roots in mathematics are old. This area involves the engineer's feel for physical behavior, the mathematician's understanding of functional behavior, and a lot of imagination, with perhaps a little help from Urania. The physics of the problem at hand must ultimately direct the grid points to congregate so that a functional relationship on these points can represent the physical solution with sufficient accuracy. The mathematics controls the points by sensing the gradients in the evolving physical solution, evaluating the accuracy of the discrete representation of that solution, communicating the needs of the physics to the points, and, finally, by providing mutual communication among the points as they respond to the physics.

The basic techniques involved then are as follows:

- (1) a means of distributing points over the field in an orderly fashion, so that neighbors may be easily identified and data can be stored and handled efficiently.
- (2) a means of communication between points, so that a smooth distribution is maintained as points shift their positions.
- (3) a means of representing continuous functions by discrete values on a collection of points with sufficient accuracy, and a means for evaluation of the error in this representation.
- (4) a means for communicating the need for a re-distribution of points in the light of the error evaluation, and a means of controlling this re-distribution.

It should be borne in mind that the requirements, e.g., smoothness, orthogonality, etc., that must be met by the grid are ultimately determined by the numerical algorithm to be run on the grid. Thus, at the same time that effort is made to generate better grids, a like effort should be made to develop hosted algorithms that are more tolerant of the grids.

Considerable progress has been made in the past decade, especially in the last few years, toward the development of these techniques and

and toward casting them in forms that can be readily applied. A comprehensive survey of procedures and applications through 1981 has been published (Ref. 212), and two conferences specifically on the area of numerical grid generation have been held, the proceedings of which have been published (Ref. 189 and 210). Some expository papers are included in the latter proceedings (Ref. 210) which can serve as an introduction to the area. A later review and correlation is given in Ref. 211.

#### Derivative Representations

Derivatives of a function may be approximated on a discrete grid either by interpolation or by mapping. In the first case the function is approximated directly in the physical region by an interpolation function which matches the given function at certain grid points. This interpolation function then is differentiated, and the derivative is evaluated at the point in question. The resulting difference expressions are simple on uniform grids, but are usually complicated on nonuniform grids, and may have to be rederived as different grid configurations occur. This is especially troublesome in higher dimensions.

In the mapping method, the derivative in the physical region (with respect to the cartesian coordinates) is transformed analytically to be expressed in terms of derivatives in the transformed region (with respect to the curvilinear coordinates) and the metric coefficients, i.e., the derivatives of the cartesian coordinates with respect to the curvilinear coordinates (cf. Ref. 209). The derivatives in the transformed region are then evaluated from an interpolation function as discussed above. Since the grid in the transformed region is uniform by construction, the resulting formulas are straightforward. Grid configurations and higher dimensions present no problems in this procedure, since the transformation relations account for the general case through the metric coefficients. However,

the accuracy of the difference representation obtained by the mapping method depends on the smoothness of the grid, as well as on that of the given function, as discussed in the following subsection.

#### Nonuniform Grid - Exact Metric

With the mapping method, the truncation error in a difference representation is dependent not only on the higher derivatives of the solution that appear in the coefficients of the Taylor series expansion, but also on the distribution of the grid points, as reflected by the appearance of the metric coefficients, i.e., derivatives of the cartesian coordinates with respect to the curvilinear coordinates. Therefore, as is discussed in Ref. 212 and further in Ref. 142, the formal order of accuracy of difference expressions may be reduced as the coordinate system departs from uniform spacing or from orthogonality. There are thus elements of the truncation error that arise from the rate-of-change of the grid spacing, and sudden transitions between regions of fine and coarse grids can introduce significant error into the numerical solution, in the form of a numerical diffusion which may even be negative and hence destabilizing. This effect has been mentioned by a number of investigators, but there still does not seem to be a complete awareness of this need for smoothness in the grid.

As an example of this effect, consider the one-dimensional transformation of the first derivative  $f_x$ :  $f_x = f_\xi / x_\xi$  (1)

Now if  $f_\xi$  is represented by the usual two-point central difference expression, the leading term of the truncation error of  $f_\xi$  will be

$\frac{1}{6} f_{\xi\xi\xi} \Delta\xi^2$ . However, it is clear that  $\Delta\xi$  will cancel from a difference representation of the above expression for  $f_x$ , and therefore may as well be taken to be unity. (This cancellation is reflected also in the terms

of the truncation error, since a multiplication of  $\xi$  by any constant will leave all terms inversely proportional to that constant, e.g.,  $f_{\xi\xi\xi} \Delta\xi^2 \sim \frac{1}{c}$ . The division by  $x_\xi$  that occurs in the expression for  $f_x$  will then cancel the constant).

Therefore it is not correct to ascribe second-order to the central difference expression on the basis of the appearance of  $\Delta\xi^2$  in the leading term of the truncation error. In fact, the truncation of the Taylor series expansion at this term is not even justified without further consideration. The crux of the matter is that truncation error is not properly expressed in terms of derivatives of the solution with respect to the curvilinear coordinates since such derivatives, unlike the cartesian derivatives, are grid-dependent. All derivatives in the Taylor series must therefore be transformed back to the physical plane before a meaningful expression of the truncation error can be obtained.

For the above one-dimensional example, the transformed expression of  $f_{\xi\xi\xi}$  is

$$f_{\xi\xi\xi} = x_{\xi\xi\xi} f_x + 3x_\xi x_{\xi\xi} f_{xx} + x_\xi^3 f_{xxx} \quad (2)$$

With  $\Delta\xi$  taken as unity, the leading term of the truncation error of the difference expression of  $f_x$  is then

$$-\frac{1}{6} \frac{x_{\xi\xi\xi}}{x_\xi} f_x - \frac{1}{2} x_{\xi\xi} f_{xx} - \frac{1}{6} \frac{x_\xi^2}{\xi} f_{xxx} \quad (3)$$

However, since the truncation error terms are not affected by a normalization of  $\xi$ , there is no basis at this point for truncating the Taylor series. The next non-vanishing term contains  $f_{\xi\xi\xi\xi\xi}$ , which is transformed in terms of products of the first five derivatives of  $f$  with respect to  $x$  and derivatives of  $x$  with respect to  $\xi$ , in each term of which the total number of differentiations with respect to  $\xi$  equals five. The successive

terms of the Taylor series would involve odd derivatives of  $f$  and successively higher total number of  $\xi$ -differentiations of  $x$ . (All the terms with even derivatives of  $f$  with respect to  $\xi$  vanish.) In general, therefore, all of the terms of the series must be retained. The severity with which the rate of change of spacing is limited can be seen from the fact that the first term in the expressions above causes a percentage error in  $f_x$  of  $\frac{100}{6} \frac{x_{\xi\xi\xi}}{x_\xi}$ . If the percentage increase in  $x_\xi$  from one point to the next is  $\alpha$ , then the percentage error in  $f_x$  from this term is approximately  $\alpha^2/600$ . This means that an 8% increase in spacing will cause a 0.1% error, while a 24% increase in spacing will lead to a 1% error. Doubling the spacing at each point will produce a 17% error in  $f_x$  just from this term alone.

The crucial point then is how the higher derivatives of  $x$  are related to  $x_\xi$ . For the truncation error to be formally second order in general, these higher derivatives must be proportional to the corresponding powers of  $x_\xi$ , i.e.,  $x_{(q)} \sim x_\xi^q$ , where  $x_{(q)}$  indicates the  $q$ -derivative of  $x$  with respect to  $\xi$ . With this relationship we have  $x_{\xi\xi} \sim x_\xi^2$  and  $x_{\xi\xi\xi}/x_\xi \sim x_\xi$  in the leading term, and in the succeeding terms the products involving a total of  $n$  differentiations with respect to  $\xi$  will be of order  $x_\xi^n$ . These succeeding terms will thus be of order greater than 2 in  $x_\xi$ , and therefore the series can be truncated after the lead term shown above. The representation is then second order. The above condition thus assures the retention of order on a nonuniform grid in general. In fact, if  $x_{(q)} \sim x_\xi^p$ , where  $p \leq q$ , then the order of the difference representations will be degraded by  $q-p$  on the nonuniform grid.

If the spacing increases by a fraction  $\alpha$  at each point, we have, approximately,  $x_{(q)} \sim \alpha^{q-1} x_\xi$ . It is then sufficient to have  $\alpha \sim x_\xi$  to get second order. This can be accomplished, with correct dimensionality,

if  $\alpha = x_\xi / \Delta t$ , where  $\Delta x_t$  is the total range of  $x$  in the field. Thus second order is assured in general if the fractional change in spacing is limited to the ratio of the spacing to the total distance over the field.

This, however, is not the case for some commonly used point distributions. For instance, consider the exponential distribution

$$x(\xi) = x_1 + (x_2 - x_1) \frac{e^{\alpha\xi} - 1}{e^{\alpha I} - 1} \quad (4)$$

where  $[x_1, x_2]$  is the range of  $x$ , and  $[0, I]$  is that of  $\xi$ . Then

$$x_{(q)} = \frac{x_2 - x_1}{e^{\alpha I} - 1} \alpha^q e^{\alpha\xi} \quad q = 1, 2, \dots \quad (5)$$

so that  $x_{(q)} \sim \alpha^{q-1} x_\xi$ . If the slope,  $S$ , is specified at  $\xi = 0$  we have

$$S = \frac{x_2 - x_1}{e^{\alpha I} - 1} \alpha \quad (6)$$

which determines the parameter  $\alpha$ .

Now there are two ways of looking at order on a nonuniform grid. For a difference representation to be  $q$ -order, the truncation error must go to zero with the spacing,  $x_\xi$ , as  $x_\xi^q$ . From the above expressions for the minimum spacing,  $S$ , it is clear that  $x_\xi$  can be driven to zero either by adjusting the parameter  $\alpha$  with a fixed number of points, or by increasing the number of points,  $I$ , with fixed  $\alpha$ . Since the latter case has no effect on the parameter  $\alpha$ , we have  $x_{(q)} \sim x_\xi$  as  $x_\xi \rightarrow 0$  in this case, and in this sense of order all the difference representations are inconsistent. In the other sense we make  $S$ , and therefore  $x_\xi$ , approach zero by having  $\alpha$  approach infinity. In this case,  $\alpha$  varies as  $\ln \frac{1}{x_\xi}$  for small  $S$ , so that as the spacing approaches zero we have  $x_{(q)} \sim (\ln \frac{1}{x_\xi})^{q-1} x_\xi$ , so that

all difference expressions are inconsistent in this sense also.

In the first term of the truncation error expression, (3), for the first derivative, we have  $x_{\xi\xi\xi}/x_\xi \sim \alpha^2$ . This term alone will cause a  $(100/6)(\alpha^2)$  percent error in  $f_x$ . That these limits are meaningful is evidenced by the fact that the  $f_x$  term in the leading term of the truncation error, (3), causes a 0.1% error in  $f_x$  when  $\alpha^2 = 0.6/100$ , which corresponds to a minimum spacing of 9% of the average spacing for 50 points. With more points the situation improves somewhat, with the 0.1% error occurring for a minimum spacing of about 0.4% of the average for 100 points. Thus the exponential distribution is not a reasonable choice for cases in which the spacing is to have a wide variation over the field.

The determination of a point distribution function for which the order of difference representations will be retained on the nonuniform grid is the subject of Ref. 217. The conditions obtained are less restrictive on the change in grid spacing than those given above, but, unlike the above conditions, are dependent on the solution being done on the grid. The results can be understood by consideration of the truncation error for a first derivative, using first-order derivatives with respect to the curvilinear coordinates:

$$-\frac{1}{2} \frac{x_{\xi\xi}}{x_\xi} f_x - \frac{1}{2} x_\xi f_{xx} \quad (7)$$

Here the second term is first order in any case. For the first term to be first order we must have

$$\frac{x_{\xi\xi}}{x_\xi} f_x \sim x_\xi f_{xx} \quad \text{or} \quad \frac{x_{\xi\xi}}{x_\xi^2} \sim \frac{f_{xx}}{f_x}$$

Now the least restriction on the grid is made if we satisfy this condition by requiring

$$x_{\xi\xi} \sim x_\xi \quad \text{and} \quad x_\xi \sim \frac{f_x}{f_{xx}}$$

which are the conditions obtained in Ref. 217. It should be noted that the second of these conditions implies a lower limit on the spacing,  $x_\xi$ .

In the same way for the truncation error with second-order derivatives with respect to the curvilinear coordinates, (3), to be second order we must have

$$\frac{x_{\xi\xi\xi}}{x_\xi} f_x \sim x_\xi^2 f_{xxx} \quad \text{and} \quad x_{\xi\xi} f_{xx} \sim x_\xi^2 f_{xxx}$$

The first of these is satisfied with least restriction on the grid by requiring

$$x_{\xi\xi\xi} \sim x_\xi^2 \quad \text{and} \quad x_\xi^2 \sim \frac{f_x}{f_{xxx}}$$

These conditions, together with the conditions already imposed for first order, (8), are sufficient to make  $x_{\xi\xi} f_{xx} \sim x_\xi^2 f_{xxx}$  also. Therefore, the conditions for second order are

$$x_{\xi\xi} \sim x_\xi, \quad x_{\xi\xi\xi} \sim x_\xi, \quad x_\xi \sim \frac{f_x}{f_{xx}}, \quad \text{and} \\ x_\xi^2 \sim \frac{f_x}{f_{xxx}} \quad (9)$$

which, again, are those obtained in Ref. 217. The development of these conditions in Ref. 217 follows a more abstract line which does not require derivation of the actual truncation error expression.

The generalization to arbitrary higher order,  $Q$ , is now clear:

$$x_{(q)} \sim x_\xi \quad \text{and} \quad x_\xi^{q-1} \sim \frac{f_x}{f_{(q)}} \quad q = 2, 3, \dots, Q+1 \quad (10)$$

where the subscript,  $(q)$ , on  $x$  indicates differentiation with respect to the curvilinear coordinate, while that on  $f$  indicates differentiation with respect to the cartesian coordinate. For higher derivatives,  $P$ , the conditions for order  $Q$  are the same as the above except that  $q$  ranges

up to  $Q + P$ .

Several distribution functions,  $x(\xi)$ , with specified slope (grid spacing) at one end and zero curvature at the other are evaluated in Ref. 217 in regard to satisfaction of the parts of the above conditions that depend only on the grid. This evaluation is based on examining the behavior of the ratio,  $x_{(q)}/x_{\xi}$ , as the specified slope approaches zero. Although this ratio becomes unbounded for all the functions considered, some functions yield a logarithmic approach to infinity, and thus will have this ratio of much lower order at small non-zero spacing than will functions for which the approach to infinity is stronger. Functions producing this stronger approach to infinity will provide the specified small spacing at the clustered end, but will leave the other end seriously depleted of points. In this respect, the hyperbolic tangent and the error function were found to be satisfactory, with the former having a lower value of the ratio at any given slope. The exponential, sine, inverse tangent, and inverse hyperbolic sine were all unsatisfactory. These results apply also to functions with individually specified slope at each end and no curvature specification.

Also considered are functions having the zero curvature at the end with the specified slope. Among these functions, the hyperbolic sine was satisfactory, while the tangent, inverse sine, and inverse hyperbolic tangent were not. These results apply also to functions having the slope and zero curvature specified at a common interior point.

With zero curvature specified at one end, the hyperbolic sine function gives a more sparse point distribution at the unclustered end than does the hyperbolic tangent function for the same specified slope. The maximum value of the ratio  $x_{(q)}/x_{\xi}$  occurs at the unclustered end

with the former and at the clustered end with the latter. Therefore, aside from consideration of the solution derivatives, the hyperbolic sine would have the lower truncation error at the clustered end. For specified slope (square root of the product of the slopes when specified at both ends) that is greater than the average slope over the field, the hyperbolic functions must be replaced by the corresponding circular functions in each of these cases.

As noted above, these conclusions are based on consideration only of the condition  $x_{(q)} \sim x_{\xi}$ . The other conditions given above are conditions directly on the spacing, and therefore can be satisfied in any given case by limiting the spacing. The conditions given by (10) are probably more reasonable than those given earlier, i.e.,  $x_{(q)} \sim x_{\xi}^q$ , for general application. The latter condition guarantees the order of the difference representations regardless of the function to which they are applied, in the strict sense of order, i.e., that the truncation error go to zero as a power of the spacing. The former conditions, however, actually relate to the behavior of the representations at small but finite spacings, with a lower limit being imposed on the spacing by the solution function to which the difference representations are applied.

#### Nonuniform Grid - Difference Metric

All of the above considerations have assumed that the derivatives of  $x$  with respect to  $\xi$  are evaluated exactly. The use of difference expressions, rather than analytical evaluations, for these derivatives does not necessarily decrease the accuracy, but may in fact actually reduce the truncation error. Returning to the central difference

expression for the first derivative, we have by the Taylor expansion

$$\frac{f_{\xi}}{x_{\xi}} \cong \frac{f_{i+1} - f_{i-1}}{2x_{\xi}} = \frac{1}{2x_{\xi}} [f_x (2x_{\xi} + \frac{1}{3} x_{\xi\xi\xi} + \dots) + \text{other terms}] \quad (11)$$

If  $x_{\xi}$  in the denominator is evaluated analytically we have for the first term,  $f_x (1 + \frac{1}{6} \frac{x_{\xi\xi\xi}}{x_{\xi}})$ , which yields the first term of the truncation error discussed above. However if  $x_{\xi}$  in the denominator is evaluated by the central difference expression

$$x_{\xi} \cong \frac{1}{2}(x_{i+1} - x_{i-1}) = x_{\xi} + \frac{1}{6} x_{\xi\xi\xi} + \dots \quad (12)$$

we will have for the first term above,

$$\frac{f_x (2x_{\xi} + \frac{1}{3} x_{\xi\xi\xi} + \dots)}{2(x_{\xi} + \frac{1}{6} x_{\xi\xi\xi} + \dots)} = f_x \text{ exactly}$$

Thus, if the derivative  $x_{\xi}$  in the expression  $f_x = f_{\xi}/x_{\xi}$  is evaluated by the same difference expression used for  $f_{\xi}$ , rather than by analytic evaluation, then the  $f_x$  term disappears from the truncation error.

Thus, even though analytical expressions for the metric coefficient may be available, it is still generally better to evaluate the metric coefficients by the difference representations used for the dependent variables. This point is also noted in Ref. 217. Ref. 114 gives an example of a case when such numerical evaluation gave smoother results than analytical evaluation.

#### Nonorthogonality

The general two-dimensional case can be analyzed by the same procedures used above, transforming all derivatives of the dependent variable with respect to the curvilinear coordinates that appear in the truncation error into derivatives with respect to the cartesian

coordinates. The order is preserved with the nonuniform spacing in the physical field provided the higher derivatives of the cartesian coordinates with respect to the curvilinear coordinates are proportional to powers of the first derivatives of a total degree equal to the total order of the derivative.

In this case an additional element of the error due to departure from orthogonality appears in the following form for a sheared one-dimensional system:

$$-x_{\xi\xi} \cot\theta \left( \frac{1}{2} f_{xx} \cot\theta + f_{xy} \right) \quad (13)$$

where  $\theta$  is the angle between the coordinate lines. Thus for formal second order it is necessary that  $x_{\xi\xi} \cot\theta \sim x_{\xi}^2$ . Note that this condition will be satisfied when  $x_{(q)} \sim x_{\xi}^q$ , as already required for formal second order above, provided the departure from orthogonality is less than  $45^\circ$ .

Reasonable departure from orthogonality is therefore of little concern when the rate-of-change of grid spacing is reasonable.

Large departure from orthogonality may be more of a problem at boundaries, where one-sided difference expressions are needed. Therefore, grids should probably be made as nearly orthogonal at the boundaries as is practical, as has been mentioned earlier.

#### Conservative Forms

When the partial differential equations to be solved on the grid are differenced in conservative form, it is possible for the metric coefficients to introduce spurious source terms into the equations, as has been noted in several works cited in Ref. 212 and discussed also in Ref. 209 and 196. This occurs because in the conservative form, the metric coefficients are brought inside the difference operators, and if the differencing of these coefficients does not result in exact numerical

satisfaction of the metric identities, then non-vanishing terms will remain in the expressions of the gradients of uniform physical quantities. These metric identities are obtained from the differential equations when the dependent variables are all uniform.

This effect is illustrated simply by consideration of the following conservative and non-conservative forms of a first derivative:

$$f_x = \frac{1}{J}[(fy_\eta)_\xi - (fy_\xi)_\eta] = \frac{1}{J}(f_\xi y_\eta - f_\eta y_\xi) \quad (14)$$

If  $f$  is uniform the non-conservative form clearly gives a vanishing  $f_x$ . However, this is not the case with the conservative form unless the differencing is such that  $(y_\eta)_\xi = (y_\xi)_\eta$  numerically. In particular, if the metric coefficients are evaluated analytically, this identity will not be satisfied numerically when these coefficients are differenced. (This is true even in the simple case of cylindrical coordinates.)

This illustrates the important fact, also alluded to above, that it is not how accurately the metric coefficients are evaluated that is important, but how accurate are the overall difference expressions.

This effect extends also to metric identities between space and time differences when the grid is time-dependent. Here the conservative difference form of the continuity equation will reduce to a metric identity, which involves the time derivative of the Jacobian, when the dependent variable is uniform. If this identity is not satisfied exactly, this equation becomes an evolution equation for the Jacobian. It thus may be necessary to evaluate the Jacobian from this equation, rather than directly from the coordinate derivatives, for use in some places in the equation, while the direct evaluation is used in others. Several relevant references are cited in Ref. 212.

It is possible in many cases to achieve exact numerical satisfaction of the metric identities through careful attention to the differencing and the evolution of the metric coefficients. As noted above, these coefficients should be expressed by differences, not analytically. The metric coefficients should be evaluated directly from coordinate values wherever they are needed. The metric coefficients should never be averaged, since use of average values will almost certainly result in lack of satisfaction of the metric identities. Values of the coordinates at points between the grid points that are needed to construct difference expressions that will satisfy the metric identities can be obtained by averaging between the grid points. Another alternative is to generate a coordinate grid with twice as many points in each direction as are to be used in the physical solution. In Ref. 185 this direct evaluation of the metric coefficients at all points needed in the difference expressions did, in fact, eliminate problems with the metric identities.

The exact satisfaction of the identities becomes more difficult in three dimensions and in schemes involving higher-order operators or unsymmetric difference expressions. When exact satisfaction is not achieved, the effects of the spurious source terms can be partially corrected, as discussed in Ref. 196, by subtracting off the product of the metric identities with either a uniform solution or the local solution. The former amounts to using a kind of perturbation form, while the latter is, in effect, expansion of the product derivatives involving the metric coefficients and retention of the supposedly vanishing terms, thus putting the equations into a weak conservation law form. Subtraction of the product with the uniform free stream solution was used in Ref. 34, because of the difficulty in satisfying the metric identities exactly with

flux vector splitting which involves directional differences.

Finally, Zalesak (Ref. 226 and 225) states that nonuniform grids are best handled by coordinate transformation. Ciment, Ref. 49, discusses the matching of difference schemes across grid interfaces using overlapping points. Browning, Kreiss, and Olinger (Ref. 33) note that waves that are poorly represented on a coarse grid will change phase speed when passing through an interface to a finer grid.

## VIII. CONCLUSION

The computer simulation of convection of concentration profiles having large gradients requires a numerical scheme that has very low dispersion, so that phase errors are reduced, and also low dissipation, so that concentration peaks are not eroded. Baker (Ref. 17) notes that the dispersion inherent in the difference representations is the dominant source of error in convection problems.

In finite difference solutions the true phase can be approximated accurately only for the longer wavelengths, cf. Turkel (Ref. 214) and Gottlieb and Turkel (Ref. 84). It is thus more important that a scheme have small dispersion at longer wavelengths than at the shorter wavelengths. The inaccurately represented shorter wavelengths are of little significance and are appropriately damped or filtered to preserve stability. The shortest wavelength mode, i.e.,  $2\Delta x$ , that can appear on the grid is, in fact, stationary for all difference methods (Fromm, Ref. 74), and therefore must be damped. Dissipation thus should be largest at the shorter wavelengths. Ideally a scheme should be highly selective in damping or filtering only the shortest wavelength present.

Several investigations have indicated that there is no point in searching for lower-order schemes with sufficiently good phase quality and sufficiently small dissipation to represent the convection of strong concentrations over long time. It is necessary to use higher-order methods with appropriate filtering of only the shortest wavelengths. As noted by Forester (Ref. 74), higher-order schemes can handle steeper gradients without introducing spurious oscillations, i.e., computational noise. The steeper the gradient, the higher the order that is required. Both the amplitude and the wavelength of the noise decrease as the order increases.

The amplitude increases with the solution gradients. The wavelength increases with the Courant number.

Since small phase error is of greatest importance, higher-order schemes should be used. An increase in order seems to be more effective than an increase in the number of grid points, cf. Williamson and Browning (Ref.223). Similarly, in finite element methods an increase in nodal continuity is more effective than an increase in nodes, cf. Sobey (Ref. 190). However, extensions to continuity of second derivatives seems to be beyond the point of diminishing returns with finite elements.

With no physical diffusion present, symmetric space differences can lead to spatial oscillations, often called "wiggles," near sharp gradients when the cell Reynolds number exceeds 2. This is due to a nonlinear instability that is essentially independent of the Courant number, cf. Ref. 124. These oscillations occur with implicit methods as well as with explicit. These oscillations can be suppressed by using methods with large artificial dissipation, but this effectively lowers the Reynolds number of the solution. It has been shown by several investigators that proper grid resolution can remove these oscillations without adding dissipation. Monotonic schemes, cf. Kholodov (Ref.112) and van Leer (Ref.) suppress the oscillations but at the expense of unacceptable dissipation.

Fromm (Ref. 72) notes that dissipation is absent from time-centered schemes. However, since short wavelength components are never represented accurately, there must be some dissipation, either inherent or artificial, to damp these components, unless the physical problem contains sufficient diffusion to suppress the oscillations that result. First-order upwind differences damp the oscillations quite effectively, but are entirely too dissipative for use in modeling convection of strong concentration gradients.

As noted by Leonard in Ref. 130, higher-order polynomial interpolation methods are progressively less diffusive, and odd-order methods tend to be less dissipative than adjacent even-order methods. Dispersion depends on the odd derivatives in the truncation error, while dissipation results from the even derivatives. In general, odd-order methods are more dissipative, and even-order methods are more dispersive. The increased dispersion of the even-order methods becomes worse at smaller Courant numbers.

The phase error of the odd-order schemes reverses sign at a Courant number of  $1/2$ , leading at the lower values, while even-order schemes have a phase lead for all values. Lagging phase errors cause oscillations behind strong gradients, with upstream skewing of concentration, while leading errors have the opposite effect. Both dissipation and dispersion generally decrease with increasing order. Dispersion generally increases with the Courant number especially for the even-order schemes which have very low damping at low Courant number, cf. Davies (Ref. 58). The use of symmetrically placed points, as in Chan (Ref. 39), eliminates all even derivatives in the truncation error (with uniform velocity) and hence removes the dissipation even with an upwind bias.

In many schemes, improvements in phase error are accomplished at the price of tighter limits on the time step, although there are exceptions. In linear problems the effect of dissipation on the phase error is not independent of the dissipation introduced by the scheme. Turkel (Ref. 214) notes that correct boundary treatment is less important for phase quality than it is for stability. One way that higher-order schemes can be constructed is through the use of successive lower-order stages as in Abarbanel and Gottlieb (Ref. 3) and Reddy (Ref. 169).

For methods that are of equal order in both space and time, the dispersion and dissipation generally decrease as the time step increases, cf. Turkel, Abarbanel and Gottlieb (Ref. 216). This is not necessarily true when the temporal order is less than the spatial. Here the optimal time step may depend on the error tolerance and on the wavelengths present in the solution. Time step selection is thus more simple with equal order. At high frequencies the unequal temporal and spatial order methods are at a disadvantage.

In many cases with explicit methods, however, there is less need for increased order in time than there is in space, cf. Turkel (Ref. 215), and higher-order methods in time are more complicated algorithms requiring more work per time step. The results of Forester (Ref. 74) and others show that both dispersion and dissipation can be controlled by the spatial order alone, with little effect from the temporal order. In fact, Fisk (Ref. 69) notes that the spatial oscillations occur even in schemes in which time is treated continuously. These oscillations occur as readily in implicit methods as in explicit, cf. Hirsh and Rudy (Ref. 102). For explicit methods, where the time step is limited by stability, high temporal order is needed only when high frequency physical phenomena are involved.

The time step should be chosen small enough that the temporal and spatial errors are about equal, cf. Turkel (Ref. 215), so that the low spatial error is not swamped by the temporal. It seems to be more effective to restrict the Courant number to being less than unity from accuracy considerations, and hence there is little point in using implicit methods, cf. Fischer (Ref. 68). With implicit methods the temporal and spatial orders should be the same if the larger time steps that are possible with such methods are to be used. Generally, the combination

of a small time step and high spatial order seems to be the most effective in reducing dispersion while still maintaining enough dissipation at lower wavelengths, cf. Gottlieb and Turkel (Ref. 84).

Essentially infinite spatial order is attained by the spectral and pseudospectral methods, cf. Orszag (Ref. 154) and Gazdag (Ref. 77), but these methods are still complicated and not as versatile as other methods. The pseudospectral methods are faster than the spectral methods.

Fischer (Ref. 68) indicates that the achievement of higher order through an increase in the number of dependent variables, i.e., use of Hermite interpolation to produce compact schemes, rather than an increased number of grid points seems to be more effective. This is confirmed by Holly and Preissman (Ref. 104) in regard to both accuracy and ease of application. The results improve with increasing Courant number. Sobey (Ref. 190) states that compact methods are more effective in resolving the shorter wavelengths. The representation of boundary conditions may be easier in operator compact methods, cf. Ciment, Leventhal and Weinberg (Ref. 50), than in other compact methods, since the individual higher derivatives do not have to be represented, but these methods tend to be more complicated overall.

Gottlieb and Turkel (Ref. 84) state that phase error for infinite spatial order with second-order time is about the same as with fourth-order space. In general, fourth-order methods in space are much more efficient than second-order methods. Order, per se, is not always a complete measure of accuracy since the higher multiplying derivatives involved may be large. With shocks higher-order schemes offer no real advantage at the shock, since all schemes are basically first order in the shock region. The higher order is still effective, however, in the smooth regions.

Decreasing the time step greatly increases the phase error for second-order space, second-order time methods, but decreases the phase error for fourth-order space. Also, decreasing the dissipation of a scheme does not necessarily increase the accuracy. In many cases it may be more desirable to decrease the phase error than the dissipation. Dissipation may be reduced overall by alternating dissipative and non-dissipative schemes. Both phase error and dissipation generally decrease as order increases. Ciment, Leventhal and Weinberg (Ref. 50) note that many model problems have shown that higher-order methods significantly decrease the storage and computer time required for a desired accuracy, since fewer grid points are required with higher order. This is confirmed by Turkel, Abarbanel, and Gottlieb (Ref. 216), especially for more complicated equations and for smaller error tolerance. For a given order, more grid points per wavelength will be required the longer the time of the simulation. It should be noted that the use of Hermite interpolation, splines, and Pade approximations can all be made to produce the same overall representations on uniform grids. However, certain useful relationships may not be obtained in some approaches, cf. Rubin and Khosla (Ref. 180).

Symmetric schemes tend to be more dispersive than upwind-biased schemes, and this effect becomes more pronounced at lower Courant numbers. The use of an upstream bias and odd-ordered schemes improves the phase properties, as noted by Chan (Ref. 39), Davies (Ref. 58), Fischer (Ref. 68), van Leer (Ref. 124), Holly and Preissman (Ref. 104), and others. In Ref. 125, van Leer states that all second-order properly upstream-centered schemes have maximum dissipation and zero phase error at Courant number  $1/2$ .

The simplest extensions to multiple dimensions is through time-splitting (cf. Turkel, Ref. 215). Time-splitting does not reduce the spatial order, nor does it increase the dispersion. Larger time steps are made possible by the factoring into one-dimensional forms. It may be desirable to time-split the convective terms from the diffusion terms, using implicit schemes for the latter (cf. Gottlieb and Turkel, Ref. 84). Van Leer (Ref. 126 and 121) also recommends that higher dimensions be treated by time-splitting unless the temporal order is higher than two. Time-splitting requires that there be a time derivative in each equation. It is also recommended that diffusion be included through time-splitting, i.e., by convecting and then diffusing the solution.

Reference should be made directly to the comparisons given in the foregoing text, especially in regard to higher-order methods and filters. The following list provides a summary of some desirable features of schemes for convection of strong concentrations using general curvilinear coordinate systems:

1. Explicit, with Courant number well below unity.
2. Second order in time.
3. At least third order in space, preferably odd order. Order higher than third may be necessary, but order beyond fifth is probably past the point of diminishing returns.
4. Compact difference expressions.
5. Upwind-bias.
6. Symmetric time-splitting into 1D schemes (factoring).
7. Strong, sharp filter on smallest noise wavelengths.
8. Non-orthogonal grid, but skewness not too great. Orthogonal at boundary.
9. Grid lines concentrated in regions of large gradients, but spacing not changing too rapidly.
10. Dynamically adaptive grid coupled with evolving physical solution.

Some particular schemes of interest are listed below (without ranking). These schemes do not exhibit all of the desirable properties, so reference should be made to the specific discussions in the text.

Davies third and fifth-order schemes (p. 62)

Chan fourth and sixth-order schemes (p. 69)

Leonard third-order QUICKEST scheme (p. 73)

van Leer third-order III and V schemes (p. 78)

MacCormack-type fourth-order scheme (p. 85)

Reddy fourth-order schemes (p. 90)

Holly and Preissman fourth-order schemes (p. 98)

Sobey finite element scheme 5 (p. 102)

Baker finite element scheme (p. 139)

Forester quintic spline scheme (p. 158)

The results of Forester (p.204) and Zalesak (p.186) show clearly that very low dispersion and dissipation can be achieved by using a high-order scheme with a filtering procedure for removing the short wavelength computational noise.

The best course then seems to be either (1) to couple a high-order scheme with one of low order in the hybrid form of FCT (p.185), using the flux limiter that takes account of past history (p.187), or (2) to use a high-order scheme with the Forester wavelength filter (p.204). In either case the high-order scheme should have very low dissipation and dispersion. The low-order scheme in the FCT framework should be very dissipative and probably should simply be first-order upwind. As noted above, the high-order scheme should be compact with upstream bias and preferably odd order.

The hybrid form may be better in principle than the filtered form. However, the hybrid form must use a flux limiter based on past history,

else the dissipation will be too large for long-term integrations, and such a limiter is somewhat involved for multiple dimensions. The filtered form is more straightforward to implement, and therefore might be preferable from a practical standpoint at present.

Of the schemes mentioned above, those of van Leer, Holly and Preissman, Baker, and Forester show considerable promise. The sixth-order Chan scheme also shows promise, but this order is degraded with variable velocity. The stronger the concentration peaks, the higher the order that will be necessary. Several very high-order schemes have been applied with the Forester filter and with hybrid FCT, as discussed in the foregoing text, and these schemes should be considered when very high order is needed. The quintic spline scheme of Forester, operating with the Forester filter, has shown what seems to be the best published results for the Gaussian concentration peak.

In conclusion, the general recommendation is the use of the highest-order scheme that is reasonable from a programming standpoint with either hybrid FCT, with a flux limiter dependent on past history, or the Forester filter to control the computational noise at short wavelengths.

## REFERENCES

- <sup>1</sup> Abarbanel, S. and Goldberg, M., "Numerical Solution of Quasi-Conservative Hyperbolic Systems - The Cylindrical Shock Problem," Journal of Computational Physics, Vol. 10, 1972, pp. 1-21.
- <sup>2</sup> Abarbanel, Saul and Gottlieb, David, "Optimal Time Splitting for Two- and Three-Dimensional Navier-Stokes Equations with Mixed Derivatives," Journal of Computational Physics, Vol. 41, 1981, pp. 1-33.
- <sup>3</sup> Abarbanel, S. and Gottlieb, D., "Higher Order Accuracy Finite Difference Algorithms for Quasi-Linear, Conservative Law Hyperbolic Systems," Mathematics of Computation, Vol. 27, 1973, pp. 505-523.
- <sup>4</sup> Abarbanel, S.; Gottlieb, D. and Turkel, E., "Difference Schemes with Fourth Order Accuracy for Hyperbolic Equations," SIAM J. Appl. Math., Vol. 29, 1975, pp. 329-351.
- <sup>5</sup> Adam, Y., Journal of Computational Physics, Vol. 24, 1977, p. 24.
- <sup>6</sup> Adam, Yves, "Highly Accurate Compact Implicit Methods and Boundary Conditions," Journal of Computational Physics, Vol. 24, 1977, pp. 10-22.
- <sup>7</sup> Adam, Y. Computational Math. Appl., Vol. 1, 1975, p. 393.
- <sup>8</sup> Agarwal, R. K., "A Fourth-Order-Accurate Compact Differencing Scheme for Steady Navier-Stokes Equations," AIAA Paper 82-0977, 1982.
- <sup>9</sup> Agarwal, R. K., "A Third-Order Accurate Upwind Scheme for Navier-Stokes Solutions at High Reynolds Numbers," AIAA Paper 81-0112, 1981.
- <sup>10</sup> Akima, Hiroshi, "A New Method of Interpolation and Smooth Curve Fitting Based on Local Procedures," Journal of the Association for Computing Machinery, Vol. 17, No. 4, 1970, pp. 589-602.
- <sup>11</sup> Allen, D. N. De G. and Southwell, R. V., "Relaxation Methods Applied to Determine the Motion in Two Dimensions of a Viscous Fluid Past a Fixed Cylinder," Quart. J. Mech. Appl. Math., Vol. 8, 1955, pp. 129-145.
- <sup>12</sup> Alpert, Pinhas, "Implicit Filtering in Conjunction with Explicit Filtering," Journal of Computational Physics, Vol. 44, 1981, pp. 212-219.
- <sup>13</sup> Anderson, D. A., "A Comparison of Numerical Solutions to the Inviscid Equations of Fluid Motion," Journal of Computational Physics, Vol. 15, 1974, pp. 1-20.
- <sup>14</sup> Anderson, D. V., "Axisymmetric Multifluid Simulation of High Beta Plasmas with Anisotropic Transport Using a Moving Flux Coordinate Grid," Journal of Computational Physics, Vol. 17, 1975, pp. 246-275.
- <sup>15</sup> Arakawa, A. "Computational Design of Long-Term Numerical Integration of the Equations of Fluid Motion: I. Two-Dimensional Incompressible Flow," Journal of Computational Physics, Vol. 1, 1966, pp. 119-143.

- <sup>16</sup> Baker, A. J., "Research on a Finite Element Numerical Algorithm for the Three-Dimensional Navier-Stokes Equations," AFWAL-TR-82-3012, Wright-Patterson AFB, 1982.
- <sup>17</sup> Baker, A. J., "Research on Numerical Algorithms for the Three-Dimensional Navier-Stokes Equations, II. Dissipative Finite Element," AFWAL-TR-80-3157, Wright-Patterson AFB, 1981.
- <sup>18</sup> Baker, A. J., "Research on Numerical Algorithms for the Three-Dimensional Navier-Stokes Equations, I. Accuracy, Convergence and Efficiency," AFFDL-TR-79-3141, Wright-Patterson AFB, 1979.
- <sup>19</sup> Baker, A. J. and Soliman, M. O., "On the Accuracy and Efficiency of a Finite Element Algorithm for Hydrodynamic Flows," Presented at the 4th International Conference On Finite Element in Water Resources, University of Hannover, FRG, June 1982.
- <sup>20</sup> Baker, A. J. and Soliman, M. O., "On the Utility of Finite Element Theory for Computational Fluid Dynamics," AIAA Paper 81-1031, 1981.
- <sup>21</sup> Baker, A. J. and Soliman, M. O., "Analysis of a Finite Element Algorithm for Numerical Predictions in Water Resources Research," Presented at the 3rd International Conference on Finite Elements in Water Resources, University of Mississippi, 1980.
- <sup>22</sup> Baker, A. J. and Soliman, M. O., "Utility of a Finite Element Solution Algorithm for Initial-Value Problems," Journal of Computational Physics, Vol. 32, 1979, pp. 289-324.
- <sup>23</sup> Baker, A. J.; Soliman, M. O.; and Pepper, D. W., "A Time-Split Finite Element Algorithm for Environmental Release Prediction," Presented at the Second International Conference on Finite Elements in Water Resources, July, 1978, Imperial College, London, England.
- <sup>24</sup> Beam, Richard A. and Warming R. F., "An Implicit Finite-Difference Algorithm for Hyperbolic Systems in Conservation-Law Form," Journal of Computational Physics, Vol. 22, 1976, pp. 87-110.
- <sup>25</sup> Bellman, Richard; Kashef B. G.; and Casti J., "Differential Quadrature: A Technique for the Rapid Solution of Nonlinear Partial Differential Equations," Journal of Computational Physics, Vol. 10, 1972, pp. 40-52.
- <sup>26</sup> Ben-Sabar, Ehud and Caswell, Bruce, "A Stable Finite Element Simulation of Convective Transport," International Journal for Numerical Methods in Engineering, Vol. 14, 1979, pp. 545-565.
- <sup>27</sup> Blottner, F. G., "Numerical Solution of Diffusion-Convection Equations," Computers and Fluids, Vol. 6, 1978, pp. 15-24.
- <sup>28</sup> Book, D. L.; Boris, J. P.; and Hain, K., "Flux-Corrected Transport. II: Generalizations of the Method," Journal of Computational Physics, Vol. 18, 1975, pp. 248-283.

- <sup>29</sup>Book, D. L. and Ott, Edward, "Rayleigh-Taylor Instability in the 'Shallow-water' Approximation," The Physics of Fluids, Vol. 17, 1974, pp. 676-678.
- <sup>30</sup>Boris, J. P., "Numerical Solution of Continuity Equations," NRL Memorandum Report 3326, Naval Research Laboratory, 1976.
- <sup>31</sup>Boris, J. P. and Book, D. L., "Flux-Corrected Transport. III. Minimal-Error FCT Algorithms," Journal of Computational Physics, Vol. 20, 1976, pp. 397-431.
- <sup>32</sup>Boris, Jay P. and Book David L., "Flux-Corrected Transport. I. SHASTA, A Fluid Transport Algorithm That Works," Journal of Computational Physics, Vol. 11, 1973, pp. 38-69.
- <sup>33</sup>Browning, Gerald; Kreiss, Heinz-Otto; and Olinger, Joseph, "Mesh Refinement," Mathematics of Computation, Vol. 27, 1973, pp. 29-39.
- <sup>34</sup>Buning, P. G. and Steger, J. L., "Solution of the Two-Dimensional Euler Equations with Generalized Coordinate Transformation Using Flux Vector Splitting," AIAA Paper 82-0971, 1982.
- <sup>35</sup>Burstein, Samuel Z. and Mirin, Arthur A., "Third Order Difference Methods for Hyperbolic Equations," Journal of Computational Physics, Vol. 5., 1970, pp. 547-571.
- <sup>36</sup>Burstein, Samuel Z., "Finite-Difference Calculations for Hydrodynamic Flows Containing Discontinuities," Journal of Computational Physics, Vol. 2, 1967, pp. 198-222.
- <sup>37</sup>Carver, Michael, B., "Pseudo Characteristic Methods of Lines Solution of the Conservation Equations," Journal of Computational Physics, Vol. 35, 1980, pp. 57-76.
- <sup>38</sup>Chakravarthy, S. and Osher, S., "Numerical Experiments with the Osher Upwind Scheme for the Euler Equations," AIAA Paper 82-0975, 1982.
- <sup>39</sup>Chan, Robert K. C., "A Balanced Expansion Technique for Constructing Accurate Finite Difference Advection Schemes," International Journal for Numerical Methods in Engineering, Vol. 12, 1978, pp. 1131-1150.
- <sup>40</sup>Chan, Robert K. C., "A Second-Order, Time Integration Scheme for Calculating Stratified Incompressible Flows," Journal of Computational Physics, Vol. 22, 1976, pp. 74-86.
- <sup>41</sup>Chapman, Milt, "FRAM - Nonlinear Damping Algorithms for the Continuity Equation," Journal of Computational Physics, Vol. 44, 1981, pp. 84-103.

- <sup>42</sup> Chattot, J. J.; Guiu-Roux, J.; and Lamine, J., "Numerical Solution of a First-Order Conservation Equation by a Least Square Method," International Journal for Numerical Methods in Fluids, Vol. 2, 1982, pp. 209-219.
- <sup>43</sup> Chien, John C., "A General Finite-Difference Formulation with Application to Navier-Stokes Equations," Journal of Computational Physics, Vol. 20, 1976, pp. 268-278.
- <sup>44</sup> Chin, R. C. Y. and Hedstrom, G. W., "A Dispersion Analysis for Difference Schemes: Tables of Generalized Airy Functions," Mathematics of Computation, Vol. 32, 1978, pp. 1163-1170.
- <sup>45</sup> Chin, R. C. Y.; Hedstrom, G. W.; and Karlsson, K. E., "A Simplified Galerkin Method for Hyperbolic Equations," Mathematics of Computation, Vol. 33, 1979, pp. 647-658.
- <sup>46</sup> Chorin, Alexandre Joel, "Random Choice Solution of Hyperbolic Systems," Journal of Computational Physics, Vol. 22, 1976, pp. 517-533.
- <sup>47</sup> Chorin, Alexandre Joel, "Random Choice Methods with Applications to Reacting Gas Flow," Journal of Computational Physics, Vol. 25, 1977, pp. 253-272.
- <sup>48</sup> Christensen, Ove and Prahm, Lars P., "A Pseudospectral Model for Dispersion of Atmospheric Pollutants," Journal of Applied Meteorology, Vol. 15, 1976, pp. 1284-1294.
- <sup>49</sup> Ciment, Melvyn, "Stable Matching of Difference Schemes," SIAM J. Numer. Anal., Vol. 9, 1972, pp. 695-701.
- <sup>50</sup> Ciment, Melvyn; Leventhal, Stephen H.; and Weinberg, Bernard C., "The Operator Compact Implicit Method for Parabolic Equations," Journal of Computational Physics, Vol. 28, 1978, pp. 135-166.
- <sup>51</sup> Colella, Phillip, "Glimm's Method for Gas Dynamics," SIAM J. Sci. Stat. Comput., Vol. 3, 1982, pp. 76-110.
- <sup>52</sup> Collatz, L., The Numerical Treatment of Differential Equations, Springer-Verlag, Berlin, 1960.
- <sup>53</sup> Concus, Paul and Proskurowski, Wlodzimierz, "Numerical Solution of a Nonlinear Hyperbolic Equation by the Random Choice Method," Journal of Computational Physics, Vol. 30, 1979, pp. 153-166.
- <sup>54</sup> Courant, R.; Isaacson, E.; and Rees, M., "On the Solution of Non-linear Hyperbolic Differential Equations by Finite Differences," Communications on Pure and Applied Mathematics, Vol 5, 1959, pp. 243-255.

- <sup>55</sup> Crowley, W. P. "Numerical Advection Experiments," Monthly Weather Review, Vol. 96, 1968, pp. 1-11.
- <sup>56</sup> Cushman, John H., "Difference Schemes or Element Schemes," International Journal for Numerical Methods in Engineering, Vol. 14, 1979, pp. 1643-1651.
- <sup>57</sup> Cushman, John H., "Continuous Families of Lax-Wendroff Schemes," International Journal for Numerical Methods in Engineering, Vol. 17, 1981, pp. 975-989.
- <sup>58</sup> Davies, Huw C., "A Pseudo-Upstream Differencing Scheme for Advection," Journal of Computational Physics, Vol. 37, 1980, pp. 280-286.
- <sup>59</sup> Davis, G. De Vahl and Mallinson, G. D., "An Evaluation of Upwind and Central Difference Approximations by a Study of Recirculating Flow," Computers and Fluids, Vol. 4, 1976, pp. 29-43.
- <sup>60</sup> Davis, Stephen F. and Flaherty, Joseph E., "An Adaptive Finite Element Method for Initial-Boundary Value Problems for Partial Differential Equations," SIAM J. Sci. Stat. Comput., Vol. 3, 1982, pp. 6-27.
- <sup>61</sup> DiPerna, Ronald J., "Finite Difference Schemes for Conservation Laws," Communications on Pure and Applied Mathematics, Vol. XXV, 1982, pp. 379-450.
- <sup>62</sup> Dukowicz, J. K. and Ramshaw, J. D., "Tensor Viscosity Method for Convection in Numerical Fluid Dynamics," Journal of Computational Physics, Vol. 32, 1979, pp. 71-79.
- <sup>63</sup> Dwoyer, Douglas L. and Thames, Frank C., "Temporal and Spatial Inconsistencies of Time-Split Finite-Difference Schemes," NASA Technical Paper 1790, Langley Research Center, 1981.
- <sup>64</sup> Egan, Bruce A. and Mahoney, James R., "Numerical Modeling of Advection and Diffusion of Urban Area Source Pollutants," Journal of Applied Meteorology, Vol. 12, 1972, pp. 312-322.
- <sup>65</sup> Eilon, B.; Gottlieb, D.; and Zwas, G., "Numerical Stabilizers and Computing Time for Second-Order Accurate Schemes," Journal of Computational Physics, Vol. 9, 1972, pp. 387-397.
- <sup>66</sup> El-Mistakawy, T. M. and Werle, M. J., "Numerical Method for Boundary Layers with Blowing - the Exponential Box Scheme," AIAA Journal, Vol. 16, 1978, pp. 749-751.
- <sup>67</sup> Emery, Ashley F., "An Evaluation of Several Differencing Methods for Inviscid Fluid Flow Problems," Journal of Computational Physics, Vol. 2, 1968, pp. 306-331.

<sup>68</sup>Fischer, Karsten, "Convective Difference Schemes and Hermite Interpolation," International Journal for Numerical Methods in Engineering, Vol. 12, 1978, pp. 931-940.

<sup>69</sup>Fisk, Robert S., "On An Oscillation Phenomenon in the Numerical Solution of the Diffusion-Convection Equation," SIAM J. Numer. Anal., Vol. 19, 1982, pp. 721-724.

<sup>70</sup>Flores, Jolen and Holt, Maurice, "Glimm's Method Applied to Underwater Explosion," Journal of Computational Physics, Vol. 44, 1981, pp. 377-387.

<sup>71</sup>Fromm, J. E., "Practical Investigation of Convective Difference Approximations of Reduced Dispersion," High-Speed Computing in Fluid Dynamics, The Physics of Fluids Supplement II, 1969.

<sup>72</sup>Fromm, Jacob E., "A Method for Reducing Dispersion in Convective Difference Schemes," Journal of Computational Physics, Vol. 3, 1968, pp. 176-189.

<sup>73</sup>Fromm, J. E., Comments on "Numerical Advection Experiments," Monthly Weather Review, Vol. 96, 1968, p. 573.

<sup>74</sup>Forester, C. K., "Higher Order Monotonic Convective Difference Schemes," Journal of Computational Physics, Vol. 23, 1977, pp. 1-22.

<sup>75</sup>Fox, Douglas G. and Orszag, Steven A., "Pseudospectral Approximation to Two-Dimensional Turbulence," Journal of Computational Physics, Vol. 11, 1973, pp. 612-619.

<sup>76</sup>Gadd, A. J., Quart. J. Roy. Met. Soc., Vol. 104, 1978, pp. 583-594.

<sup>77</sup>Gazdag, Jenő, "Numerical Convective Schemes Based on Accurate Computation of Space Derivatives," Journal of Computational Physics, Vol. 13, 1973, pp. 100-113.

<sup>78</sup>Gelinas, R. J. and Doss, S. K., "The Moving Finite Element Method: Applications to General Partial Differential Equations with Multiple Large Gradients," Journal of Computational Physics, Vol. 40, 1981, pp. 202-249.

<sup>79</sup>Gerrity, Joseph P., Jr., "A Note on the Computational Stability of the Two-Step Lax-Wendroff Form of the Advection Equation," Monthly Weather Review, Vol. 100, 1972, pp. 72-73.

<sup>80</sup>Gerrity, Joseph P., Jr.; McPherson, Ronald D.; and Polger, Paul D., "On the Efficient Reduction of Truncation Error in Numerical Weather Prediction Models," Monthly Weather Review, Vol. 100, 1972, pp. 637-643.

- <sup>81</sup>Glimm, J., Comm. Pure Appl. Math., Vol. 18, 1965, p. 697.
- <sup>82</sup>Gottlieb, David, "Strang-Type Difference Schemes for Multi-Dimensional Problems," SIAM J. Numer. Anal., Vol. 9, 1972, pp. 650-661.
- <sup>83</sup>Gottlieb, D. and Orszag, S., "Numerical Analysis of Spectral Methods: Theory and Applications," SIAM, 1977.
- <sup>84</sup>Gottlieb, David and Turkel, Eli, "Dissipative Two-Four Methods for Time-Dependent Problems," Mathematics of Computation, Vol. 30, 1976, pp. 703-732.
- <sup>85</sup>Gourlay, A. R. and Morris, J. L., Math. of Comp., Vol. 22, 1968, p. 28.
- <sup>86</sup>Gourlay, A. R. and Morris, J. L., "On the Comparison of Multi-step Formulations of the Optimized Lax-Wendroff Method for Nonlinear Hyperbolic Systems in Two Space Variables," Journal of Computational Physics, Vol. 5, 1970, pp. 229-243.
- <sup>87</sup>Grammeltvedt, Arne, "A Survey of Finite-Difference Schemes for the Primitive Equations for a Barotropic Fluid," Monthly Weather Review, Vol. 97, 1969, pp. 384-404.
- <sup>88</sup>Graves, Randolph A., "Solutions to Divergence Form Equations Using the Method of Partial Implicitization," Journal of Computational Physics, Vol. 21, 1976, pp. 340-342.
- <sup>89</sup>Graves, Randolph A., "Partial Implicitization," Journal of Computational Physics, Vol. 13, 1973, pp. 439-444.
- <sup>90</sup>Gresho, Philip M. and Lee, Robert L., "Don't Suppress the Wiggles - They're Telling You Something," Computers and Fluids, Vol. 9, 1981, pp. 223-253.
- <sup>91</sup>Griffiths, D. F., "On the Approximation of Convection Problems in Fluid Dynamics," Int. Journal for Numerical Methods in Engineering, Vol. 12, 1977, pp. 1477-1483.
- <sup>92</sup>Griffiths, D. F.; Christie, I.; and Mitchell, A. R., "Analysis of Error Growth for Explicit Difference Schemes in Conduction-Convection Problems," International Journal for Numerical Methods in Engineering, Vol. 15, 1980, pp. 1075-1081.
- <sup>93</sup>Gustafsson, Bertil, "The Convergence Rate for Difference Approximations to Mixed Initial Boundary Value Problems," Mathematics of Computation, Vol. 29, 1975, pp. 396-406.
- <sup>94</sup>Haidvogel, D. B.; Robinson, A. R.; and Schulman, E. E., "The Accuracy, Efficiency, and Stability of Three Numerical Models with Application to Open Ocean Problems," Journal of Computational Physics, Vol. 34, 1980, pp. 1-53.

- <sup>95</sup>Han, T.; Humphrey, J. A. C.; and Launder, B. E., "A Comparison of Hybrid and Quadratic-Upstream Differencing in High Reynolds Number Elliptic Flows," Computer Methods in Applied Mechanics and Engineering, Vol. 29, 1981, pp. 81-95.
- <sup>96</sup>Harten, A., Comm. Pure Appl. Math., Vol. 30, 1977, p. 611.
- <sup>97</sup>Harten, A. and Tal-Ezer, H., "On a Fourth Order Implicit Finite Difference Scheme for Hyperbolic Conservation Laws. II. Five-Point Schemes," Journal of Computational Physics, Vol. 41, 1981, pp. 329-356.
- <sup>98</sup>Harten, A. and Zwas, G., "Self-Adjusting Hybrid Schemes for Shock Computations," Journal of Computational Physics, Vol. 9, 1972, pp. 568-583.
- <sup>99</sup>Harten, A. and Zwas, G., "Switched Numerical Shuman Filters for Shock Calculations," Journal of Engineering Mathematics, Vol. 6, 1972, pp. 207-216.
- <sup>100</sup>Heydweiller, J. C., "A Stable Difference Scheme for the Solution of Hyperbolic Equations Using the Method of Lines," Journal of Computational Physics, Vol. 22, 1976, pp. 377-388.
- <sup>101</sup>Hirsh, Richard S., "Higher Order Accurate Difference Solutions of Fluid Mechanics Problems by a Compact Differencing Technique," Journal of Computational Physics, Vol. 19, 1975, pp. 90-109.
- <sup>102</sup>Hirsh, R. S. and Rudy, D. H., "The Role of Diagonal Dominance and Cell Reynolds Number in Implicit Difference Methods for Fluid Mechanics Problems," Journal of Computational Physics, Vol. 16, 1974, pp. 304-310.
- <sup>103</sup>Holla, D. N. and Jain, P. C., "Implicit Dissipative Schemes for Solving Systems of Conservation Laws," Journal of Engineering Mathematics, Vol. 13, 1979, pp. 257-270.
- <sup>104</sup>Holly, Forrest M., Jr. and Preissman, Alexandre, "Accurate Calculation of Transport in Two Dimensions," Journal of the Hydraulics Division, ASCE, Vol. 103, 1977, pp. 1259-1277.
- <sup>105</sup>van der Houwen, P. J., "Multistep Splitting Methods of High Order for Initial Value Problems," SIAM J. Numer. Anal. Vol. 17, 1980, pp. 410-427.
- <sup>106</sup>Huffenus, J. P. and Khaletzky, D., "The Lagrangian Approach of Advective Term Treatment and its Application to the Solution of Navier-Stokes Equations," International Journal for Numerical Methods in Fluids, Vol. 1, 1981, pp. 365-387.
- <sup>107</sup>Jones, D. J.; South, J. C.; and Klunker, E. B., Journal of Computational Physics, Vol. 9, 1972, p. 496.

- 108 Keller, H. G., "A New Difference Scheme for Parabolic Problems," Numerical Solution of Partial Differential Equations (SYNSPADE 1970), B. Hubbard, Ed., Vol. 2, Academic Press, New York, 1970.
- 109 Kellogg, R. B.; Shubin, G. R.; and Stephens, A. B., "Uniqueness and the Cell Reynolds Number," SIAM J. Numer. Anal., Vol. 17, 1980, pp. 733-739.
- 110 Kerr, Christopher L. and Blumberg, Alan F., "An Analysis of a Local Second-Moment Conserving Quasi-Lagrangian Scheme for Solving the Advection Equation," Journal of Computational Physics, Vol. 32, 1979, pp. 1-9.
- 111 Khaliq, A. Q. M. and Twizell, E. H., "The Extrapolation of Stable Finite Difference Schemes for First Order Hyperbolic Equations," Intern. J. Computer Math., Vol. 11, 1982, pp. 155-167.
- 112 Kholodov, A. S., "The Construction of Difference Schemes of Increased Order of Accuracy for Equations of Hyperbolic Type," U.S.S.R. Comput. Maths. Math. Phys., Vol. 20, 1980, pp. 234-253.
- 113 Khosla, P. K. and Rubin, S. G., "A Diagonally Dominant Second-Order Accurate Implicit Scheme," Computers and Fluids, Vol. 2, 1974, pp. 207-209.
- 114 Khosla, P. K. and Rubin, S. G., "A Composite Velocity for the Compressible Navier-Stokes Equations," AIAA Paper 82-0099, 1982.
- 115 Khosla, P. K. and Rubin, S. G., "Filtering of Non-linear Instabilities," Journal of Engineering Mathematics, Vol. 13, 1979, pp. 127-141.
- 116 Krause, E.; Hirschel, E. H.; and Kordulla, W., "Fourth Order 'Mehrstellen' -Integration for Three-Dimensional Turbulent Boundary Layers," Computers and Fluids, Vol. 4, 1976, pp. 77-92.
- 117 Kreiss, H. O. and Olinger, J., Tellus, Vol. 24, 1972, p. 199.
- 118 Kreiss, H. and Olinger J., "Methods for Approximate Solution of Time Dependent Problems," Global Atmospheric Research Programme, Series No. 10, 1973.
- 119 Kutler, P.; Lomax, H.; and Warming, R. F., "Computation of Space Shuttle Flow Fields Using Noncentered Finite-Difference Schemes," AIAA Paper, 1972, pp. 72-193.
- 120 Lam, D. C. L. and Simpson, R. B., "Centered Differencing and the Box Scheme for Diffusion Convection Problems," Journal of Computational Physics, Vol. 22, 1976, pp. 486-500.
- 121 Lax, P. D. and Wendroff, B., "Difference Schemes for Hyperbolic Equations with High Order of Accuracy," Comm. Pure Appl. Math., Vol. 17, 1967, pp. 381-398.

- 122 van Leer, Bram, "Towards the Ultimate Conservative Difference Scheme. I. The Quest of Monotonicity," in Lecture Notes in Physics, Vol. 18, p. 163, Springer, Berlin, 1973.
- 123 van Leer, Bram, "Towards the Ultimate Conservative Difference Scheme. II. Monotonicity and Conservation Combined in a Second-Order Scheme," Journal of Computational Physics, Vol. 14, 1974, pp. 361-370.
- 124 van Leer, Bram, "Towards the Ultimate Conservative Difference Scheme. III. Upstream-Centered Finite-Difference Schemes for Ideal Compressible Flow," Journal of Computational Physics, Vol. 23, 1977, pp. 263-275.
- 125 van Leer, Bram, "Towards the Ultimate Conservative Difference Scheme. IV. A New Approach to Numerical Convection," Journal of Computational Physics, Vol. 23, 1977, pp. 276-299.
- 126 van Leer, Bram, "Towards the Ultimate Conservative Difference Scheme. V. A Second-Order Sequel to Godunov's Method," Journal of Computational Physics, Vol. 32, 1979, pp. 101-136.
- 127 van Leer, B., "Stabilization of Difference Schemes for the Equations of Inviscid Compressible Flow by Artificial Diffusion," Journal of Computational Physics, Vol. 3, 1969, pp. 473-495.
- 128 Leith, C. E., "Numerical Simulation of the Earth's Atmosphere," Meths. Comp. Phys., Vol. 4, 1965, pp. 1-28.
- 129 Leonard, B. P., "A Stable and Accurate Convective Modelling Procedure Based on Quadratic Upstream Interpolation," Computer Methods in Applied Mechanics and Engineering, Vol. 19, 1979, pp. 59-98.
- 130 Leonard, B. P., "Adjusted Quadratic Upstream Algorithms for Transient Incompressible Convection," AIAA Paper 79-1469, 1979.
- 131 Leschziner, M. A. and Rodi, W., "Calculation of Annular and Twin Parallel Jets Using Various Discretization Schemes and Turbulence-Model Variations," Journal of Fluids Engineering, Vol. 103, 1981, pp. 352-360.
- 132 Leventhal, Stephen H., "An Operator Compact Implicit Method of Exponential Type," Journal of Computational Physics, Vol. 46, 1982, pp. 138-165.
- 133 Lilly, Douglas, K., "On the Computational Stability of Numerical Solutions of Time-Dependent Non-Linear Geophysical Fluid Dynamics Problems," Monthly Weather Review, Vol. 93, 1965, pp. 11-26.
- 134 Livine, Avishai, "Seven-Point Difference Schemes for Hyperbolic Equations," Mathematics of Computation, Vol. 29, 1975, pp. 425-433.

- 135 MacCormack, R. W., "Numerical Solution of the Interaction of a Shock Wave with a Laminar Boundary Layer," Springer-Verlag Lecture Notes in Physics, Vol. 8, 1970.
- 136 MacCormack, R. W., "A Numerical Method for Solving the Equations of Compressible Viscous Flow," AIAA Paper 81-0110, 1981.
- 137 MacCracken, Michael C. and Bornstein, Robert D., "On the Treatment of Advection in Flux Formulations for Variable Grid Models with Application to Two Models of the Atmosphere," Journal of Computational Physics, Vol. 23, 1977, pp. 135-149.
- 138 Mahlman, J. D. and Sinclair, R. W., Advances in Environmental Science and Technology, Vol. 8, Wiley, 1977.
- 139 Mahrer, Y. and Phiki, R. A., Monthly Weather Review, Vol. 196, 1978, p. 106.
- 140 Majda, Andrew and Osher, Stanley, "Propagation of Error into Regions of Smoothness for Accurate Difference Approximations to Hyperbolic Equations," Communications on Pure and Applied Mathematics, Vol. 30, 1977, pp. 671-705.
- 141 Martin, Brian, "Numerical Representations Which Model Properties of the Solution to the Diffusion Equation," Journal of Computational Physics, Vol. 17, 1975, pp. 358-383.
- 142 Mastin, C. Wayne, "Error Induced by Coordinate Systems," Numerical Grid Generation, ed. Joe F. Thompson, North-Holland, 1982.
- 143 Matsuno, T., "Numerical Integrations of the Primitive Equations by a Simulated Backward Difference Method," J. Meteorol. Soc. Japan, Vol. 44, 1966, pp. 76-84.
- 144 McGuire, G. R. and Morris, J. L., "A Class of Implicit, Second-Order Accurate, Dissipative Schemes for Solving Systems of Conservation Laws," Journal of Computational Physics, Vol. 14, 1974, pp. 126-147.
- 145 McGuire, G. R. and Morris, J. L., "A Class of Second-Order Accurate Methods for the Solution of Systems of Conservation Laws," Journal of Computational Physics, Vol. 11, 1973, pp. 531-549.
- 146 McRae, Gregory J.; Goodin, William R.; and Seinfeld, John H., "Numerical Solution of the Atmospheric Diffusion Equation for Chemically Reacting Flows," Journal of Computational Physics, Vol. 45, 1982, pp. 1-42.

- 147 Miller, Keith, "Moving Finite Elements. II.," SIAM J. Numer. Anal., Vol. 18, 1981, pp. 1033-1057.
- 148 Miller, Keith and Miller, Robert N., "Moving Finite Elements. I," SIAM. J. Numer. Anal. Vol. 18, 1981, pp. 1019-1032.
- 149 Morchoisn, Y., "Pseudo-Spectral Space-Time Calculations of Incompressible Viscous Flows," AIAA Paper 81-0109, 1981.
- 150 Morton, K. W. and Parrott, A. K., Journal of Computational Physics, Vol. 36, 1980, p. 249.
- 151 Narayanan, M. and Shankar, N. Jothi, "A Numerical Model for the Simulation of Two-Dimensional Convective-Dispersion in Shallow Estuaries," International Journal for Numerical Methods in Engineering, Vol. 10, 1976, pp. 873-883.
- 152 Oey, Li-Yauw, "Implicit Schemes for Differential Equations," Journal of Computational Physics, Vol. 45, 1982, pp. 443-468.
- 153 Olinger, Joseph, "Fourth Order Difference Methods for the Initial Boundary-Value Problem for Hyperbolic Equations," Mathematics of Computation, Vol. 28, 1974, pp. 15-25.
- 154 Orszag, Steven A., "Numerical Simulation of Incompressible Flows within Simple Boundaries: Accuracy," J. Fluid Mech., Vol. 49, 1971, pp. 75-112.
- 155 Orszag, S. and Israel, M., Annual Rev. Fluid Mech., Vol. 6, 1974, p. 281.
- 156 Orszag, Steven A. and Jayne, Lance W., "Local Errors of Difference Approximations to Hyperbolic Equations," Journal of Computational Physics, Vol. 14, 1974, pp. 93-103
- 157 Osher, Stanley and Solomon, Fred, "Upwind Difference Schemes for Hyperbolic Systems of Conservation Laws," Mathematics of Computation, Vol. 38, 1982, pp. 339-374.
- 158 Pedersen, L. B. and Prahm, L. P., "A Method for Numerical Solution of the Advection Equation," Tellus, Vol. 26, 1974, p. 594.
- 159 Pepper, D. W. and Baker, A. J., "A High-Order Accurate Numerical Algorithm for Three-Dimensional Transport Prediction," Computers and Fluids, Vol. 8, 1980, pp. 371-390.
- 160 Pepper, D. W.; Kern, C. D.; and Long, P. E., Jr., "Modeling the Dispersion of Atmospheric Pollution Using Cubic Splines and Chapeau Functions," Atmospheric Environment, Vol. 13, 1979, pp. 223-238.
- 161 Pepper, D. W. and Long, P. E., "A Comparison of Results Using Second-Order Moments With and Without Width Correction to Solve the Advection Equation," Journal of Applied Meteorology, Vol. 12, 1978, pp. 228-233.

- 162 Peters, N., "Boundary Layer Calculations by a Hermitian Finite Difference Method," in Proceedings of the Fourth International Conference on Numerical Method in Fluid Mechanics, Boulder, Colorado, Springer-Verlag, Berlin, 1974.
- 163 Philips, Richard B. and Rose, Milton E., "Compact Finite Difference Schemes for Mixed Initial-Boundary Value Problems," SIAM J. Numer. Anal., Vol. 19, 1982, pp. 698-720.
- 164 Piacsek, Steve A. and Williams, Gareth P., "Conservation Properties of Convection Difference Schemes," Journal of Computational Physics, Vol. 6, 1970, pp. 392-405.
- 165 Pironneau, O., "On the Transport-Diffusion Algorithm and Its Applications to the Navier-Stokes Equations," Numer. Math., Vol. 38, 1982, pp. 309-332.
- 166 Price, G. V. and MacPherson, A. K., "A Numerical Weather Forecasting Method Using Cubic Splines on a Variable Mesh," Journal of Applied Meteorology, Vol. 12, 1973, pp. 1102-1113.
- 167 Price, H. S.; Varga, R. S.; and Warren, J. E., J. Math. Phys., Vol. 45, 1966, p. 301.
- 168 Raithby, G. D. and Torrance, K. E., "Upstream-Weighted Differencing Schemes and Their Application to Elliptic Problems Involving Fluid Flow," Computers and Fluids, Vol. 2, 1974, pp. 191-206.
- 169 Reddy, A. Sivasankara, "Higher Order Accuracy Finite-Difference Schemes for Hyperbolic Conservation Laws," International Journal for Numerical Methods in Engineering, Vol. 18, 1982, pp. 1019-1029.
- 170 Rhie, C. M., "A Numerical Study of the Turbulent Flow Past an Isolated Airfoil with Trailing Edge Separation," AIAA Paper 82-0998, 1982.
- 171 Richtmyer, R. D., NCAR Tech. Notes, Vol 63, 1962.
- 172 Roache, Patrick J., Computational Fluid Dynamics, Hermosa Publishers, 1976.
- 173 Robert, Andre J.; Shuman, Frederick G.; and Gerrity, Joseph P., Jr., "On Partial Difference Equations in Mathematical Physics," Monthly Weather Review, Vol. 98, 1970, pp. 1-6.
- 174 Roberts, K. V. and Weiss, N. O., "Convective Difference Schemes," Mathematics of Computation, Vol. 20, 1966, p. 272.
- 175 Roe, P. L., "Approximate Riemann Solvers, Parameter Vectors, and Difference Schemes," Journal of Computational Physics, Vol. 43, 1981, pp. 357-372.
- 176 Roscoe, D. F., "New Methods for the Derivation of Stable Difference Representations for Differential Equations," J. Inst. Maths. Applics., Vol. 16, 1975, pp. 291-301.

- 177 Rubin, Ephraim, L. and Burstein, Samuel Z., "Difference Methods for the Inviscid and Viscous Equations of a Compressible Gas," Journal of Computational Physics, Vol. 2, 1967, pp. 178-196.
- 178 Rubin, S. G. and Graves, Randolph A., "Viscous Flow Solutions with a Cubic Spline Approximation," Computers and Fluids, Vol. 3, 1975, pp. 1-36.
- 179 Rubin, S. G. and Khosla, P. K., "Higher-Order Numerical Solutions Using Cubic Splines," AIAA Journal, Vol. 14, 1976, pp. 851-858.
- 180 Rubin, S. G. and Khosla, P. K., "Polynomial Interpolation Methods for Viscous Flow Calculations," Journal of Computational Physics, Vol. 24, 1977, pp. 217-244.
- 181 Runchal, Akshai K., "Comparative Criteria for Finite-Difference Formulations for Problems of Fluid Flow," International Journal for Numerical Methods in Engineering, Vol. 11, 1977, pp. 1667-1679.
- 182 Runchal, A. K., "Convergence and Accuracy of Three Finite Difference Schemes for a Two-Dimensional Conduction and Convection Problem," International Journal for Numerical Methods in Engineering, Vol. 4, 1972, pp. 541-550.
- 183 Rusanov, V. V., "On Difference Schemes of Third Order Accuracy for Nonlinear Hyperbolic Systems," Journal of Computational Physics, Vol. 5, 1970, pp. 507-516.
- 184 Rusanov, V. V., "The Calculation of the Interaction of Non-Stationary Shock Waves and Obstacles," Zh. Vych. Mat., Vol. 1, 1961, pp. 267-279.
- 185 Sankar, N. L., "A Multigrid Strongly Implicit Procedure for Two-Dimensional Transonic Potential Flow Problems," AIAA Paper 82-0931, 1982.
- 186 Sasaki, Y. K. and Reddy, J. N., "A Comparison of Stability and Accuracy of Some Numerical Models of Two-Dimensional Circulation," International Journal for Numerical Methods in Engineering, Vol. 16, 1980, pp. 149-170.
- 187 Shapiro, Ralph, "The Use of Linear Filtering as a Parameterization of Atmospheric Diffusion," Journal of the Atmospheric Sciences, Vol. 28, 1971, pp. 523-531.
- 188 Siemieniuch, J. L. and Gladwell, I., "Analysis of Explicit Difference Methods for a Diffusion-Convection Equation," International Journal for Numerical Methods in Engineering, Vol. 12, 1978, pp. 899-916.

- 189 Smith, Robert E., Numerical Grid Generation Techniques, NASA Conference Publication 2166, NASA Langley Research Center, 1980.
- 190 Sobey, R. J., "Hermitian Space-Time Finite Elements for Estuarine Mass Transport," International Journal for Numerical Methods in Fluids, Vol. 2, 1982, pp. 277-297.
- 191 Sod, Gary A., "A Survey of Several Finite Difference Methods of Systems of Nonlinear Hyperbolic Conservation Laws," Journal of Computational Physics, Vol. 27, 1978, pp. 1-31.
- 192 Spalding, D. G., "A Novel Finite Difference Formulation for Differential Expressions Involving Both First and Second Derivatives," International Journal for Numerical Methods in Engineering, Vol. 4, 1972, pp. 551-559.
- 193 Srinivas, K. and Gururaja, J., "An Improved Form of the Artificial Diffusion Parameter-X," Journal of Computational Physics, Vol. 31, 1979, pp. 289-292.
- 194 Srinivas, K.; Gururaja, J.; and Prasad, K. Krishna, "On the First Order Local Stability Scheme for the Numerical Solution of Time-Dependent Compressible Flows," Computers and Fluids, Vol. 5, 1977, pp. 87-97.
- 195 Srinivas, K.; Gururaja, J.; and Prasad, K. Krishna, "An Assessment of the Quality of Selected Finite Difference Schemes for Time Dependent Compressible Flows," Journal of Computational Physics, Vol. 20, 1976, pp. 140-159.
- 196 Steger, Joseph L., "On Application of Body Conforming Curvilinear Grids for Finite Difference Solution of External Flow," Numerical Grid Generation, ed. Joe F. Thompson, North-Holland, 1982.
- 197 Steger, Joseph L. and Warming R. F., "Flux Vector Splitting of the Inviscid Gasdynamic Equations with Application to Finite-Difference Methods," Journal of Computational Physics, Vol. 40, 1981, pp. 263-293.
- 198 Steppeler, J., "Difference Schemes with Uniform Second and Third Order Accuracy and Reduced Smoothing," Journal of Computational Physics, Vol. 31, 1979, pp. 438-449.
- 199 Steppeler, J., "The Application of the Second and Third Degree Methods," Journal of Computational Physics, Vol. 22, 1976, pp. 295-318.
- 200 Steppeler, J., "On a High Accuracy Finite Difference Method," Journal of Computational Physics, Vol. 19, 1975, pp. 390-403.

- 201 Strang, G., "Accurate Partial Difference Methods, I. Linear Cauchy Problems," Arch. Rational Mech. Anal., Vol. 12, 1963, pp. 392-402.
- 202 Strang, Gilbert, "Accurate Partial Methods, II. Non-linear Problems," Numerische Mathematik, Vol. 28 1964, pp. 37-46.
- 203 Strang, G., "On the Construction and Comparison of Difference Schemes," SIAM J. Numer. Anal., Vol. 5, 1968, pp. 506-517.
- 204 Strang, G. and Fix, G. J., An Analysis of the Finite Element Method, Prentice-Hall, Englewood Cliffs, NJ.
- 205 Strauss, H. R., "An Artificial Viscosity for Two-Dimensional Hydrodynamics," Journal of Computational Physics, Vol. 28, 1978, pp. 437-438.
- 206 Takeo, Saitoh, "A Numerical Method for Two-Dimensional Navier-Stokes Equation by Multi-Point Finite Differences," International Journal for Numerical Methods in Engineering, Vol. 11, 1977, pp. 1439-1454.
- 207 Taylor, T. D.; Ndefo, E.; and Masson, B. S., "A Study of Numerical Methods for Solving Viscous and Inviscid Flow Problems," Journal of Computational Physics, Vol. 9, 1972, pp. 99-119.
- 208 Thiele, F., "Accurate Numerical Solutions of Boundary Layer Flows by the Finite-Difference Method of Hermitian Type" Journal of Computational Physics, Vol. 27, 1978, pp. 138-15.
- 209 Thompson, Joe F., "General Curvilinear Coordinate Systems," Numerical Grid Generation, ed. Joe F. Thompson, North-Holland, 1982.
- 210 Thompson, Joe F., (ed.) Numerical Grid Generation, North-Holland, 1982.
- 211 Thompson, Joe F., "A Survey of Grid Generation Techniques in Computational Fluid Dynamics," AIAA Paper 83-0447, AIAA 21st Aerospace Sciences Meeting, Reno, Nevada, January 1983.
- 212 Thompson, Joe F.; Warsi, Z. U. A.; and Mastin, C. W., "Boundary-Fitted Coordinate Systems for Numerical Solution of Partial Differential Equations - A Review," Journal of Computational Physics, Vol. 47, 1982, pp. 1-108.
- 213 Trefethen, Lloyd N., "Group Velocity in Finite Difference Schemes," SIAM Review, Vol. 24, 1982, pp. 113-136.

214. Turkel, Eli, "Phase Error and Stability of Second Order Methods for Hyperbolic Problems, I," Journal of Computational Physics, Vol. 15, 1974, pp. 226-250
215. Turkel, Eli, "On the Practical Use of High Order Methods for Hyperbolic Systems," Journal of Computational Physics, Vol. 35, 1980, pp. 319-340.
216. Turkel, E.; Abarbanel, S.; and Gottlieb, D., "Multidimensional Difference Schemes with Fourth Order Accuracy," Journal of Computational Physics, Vol. 21, 1976, pp. 85-113.
217. Vinokur, Marcel, "On One-Dimensional Stretching Functions for Finite-Difference Calculations," NASA CR 3313, Ames Research Center, 1980.
218. Vliegenthart, A. C., "The Shuman Filtering Operator and the Numerical Computation of Shock Waves," Journal of Engineering Mathematics, Vol. 4, 1970, pp. 341-348.
219. Warming, R. F. and Beam, Richard M., "Upwind Second-Order Difference Schemes and Applications in Aerodynamic Flows," AIAA Journal, Vol. 14, 1976, pp. 1241-1249.
220. Watanabe, Daniel S. and Flood, J. Richard, "An Implicit Fourth Order Difference Method for Viscous Flows," Mathematics of Computation Vol. 28, 1974, pp. 27-32.
221. Weber, W. J.; Boris, J.; and Gardner, J. H., "ALFVEN - A Two-Dimensional Code Based on SHASTA, Solving the Radiative, Diffusive MHD Equations," Physics Communications, Vol. 16, 1979, pp. 243-265.
222. Wesseling, P., "On the Construction of Accurate Difference Schemes for Hyperbolic Partial Differential Equations," Journal of Engineering Mathematics, Vol. 7, 1973, pp. 19-31.
223. Williamson, David L. and Browning, Gerald L., "Comparison of Grids and Difference Approximations for Numerical Weather Prediction Over a Sphere," Journal of Applied Meteorology, Vol. 12, 1973, pp. 264-274.
224. Wilson, J., J. Inst. Math. Appl., Vol. 20, 1972, p. 238.
225. Zalesak, Steven T., "High Order 'ZIP' Differencing of Convective Terms," NRL Memorandum Report 4218, Naval Research Lab, 1980.
226. Zalesak, Steven T., "Very High Order and Pseudospectral Flux-Coorect Transport (FCT) Algorithms for Conservation Laws," in Advances in Computer Methods, for Partial Differential Equations, IV (R. Vichnevetsky and R. S. Stepleman, Eds.), 1981.

<sup>227</sup>Zalesak, Steven T., "Fully Multidimensional Flux-Corrected Transport Algorithms for Fluids," Journal of Computational Physics, Vol. 31, 1979, pp. 335-362.

<sup>228</sup>Zhmakin, A. I. and Fursenko, A. A., "On a Monotonic Shock-Capturing Difference Scheme," U.S.S.R. Comput. Maths. Math. Phys., Vol. 20, 1981, pp. 218-227.

<sup>229</sup>Zwas, Gideon and Abarbanel, Saul, "Third and Fourth Order Accurate Schemes for Hyperbolic Equations of Conservation Law Form," Mathematics of Computation, Vol. 25, 1971, pp. 229-236.